

Mechanistic Studies of Hydride Transfer to Imines from a Highly Active and Chemoselective Manganate Catalyst

Frederik Freitag, Torsten Irrgang, Rhett Kempe*

Inorganic Chemistry II – Catalyst Design, University of Bayreuth, 95440 Bayreuth, Germany

Table of contents

1	General Considerations	3
2	Hydrogenation of Imines	4
2.1	Parameter Screening	4
2.2	Substrate Synthesis	6
2.2.1.	Aldimine Reduction	6
2.2.2.	Ketimine Reduction	20
3	Mechanistic Investigations	23
3.1	Reaction Intermediates	23
3.1.1.	Activation of the Manganese Complexes	23
3.1.2.	Syntheses of [Mn]K, [Mn-H]HK and [Mn-H]K ₂	32
3.1.2.1.	[Mn]K	32
3.1.2.2.	[Mn-H]HK	32
3.1.2.3.	[Mn-H]K ₂	33

3.1.3.	Crystals for X-Ray Crystal Analysis.....	33
3.1.4.	Investigation of a Hypothetical Amide Complex	33
3.1.5.	Time-dependent Stability of [Mn-H]H₂ and [Mn-H]K₂	35
3.2	Stoichiometric Hydride Transfer Reactions	37
3.2.1.	General Procedure.....	37
3.2.2.	Experimental Probing of the Catalytic Cycle	38
3.2.3.	Partial Reaction Orders	40
3.2.3.1.	Base Concentration	41
3.2.3.2.	HO ^t Bu Concentration	42
3.2.3.3.	Imine Concentration	42
3.2.3.4.	Concentration of [Mn-H]K₂	44
3.2.4.	Reaction Constant <i>k</i> and Reaction Order	46
3.2.5.	Reaction under CO Atmosphere	47
3.2.6.	Alkali Metal Ion Testing	48
3.2.7.	Hammett Study	49
3.3	Hydrogenation Experiments	52
3.3.1.	Crown Ether Addition.....	52
3.3.1.	Hydrogenation with [Mn-H]K₂ and HO ^t Bu.....	53
4	NMR Spectra.....	54
5	UV-vis Data.....	95
6	IR Data	96
7	Crystallographic Data.....	99
8	References	102

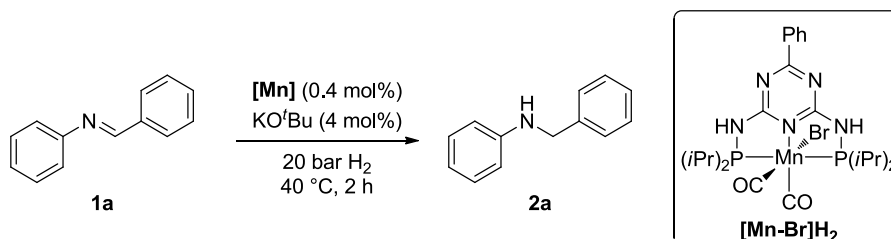
1 General Considerations

All reactions were carried out under nitrogen or argon atmosphere using standard Schlenk or glove box techniques. Solvents were purified by distillation (pentane, Et₂O, CH₂Cl₂). Dry solvents were distilled over sodium benzophenone or over CaH₂ (2-methyl-thf) or were obtained from Acros. Dry solvents were stored over molecular sieves (3 Å). Chemicals were purchased from commercial vendors and used without further purification if not noted otherwise. Imines were purchased from commercial vendors, or were synthesized according to literature procedures^{1, 2} and purified using distillation, recrystallization or sublimation. NMR spectra were collected on a Varian INOVA 300 (300 MHz for ¹H, 75 MHz for ¹³C), a Varian INOVA 400 (400 MHz for ¹H, 101 MHz for ¹³C, 162 MHz for ³¹P), or a Bruker Avance III HD 500 (500 MHz for ¹H, 125.7 MHz for ¹³C, 202 MHz for ³¹P). Chemical shifts are reported in ppm relative to the residual solvent signal [CDCl₃: 7.26 ppm (¹H); 77.16 ppm (¹³C). CD₂Cl₂: 5.32 ppm (¹H); 53.84 ppm (¹³C). thf_{D8}: 3.58 ppm, 1.72 ppm (¹H); 67.2 ppm, 25.3 ppm (¹³C)]. Coupling constants (*J*) are reported in Hz (coupling patterns: s = singlet, d = doublet, t = triplet, q = quartet, hept = heptet, bs = broad singlet, m = multiplet). ¹³C NMR spectra were measured ¹H decoupled. GC analyses were carried out on an Agilent 6850 network system with an Optima 17 column (30 m x 320 μm, 0.25 μm) and GC/MS analyses were conducted on an Agilent 7890A GC system equipped with a HP 5MS column (30 m x 320 μm x 0.25 μm) and a 5975C inert MSD detector (EI, 70 eV). Elemental analyses were carried out on an Elementar Unicube. Melting points were measured on a Stuart Scientific Melting Point Apparatus SMP3. UV-vis measurements were conducted on an Agilent Cary 60 UV-Vis. IR spectra were collected on a Shimadzu IRTracer-100 with KBr pellets. The pellets of the compounds were prepared in a glove box with dry KBr and subsequently measured under air. Macherey Nagel silica gel 60 (40–63 μm particle size) was used for column chromatography. All organic compounds were characterized by ¹H and ¹³C NMR analysis. Unknown compounds or compounds with incomplete spectroscopic literature data were further analyzed via elemental analysis. The ligands were synthesized according to literature procedures³ and the precatalysts were also synthesized similar to literature procedures⁴, in thf under reflux for 1.5 h and subsequent removal of the solvent. Hydrogenations were conducted in PARR Instrument stainless steel autoclaves N-MT5 300 mL equipped with heating mantles and temperature controllers. X-ray crystal structure analysis was performed on a STOE STADIVARI [$\lambda(\text{Mo-K}\alpha) = 0.71073 \text{ \AA}$] equipped with an Oxford Cryostream low temperature unit. Structure solution and refinement was accomplished with OlexSys 2⁵, SHELXL-2014⁶, WinGX⁷, and Mercury 3.9⁸.

2 Hydrogenation of Imines

2.1 Parameter Screening

N-benzylideneaniline (**1a**) was chosen as the model substrate for the imine hydrogenation reaction (Scheme S 1).



Scheme S 1. Starting conditions for the imine hydrogenation with *N*-benzylideneaniline (**1a**).

General screening procedure: Under nitrogen atmosphere in a glove box screw-vials were charged with magnetic stir bars, base, Mn precatalyst, **1a** (1.00 mmol, 1.00 eq.), and solvent (2 mL). The vials were placed in an autoclave, which was sealed and purged three times with hydrogen, before adjusting the pressure to 20 bar. The reactions were stirred and heated to the desired temperature. After the reaction, hydrogen was released, 1 mL H₂O, 100 μ L dodecane as internal standard, and 7 mL Et₂O were added to each vial and the mixtures were homogenized. A sample of the organic phase was dried over Na₂SO₄ and analyzed via GC.

Screenings are listed in Table S 1–Table S 5.

Table S 1. Solvent screening.^a

Entry	Solvent	Yield of 2a [%] ^b
1	thf	61
2	1,4-dioxane	23
3	toluene	12
4	2-methyl-2-butanol	0
5	diglyme	20
6	dimethoxyethane	0
7	2-methyl-thf	33

^a **1a** (1.0 mmol), KO^tBu (4 mol%), [Mn-Br]H₂ (0.4 mol%), solvent (2 mL), 40 °C, 20 bar H₂, 2 h. ^b Determined by GC with dodecane as internal standard.

Table S 2. Base screening.^a

Entry	Base	Yield of 2a [%] ^b
1	LiO ^t Bu	0
2	NaO ^t Bu	8
3	KO ^t Bu	61
4	NaHMDS ^c	3
5	KHMDS ^d	12
6	Cs ₂ CO ₃	0
7	KOH	0
8	NaOH	0
9	KH	13

^a **1a** (1.0 mmol), Base (4 mol%), [**Mn-Br**]**H₂** (0.4 mol%), thf (2 mL), 40 °C, 20 bar H₂, 2h. ^b Determined by GC with dodecane as internal standard. ^c Sodium bis(trimethylsilyl)amide. ^d Potassium bis(trimethylsilyl)amide.

Table S 3. Base amount screening.^a

Entry	Base amount [eq. with respect to the precatalyst]	Yield of 2a [%] ^b
1	1	0
2	2	0
3	5	16
4	8	54
5	10	61
6	12	54

^a **1a** (1.0 mmol), KO^tBu, [**Mn-Br**]**H₂** (0.4 mol%), thf (2 mL), 40 °C, 20 bar H₂, 2 h. ^b Determined by GC with dodecane as internal standard.

Table S 4. Precatalyst screening.^a

Entry	Precatalyst	Yield of 2a [%] ^b
1	R = Ph, X = N	37
2	R = 4-F ₃ C-C ₆ H ₄ , X = N	11
3	R = NH-cyclopropyl, X = N	20
4	R = NEt ₂ , X = N	14
5	R = Me, X = N	28
6	R = H, X = CH	2
7	PN ₅ P[MnCl ₂]	0
8	[Mn(CO) ₅ Br]	1

^a **1a** (1.0 mmol), KO^tBu (1.6 mol%), precatalyst (0.2 mol%), thf (2 mL), 40 °C, 20 bar H₂, 2 h. ^b Determined by GC with dodecane as internal standard.

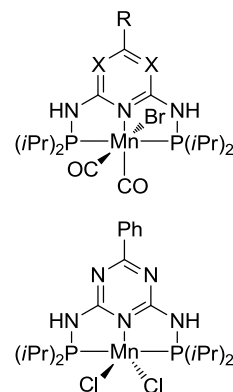


Table S 5. Screening of the catalyst loading at 40 °C and 50 °C.^a

Entry	Catalyst Loading [mol%]	Temperature [°C]	Yield of 2a [%] ^b
1	0.4	40	95
2	0.3	40	69
3	0.05	40	0
4	0.4	50	>99
5	0.3	50	79
6	0.05	50	0

^a **1a** (1.0 mmol), KO^tBu (10 eq. with respect to [Mn-Br]H₂), [Mn-Br]H₂, thf (2 mL), 20 bar H₂, 4 h.
^b Determined by GC with dodecane as internal standard.

2.2 Substrate Synthesis

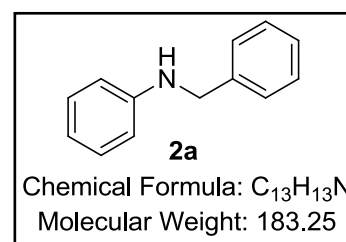
2.2.1. Aldimine Reduction

General procedure for aldimine reduction: Under nitrogen atmosphere in a glove box screw-vials were charged with magnetic stir bars, KO^tBu (4 mol%), [Mn-Br]H₂ (0.4 mol%), imine **1** (1.00 mmol, 1.00 eq.), and thf (2 mL). The vials were placed in an autoclave, which was sealed and purged three times with hydrogen, before adjusting the pressure to 20 bar. The reactions were stirred and heated to 50 °C. After 4 h, the hydrogen was released, 1 mL H₂O and 7 mL Et₂O were added to each vial, and the mixtures were homogenized. The mixture was dried with Na₂SO₄, filtered, washed with Et₂O or CH₂Cl₂, and the solvent was removed under reduced pressure. The product was isolated via a short silica column.

N-benzylaniline (**2a**)

According to the general procedure with *N*-benzylideneaniline (**1a**) (181 mg, 1.00 mmol, 1.00 eq.). Purification by column chromatography (silica gel, pentane/diethylether, 9:1).

Yield: 98 % (982 μmol, 180 mg) yellowish solid.



Upscaling: According to the general procedure with *N*-benzylideneaniline (**1a**) (3.62 g, 20.0 mmol, 1.00 eq.) and 20 mL thf. Purification by column chromatography (silica gel, pentane/diethylether, 9:1).

Yield: 98 % (19.6 mmol, 3.59 g) yellowish solid.

¹H NMR (500 MHz, CDCl₃): δ 7.43 – 7.36 (m, 4H), 7.34 – 7.28 (m, 1H), 7.24 – 7.18 (m, 2H), 6.76 (t, *J* = 7.3 Hz, 1H), 6.67 (d, *J* = 7.8 Hz, 2H), 4.36 (s, 2H), 4.07 (s, 1H).

^{13}C NMR (126 MHz, CDCl_3): δ 148.2, 139.5, 129.4, 128.8, 127.6, 127.4, 117.7, 113.0, 48.4.

The spectroscopic data correspond to those reported in literature.⁹

***N*-benzyl-4-fluoroaniline (2b)**

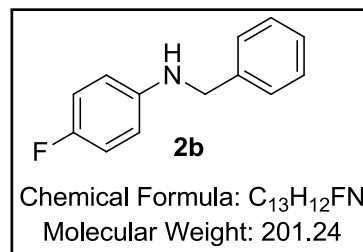
According to the general procedure with *N*-benzylidene-4-fluoroaniline (**1b**) (199 mg, 1.00 mmol, 1.00 eq.). Purification by column chromatography (silica gel, pentane/diethylether, 9:1).

Yield: 95 % (954 μmol , 192 mg) yellowish solid.

^1H NMR (500 MHz, CDCl_3): δ 7.42 – 7.35 (m, 4H), 7.35 – 7.28 (m, 1H), 6.95 – 6.87 (m, 2H), 6.62 – 6.55 (m, 2H), 4.31 (s, 2H), 3.95 (bs, 1H).

^{13}C NMR (126 MHz, CDCl_3): δ 156.0 (d, $J = 235.0$ Hz), 144.6 (d, $J = 1.8$ Hz), 139.4, 128.8, 127.6, 127.4, 115.8 (d, $J = 22.3$ Hz), 113.7 (d, $J = 7.4$ Hz), 49.0.

The spectroscopic data correspond to those reported in literature.⁹



***N*-benzyl-4-chloroaniline (2c)**

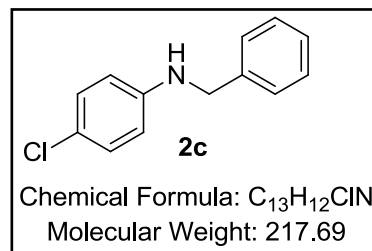
According to the general procedure with *N*-benzylidene-4-chloroaniline (**1c**) (215 mg, 1.00 mmol, 1.00 eq.). Purification by column chromatography (silica gel, pentane/diethylether, 9:1).

Yield: 98 % (983 μmol , 214 mg) orange solid.

^1H NMR (500 MHz, CDCl_3): δ 7.40 – 7.33 (m, 4H), 7.33 – 7.27 (m, 1H), 7.15 – 7.09 (m, 2H), 6.58 – 6.53 (m, 2H), 4.31 (s, 2H), 4.09 (s, 1H).

^{13}C NMR (126 MHz, CDCl_3): δ 146.7, 139.0, 129.2, 128.8, 127.5, 127.5, 122.2, 114.0, 48.5.

The spectroscopic data correspond to those reported in literature.⁹



***N*-benzyl-4-bromoaniline (2d)**

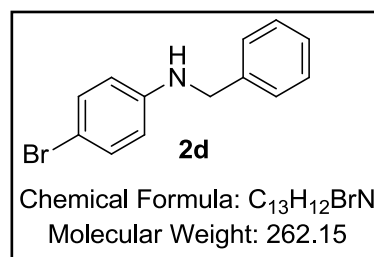
According to the general procedure with *N*-benzylidene-4-bromoaniline (**1d**) (260 mg, 1.00 mmol, 1.00 eq.). Purification by column chromatography (silica gel, pentane/diethylether, 9:1).

Yield: 96 % (957 μ mol, 251 mg) yellow solid.

^1H NMR (500 MHz, CDCl_3): δ 7.38-7.31 (m, 4H), 7.31 – 7.26 (m, 1H), 7.24 (d, J = 8.7 Hz, 2H), 6.50 (d, J = 8.7 Hz, 2H), 4.29 (s, 2H), 4.23 (bs, 1H).

^{13}C NMR (126 MHz, CDCl_3): δ 147.0, 138.9, 132.1, 128.8, 127.6, 127.5, 114.6, 109.4, 48.4.

The spectroscopic data correspond to those reported in literature.¹⁰



***N*-benzyl-4-iodoaniline (2e)**

According to the general procedure with *N*-benzylidene-4-iodoaniline (**1e**) (307 mg, 1.00 mmol, 1.00 eq.). Purification by column chromatography (silica gel, pentane/diethylether, 9:1).

Yield: 99 % (987 μ mol, 305 mg) yellowish oil.

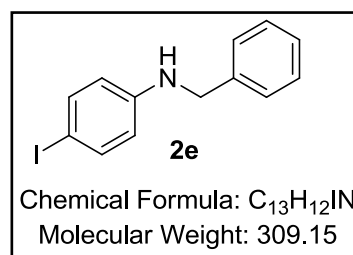
Upscaling: According to the general procedure with *N*-benzylidene-4-iodoaniline (**1e**) (6.14 g, 20.0 mmol, 1.00 eq.) and 20 mL thf. Purification by column chromatography (silica gel, pentane/diethylether, 95:5).

Yield: 98 % (19.5 mmol, 6.04 g) yellowish oil.

^1H NMR (300 MHz, CDCl_3): δ 7.44 – 7.38 (m, 2H), 7.37 – 7.32 (m, 4H), 7.32 – 7.26 (m, 1H), 6.45 – 6.40 (m, 2H), 4.30 (s, 2H), 4.19 (s, 1H).

^{13}C NMR (75 MHz, CDCl_3): δ 147.7, 138.9, 137.9, 128.8, 127.5, 115.2, 78.3, 48.2.

The spectroscopic data correspond to those reported in literature.¹¹



***N*-benzyl-3,5-dichloroaniline (2f)**

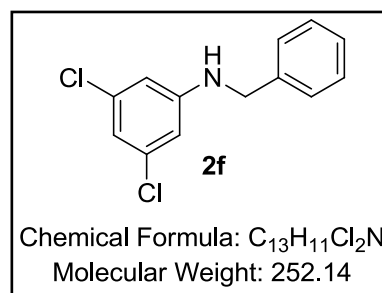
According to the general procedure with *N*-benzylidene-3,5-dichloroaniline (**1f**) (250 mg, 1.00 mmol, 1.00 eq.). Purification by column chromatography (silica gel, pentane/diethylether, 9:1).

Yield: 94 % (940 μ mol, 237 mg) yellow oil.

^1H NMR (500 MHz, CDCl_3): δ 7.40 – 7.28 (m, 5H), 6.69 (t, J = 1.7 Hz, 1H), 6.49 (d, J = 1.7 Hz, 2H), 4.32 (bs, 1H), 4.29 (s, 2H).

^{13}C NMR (126 MHz, CDCl_3): δ 149.5, 138.0, 135.5, 128.9, 127.7, 127.5, 117.4, 111.1, 48.0.

The spectroscopic data correspond to those reported in literature.¹²



***N*-benzyl-3,5-bis(trifluoromethyl)aniline (2g)**

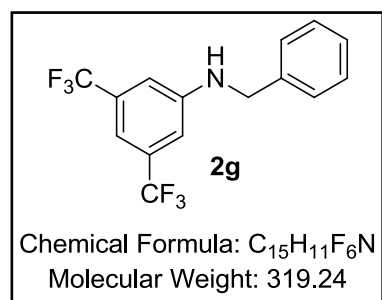
According to the general procedure with *N*-benzylidene-3,5-bis(trifluoromethyl)aniline (**1g**) (317 mg, 1.00 mmol, 1.00 eq.). Purification by column chromatography (silica gel, pentane/diethylether, 9:1).

Yield: 95 % (952 μ mol, 304 mg) yellow oil.

^1H NMR (500 MHz, CDCl_3): δ 7.43 – 7.29 (m, 5H), 7.18 (s, 1H), 6.98 (s, 2H), 4.50 (bs, 1H), 4.38 (s, 2H).

^{13}C NMR (126 MHz, CDCl_3): δ 148.7, 137.7, 132.6 (q, J = 32.7 Hz), 129.1, 128.0, 127.7, 123.7 (q, J = 273 Hz), 112.1, 110.6, 48.2.

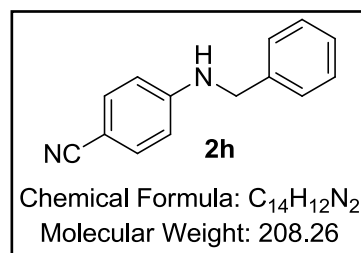
The spectroscopic data correspond to those reported in literature.¹³



4-(benzylamino)benzonitrile (2h)

According to the general procedure with 4-(benzylideneamino)benzonitrile (**1h**) (206 mg, 1.00 mmol, 1.00 eq.). Purification by column chromatography (silica gel, pentane/diethylether, 8:2).

Yield: 94 % (941 μ mol, 196 mg) yellowish solid.



Upscaling: According to the general procedure with 4-(benzylideneamino)benzonitrile (**1g**) (4.12 g, 20.0 mmol, 1.00 eq.) and 20 mL thf. Purification by column chromatography (silica gel, pentane/diethylether, 8:2).

Yield: 90 % (18.0 mmol, 3.75 g) yellowish solid.

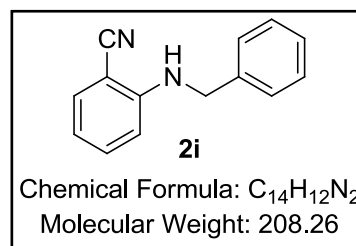
¹H NMR (500 MHz, CDCl₃): δ 7.41 (d, *J* = 8.8 Hz, 2H), 7.39 – 7.28 (m, 5H), 6.59 (d, *J* = 8.8 Hz, 2H), 4.69 (bs, 1H), 4.38 (s, 2H).

¹³C NMR (126 MHz, CDCl₃): δ 151.2, 137.9, 133.8, 129.0, 127.8, 127.4, 120.5, 112.5, 99.1, 47.6.

The spectroscopic data correspond to those reported in literature.¹⁴

2-(benzylamino)benzonitrile (**2i**)

According to the general procedure with 2-(benzylideneamino)benzonitrile (**1i**) (206 mg, 1.00 mmol, 1.00 eq.). Purification by column chromatography (silica gel, pentane/diethylether, 9:1).



Yield: 86 % (864 μmol, 180 mg) yellow solid.

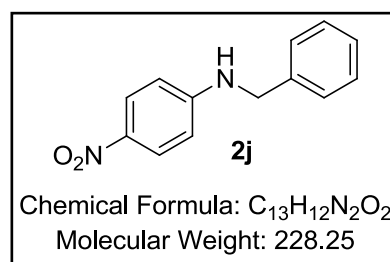
¹H NMR (500 MHz, CDCl₃): δ 7.42 (dd, *J* = 7.7, 1.4 Hz, 1H), 7.39 – 7.28 (m, 6H), 6.69 (td, *J* = 7.7, 0.7 Hz, 1H), 6.64 (d, *J* = 8.5 Hz, 1H), 5.04 (bs, 1H), 4.44 (d, *J* = 5.6 Hz, 2H).

¹³C NMR (126 MHz, CDCl₃): δ 150.2, 137.8, 134.4, 132.9, 129.0, 127.8, 127.3, 118.0, 117.0, 111.1, 96.0, 47.6.

The spectroscopic data correspond to those reported in literature.¹⁵

N-benzyl-4-nitroaniline (**2j**)

According to the general procedure with *N*-benzylidene-4-nitroaniline (**1j**) (226 mg, 1.00 mmol, 1.00 eq.) with 0.6 mol% [Mn-Br]H₂ and a reaction time of 16 h. Purification by column chromatography (silica gel, pentane/CH₂Cl₂, 9:1).



Yield: 85 % (854 μmol, 195 mg) orange solid.

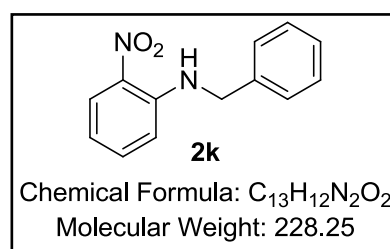
^1H NMR (500 MHz, CDCl_3): δ 8.13 – 8.04 (m, 2H), 7.43 – 7.29 (m, 5H), 6.62 – 6.52 (m, 2H), 4.91 (s, 1H), 4.44 (s, 2H).

^{13}C NMR (126 MHz, CDCl_3): δ 153.2, 138.4, 137.5, 129.1, 128.0, 127.5, 126.5, 111.5, 47.8.

The spectroscopic data correspond to those reported in literature.¹⁶

***N*-benzyl-2-nitroaniline (2k)**

According to the general procedure with *N*-benzylidene-2-nitroaniline (**1k**) (226 mg, 1.00 mmol, 1.00 eq.) with 0.6 mol% **[Mn-Br] H_2** and a reaction time of 18 h. Purification by column chromatography (silica gel, pentane/diethylether, 8:2).



Yield: 81 % (806 μmol , 184 mg) orange oil.

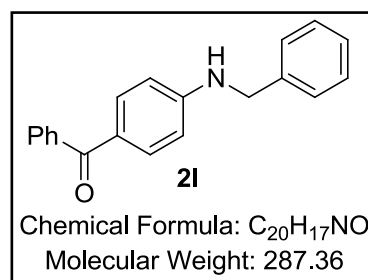
^1H NMR (500 MHz, CDCl_3): δ 8.44 (bs, 1H), 8.20 (dd, J = 8.6, 1.5 Hz, 1H), 7.44 – 7.33 (m, 5H), 7.33 – 7.28 (m, 1H), 6.82 (d, J = 8.6 Hz, 1H), 6.72 – 6.63 (m, 1H), 4.56 (d, J = 5.7 Hz, 2H).

^{13}C NMR (126 MHz, CDCl_3): δ 145.4, 137.5, 136.4, 132.4, 129.1, 127.8, 127.2, 127.0, 115.9, 114.3, 47.2.

The spectroscopic data correspond to those reported in literature.¹⁷

(4-(benzylamino)phenyl)(phenyl)methanone (2l)

According to the general procedure with (4-(benzylideneamino)phenyl)(phenyl)methanone (**1l**) (285 mg, 1.00 mmol, 1.00 eq.). Purification by column chromatography (silica gel, pentane/diethylether, 8:2).



Yield: 77 % (773 μmol , 222 mg) brightly-yellow solid.

^1H NMR (500 MHz, CDCl_3): δ 7.82 – 7.63 (m, 4H), 7.58 – 7.20 (m, 8H), 6.63 (d, J = 7.9 Hz, 2H), 4.72 (bs, 1H), 4.42 (s, 2H).

^{13}C NMR (126 MHz, CDCl_3): δ 195.3, 152.0, 139.2, 138.3, 133.1, 131.4, 129.6, 128.9, 128.1, 127.7, 127.5, 126.5, 111.6, 47.7.

The spectroscopic data correspond to those reported in literature.¹⁸

***N*-benzyl-4-styrylaniline (2m)**

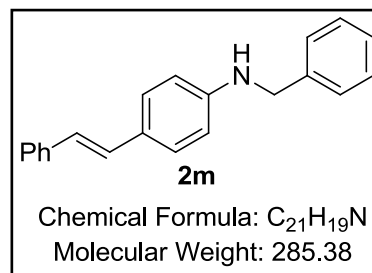
According to the general procedure with *N*-benzylidene-4-((*E*)-styryl)aniline (**1m**) (283 mg, 1.00 mmol, 1.00 eq.) and 0.6 mol% **[Mn-Br]H₂**. Purification by column chromatography (silica gel, pentane/diethylether, 9:1).

Yield: 94 % (943 μ mol, 269 mg) orange-yellow solid.

¹H NMR (500 MHz, CDCl₃): δ 7.49 (d, J = 7.5 Hz, 2H), 7.42 – 7.28 (m, 9H), 7.22 (t, J = 7.3 Hz, 1H), 7.05 (d, J = 16.3 Hz, 1H), 6.92 (d, J = 16.3 Hz, 1H), 6.65 (d, J = 8.6 Hz, 2H), 4.38 (s, 2H), 4.30 (s, 1H).

¹³C NMR (126 MHz, CDCl₃): δ 147.8, 139.2, 138.2, 128.9, 128.8, 128.7, 127.9, 127.6, 127.5, 127.2, 126.9, 126.2, 124.8, 113.1, 48.4.

The spectroscopic data correspond to those reported in literature.¹⁹



***N*-benzyl-4-methylaniline (2n)**

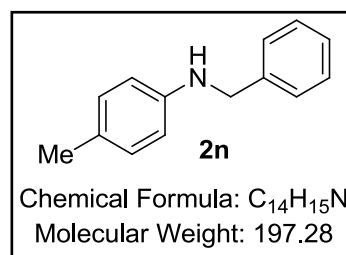
According to the general procedure with *N*-benzylidene-4-methylaniline (**1n**) (195 mg, 1.00 mmol, 1.00 eq.). Purification by column chromatography (silica gel, pentane/diethylether, 9:1).

Yield: 85 % (847 μ mol, 167 mg) yellowish oil.

¹H NMR (500 MHz, CDCl₃): δ 7.47 – 7.37 (m, 4H), 7.37 – 7.30 (m, 1H), 7.07 (d, J = 7.1 Hz, 2H), 6.63 (d, J = 6.8 Hz, 2H), 4.37 (s, 2H), 3.95 (bs, 1H), 2.32 (s, 3H).

¹³C NMR (126 MHz, CDCl₃): δ 146.0, 139.8, 129.8, 128.7, 127.6, 127.2, 126.8, 113.1, 48.7, 20.5.

The spectroscopic data correspond to those reported in literature.⁹



***N*-benzyl-4-isopropylaniline (2o)**

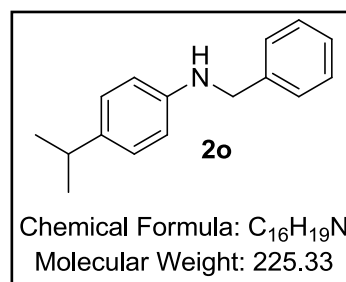
According to the general procedure with *N*-benzylidene-4-isopropylaniline (**1o**) (223 mg, 1.00 mmol, 1.00 eq.). Purification by column chromatography (silica gel, pentane/diethylether, 9:1).

Yield: 93 % (932 μ mol, 210 mg) orange oil.

^1H NMR (500 MHz, CDCl_3): δ 7.47 – 7.37 (m, 4H), 7.37 – 7.31 (m, 1H), 7.12 (d, J = 8.3 Hz, 2H), 6.66 (d, J = 8.4 Hz, 2H), 4.36 (s, 2H), 4.03 (s, 1H), 2.88 (hept, J = 6.9 Hz, 1H), 1.28 (d, J = 6.9 Hz, 6H).

^{13}C NMR (126 MHz, CDCl_3): δ 146.3, 139.8, 138.2, 128.7, 127.7, 127.3, 127.2, 113.0, 48.8, 33.3, 24.4.

The spectroscopic data correspond to those reported in literature.²⁰



***N*-benzyl-4-methoxyaniline (2p)**

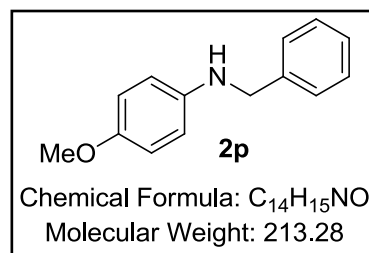
According to the general procedure with *N*-benzylidene-4-methoxyaniline (**1p**) (211 mg, 1.00 mmol, 1.00 eq.) and 0.6 mol% **[Mn-Br] H_2** . Purification by column chromatography (silica gel, pentane/diethylether, 9:1).

Yield: 94 % (942 μ mol, 201 mg) yellowish solid.

^1H NMR (500 MHz, CDCl_3): δ 7.44 – 7.36 (m, 4H), 7.36 – 7.29 (m, 1H), 6.85 – 6.80 (m, 2H), 6.67 – 6.62 (m, 2H), 4.32 (s, 2H), 3.87 (bs, 1H), 3.78 (s, 3H).

^{13}C NMR (126 MHz, CDCl_3): δ 152.2, 142.5, 139.7, 128.7, 127.6, 127.2, 115.0, 114.2, 55.8, 49.3.

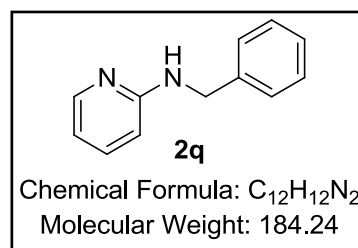
The spectroscopic data correspond to those reported in literature.⁹



***N*-benzylpyridin-2-amine (2q)**

According to the general procedure with *N*-benzylidenepyridin-2-amine (**1q**) (182 mg, 1.00 mmol, 1.00 eq.). Purification by column chromatography (silica gel, pentane/diethylether, 7:3).

Yield: 92 % (923 μ mol, 170 mg) white solid.



¹H NMR (500 MHz, CDCl₃): δ 8.11 (dd, J = 5.0, 0.9 Hz, 1H), 7.44 – 7.32 (m, 5H), 7.32 – 7.26 (m, 1H), 6.60 (ddd, J = 7.0, 5.1, 0.6 Hz, 1H), 6.39 (d, J = 8.4 Hz, 1H), 5.03 (bs, 1H), 4.52 (d, J = 5.8 Hz, 2H).

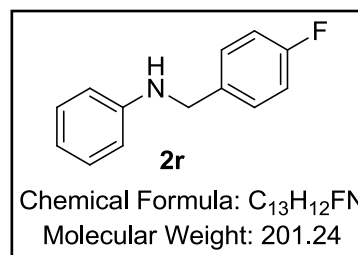
¹³C NMR (126 MHz, CDCl₃): δ 158.7, 148.2, 139.3, 137.6, 128.8, 127.5, 127.4, 113.2, 106.9, 46.4.

The spectroscopic data correspond to those reported in literature.¹³

***N*-(4-fluorobenzyl)aniline (2r)**

According to the general procedure with *N*-(4-fluorobenzylidene)aniline (**1r**) (199 mg, 1.00 mmol, 1.00 eq.) and 0.6 mol% [Mn-Br]H₂. Purification by column chromatography (silica gel, pentane/diethylether, 8:2).

Yield: 93 % (934 μ mol, 188 mg) yellowish oil.



¹H NMR (500 MHz, CDCl₃): δ 7.34 (dd, J = 7.8, 5.7 Hz, 2H), 7.22 – 7.16 (m, 2H), 7.07 – 7.00 (m, 2H), 6.75 (td, J = 7.3, 0.8 Hz, 1H), 6.67 – 6.61 (m, 2H), 4.31 (s, 2H), 4.16 (bs, 1H).

¹³C NMR (126 MHz, CDCl₃): δ 163.2, 161.2, 147.9, 135.1, 129.4, 129.2, 129.1, 118.0, 115.7, 115.5, 113.1, 47.8.

The spectroscopic data correspond to those reported in literature.²⁰

***N*-(4-chlorobenzyl)aniline (2s)**

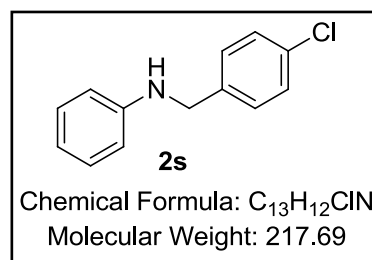
According to the general procedure with *N*-(4-chlorobenzylidene)aniline (**1s**) (215 mg, 1.00 mmol, 1.00 eq.). Purification by column chromatography (silica gel, pentane/diethylether, 9:1).

Yield: 95 % (946 μ mol, 206 mg) yellowish oil.

^1H NMR (300 MHz, CDCl_3): δ 7.32 (d, J = 2.4 Hz, 4H), 7.25 – 7.14 (m, 2H), 6.76 (t, J = 7.3 Hz, 1H), 6.63 (d, J = 6.8 Hz, 2H), 4.32 (s, 2H), 4.10 (bs, 1H).

^{13}C NMR (75 MHz, CDCl_3): δ 147.9, 138.1, 132.9, 129.4, 128.8, 128.8, 117.9, 113.0, 47.7.

The spectroscopic data correspond to those reported in literature.¹⁹



***N*-(4-bromobenzyl)aniline (2t)**

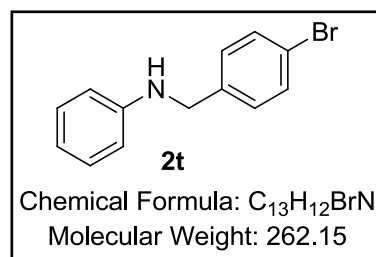
According to the general procedure with *N*-(4-bromobenzylidene)aniline (**1t**) (260 mg, 1.00 mmol, 1.00 eq.). Purification by column chromatography (silica gel, pentane/diethylether, 9:1).

Yield: 94 % (942 μ mol, 247 mg) yellow oil.

^1H NMR (500 MHz, CDCl_3): δ 7.53 (d, J = 8.3 Hz, 2H), 7.31 (d, J = 8.3 Hz, 1H), 7.27 (t, J = 7.7 Hz, 2H), 6.83 (t, J = 7.3 Hz, 1H), 6.68 (d, J = 8.3 Hz, 2H), 4.34 (s, 2H), 4.12 (s, 1H).

^{13}C NMR (126 MHz, CDCl_3): δ 147.8, 138.6, 131.7, 129.4, 129.1, 120.9, 117.8, 112.9, 47.6.

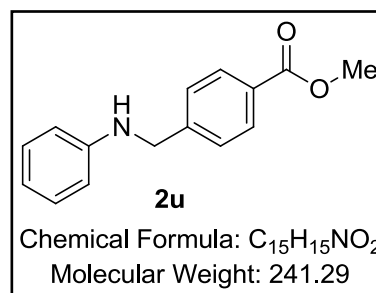
The spectroscopic data correspond to those reported in literature.¹⁹



methyl-4-((phenylamino)methyl)benzoate (2u)

According to the general procedure with methyl-4-((phenylimino)methyl)benzoate (**1u**) (239 mg, 1.00 mmol, 1.00 eq.). Purification by column chromatography (silica gel, pentane/diethylether, 9:1).

Yield: 74 % (738 μ mol, 178 mg) yellow oil.



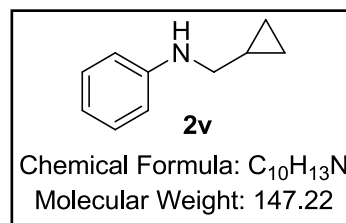
^1H NMR (500 MHz, CDCl_3): δ 8.04 – 7.99 (m, 2H), 7.45 (d, J = 8.1 Hz, 2H), 7.21 – 7.14 (m, 2H), 6.77 – 6.71 (m, 1H), 6.65 – 6.59 (m, 2H), 4.41 (s, 2H), 4.24 (bs, 1H), 3.92 (s, 3H).

^{13}C NMR (126 MHz, CDCl_3): δ 167.1, 147.8, 145.1, 130.1, 129.4, 129.2, 127.3, 118.0, 113.0, 52.2, 48.1.

The spectroscopic data correspond to those reported in literature.¹⁴

***N*-(cyclopropylmethyl)aniline (2v)**

According to the general procedure with *N*-(cyclopropylmethylene)aniline (**1v**) (145 mg, 1.00 mmol, 1.00 eq.). Purification by column chromatography (silica gel, pentane/diethylether, 98:2).



Yield: 81 % (808 μmol , 119 mg) yellow-orange oil.

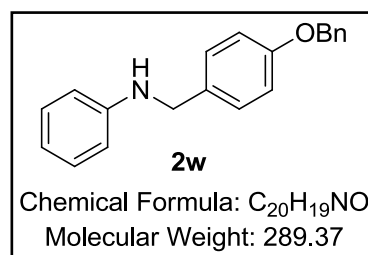
^1H NMR (500 MHz, CDCl_3): δ 7.22 – 7.15 (m, 2H), 6.71 (t, J = 7.3 Hz, 1H), 6.67 – 6.60 (m, 2H), 4.03 (bs, 1H), 2.96 (d, J = 6.9 Hz, 2H), 1.16 – 1.06 (m, 1H), 0.58 – 0.53 (m, 2H), 0.27 – 0.22 (m, 2H).

^{13}C NMR (126 MHz, CDCl_3): δ 148.6, 129.4, 117.4, 112.9, 49.2, 11.0, 3.58.

The spectroscopic data correspond to those reported in literature.²¹

***N*-(4-(benzyloxy)benzyl)aniline (2w)**

According to the general procedure with *N*-(4-(benzyloxy)benzylidene)aniline (**1w**) (287 mg, 1.00 mmol, 1.00 eq.). Purification by column chromatography (silica gel, pentane/diethylether, 9:1).



Yield: 97 % (968 μmol , 280 mg) white solid.

^1H NMR (500 MHz, CDCl_3): δ 7.50 – 7.45 (m, 2H), 7.45 – 7.39 (m, 2H), 7.39 – 7.30 (m, 3H), 7.25 – 7.18 (m, 2H), 7.02 – 6.96 (m, 2H), 6.76 (t, J = 7.3 Hz, 1H), 6.70-6.65 (m, 2H), 5.09 (s, 2H), 4.28 (s, 2H), 4.04 (bs, 1H).

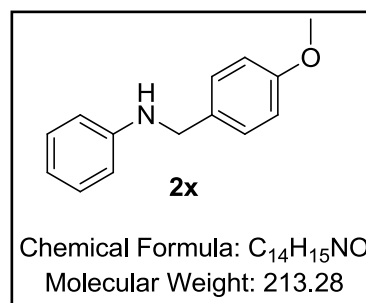
^{13}C NMR (126 MHz, CDCl_3): δ 158.2, 148.2, 137.1, 131.8, 129.4, 129.0, 128.7, 128.1, 127.6, 117.7, 115.1, 113.0, 70.1, 47.9.

The spectroscopic data correspond to those reported in literature.²²

***N*-(4-(methoxybenzyl)aniline (2x)**

According to the general procedure with *N*-(4-(methoxybenzylidene)aniline (**1x**) (211 mg, 1.00 mmol, 1.00 eq.) and 0.6 mol% [**Mn-Br**]**H**₂. Purification by column chromatography (silica gel, pentane/diethylether, 9:1).

Yield: 91 % (910 μmol , 194 mg) yellowish solid.



^1H NMR (500 MHz, CDCl_3): δ 7.30 (d, J = 8.6 Hz, 2H), 7.19 (t, J = 7.8 Hz, 2H), 6.89 (d, J = 8.5 Hz, 2H), 6.73 (t, J = 7.3 Hz, 1H), 6.66 (d, J = 7.7 Hz, 2H), 4.26 (s, 2H), 4.10 (bs, 1H), 3.81 (s, 3H).

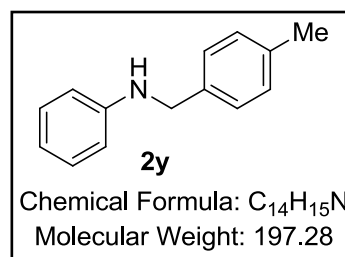
^{13}C NMR (126 MHz, CDCl_3): δ 159.0, 148.2, 131.4, 129.4, 129.0, 117.7, 114.1, 113.1, 55.4, 48.0.

The spectroscopic data correspond to those reported in literature.²⁰

***N*-(4-methylbenzyl)aniline (2y)**

According to the general procedure with *N*-(4-methylbenzylidene)aniline (**1y**) (195 mg, 1.00 mmol, 1.00 eq.). Purification by column chromatography (silica gel, pentane/diethylether, 9:1).

Yield: 86 % (862 μmol , 170 mg) white solid.



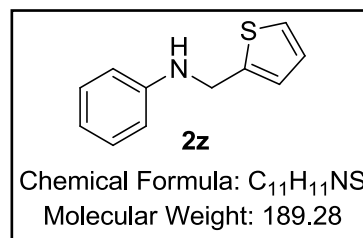
^1H NMR (300 MHz, CDCl_3): δ 7.33 – 7.26 (m, 2H), 7.26 – 7.14 (m, 4H), 6.81 – 6.71 (m, 1H), 6.71 – 6.62 (m, 2H), 4.29 (s, 2H), 3.98 (bs, 1H), 2.39 (s, 3H).

^{13}C NMR (75 MHz, CDCl_3): δ 148.3, 136.9, 136.4, 129.4, 129.3, 127.6, 117.5, 112.9, 48.1, 21.2.

The spectroscopic data correspond to those reported in literature.²⁰

***N*-(thiophen-2-ylmethyl)aniline (**2z**)**

According to the general procedure with *N*-(thiophen-2-ylmethylene)aniline (**1z**) (187 mg, 1.00 mmol, 1.00 eq.) and 0.6 mol% **[Mn-Br]H₂**. Purification by column chromatography (silica gel, pentane/diethylether, 9:1).



Yield: 93 % (925 μmol, 175 mg) orange oil.

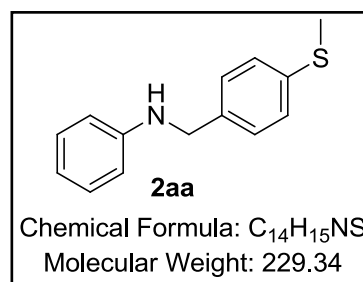
¹H NMR (500 MHz, CDCl₃): δ 7.26 – 7.19 (m, 3H), 7.07 – 7.02 (m, 1H), 7.02 – 6.98 (m, 1H), 6.82 – 6.75 (m, 1H), 6.71 (d, *J* = 7.8 Hz, 2H), 4.54 (s, 2H), 4.13 (s, 1H).

¹³C NMR (126 MHz, CDCl₃) δ 147.7, 143.0, 129.4, 127.0, 125.2, 124.7, 118.2, 113.3, 43.6.

The spectroscopic data correspond to those reported in literature.¹⁹

***N*-(4-(methylthio)benzyl)aniline (**2aa**)**

According to the general procedure with *N*-(4-(methylthio)benzylidene)aniline (**1aa**) (227 mg, 1.00 mmol, 1.00 eq.). Purification by column chromatography (silica gel, pentane/diethylether, 95:5).



Yield: 97 % (972 μmol, 223 mg) yellow solid.

¹H NMR (500 MHz, CDCl₃): δ 7.30 (d, *J* = 8.2 Hz, 2H), 7.24 (d, *J* = 8.2 Hz, 2H), 7.18 (t, *J* = 7.9 Hz, 2H), 6.73 (t, *J* = 7.3 Hz, 1H), 6.64 (d, *J* = 8.0 Hz, 2H), 4.49 – 4.03 (m, 3H), 2.48 (s, 3H).

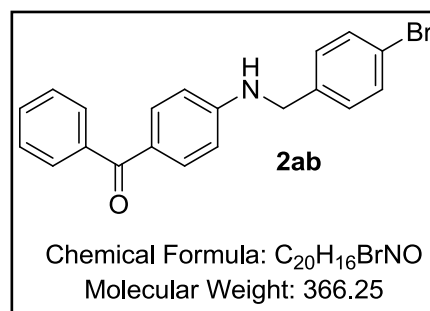
¹³C NMR (126 MHz, CDCl₃): δ 148.0, 137.3, 136.4, 129.4, 128.2, 127.1, 117.9, 113.2, 48.1, 16.1.

The spectroscopic data correspond to those reported in literature.²⁰

(4-((4-bromobenzyl)amino)phenyl)(phenyl)methanone (**2ab**)

According to the general procedure with (4-((4-bromobenzylidene)amino)phenyl)(phenyl)methanone (**1ab**) (364 mg, 1.00 mmol, 1.00 eq.). Purification by column chromatography (silica gel, pentane/diethylether, 6:4).

Yield: 93 % (926 μ mol, 339 mg) white solid.



¹H NMR (500 MHz, CD₂Cl₂): δ 7.72 – 7.66 (m, 4H), 7.56 – 7.51 (m, 1H), 7.51 – 7.43 (m, 4H), 7.28 – 7.23 (m, 2H), 6.66 – 6.58 (m, 2H), 4.89 (t, *J* = 5.4 Hz, 1H), 4.39 (d, *J* = 5.8 Hz, 2H).

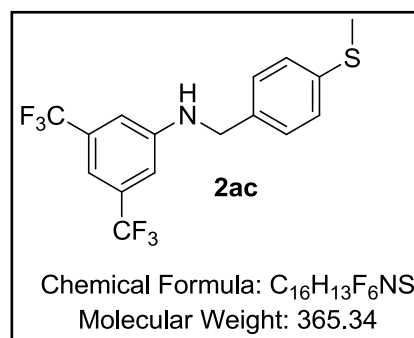
¹³C NMR (126 MHz, CD₂Cl₂): δ 195.2, 152.2, 139.6, 138.3, 133.2, 132.3, 131.8, 129.9, 129.5, 128.6, 127.0, 121.5, 112.1, 47.3.

Elemental analysis – Anal. Calcd for C₂₀H₁₆BrNO: C, 65.59; H, 4.40; N, 3.82. Found: C, 65.54; H, 4.32; N, 3.71.

N-(4-(methylthio)benzyl)-3,5-bis(trifluoromethyl)aniline (**2ac**)

According to the general procedure with *N*-(4-(methylthio)benzylidene)-3,5-bis(trifluoromethyl)aniline (**1ac**) (363 mg, 1.00 mmol, 1.00 eq.). Purification by column chromatography (silica gel, pentane/diethylether, 9:1).

Yield: 97 % (969 μ mol, 354 mg) yellow solid.



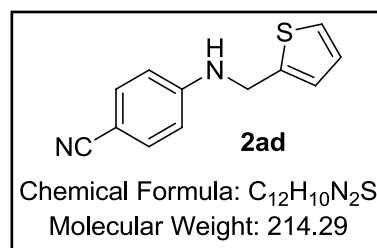
¹H NMR (500 MHz, CD₂Cl₂): δ 7.29 (d, *J* = 8.5 Hz, 2H), 7.27 – 7.23 (m, 2H), 7.17 (s, 1H), 7.00 (s, 2H), 4.64 (s, 1H), 4.35 (d, *J* = 5.6 Hz, 2H), 2.48 (s, 3H).

¹³C NMR (126 MHz, CD₂Cl₂): δ 149.3, 138.7, 135.1, 132.7 (q, *J* = 32.6 Hz), 128.5, 127.2, 124.2 (q, *J* = 272.5 Hz), 112.66 – 112.42 (m), 110.8 – 110.5 (m), 47.9, 16.0.

Elemental analysis – Anal. Calcd for C₁₆H₁₃F₆NS: C, 52.60; H, 3.59; N, 3.83. Found: C, 52.95; H, 3.72; N, 3.81.

4-((thiophen-2-ylmethyl)amino)benzonitrile (**2ad**)

According to the general procedure with 4-((thiophen-2-ylmethylene)amino)benzonitrile (**1ad**) (212 mg, 1.00 mmol, 1.00 eq.). Purification by column chromatography (silica gel, pentane/diethylether, 8:2).



Yield: 96 % (961 μ mol, 206 mg) yellow solid.

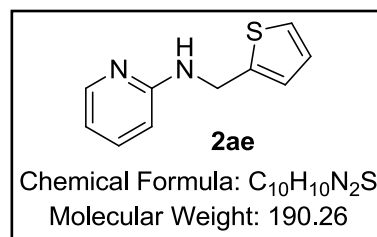
¹H NMR (500 MHz, CDCl₃): δ 7.44 – 7.39 (m, 2H), 7.24 (dd, J = 5.1, 1.1 Hz, 1H), 7.04 – 7.00 (m, 1H), 6.98 (dd, J = 5.0, 3.5 Hz, 1H), 6.66 – 6.60 (m, 2H), 4.84 (s, 1H), 4.55 (s, 2H).

¹³C NMR (126 MHz, CDCl₃): δ 150.6, 141.1, 133.7, 127.1, 125.6, 125.1, 120.4, 112.7, 99.5, 42.6.

The spectroscopic data correspond to those reported in literature.²³

N-(thiophen-2-ylmethyl)pyridin-2-amine (**2ae**)

According to the general procedure with N-(thiophen-2-ylmethylene)pyridin-2-amine (**1ae**) (188 mg, 1.00 mmol, 1.00 eq.). Purification by column chromatography (silica gel, pentane/diethylether, 7:3).



Yield: 73 % (731 μ mol, 139 mg) white-yellowish solid.

¹H NMR (500 MHz, CDCl₃): δ 8.12 (d, J = 4.8 Hz, 1H), 7.47 – 7.37 (m, 1H), 7.20 (dd, J = 5.1, 1.1 Hz, 1H), 7.03 – 6.99 (m, 1H), 6.96 (dd, J = 5.0, 3.5 Hz, 1H), 6.62 (dd, J = 6.7, 5.5 Hz, 1H), 6.43 (d, J = 8.4 Hz, 1H), 4.94 (bs, 1H), 4.70 (d, J = 5.8 Hz, 2H).

¹³C NMR (126 MHz, CDCl₃): δ 158.2, 148.2, 142.7, 137.6, 126.9, 125.3, 124.8, 113.6, 107.5, 41.4.

The spectroscopic data correspond to those reported in literature.¹⁰

2.2.2. Ketimine Reduction

General procedure for ketimine reduction: Under nitrogen atmosphere in a glove box screw-vials were charged with magnetic stir bars, KO^tBu (5 eq. with respect to [Mn-Br]H₂),

[Mn-Br]H₂, ketimine (**3**) (1.00 mmol, 1.00 eq.), and thf (2 mL). The vials were placed in an autoclave, which was sealed and purged three times with hydrogen, before adjusting the pressure to 20 bar. The reactions were heated to 50 °C and stirred for 18 h. After the reaction, the hydrogen was released, 1 mL H₂O and 7 mL Et₂O were added to each vial, and the mixtures were homogenized. Subsequently, the liquid phase was dried with Na₂SO₄, filtered, washed with Et₂O or CH₂Cl₂ and the solvent was removed under reduced pressure. The product was isolated by column chromatography.

4-(1-(phenylamino)ethyl)benzonitrile (**4a**)

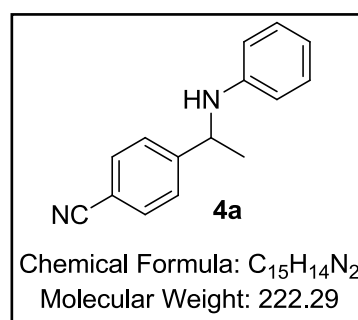
According to the general procedure with 4-(1-(phenylimino)ethyl)benzonitrile (**3a**) (220 mg, 1.00 mmol, 1.00 eq.) and 3 mol% **[Mn-Br]H₂**. Purification by column chromatography (silica gel, pentane/diethylether, 8:2).

Yield: 73 % (729 μmol, 162 mg) white solid.

¹H NMR (500 MHz, CDCl₃): δ 7.61 (d, *J* = 8.3 Hz, 2H), 7.50 (d, *J* = 8.2 Hz, 2H), 7.16 – 7.06 (m, 2H), 6.70 (t, *J* = 7.3 Hz, 1H), 6.46 (d, *J* = 7.8 Hz, 2H), 4.52 (q, *J* = 6.8 Hz, 1H), 4.24 (bs, 1H), 1.53 (d, *J* = 6.8 Hz, 3H).

¹³C NMR (126 MHz, CDCl₃): δ 151.1, 146.5, 132.7, 129.3, 126.8, 119.1, 118.1, 113.5, 110.8, 53.6, 25.0.

The spectroscopic data correspond to those reported in literature.²⁴

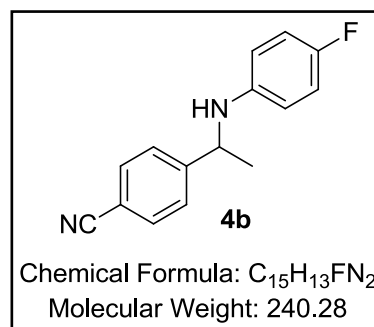


4-(1-((4-fluorophenyl)amino)ethyl)benzonitrile (**4b**)

According to the general procedure with 4-(1-((4-fluorophenyl)imino)ethyl)benzonitrile (**3b**) (238 mg, 1.00 mmol, 1.00 eq.) and 3 mol% **[Mn-Br]H₂**. Purification by column chromatography (silica gel, pentane/diethylether, 8:2).

Yield: 71 % (712 μmol, 171 mg) white solid.

¹H NMR (500 MHz, CDCl₃): δ 7.61 (d, *J* = 8.3 Hz, 2H), 7.47 (d, *J* = 8.2 Hz, 2H), 6.84 – 6.75 (m, 2H), 6.42 – 6.32 (m, 2H), 4.45 (q, *J* = 6.8 Hz, 1H), 4.07 (bs, 1H), 1.51 (d, *J* = 6.8 Hz, 3H).



^{13}C NMR (126 MHz, CDCl_3): δ 157.0, 155.1, 150.9, 142.9, 132.8, 126.8, 119.0, 115.9, 115.7, 114.3, 114.2, 111.0, 54.2, 25.0.

The spectroscopic data correspond to those reported in literature.²⁵

***N*-(1-(pyridin-4-yl)ethyl)aniline (4c)**

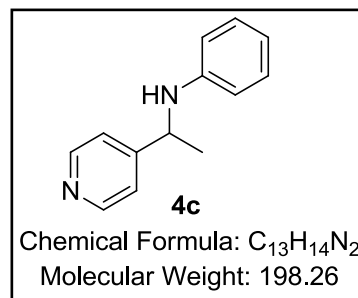
According to the general procedure with *N*-(1-(pyridin-4-yl)ethylidene)aniline (**3c**) (196 mg, 1.00 mmol, 1.00 eq.) and 3 mol% **[Mn-Br] H_2** . Purification by column chromatography (silica gel, diethylether).

Yield: 79 % (787 μmol , 156 mg) white solid.

^1H NMR (500 MHz, CDCl_3): δ 8.55 (s, 2H), 7.31 (s, 2H), 7.10 (t, J = 7.9 Hz, 2H), 6.68 (t, J = 7.3 Hz, 1H), 6.46 (d, J = 7.9 Hz, 2H), 4.46 (q, J = 6.5 Hz, 1H), 4.08 (s, 1H), 1.52 (d, J = 6.8 Hz, 3H).

^{13}C NMR (126 MHz, CDCl_3): δ 154.6, 150.2, 146.7, 129.3, 121.3, 117.9, 113.3, 52.8, 24.6.

Elemental analysis – Anal. Calcd for $\text{C}_{13}\text{H}_{14}\text{N}_2$: C, 78.75; H, 7.12; N, 14.13. Found: C, 78.88; H, 6.83; N, 14.03.



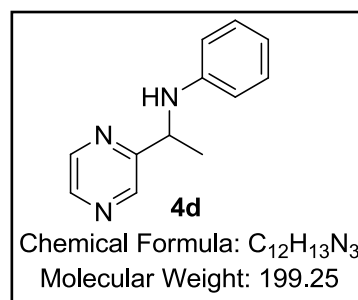
***N*-(1-(pyrazin-2-yl)ethyl)aniline (4d)**

According to the general procedure with *N*-(1-(pyrazin-2-yl)ethylidene)aniline (**3d**) (197 mg, 1.00 mmol, 1.00 eq.) and 1 mol% **[Mn-Br] H_2** . Purification by column chromatography (silica gel, pentane/diethylether, 4:6).

Yield: 85 % (853 μmol , 170 mg) brownish solid.

^1H NMR (500 MHz, CDCl_3): δ 8.66 (s, 1H), 8.53 (s, 1H), 8.48 – 8.43 (m, 1H), 7.13 (t, J = 7.8 Hz, 2H), 6.70 (t, J = 7.3 Hz, 1H), 6.58 (d, J = 8.0 Hz, 2H), 5.00 – 4.01 (bs, 1H), 4.70 (q, J = 6.8 Hz, 1H), 1.59 (d, J = 6.8 Hz, 3H).

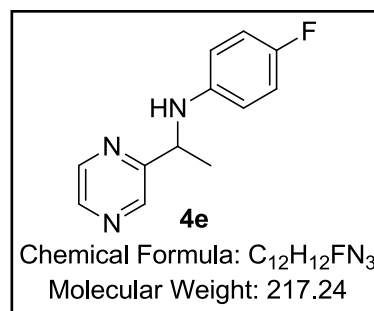
^{13}C NMR (126 MHz, CDCl_3): δ 159.1, 146.5, 144.2, 143.4, 143.2, 129.4, 118.3, 113.8, 53.1, 22.9.



Elemental analysis – Anal. Calcd for C₁₂H₁₃N₃: C, 72.33; H, 6.58; N, 21.09. Found: C, 72.35; H, 6.44; N, 20.96.

4-fluoro-*N*-(1-(pyrazin-2-yl)ethyl)aniline (**4e**)

According to the general procedure with 4-fluoro-*N*-(1-(pyrazin-2-yl)ethylidene)aniline (**3e**) (215 mg, 1.00 mmol, 1.00 eq.) and 2 mol% [Mn-Br]H₂. Purification by column chromatography (silica gel, pentane/diethylether, 1:2).



Yield: 81 % (806 μmol, 175 mg) orange oil.

¹H NMR (500 MHz, CDCl₃): δ 8.62 (s, 1H), 8.52 (s, 1H), 8.48 – 8.42 (m, 1H), 6.86 – 6.79 (m, 2H), 6.53 – 6.46 (m, 2H), 4.67 – 4.56 (m, 1H), 4.29 (s, 1H), 1.56 (d, *J* = 6.8 Hz, 3H).

¹³C NMR (126 MHz, CDCl₃): δ 159.1, 157.1, 155.2, 144.2, 143.5, 143.1, 143.1, 143.1, 116.0, 115.8, 114.6, 114.5, 53.6, 23.0.

Elemental analysis – Anal. Calcd for C₁₂H₁₂FN₃: C, 66.34; H, 5.57; N, 19.34. Found: C, 65.96; H, 5.43; N, 19.49.

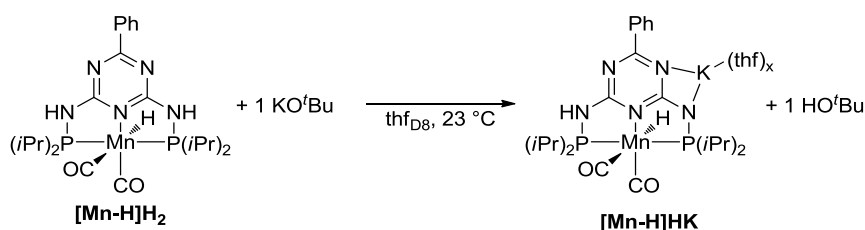
3 Mechanistic Investigations

3.1 Reaction Intermediates

3.1.1. Activation of the Manganese Complexes

[Mn-H]H₂ with 1 eq. KO^tBu

[Mn-H]H₂ (20 μmol, 1.0 eq.) and KO^tBu (20 μmol, 1.0 eq.) were stirred in thf_{D8} (500 μL) for 1 minute. The red mixture immediately turned dark red and was transferred to an NMR tube.



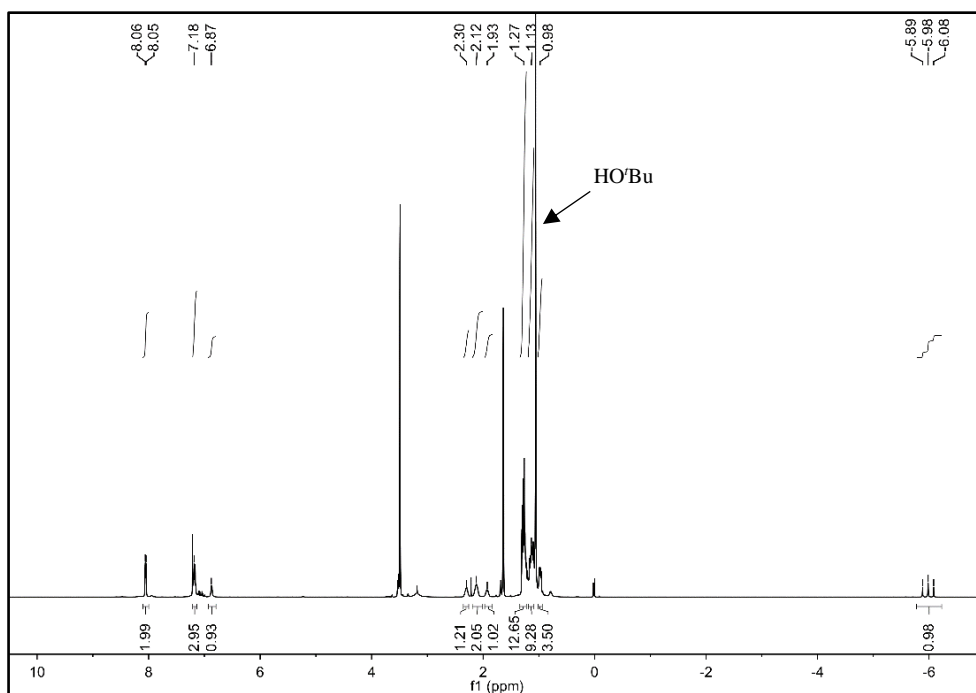


Figure S 1. ^1H NMR spectrum of the reaction of complex $[\text{Mn-H}]\text{H}_2$ and 1 eq. KOtBu in thf-D_8 .

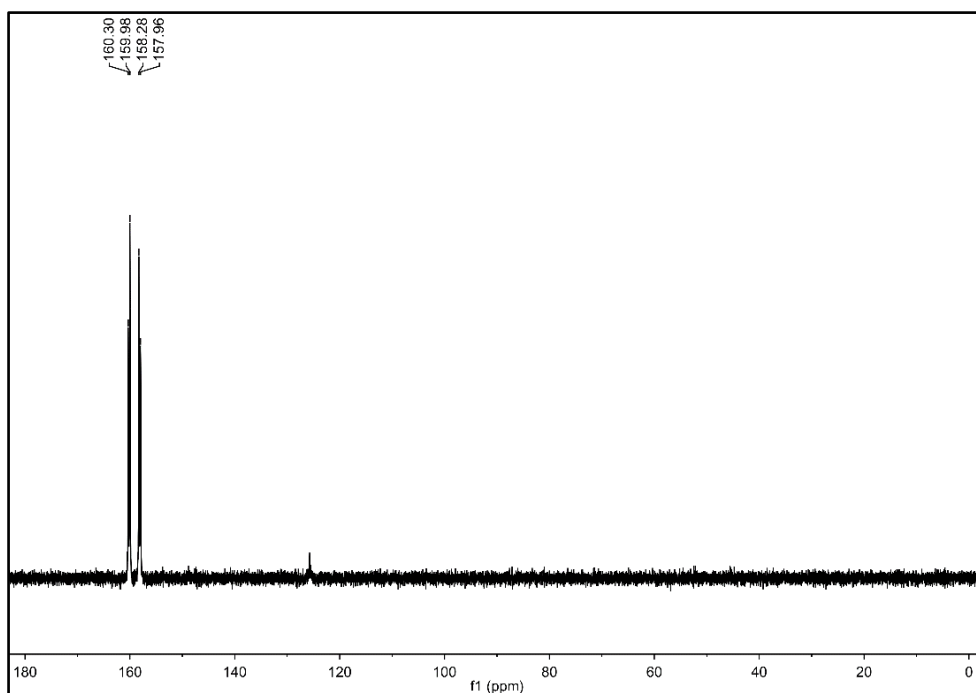


Figure S 2. ^{31}P NMR spectrum of the reaction of complex $[\text{Mn-H}]\text{H}_2$ and 1 eq. KOtBu in thf-D_8 .

^1H NMR (500 MHz, thf-D_8): δ 8.05 (d, $J = 7.1$ Hz, 2H), 7.18 (m, 3H), 6.87 (s, 1H), 2.30 (m, 1H), 2.12 (m, 2H), 1.93 (m, 1H), 1.27 (m, 12H), 1.13 (m, 9H), 0.98 (m, 3H), -5.98 (t, $J = 49.5$ Hz, 1H). ^{31}P NMR (202 MHz, thf-D_8): δ 160.14 (d, $J = 65.3$ Hz), 158.12 (d, $J = 64.6$ Hz).

Only one NH (^1H NMR: 6.87 ppm) proton is left and both phosphorus atoms (^{31}P NMR: 160.3–158.0 ppm) and the adjacent isopropyl groups (^1H NMR: three signals of CH : 2.30–1.93 ppm) are magnetically not equivalent, consistent with the proposed structure for $[\text{Mn-H}]\text{HK}$ (^1H , ^{31}P NMR: Figure S 1 and Figure S 2). Furthermore, it can be concluded that the reaction of $[\text{Mn-H}]\text{H}_2$ with KO^tBu is a quantitative and fast reaction.

$[\text{Mn-H}]\text{H}_2$ with 2 eq. KO^tBu

$[\text{Mn-H}]\text{H}_2$ (20 μmol , 1.0 eq.) and KO^tBu (40 μmol , 2.0 eq.) were stirred in $\text{thf}_{\text{D}8}$ (500 μL) for 1 minute. The red mixture immediately turned dark red and was transferred to an NMR tube.

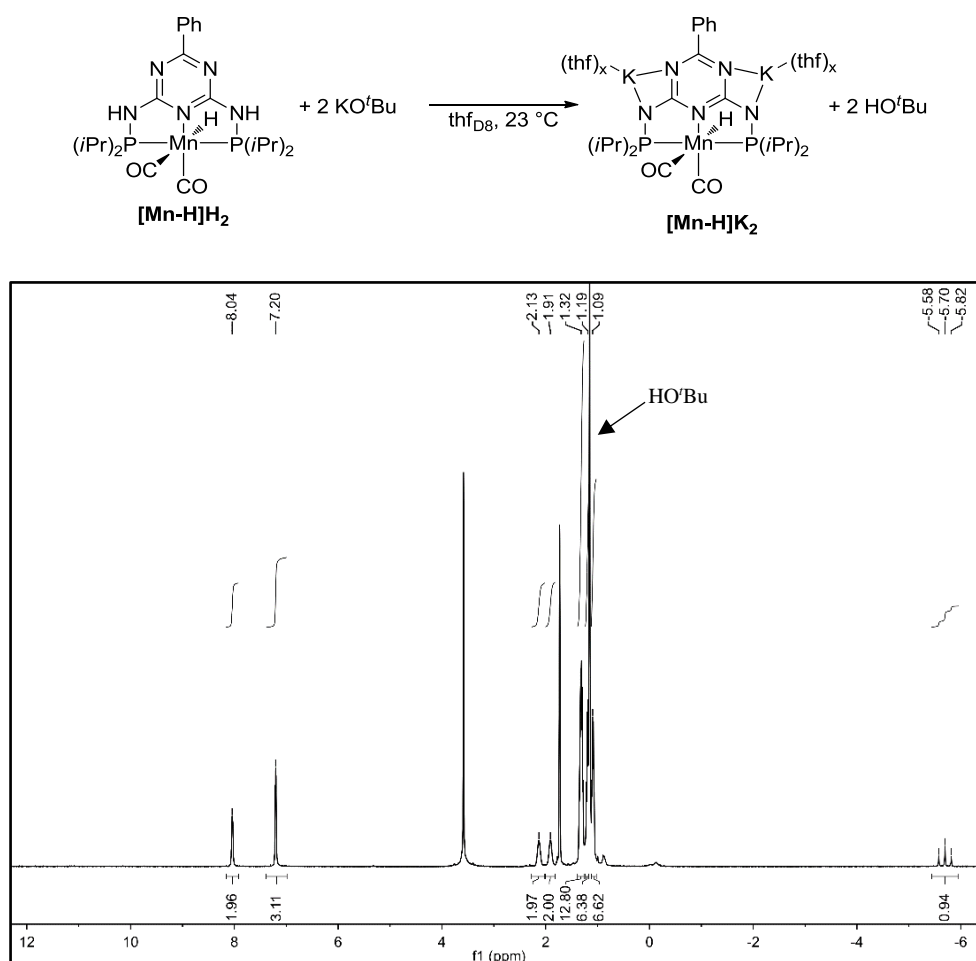


Figure S 3. ^1H NMR spectrum of the reaction of $[\text{Mn-H}]\text{H}_2$ and 2 eq. KO^tBu in $\text{thf}_{\text{D}8}$.

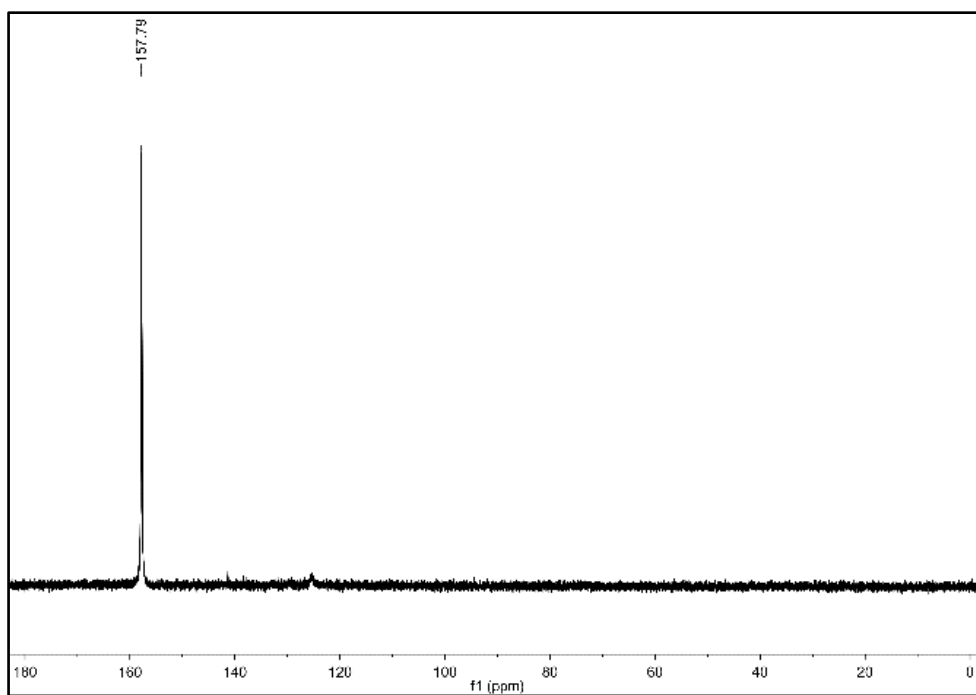


Figure S 4. ^{31}P NMR spectrum of the reaction of $[\text{Mn-H}]\text{H}_2$ and 2 eq. KO'Bu in $\text{thf}_{\text{D}8}$.

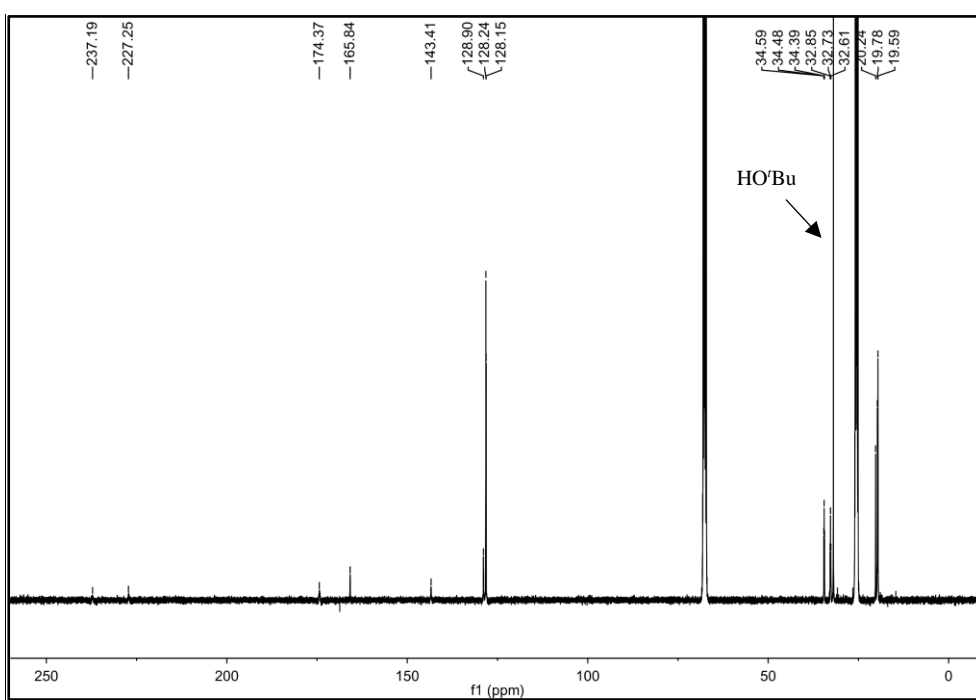


Figure S 5. ^{13}C NMR spectrum of the reaction of $[\text{Mn-H}]\text{H}_2$ and 2 eq. KO'Bu in $\text{thf}_{\text{D}8}$.

^1H NMR (400 MHz, $\text{thf}_{\text{D}8}$): δ 8.04 (m, 2H), 7.20 (m, 3H), 2.13 (m, 2H), 1.91 (m, 2H), 1.32 (m, 12H), 1.19 (m, 6H), 1.09 (m, 6H), -5.70 (t, $J = 48.0$ Hz, 1H). ^{13}C NMR (101 MHz, $\text{thf}_{\text{D}8}$): δ 237.2 (m), 227.3(m), 174.4, 165.9, 143.4, 128.9, 128.2, 128.2, 34.5 (t, $J = 10.1$), 32.7 (t, $J = 12.4$ Hz), 20.2, 19.8, 19.6 (m). ^{31}P NMR (202 MHz, $\text{thf}_{\text{D}8}$): δ 157.8 (s).

It can be stated from the ^1H and ^{31}P NMR spectra (Figure S 3 and Figure S 4), that no NH proton is left and that both phosphorus atoms (^{31}P NMR: 157.8 ppm) and the adjacent isopropyl groups (^1H NMR: two signals of CH: 2.13, 1.91 ppm) are magnetically equivalent, consistent with the proposed structure of $[\text{Mn-H}]\text{K}_2$. Furthermore, it can be concluded that the reaction of $[\text{Mn-H}]\text{H}_2$ with 2 eq. KO'Bu is also a quantitative and fast reaction.

$[\text{Mn-H}]\text{H}_2$ with 10 eq. KO'Bu

$[\text{Mn-H}]\text{H}_2$ (20 μmol , 1.0 eq.) and KO'Bu (200 μmol , 10.0 eq.) were stirred in $\text{thf}_{\text{D}8}$ (500 μL) for 1 minute. The red mixture immediately turned dark red and was transferred to an NMR tube.

No further deprotonation takes place (^1H : Figure S 6, ^{31}P : Figure S 7) in comparison to $[\text{Mn-H}]\text{K}_2$.

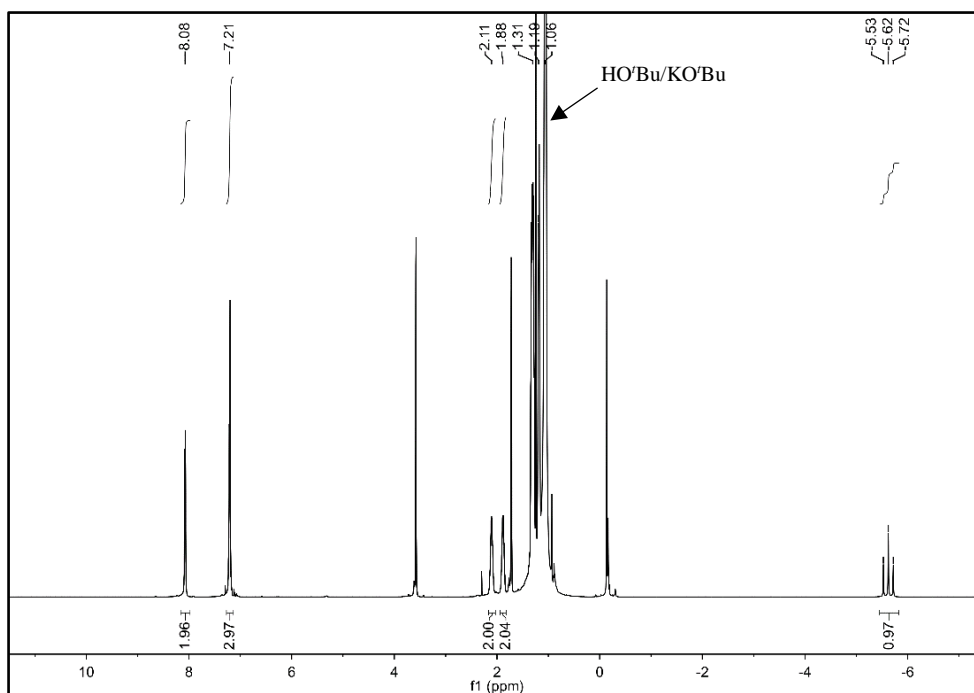


Figure S 6. ^1H NMR spectrum of the reaction of complex $[\text{Mn-H}]\text{H}_2$ and 10 eq. KO'Bu in $\text{thf}_{\text{D}8}$.

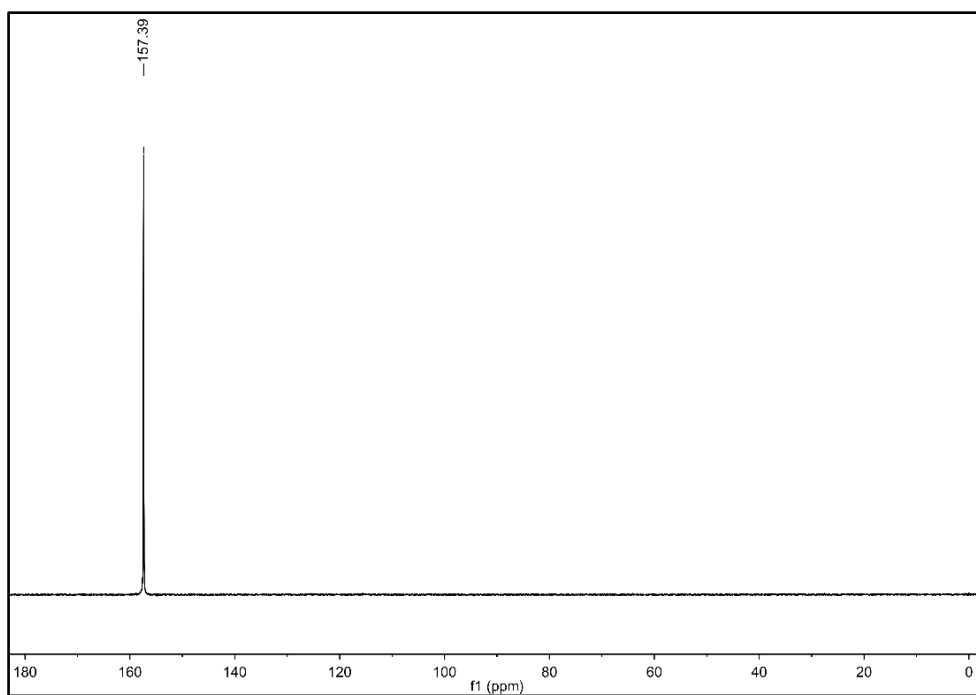


Figure S 7. ^{31}P NMR spectrum of the reaction of complex $[\text{Mn-H}]\text{H}_2$ and 10 eq. KOtBu in $\text{thf}_{\text{D}8}$.

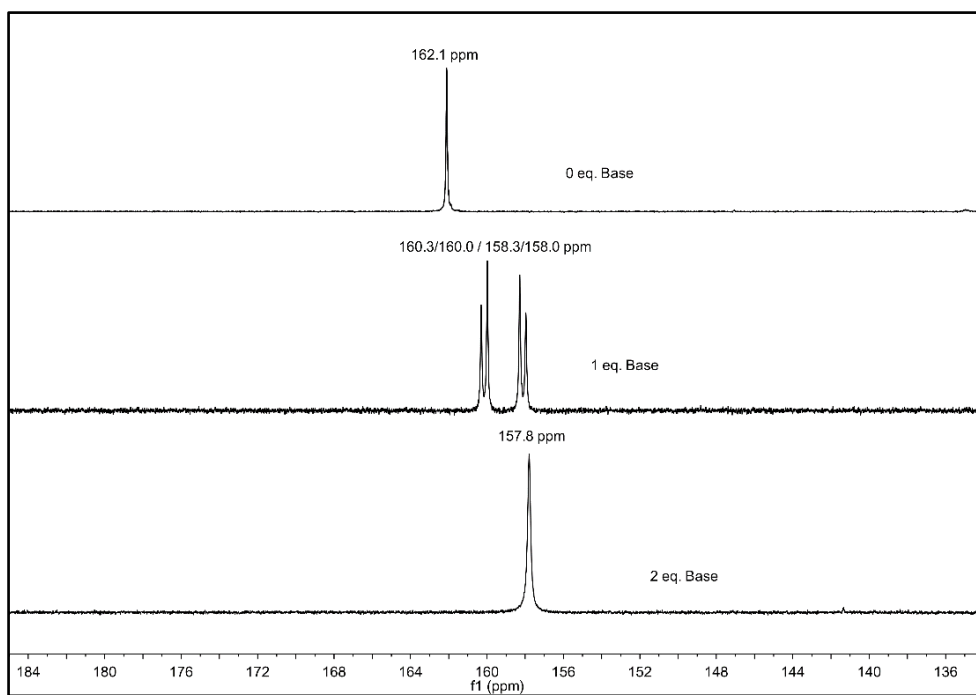


Figure S 8. Comparison of ^{31}P NMR spectra for the reactions of $[\text{Mn-H}]\text{H}_2$ with 0, 1 and 2 eq. of KOtBu.

[Mn-Br]H₂ with 2 eq. KO^tBu

[Mn-Br]H₂ (20 μmol, 1.0 eq.) and KO^tBu (40 μmol, 2.0 eq.) were stirred in thf_{D8} (500 μL) for 1 minute. The yellow mixture immediately turned dark green and was transferred to an NMR tube.

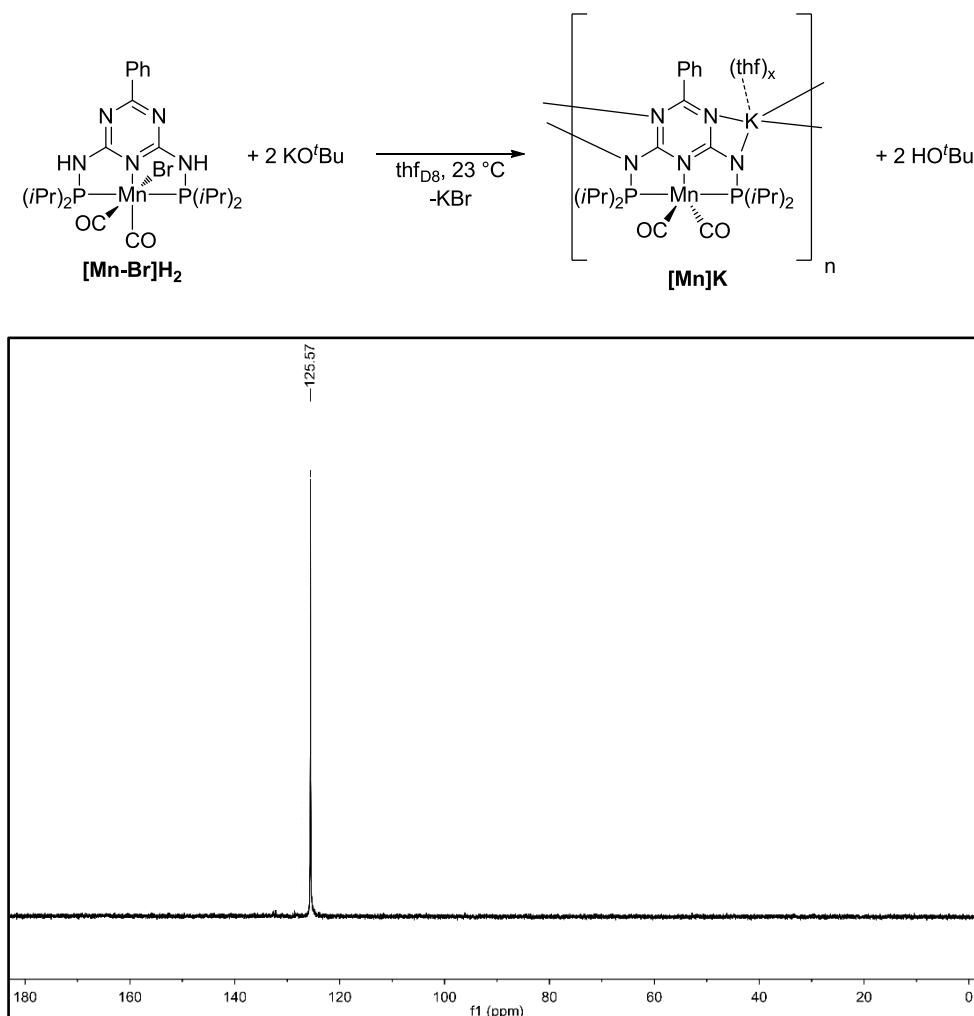


Figure S 9. ³¹P NMR spectrum of the reaction of complex [Mn-Br]H₂ with 2 eq. KO^tBu in thf_{D8}.

Considering that complex [Mn]K is a coordination polymer, it precipitates quickly. Obtaining an analyzable ¹H NMR spectrum is not easily possible in thf.

Therefore, complex [Mn]K was synthesized by mixing complex [Mn-Br]H₂ (305 mg, 500 μmol, 1.0 eq.) and KO^tBu (118 mg, 1.05 mmol, 2.1 eq.) in 2 mL thf, which was let to precipitate over night. The solvent was filtered off, the residue was washed with thf twice to remove remaining KO^tBu and HO^tBu and the remaining solvent was removed in vacuum to obtain a green powder. A few mg of the powder were dissolved in DMSO_{D6} to measure ¹H and ³¹P NMR.

In the ^1H NMR spectrum (Figure S 10) no NH proton signal is present and the CH-proton signals of the isopropyl groups are magnetically equivalent resulting in only one peak at 2.21 ppm. In the ^{31}P NMR spectrum (Figure S 11) there is also only one peak, consistent with the spectrum in thf_{D_8} (Figure S 9), indicating the magnetic equivalence of the two phosphorus atoms. The results support the postulated structure of $[\text{Mn}]\text{K}$.

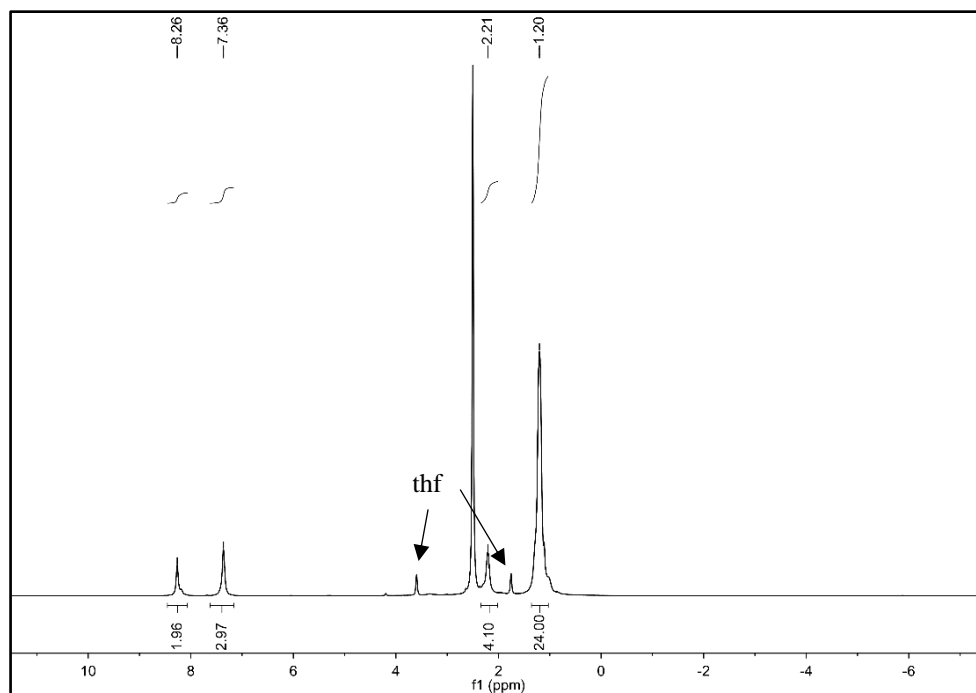


Figure S 10. ^1H NMR spectrum of $[\text{Mn}]\text{K}$ in $\text{DMSO}-d_6$.

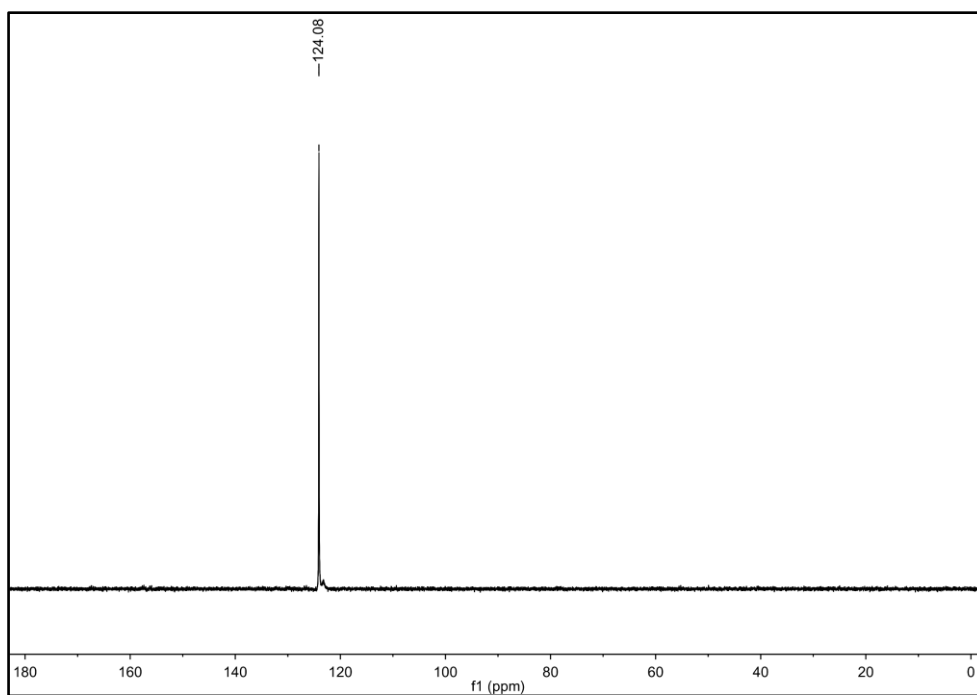


Figure S 11. ^{31}P NMR spectrum of **[Mn]K** in DMSO-D_6 .

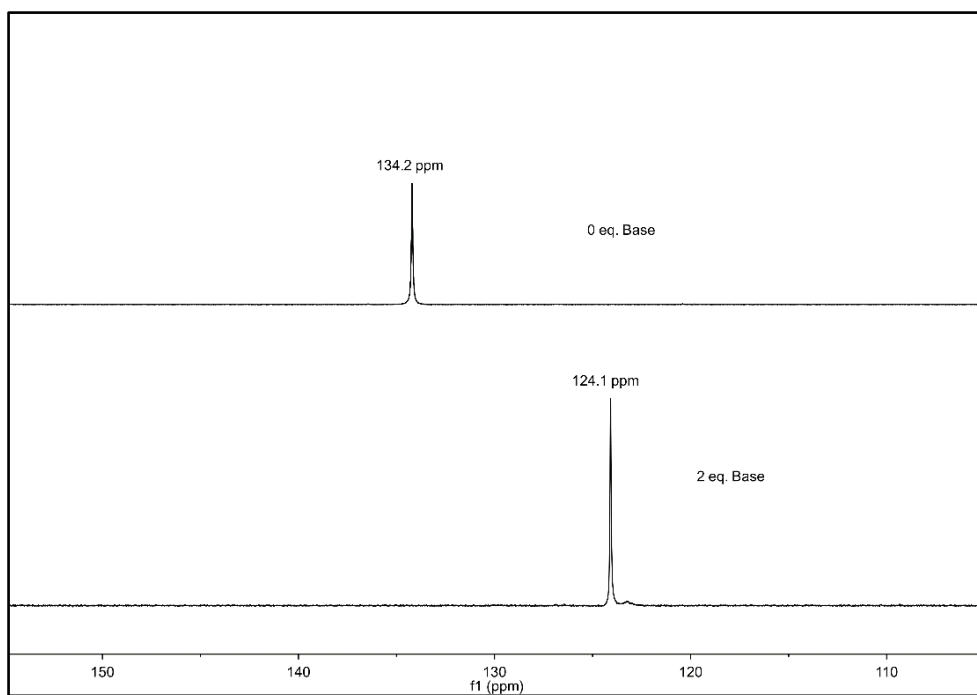


Figure S 12. Comparison of ^{31}P NMR spectra of complex **[Mn-Br]H₂** with and without KOtBu measured in DMSO-D_6 .

^1H NMR (500 MHz, DMSO-D_6): δ 8.45 – 8.07 (m, 2H), 7.36 (s, 3H), 2.21 (bs, 4H), 1.36 – 1.03 (m, 24H). ^{31}P NMR (202 MHz, DMSO-D_6): δ 124.1 (s).

3.1.2. Syntheses of [Mn]K, [Mn-H]HK and [Mn-H]K₂

3.1.2.1. [Mn]K

[Mn-H]H₂ (95.0 mg, 179 μ mol, 1.0 eq.) and imine **1a** (48.6 mg, 268 μ mol, 1.5 eq.) were dissolved in thf (210 μ L) and KO^tBu (0.2 M in thf; 1.79 mL, 358 μ mol, 2.0 eq.) was added dropwise while stirring. The dark red mixture was heated to 50 °C over night. After that, the flask was cooled down to -24 °C for 10 h, the solvent was subsequently filtered off and the solid was washed three times with 5 mL of thf. The powder was dried under vacuum and the product was obtained as a dark green powder.

Yield: 41 % (74.0 μ mol, 42.0 mg) dark green powder.

¹H NMR (400 MHz, DMSO): δ 8.27 (s, 2H), 7.37 (s, 3H), 2.20 (bs, 4H), 1.41 – 1.07 (m, 24H). ³¹P NMR (202 MHz, DMSO): δ 123.9. ¹³C NMR (101 MHz, DMSO): δ 235.2, 176.2, 168.7, 140.0, 129.4, 127.8, 127.3, 27.6 (t, *J* = 12.6 Hz), 18.6, 18.5, 17.9, 17.7. Melting point: 287 °C (Decomposition). Elemental analysis – Anal. Calcd for C₂₃H₃₃KMnN₅O₂P₂: C, 48.68; H, 5.86; N, 12.34. Found: C, 47.40; H, 6.00; N, 11.82.

3.1.2.2. [Mn-H]HK

[Mn-H]H₂ (53.1 mg, 100 μ mol, 1.0 eq.) was dissolved in 4 mL thf and KH (4.01 mg, 100 μ mol, 1.0 eq.) was added. The mixture was stirred for 10 minutes at room temperature and the solvent was subsequently removed under vacuum while keeping the temperature below 0 °C. The product was obtained as a glassy solid, which was scratched with a spatula to yield an orange powder and was further dried under vacuum.

Yield: 62 % (61.5 μ mol, 35 mg)

¹H NMR (400 MHz, thf-D₈): δ 8.14 (d, *J* = 6.9 Hz, 2H), 7.39 – 7.20 (m, 3H), 6.95 (s, 1H), 2.38 (s, 1H), 2.21 (s, 2H), 2.02 (s, 1H), 1.43 – 1.30 (m, 12H), 1.29 – 1.13 (m, 9H), 1.12 – 1.02 (m, 3H), -5.90 (t, *J* = 49.6 Hz, 1H). ³¹P NMR (202 MHz, thf-D₈): δ 160.2 (d, *J* = 65.0 Hz), 158.2 (d, *J* = 66.9 Hz). ¹³C NMR (126 MHz, thf-D₈): δ 234.6, 225.2, 174.1, 169.9, 167.2, 140.6, 130.5, 128.6, 128.5, 34.1 (m), 32.6 (m), 19.7 (m), 19.2. Melting Point: 95 °C (Decomposition). Elemental analysis – Anal. Calcd for C₂₃H₃₅KMnN₅O₂P₂: C, 48.50; H, 6.19; N, 12.30. Found: C, 48.36; H, 6.85; N, 11.86.

3.1.2.3. [Mn-H]K₂

[Mn-H]H₂ (53.1 mg, 100 μ mol, 1.0 eq.) was dissolved in 4 mL thf and KH (8.02 mg, 200 μ mol, 2.0 eq.) was added. The mixture was stirred for 30 minutes at room temperature and the solvent was subsequently removed under vacuum while keeping the temperature below 0 °C. The product was obtained as a glassy solid, which was scratched with a spatula to yield an orange powder and was further dried under vacuum.

Yield: 54 % (54.4 μ mol, 37 mg)

¹H NMR (500 MHz, thf_{D8}): δ 8.26 – 7.75 (m, 2H), 7.40 – 7.00 (m, 3H), 2.24 – 2.04 (m, 2H), 1.95 – 1.84 (m, 2H), 1.36 – 1.27 (m, 12H), 1.25 – 1.14 (m, 6H), 1.14 – 1.02 (m, 6H), -5.71 (t, J = 48.1 Hz, 1H). ³¹P NMR (202 MHz, thf_{D8}): δ 157.8 (s). ¹³C NMR (126 MHz, thf_{D8}): δ 237.3, 227.3, 174.5, 165.7, 143.6, 128.8, 128.2, 128.1, 34.5 (t, J = 10.1 Hz), 32.8 (t, J = 12.1 Hz), 20.2, 19.8, 19.6, 19.6 (m). Melting Point: 142 °C (Decomposition). Elemental analysis – Anal. Calcd for C₂₃H₃₄K₂MnN₅O₂P₂ (+thf): C, 47.71; H, 6.23; N, 10.30. Found: C, 46.37; H, 6.18; N, 10.43.

3.1.3. Crystals for X-Ray Crystal Analysis

[Mn-Br]H₂ (50 mg, 81.9 μ mol, 1.0 eq.) was dissolved in 4 mL thf and KO^tBu (164 mM; 1.00 mL, 164 μ mol, 2.0 eq.) was added dropwise while stirring. The solution immediately turned from yellow to dark green. The crystals were collected in a glove box after several days.

The same crystals were obtained by NMR experiments like shown in Table S 14.

Both crystal fractions showed the same structure obtained by X-ray crystallography.

3.1.4. Investigation of a Hypothetical Amide Complex

K•2a (produced with KH and 2a in thf over night with subsequent removal of the solvent under vacuum) (23.2 mg, 105 μ mol, 3.0 eq.) and [Mn-Br]H₂ (21.4 mg, 35 μ mol, 1.0 eq.) were dissolved in thf_{D8} while stirring. The solution turned dark red and was subsequently transferred to an NMR tube.

A CH signal of the imine (8.50 ppm) and the hydride signal (-5.61 ppm) appear in the ¹H NMR spectrum (Figure S 13). The ³¹P NMR spectrum (Figure S 14) shows that as a main product [Mn-H]K₂ was produced according to the shift of the signal at 157 ppm. There is no evidence of an amide complex in a reasonable amount.

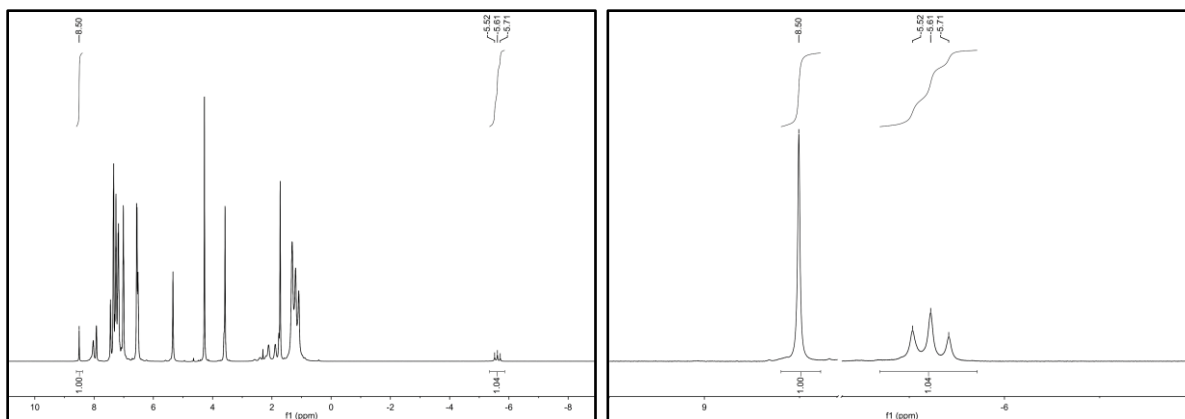


Figure S 13. ^1H NMR spectrum of the reaction of $\text{K}\cdot\mathbf{2a}$ with complex $[\text{Mn-Br}]\text{H}_2$.

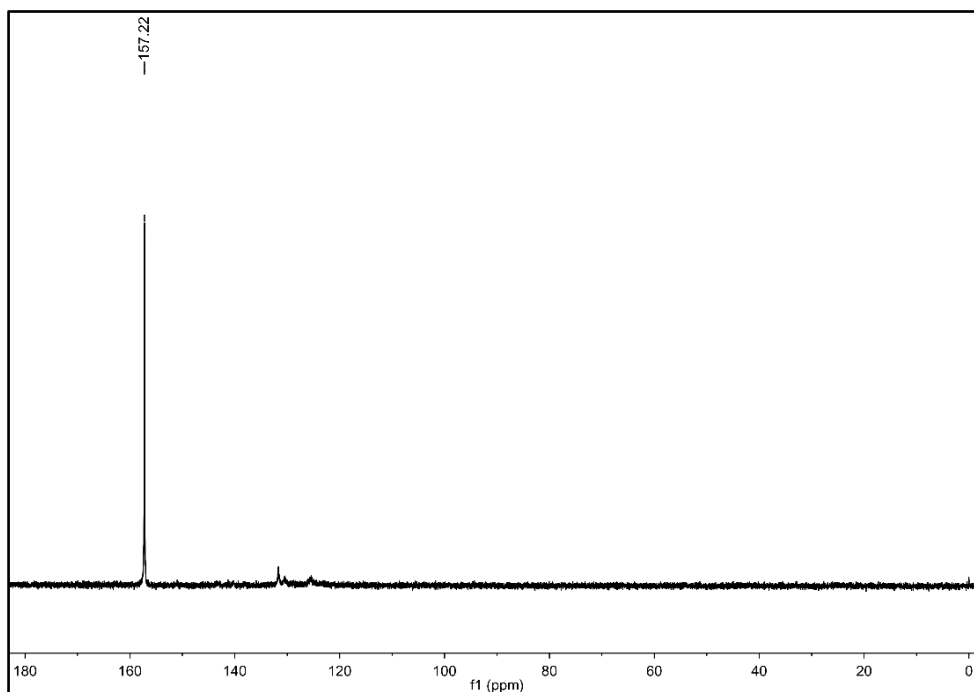


Figure S 14. ^{31}P NMR spectrum of the reaction of $\text{K}\cdot\mathbf{2a}$ with complex $[\text{Mn-Br}]\text{H}_2$.

In another experiment the activated complex $[\text{Mn}]\text{K}$ (preparation as shown in 3.1.1) (30 mg, $43.6\ \mu\text{mol}$, 1.0 eq.; calculated as 1:1 mixture with KBr) was mixed with $\text{K}\cdot\mathbf{2a}$ (46.4 mg, $219\ \mu\text{mol}$, 5.0 eq.) in $\text{thf}_{\text{D}8}$. The mixture turned dark red and was transferred to an NMR tube after 5 minutes of stirring. The observations (Figure S 15) are the same as for the experiment with the bromide complex $[\text{Mn-Br}]\text{H}_2$ above (Figure S 14).

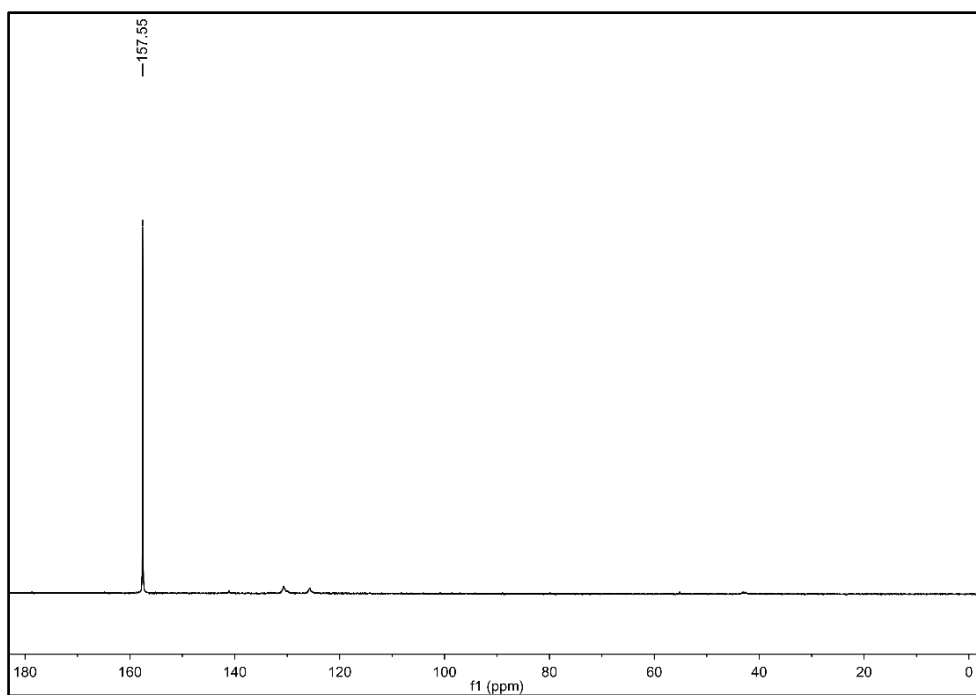


Figure S 15. ^{31}P NMR spectrum of the mixture of complex **[Mn]K** and **K•2a** in $\text{thf}_{\text{D}8}$.

3.1.5. Time-dependent Stability of **[Mn-H] H_2** and **[Mn-H] K_2**

Stability of **[Mn-H] H_2**

A stock solution of **[Mn-H] H_2** in $\text{thf}_{\text{D}8}$ (0.15 M) was stored at room temperature for 3 months and was measured subsequently via NMR (Figure S 16 and Figure S 17). No degradation of the complex is observable.

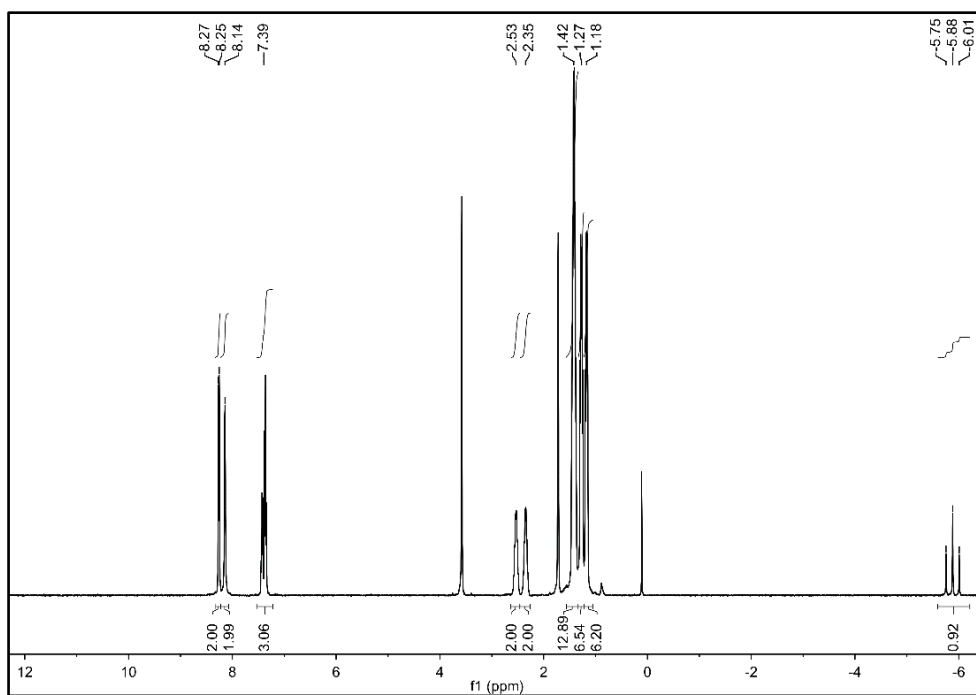


Figure S 16. ¹H NMR spectrum of a stock solution of [Mn-H]H₂ in thf-D₈ which was stored at room temperature for 3 months.

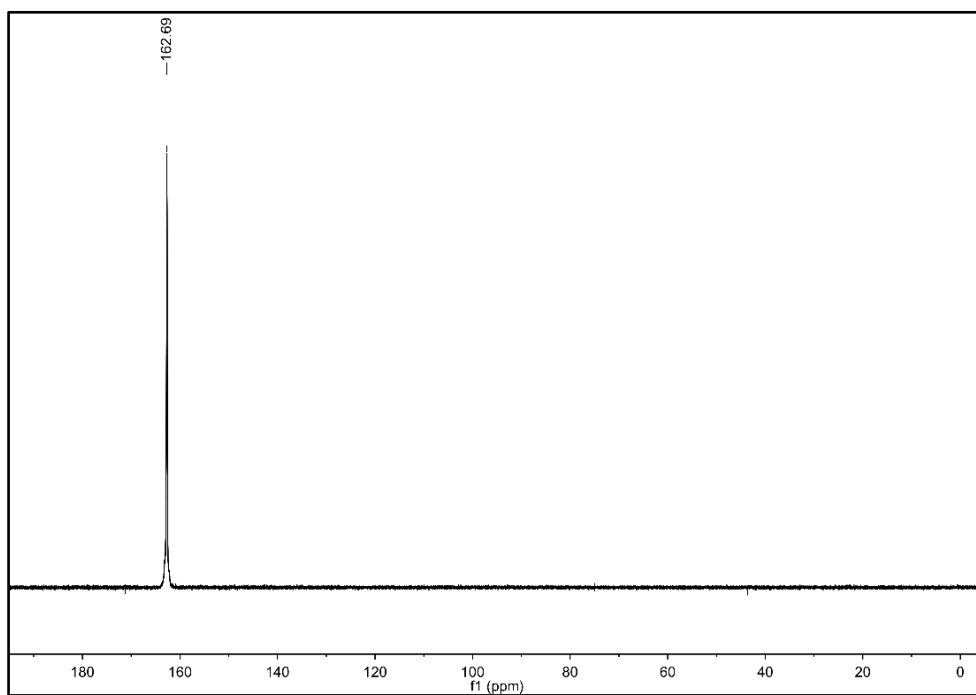


Figure S 17. ³¹P NMR spectrum of a stock solution of [Mn-H]H₂ in thf-D₈ which was stored at room temperature for 3 months.

Stability of [Mn-H]K₂

KO^tBu (30 μ mol, 2.0 eq.) was added to a solution of [Mn-H]H₂ (15 μ mol, 1.0 eq.) in thf_D₈ (500 μ L in total) at rt. The mixture immediately turned to a dark red color and was transferred to a Young NMR tube. A ¹H NMR spectrum was measured to make sure that double deprotonation took place. The solution was stored for 3 days at room temperature and an ¹H NMR spectrum was measured again (Figure S 18). The complex did not decompose over time.

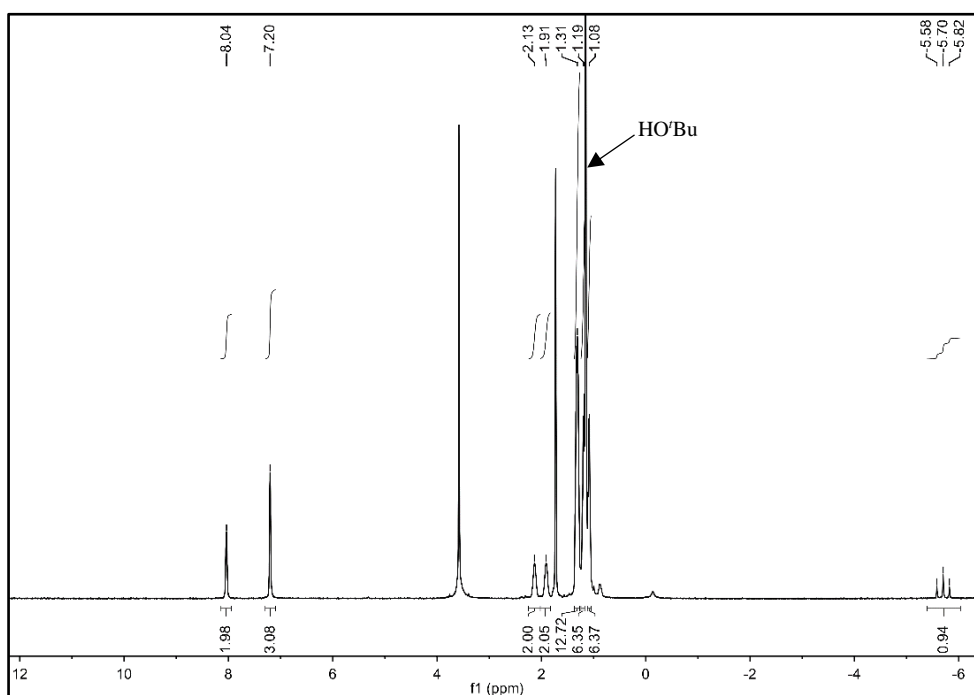


Figure S 18. ¹H NMR spectrum of [Mn-H]K₂ after 3 days at room temperature in thf_D₈.

3.2 Stoichiometric Hydride Transfer Reactions

3.2.1. General Procedure

A Young NMR tube was charged with thf_D₈ solutions of hydride complex [Mn-H]H₂ and imine and the NMR spectrometer was shimmed herewith for ¹H NMR spectra. The tube was subsequently cooled down with liquid nitrogen and KO^tBu (solution in thf_D₈) was added, resulting in a total volume of 700 μ L thf_D₈. Shortly after melting, the mixture was homogenized and cooled down with liquid nitrogen again. Directly before introducing the tube into the NMR it was brought to room temperature and the measurement was started at 23 °C.

3.2.2. Experimental Probing of the Catalytic Cycle

[**Mn-H**]**H**₂ (30 μmol, 1.0 eq.), **1a** (60 μmol, 2.0 eq.) and KO^tBu (60 μmol, 2.0 eq.) were dissolved in thf_D₈ (700 μL) in a Young NMR tube and inserted into an NMR spectrometer at 23 °C. The reaction was monitored via ¹H NMR for 5 h. After four days at 23 °C the reaction progress was checked with ¹H NMR, subsequently transferred into an autoclave and the tube was washed with 500 μL thf_D₈. The autoclave was purged three times with H₂, before the pressure was adjusted to 20 bar H₂. The reaction was stirred over night at 40 °C. Afterwards, the solution was transferred to an NMR tube.

It can be asserted from the ¹H NMR spectra in Figure S 19 that the hydride (e.g. Mn-*H* - 5.71 ppm) and partially **1a** (e.g. N=CH 8.51 ppm) is consumed under production of amine **2a** (e.g. CH₂ 4.28 ppm). The shift of the acidic hydrogen atoms (HO^tBu between about 3.5 and 7 ppm), produced at the beginning of the reaction by deprotonation of complex [**Mn-H**]**H**₂, can most likely be attributed to 1 eq. KO^tBu reproduced in the reaction. The sharp bend of the shift of the acidic protons is due to a change of the time intervals of the measurements.

After 4 days (Figure S 20) almost all the hydride was transferred (Mn-*H* -5.71 ppm). As expected, the result is a mixture of **1a** (e.g. N=CH 8.51 ppm) and **2a** (e.g. CH₂ 4.28 ppm).

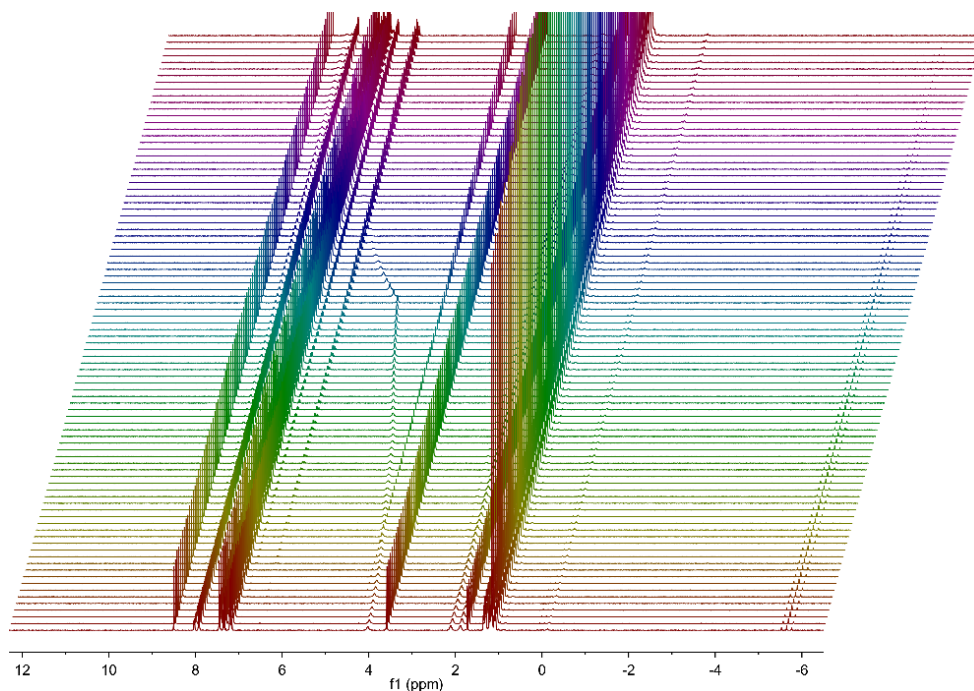


Figure S 19. ¹H NMR experiment with [**Mn-H**]**H**₂, **1a** and KO^tBu in thf_D₈.

After one night of stirring with 20 bar H₂ at 40 °C the double deprotonated complex **[Mn-H]K₂** is fully regenerated as can be concluded from ¹H NMR (8.03, 7.20, 2.12, 1.89, 1.31, 1.19, 1.08, -5.70 ppm) (Figure S 21) and ³¹P NMR (157.8 ppm) (Figure S 22). **1a** was completely transformed into amine **2a** (7.35, 7.26, 7.19, 7.01, 6.52, 5.33, 4.28 ppm). The stoichiometry of **[Mn-H]K₂** and **2a** is still 1:2. The acidic protons of HO'Bu were shifted upfield, most likely due to consumption of KO'Bu and re-formation of HO'Bu (3.5 ppm, Figure S 22). Herewith, the catalytic cycle is closed.

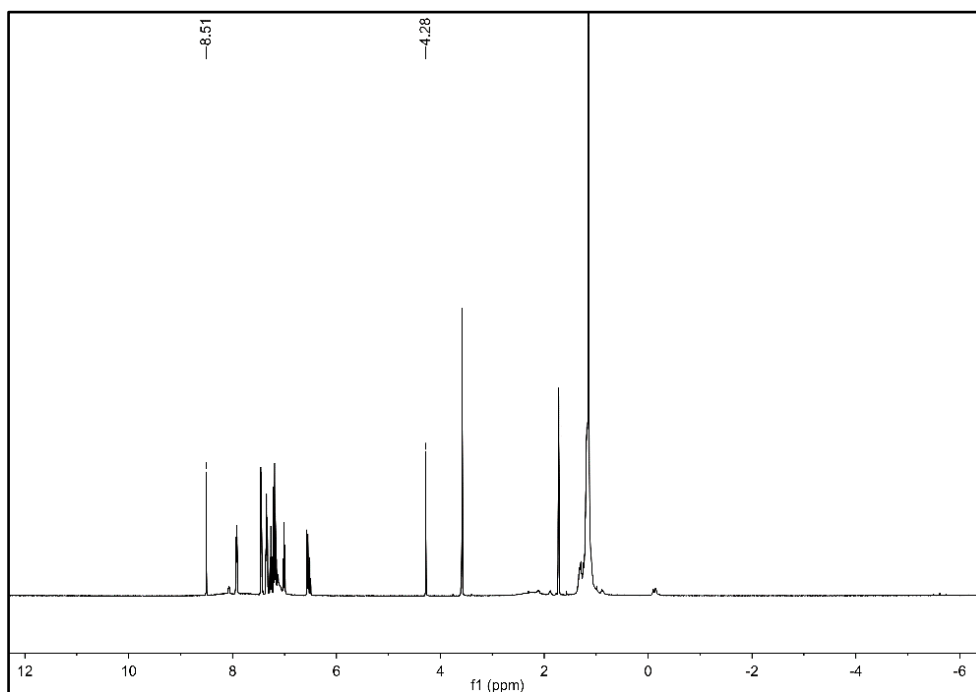


Figure S 20. ¹H NMR spectrum of the reaction mixture after 4 days at rt.

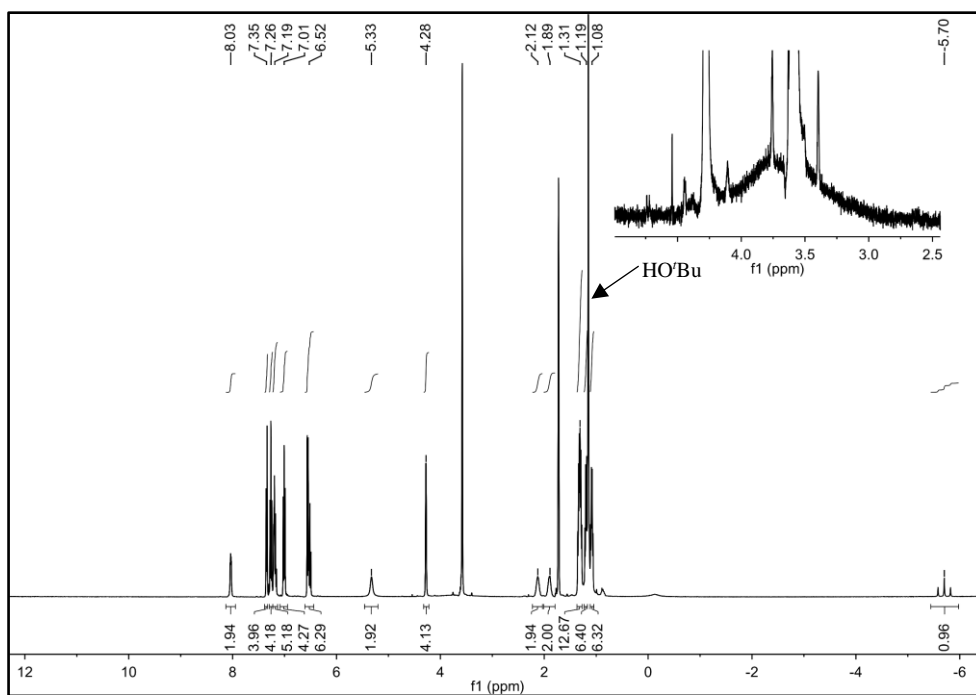


Figure S 21. ^1H NMR spectrum of the reaction mixture after 1 d of stirring at 40 °C with 20 bar H_2 .

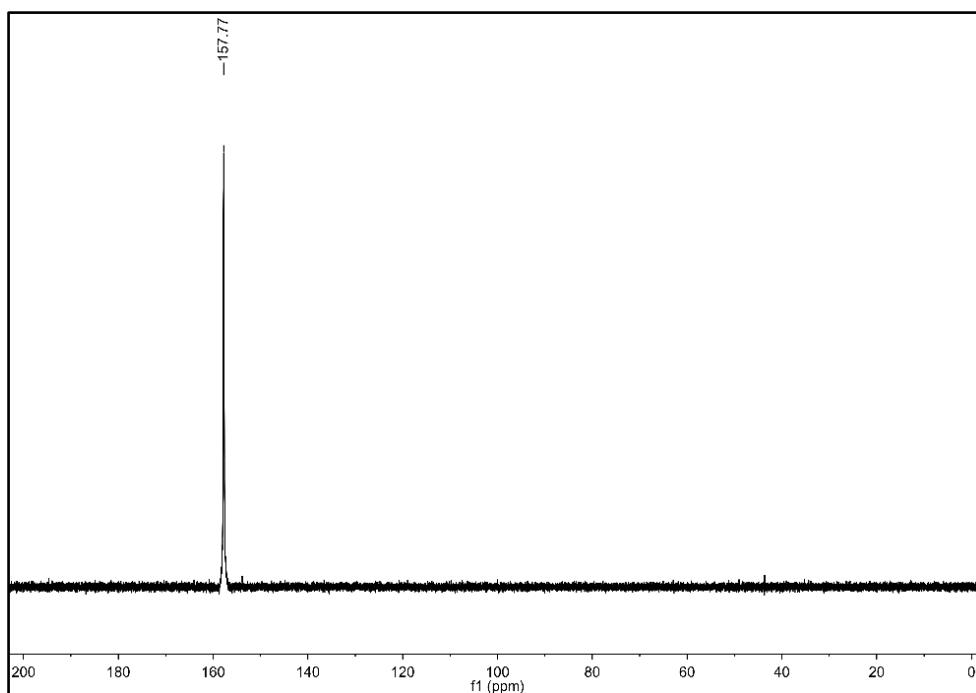


Figure S 22. ^{31}P NMR spectrum of the reaction mixture after 1 d of stirring at 40 °C with 20 bar H_2 .

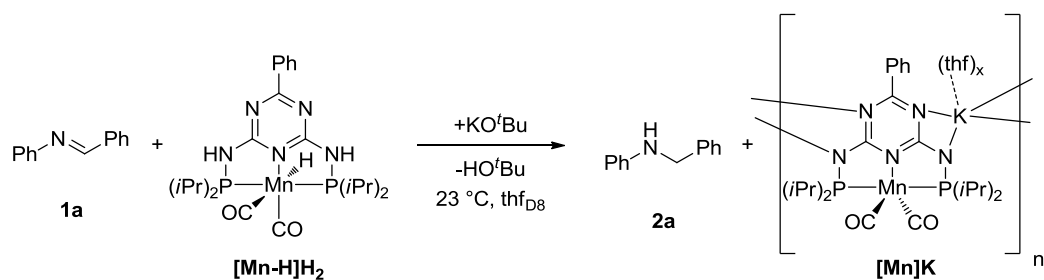
3.2.3. Partial Reaction Orders

The dependency of the reaction between $[\text{Mn-H}]\text{H}_2$ and **1a** on the reactant concentrations was investigated by ^1H NMR experiments according to the general procedure (3.2.1).

3.2.3.1. Base Concentration

The dependency of the reaction rate on the base concentration was investigated as it is shown in Table S 6. From 0 to 1 eq. of base no reaction was observed. The initial reaction rate grows drastically from 1–2 eq. of base and stagnates thereafter.

Table S 6. Variation of the amount of KO^tBu in the reaction of [Mn-H]H₂ and **1a** and correspondent initial rates (r_i).^a



Equivalents KO ^t Bu ^b	r_i [$\frac{\mu\text{mol}}{\text{mL}\cdot\text{h}}$] ^c	R^2
0	0	/
1	0.44 ± 0.09	0.319
2	8.28 ± 0.17	0.983
3 ^d	8.37 ± 0.08	0.996
4	9.12 ± 0.25	0.971

^a [Mn-H]H₂ (30 μmol), **1a** (30 μmol), KO^tBu, thf_{D8} (700 μL), 23 °C. ^b With respect to [Mn-H]H₂. ^c Initial rate of the consumption of **1a**. ^d Calculated by the production of amine.

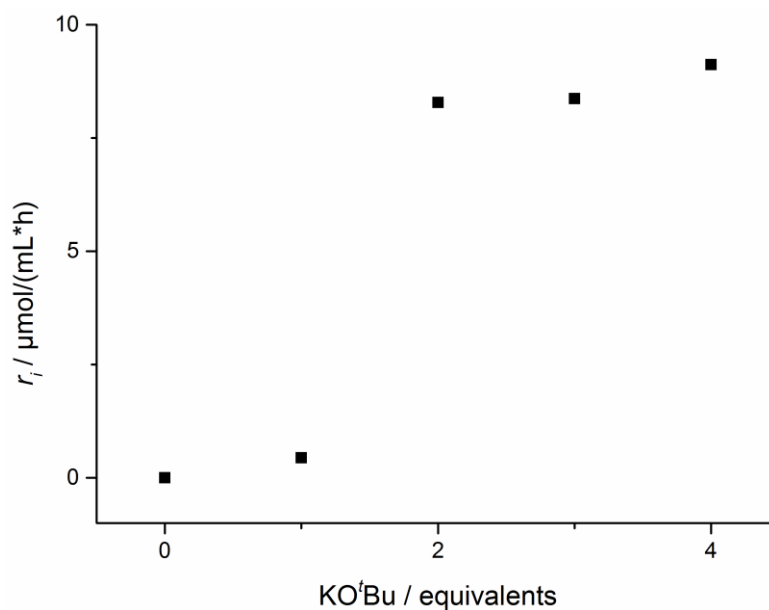
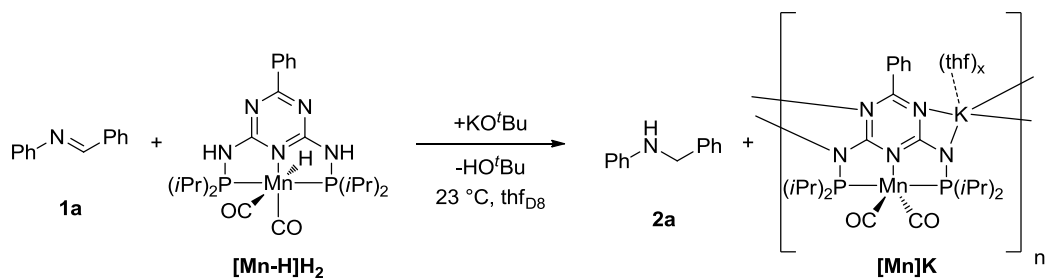


Figure S 23. Dependency of r_i on the concentration of KO^tBu.

3.2.3.2. HO'Bu Concentration

HO'Bu is produced immediately after the addition of KO'Bu because of the deprotonation of hydride complex $[\text{Mn-H}]\text{H}_2$. 1 eq. of $[\text{Mn-H}]\text{H}_2$ with 2 eq. of KO'Bu yields 2 eq. of HO'Bu (Entry 1, Table S 7).

Table S 7. Variation of the amount of HO'Bu in the reaction of $[\text{Mn-H}]\text{H}_2$ and **1a**.^a



Equivalents HO'Bu ^b	$r_i \left[\frac{\mu\text{mol}}{\text{mL}\cdot\text{h}} \right]^c$	R ²
2	8.28 ± 0.17	0.983
4	8.29 ± 0.19	0.979

^a $[\text{Mn-H}]\text{H}_2$ (30 μmol), **1a** (30 μmol), KO'Bu (60 μmol), $\text{thf}_{\text{D}8}$ (700 μL), 23 °C.

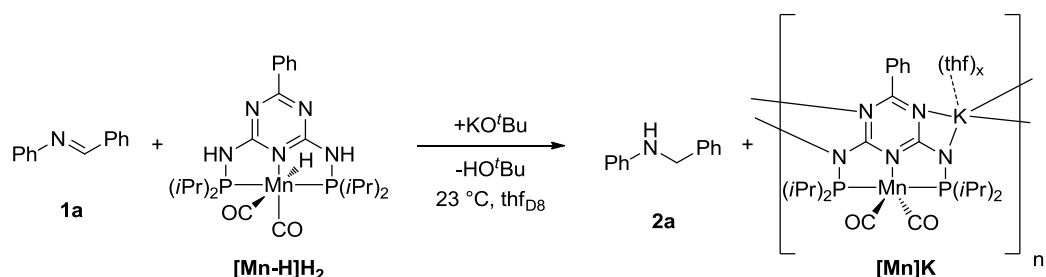
^b With respect to $[\text{Mn-H}]\text{H}_2$. ^c Initial rate of the consumption of **1a**.

Considering the results shown in Table S 7, HO'Bu has no influence on the reaction rate.

3.2.3.3. Imine Concentration

The dependency of the reduction of imine **1a** on the concentration of **1a** was determined (Table S 8).

Table S 8. Variation of the imine (**1a**) concentration.^a



Equivalents 1a ^b	$r_i \left[\frac{\mu\text{mol}}{\text{mL}\cdot\text{h}} \right]^c$	R^2
0.5	4.38 ± 0.12	0.969
1	8.28 ± 0.17	0.983
2	16.6 ± 0.4	0.989

^a **[Mn-H]₂** (30 μmol), **1a**, KO^tBu (60 μmol), thf_{D8} (700 μL), 23 °C. ^b With respect to **[Mn-H]₂**. ^c Initial rate of the consumption of **1a**.

Considering following equation:

$$r = k * [A]^a * [B]^b \dots \quad (1)$$

r is the reaction rate, $[A]$, $[B]$ are the concentrations of the components, and a and b are the partial reaction orders with respect to the components. The variables expect for $[A]$ and a can be combined to constant k' when the concentration of only one component (A) is varied (r_i is the initial rate).

$$r_i = k' * [A]^a \quad (2)$$

It follows:

$$\ln(r_i) = \ln(k') + a * \ln([A]) \quad (3)$$

This is a linear equation for the variation of the concentration of only one component at once. By plotting $\ln(r_i)$ against $\ln([A])$ the reaction order a with respect to this component follows as the slope of the line.

Table S 9. $\ln(r_i)$ and $\ln([A])$ (A is **1a**)

$\ln(r_i)$	$\ln([A])$
1.477 ± 0.027	3.065
2.114 ± 0.021	3.758
2.809 ± 0.024	4.451

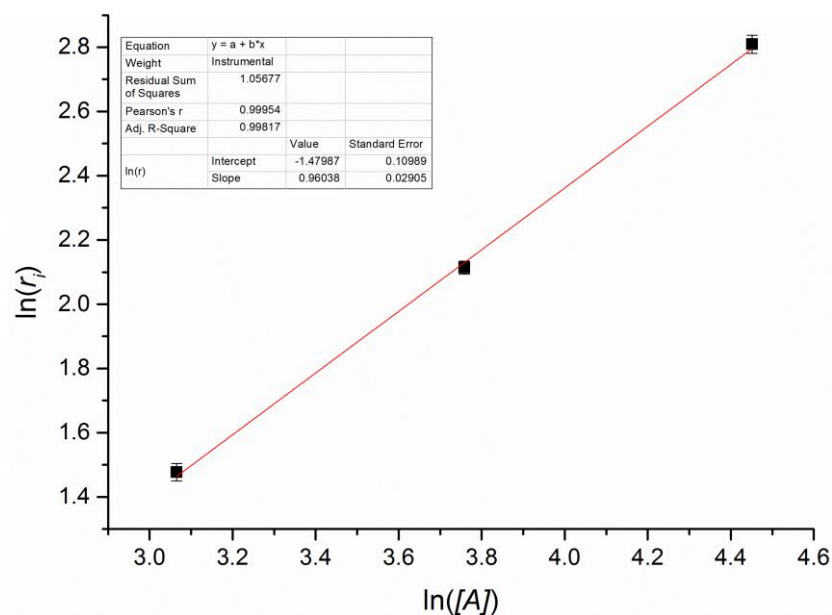


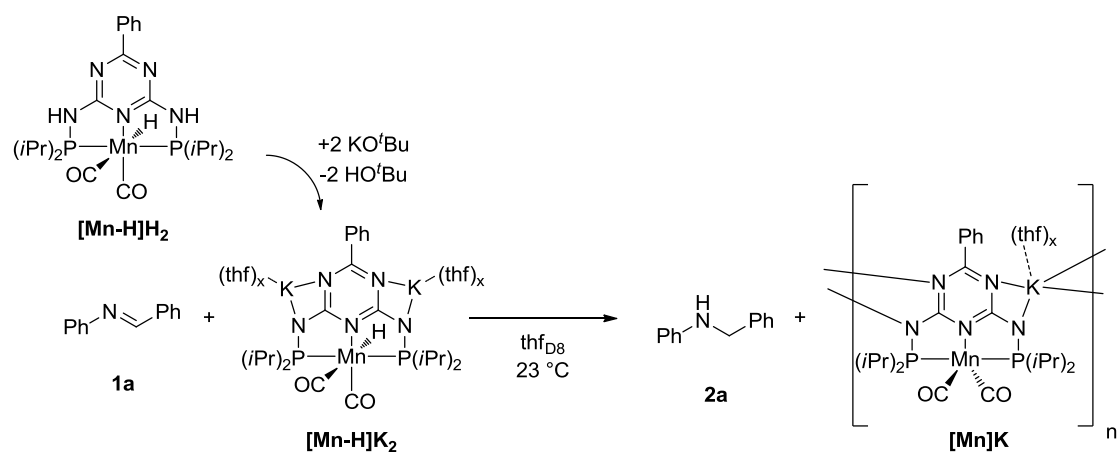
Figure S 24. $\ln(r_i)$ against $\ln([A])$.

The partial reaction order with respect to imine **1a** which equals the slope in Figure S 24 is $a = 0.960 \pm 0.029$. Therefore, the reaction order with respect to **1a** is 1. With $R^2 = 0.999$ (R = Pearson Correlation Coefficient) a good linear correlation was observed.

3.2.3.4. Concentration of $[\text{Mn-H}]\text{K}_2$

The dependency of the reduction of imine **1a** on the concentration of $[\text{Mn-H}]\text{K}_2$ was determined (Table S 10). $[\text{Mn-H}]\text{K}_2$ was produced by adding 2 eq. of KO^tBu to 1 eq. of $[\text{Mn-H}]\text{H}_2$.

Table S 10. Variation of the amount of **[Mn-H]K₂** in the hydrogenation of **1a**.^a



Equivalents [Mn-H]K₂ ^b	$r_i \left[\frac{\mu\text{mol}}{\text{mL}\cdot\text{h}} \right]^c$	R^2
0.5	4.07 ± 0.12	0.969
1	8.28 ± 0.17	0.983
2	17.96 ± 0.25	0.989

^a **1a** (30 μmol), **[Mn-H]H₂**, KO^tBu (2 eq. with respect to **[Mn-H]H₂**), thf_{D8} (700 μL), 23 °C. ^b With respect to **1a**. ^c Initial rate of the consumption of **1a**.

Table S 11. Values of $\ln(r_i)$ and $\ln([B])$ ($B = \text{[Mn-H]K}_2$).

$\ln(r_i)$	$\ln([B])$
1.404 ± 0.059	3.065
2.114 ± 0.021	3.758
2.888 ± 0.013	4.451

The reaction order with respect to **[Mn-H]K₂** which equals the slope in Figure S 25 is $a = 1.10 \pm 0.03$. Thus, the partial reaction order can be assumed as 1. With $R^2 = 0.9995$ a linear good correlation was observed.

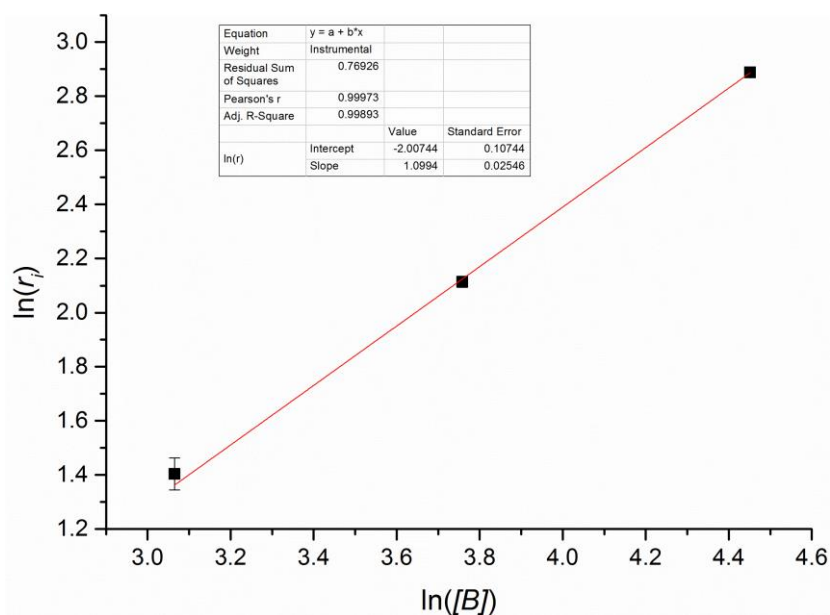


Figure S 25. Plot of $\ln(r_i)$ against $\ln([B])$.

3.2.4. Reaction Constant k and Reaction Order

Under the evidence-based assumption that the reaction order is 2 (1 with respect to **1a** and 1 with respect to **[Mn-H]K₂**) the reaction order k was calculated. The data of an equimolar reaction between **1a** and **[Mn-H]K₂** was used.

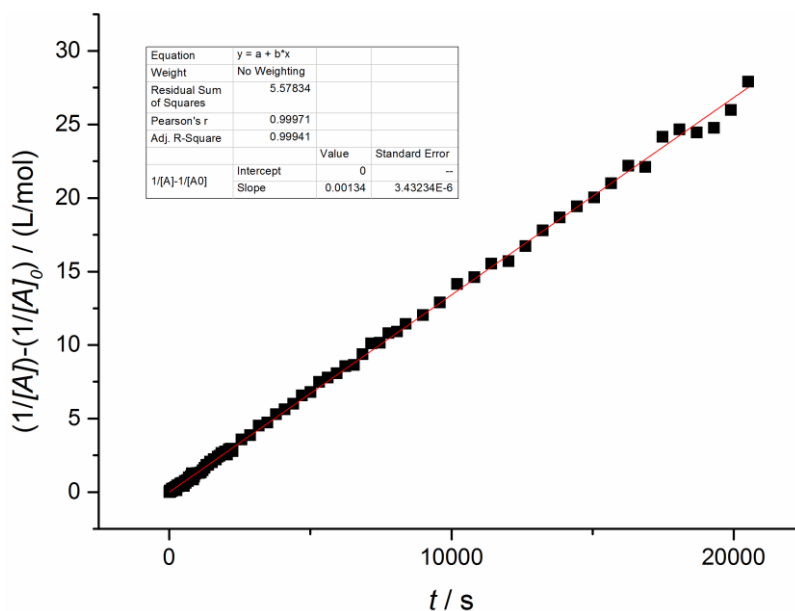


Figure S 26. Plotting of $\frac{1}{[A]} - \frac{1}{[A]_0}$ against t . A is **1a**.

Equation (4) is a linear equation shown in Figure S 26:

$$\frac{1}{[A]} - \frac{1}{[A]_0} = k * t \quad (4)$$

$[A]$ is the concentration of **1a** during the reaction and $[A]_0$ is the concentration of **1a** at $t = 0$.

As it can be seen from Figure S 26 the plot for a reaction order of 2 produces an almost perfectly straight line with $R^2 = 0.999$. Furthermore, the reaction constant k at 23 °C for the reaction between **1a** and **[Mn-H]K₂** was calculated as:

$$k = (1.34 * 10^{-3} \pm 3.43 * 10^{-6}) \frac{L}{mol * s} \quad (5)$$

3.2.5. Reaction under CO Atmosphere

In order to evaluate if CO has an influence on the reaction rate, a reaction was carried out analogous to 3.2.1 with an equimolar ratio of **[Mn-H]H₂** (30 µmol, 1.0 eq.) and **1a** (30 µmol, 1.0 eq.) but after adding KO^tBu (60 µmol, 2 eq.) and cooling down the NMR tube with liquid nitrogen it was evacuated and purged with CO three times. The CO pressure was adjusted to 0.5 bar overpressure, the NMR was then heated up to room temperature and immediately inserted into the NMR.

Table S 12. CO experiment for the stoichiometric reduction of **1a** with **[Mn-H]H₂**.^a

CO [bar]	$r_i [\frac{\mu mol}{mL * h}]^b$	R^2
0	8.28 ± 0.17	0.983
1.5	7.56 ± 0.14	0.989
^a [Mn-H]H₂ (30 µmol), 1a (30 µmol), KO ^t Bu (60 µmol), thf _{D8} (700 µL), 23 °C.		
^b Initial rate of the consumption of 1a .		

According to the results, CO does not have an essential influence on the reaction rate (Table S 12). The difference between the experiment with and without CO can be explained with the fact, that the first points in time could not be used for the regression line (Figure S 27), probably because of equilibrium effects due to the CO overpressure.

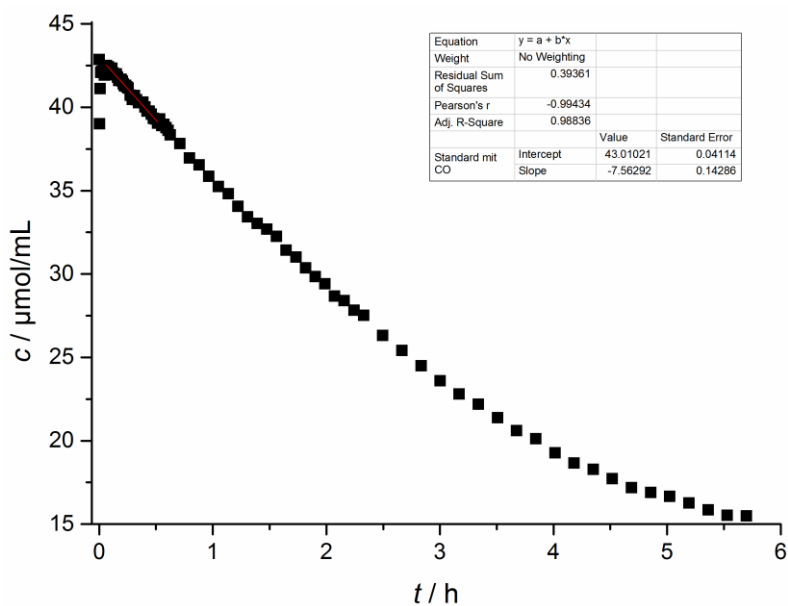


Figure S 27. Consumption of **1a** in the reaction of **1a** and **[Mn-H]K₂** under CO atmosphere.

3.2.6. Alkali Metal Ion Testing

LiO'Bu, NaO'Bu and KO'Bu were tested as bases in the stoichiometric reaction of **1a** and **[Mn-H]H₂**. The reactions were conducted according to the general procedure (3.2.1) at 50 °C with **[Mn-H]H₂** (30 μmol, 1.0 eq.), **1a** (30 μmol, 1.0 eq.) and base (60 μmol, 2.0 eq.).

The initial rates are listed in Table S 13.

Table S 13. Initial rates of the amine production in the reaction between **1a** and **[Mn-H]H₂**.

	LiO'Bu	NaO'Bu	KO'Bu
Initial rate [$\frac{mM}{h}$]	0.68 ± 0.01	5.50 ± 0.05	48.1 ± 1.07

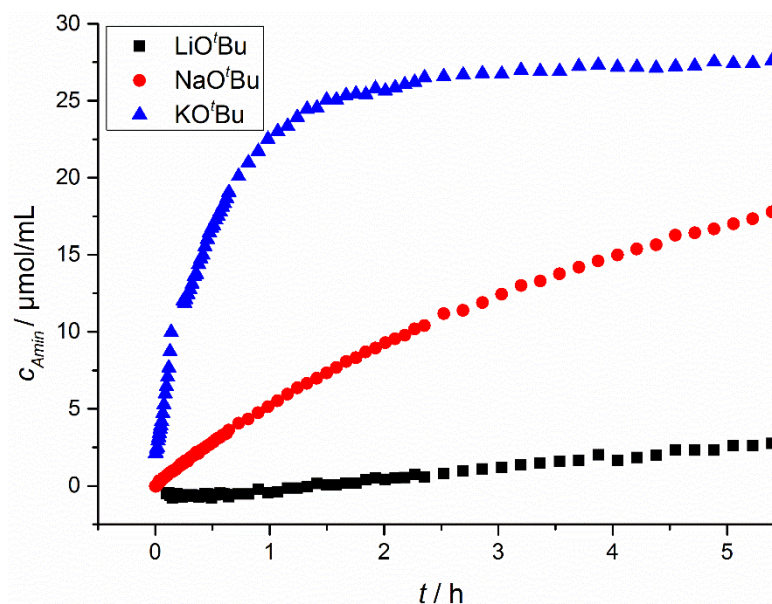


Figure S 28. Comparison between the initial rates of the amine (**2a**) production in the stoichiometric reaction between **[Mn-H]H₂** and **1a** employing KO'Bu, NaO'Bu or LiO'Bu as the base.

3.2.7. Hammett Study

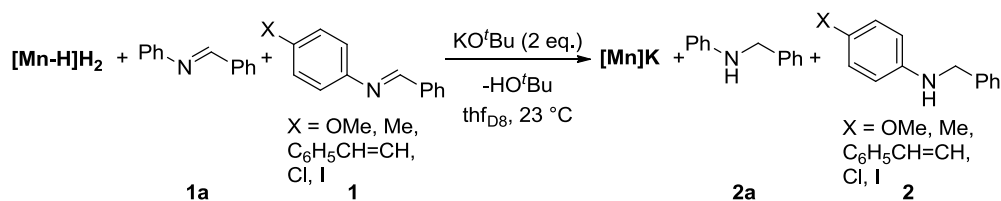
Competition experiments between standard imine **1a** and other imines **1** with various functional groups were carried out in order to gain further insight into the electronic structure of the intermediates which are involved in the rate-determining step (Hammett study^{26, 27}).

With a first-order dependency on imine **1a** (see 3.2.3.3) and the assumption that the reaction order is the same for different imines, following equation applies:

$$\ln\left(\frac{X_0}{X}\right) = \frac{k_X}{k_H} * \ln\left(\frac{H_0}{H}\right) \quad (6)$$

X_0 is the initial concentration of a substrate **1** with a functional group other than H, X is the corresponding concentration during the reaction, H_0 is the initial concentration of standard imine **1a** and H is the corresponding concentration during the reaction. k_X is the reaction constant for the reaction with the substituted imine **1** and k_H is the reaction constant for **1a**. By plotting $\ln\left(\frac{X_0}{X}\right)$ against $\ln\left(\frac{H_0}{H}\right)$ $\frac{k_X}{k_H} = k_{rel}$ can be obtained as the slope of the line. Subsequent plotting of k_{rel} against different σ -values^{26,28} allows the gathering of information if anions, cations or radicals are involved in the rate-determining step.

Table S 14. Values obtained from competition experiments with substrates with different functional groups and values obtained from plotting $\log(k_{rel})$ against different σ -values^{26, 28, a}



Functional Group (X)	R^2	k_{rel}	$\log(k_{rel})$	σ^{26}	σ^{+26}	σ^{+28}	σ^{26}
OMe	0.993	0.0780 ± 0.0007	-1.108 ± 0.004	-0.27	-0.78	0.24	-0.26
Me	0.997	0.183 ± 0.001	-0.738 ± 0.002	-0.17	-0.31	0.11	-0.17
C ₆ H ₅ -CH=CH	0.979	15.36 ± 0.30	1.186 ± 0.008	-0.07	-1.00	/ ^b	0.13
Cl	0.981	23.25 ± 0.46	1.366 ± 0.009	0.23	0.11	0.12	0.19
I	0.923	56.84 ± 2.30	1.755 ± 0.018	0.18	0.14	/ ^b	0.27
R^2				0.61	0.01	0.11	0.94

^a [Mn-H]₂ (30 μmol, 1.0 eq.), **1a** (15 μmol, 0.5 eq.), **1** (15 μmol, 0.5 eq.) KO^tBu (60 μmol, 2.0 eq.), thf_{D8} (700 μL), 23 °C. ^b No data available in literature.

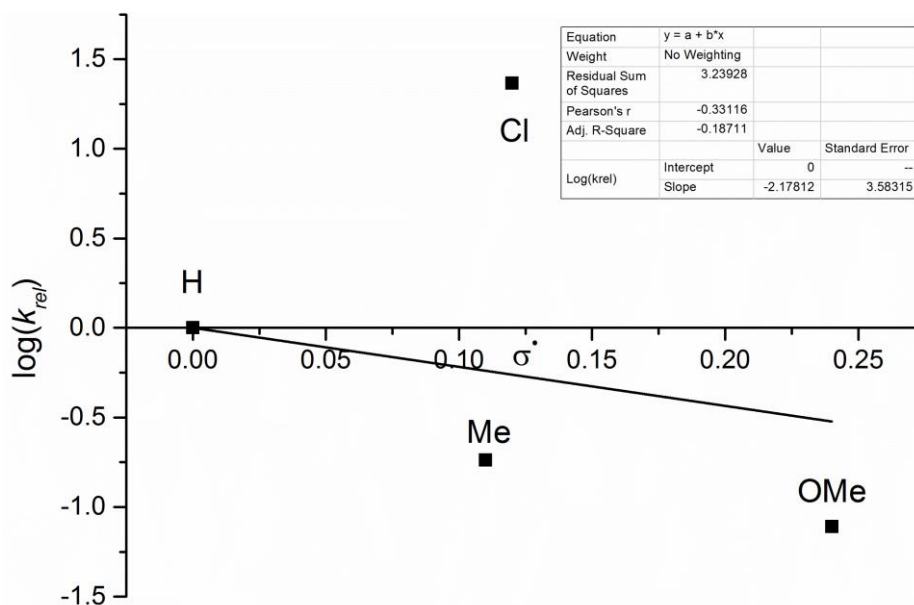


Figure S 29. Hammett plot with σ -values for radical reactions²⁸.

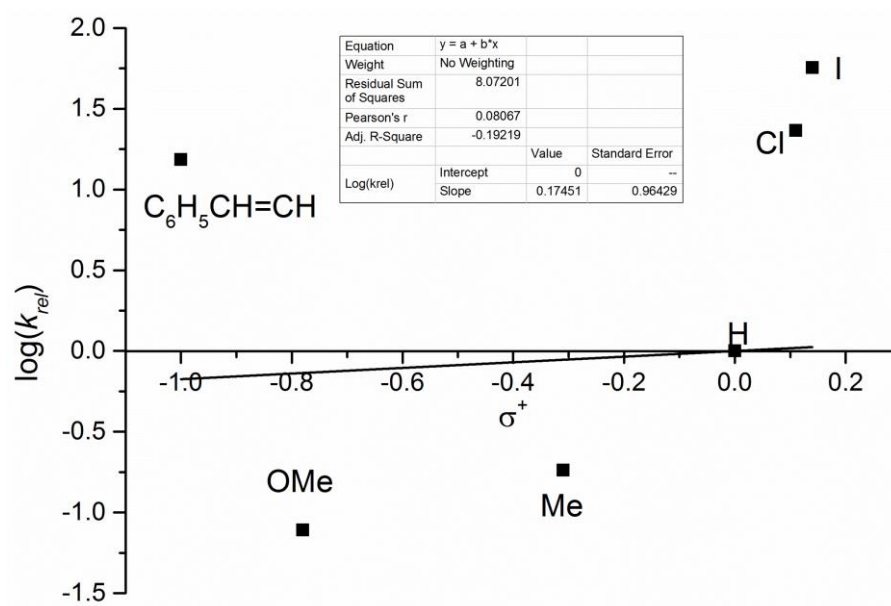


Figure S 30. Hammett plot with σ -values optimized for reactions with an evolving positive charge in conjugation with the substituent²⁶.

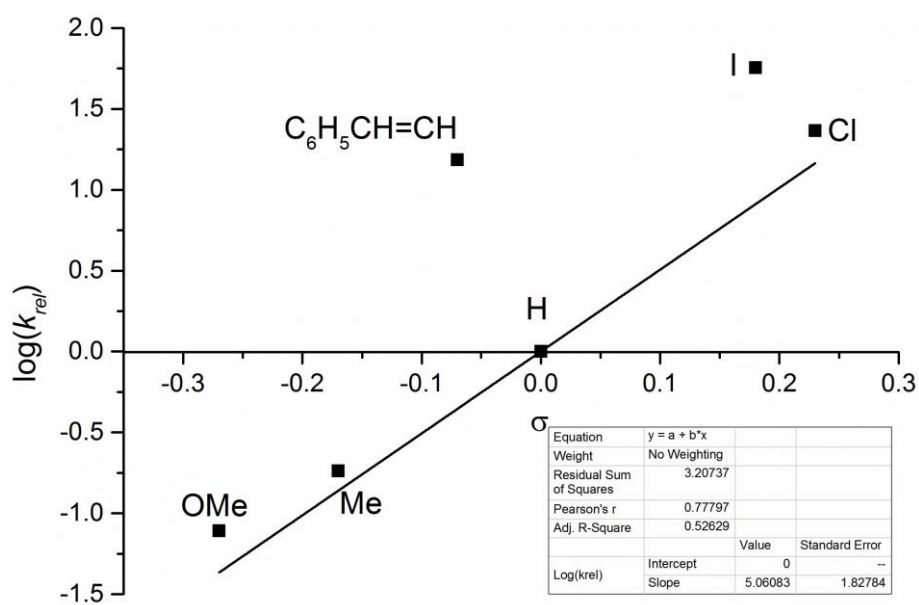


Figure S 31. Hammett plot with standard σ -values²⁶.

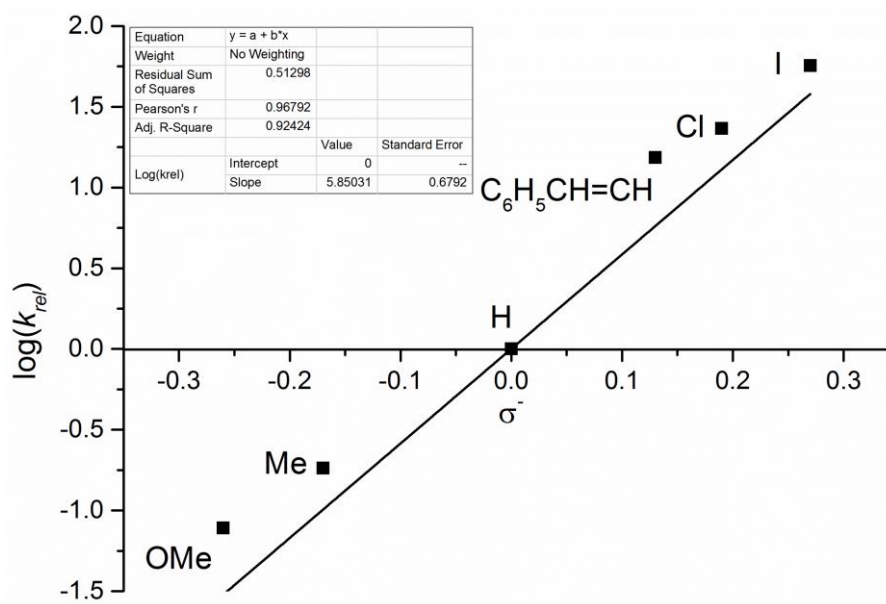


Figure S 32. Hammett plot with sigma σ^- -values (values for a reaction with an evolving negative charge in conjugation with the substituent).

Plotting of $\ln\left(\frac{X_0}{X}\right)$ against $\ln\left(\frac{H_0}{H}\right)$ yielded lines with high R^2 -values, indicating good linear dependencies (Table S 14). The Hammett plots (Figure S 29 –Figure S 32) show, that the only fitting σ -values are the σ^- -values, optimized for reactions in which a negative charge is built up which is resonance-stabilized by the substituent. The slope, which is the reaction constant $\rho = 5.85$, is relatively high, indicating that a strong negative charge is built up during the rate-determining step. It can be concluded, that there are most likely no radical or cationic intermediates present during the rate determining step and a strong negative charge is built up, which is delocalized over the substituent, consistent with a hydride transfer, producing a transiently negative charge on the nitrogen atom at the former imine.

3.3 Hydrogenation Experiments

3.3.1. Crown Ether Addition

According to the general procedure for hydrogenation reactions (2.2.1) an autoclave was charged with **1a** (181 mg, 1.00 mmol, 1.0 eq.), KO^tBu (0.16 M in thf; 250 μ L, 40 μ mol, 4 mol%), [Mn-Br]H₂ (0.008 M in thf, 500 μ L, 4 μ mol, 0.4 mol%), 18-crown-6 (0.16 M in thf; 250 μ L, 40 μ mol, 4 mol%) and 1 mL thf. The reaction was stirred for 4 h at 50 °C. After the

reaction, 1 mL H₂O, 100 μ L dodecan and 7 mL Et₂O were added, the mixture homogenized, and a sample for GC analysis was dried over Na₂SO₄.

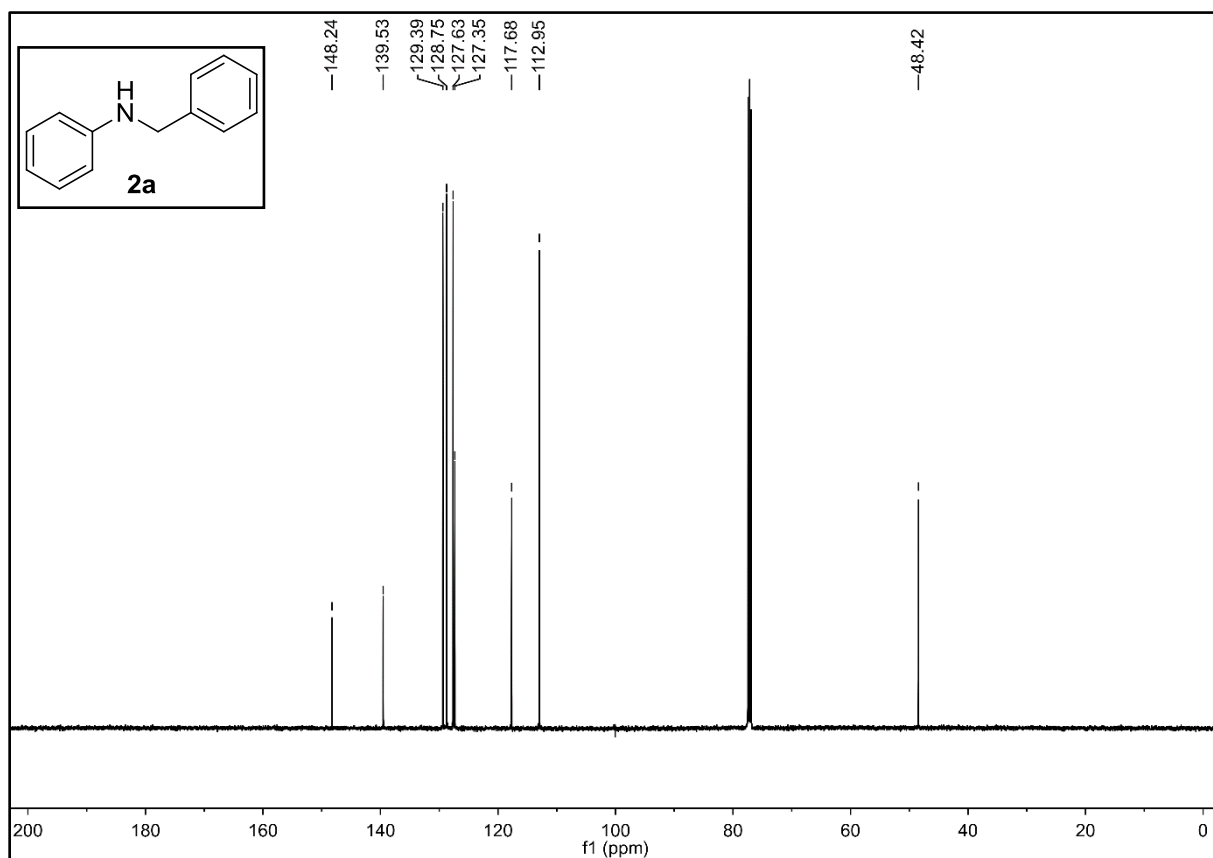
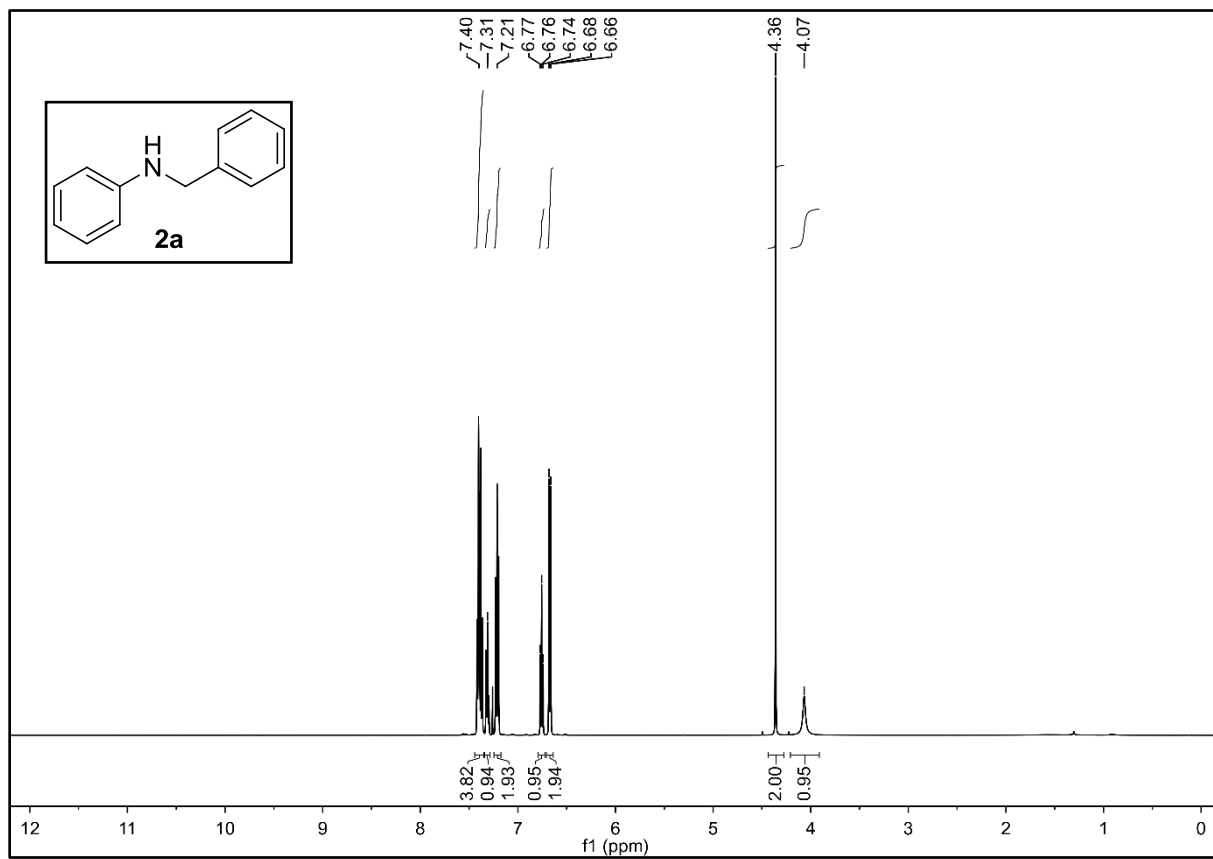
Yield of **2a** (determined by GC): 38 %.

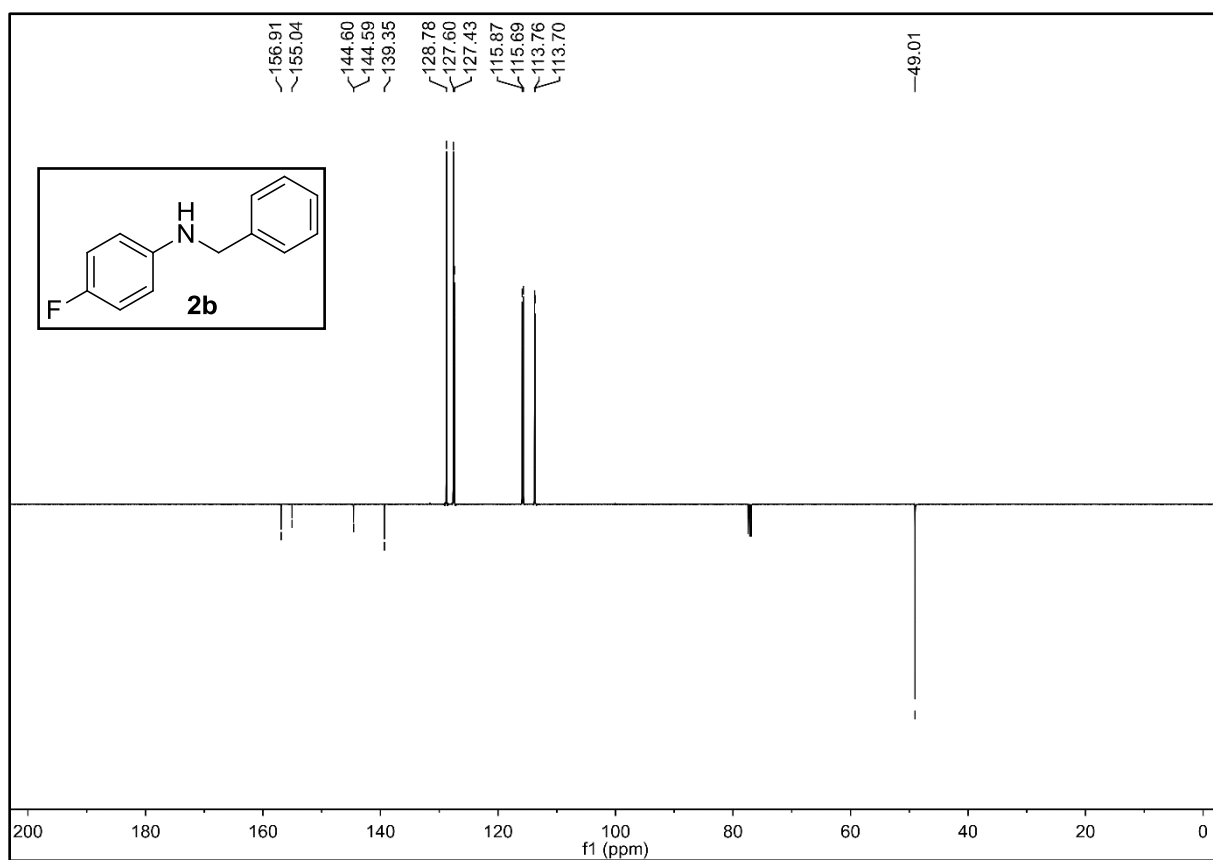
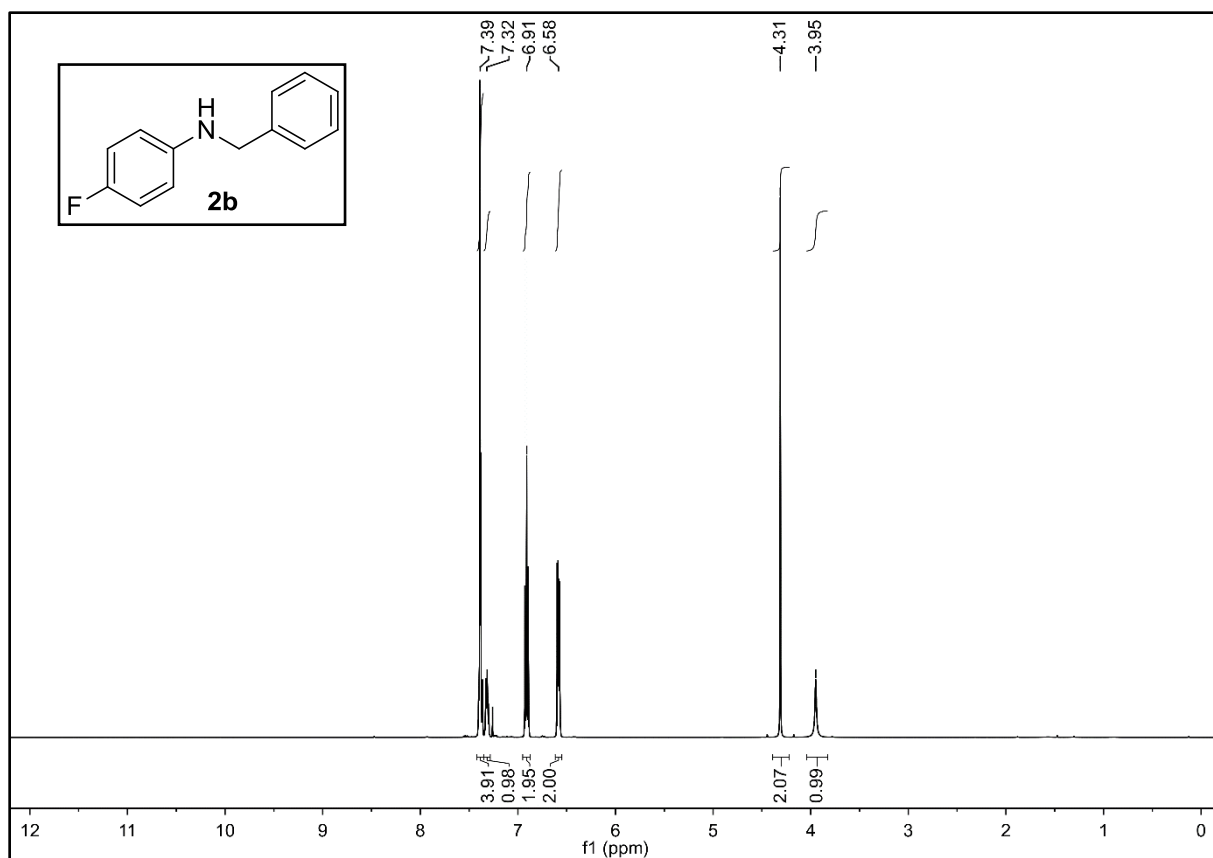
3.3.1. Hydrogenation with [Mn-H]K₂ and HOtBu

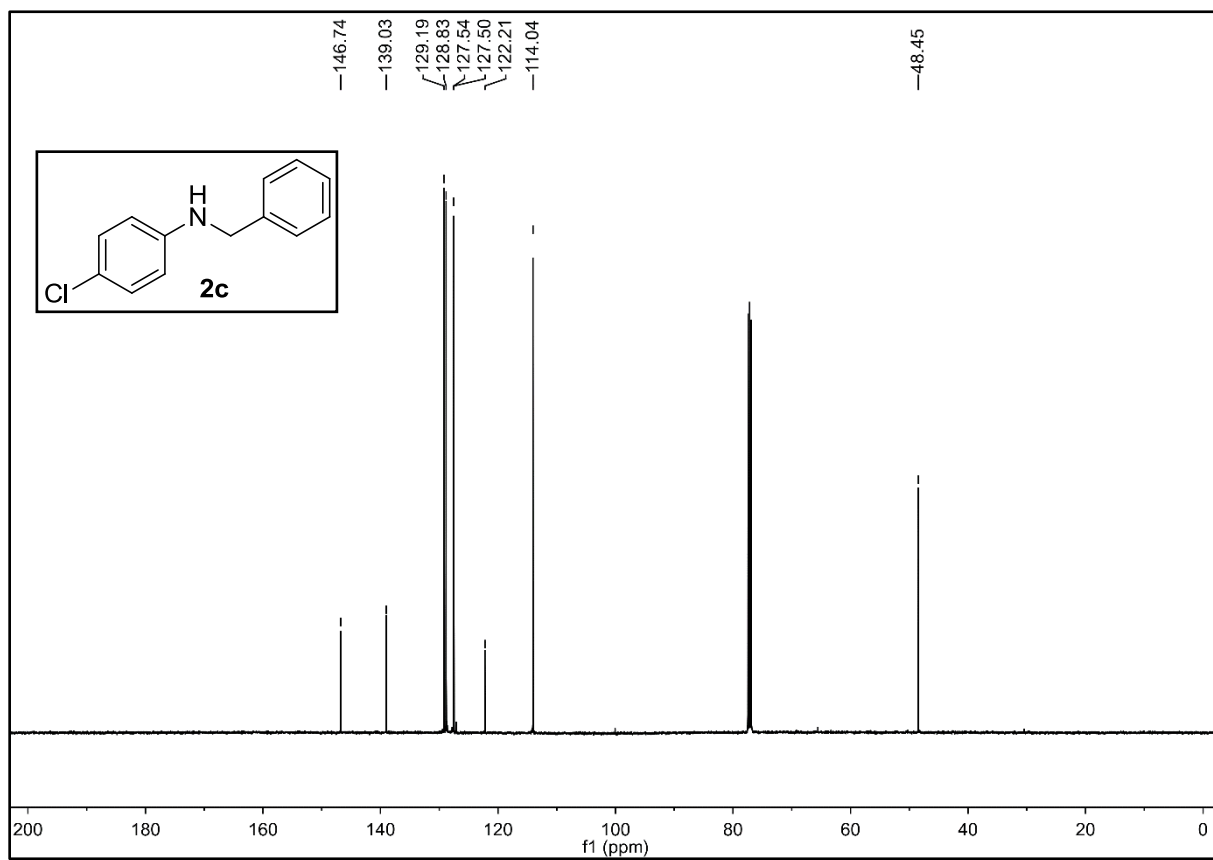
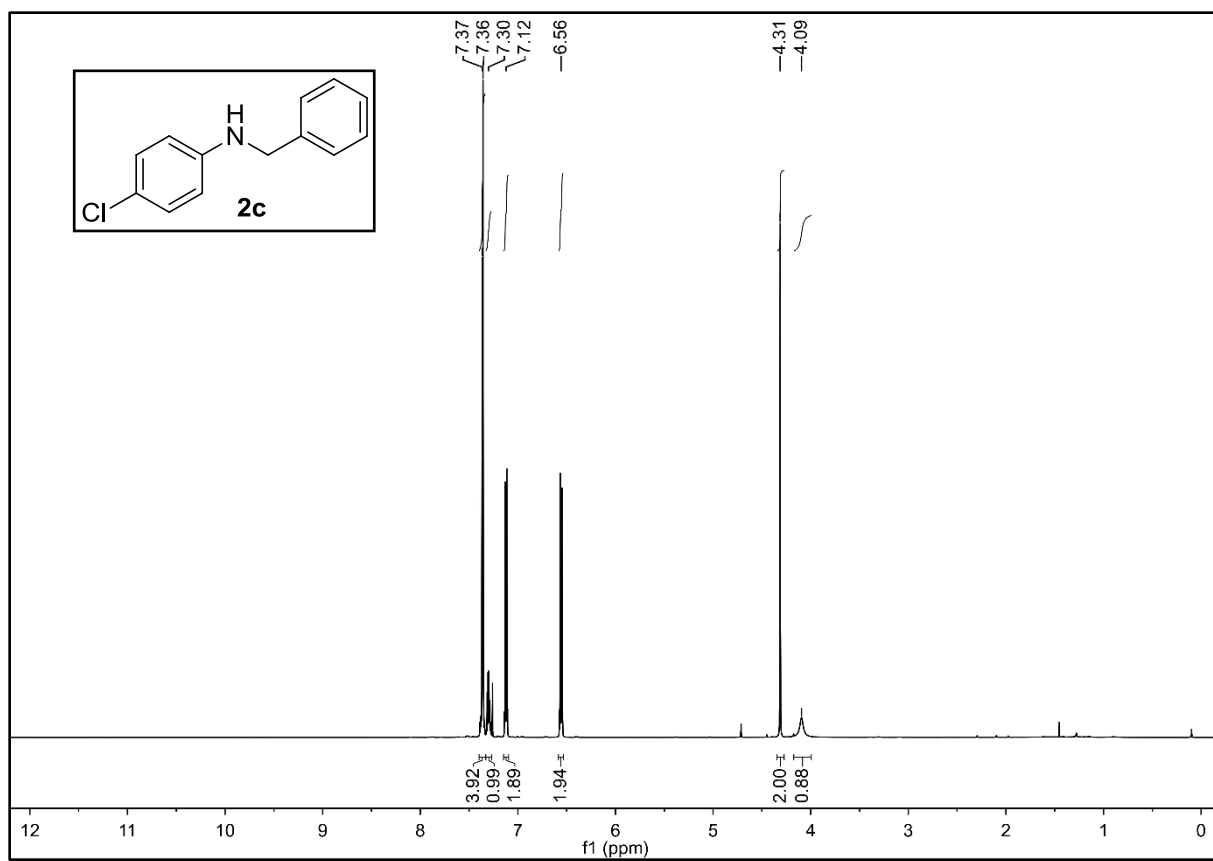
An autoclave was charged with **1a** (181 mg, 1.00 mmol, 1.0 eq.) [Mn-H]K₂ (0.004 M in thf, 1.00 mL, 4 μ mol, 0.4 mol%), HOtBu (0.04 M in thf; 100 μ L, 4 μ mol, 0.4 mol%) and 900 μ L thf. The reaction was stirred for 24 h at 50 °C. After the reaction, 1 mL H₂O, 100 μ L dodecan and 7 mL Et₂O were added, the mixture homogenized, and a sample for GC analysis was dried over Na₂SO₄.

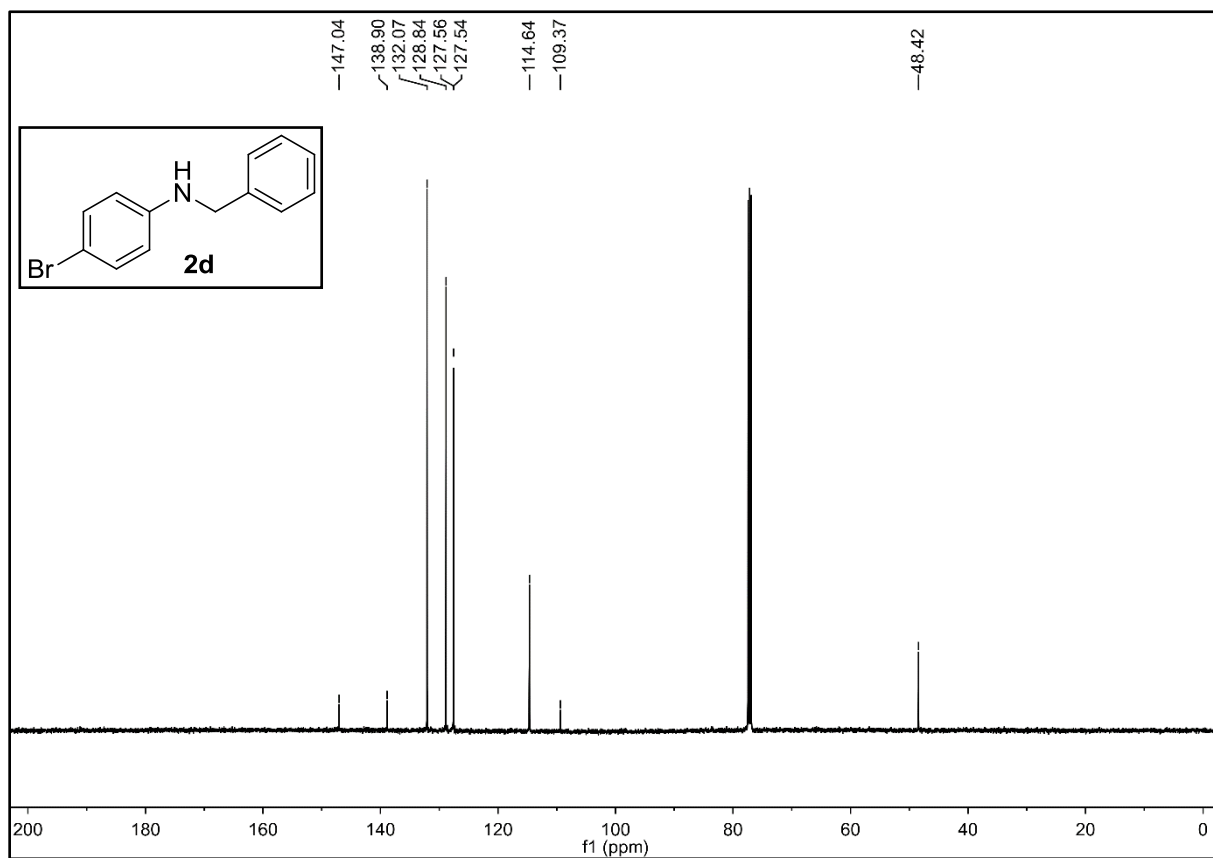
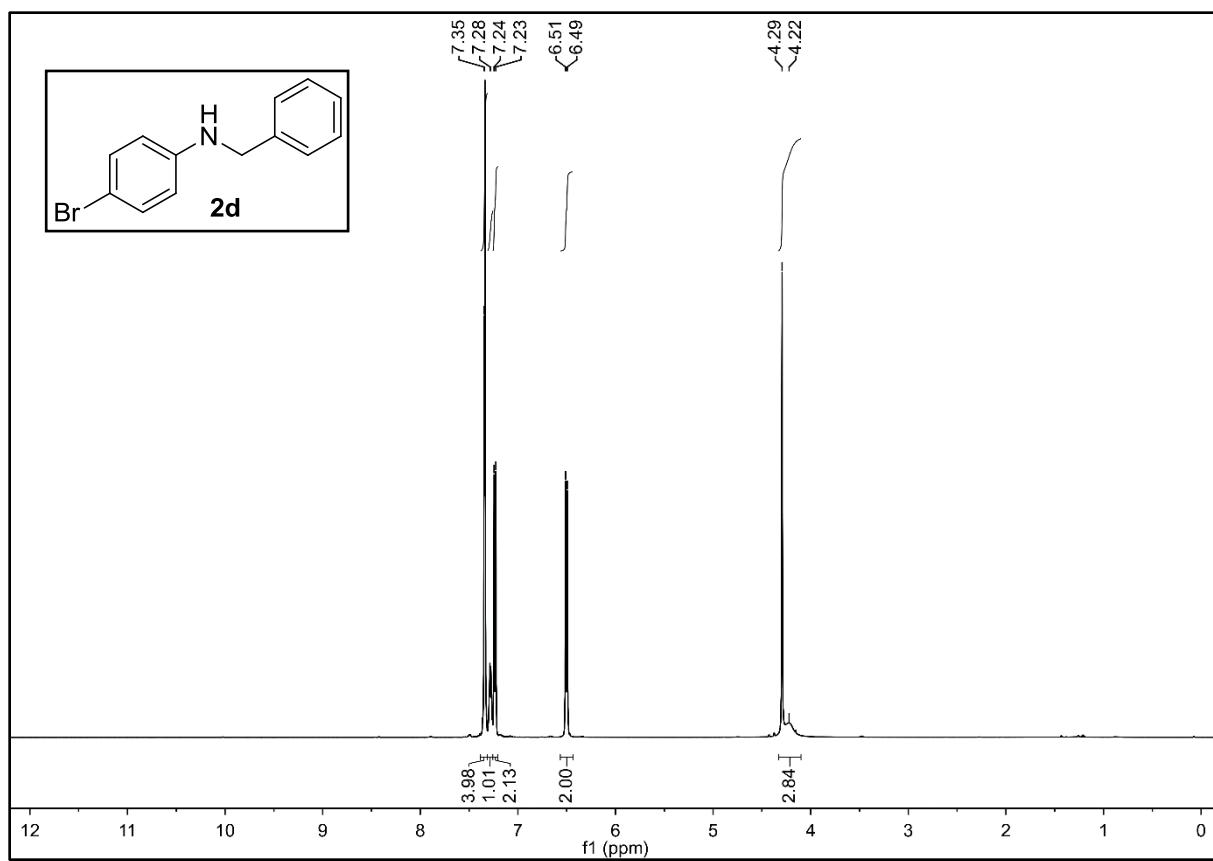
Yield of **2a** (determined by GC): 28 %.

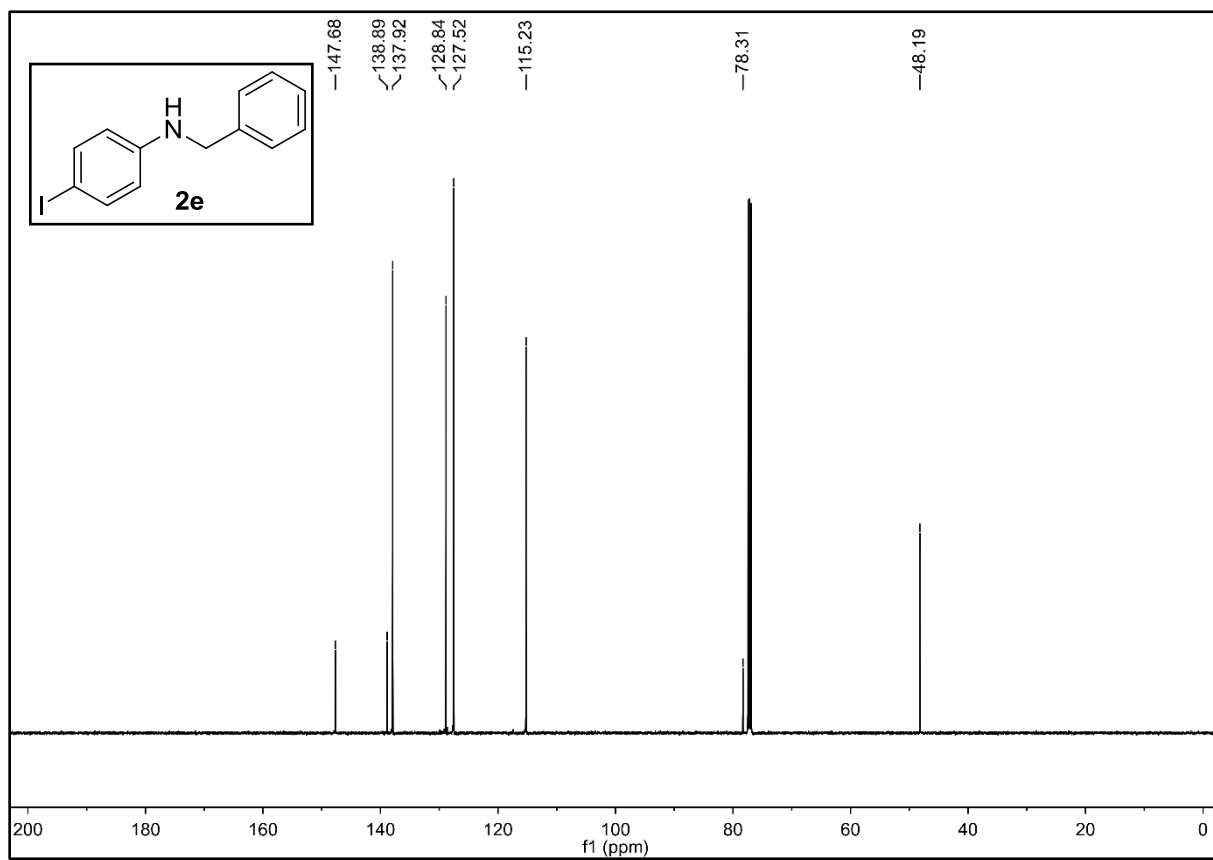
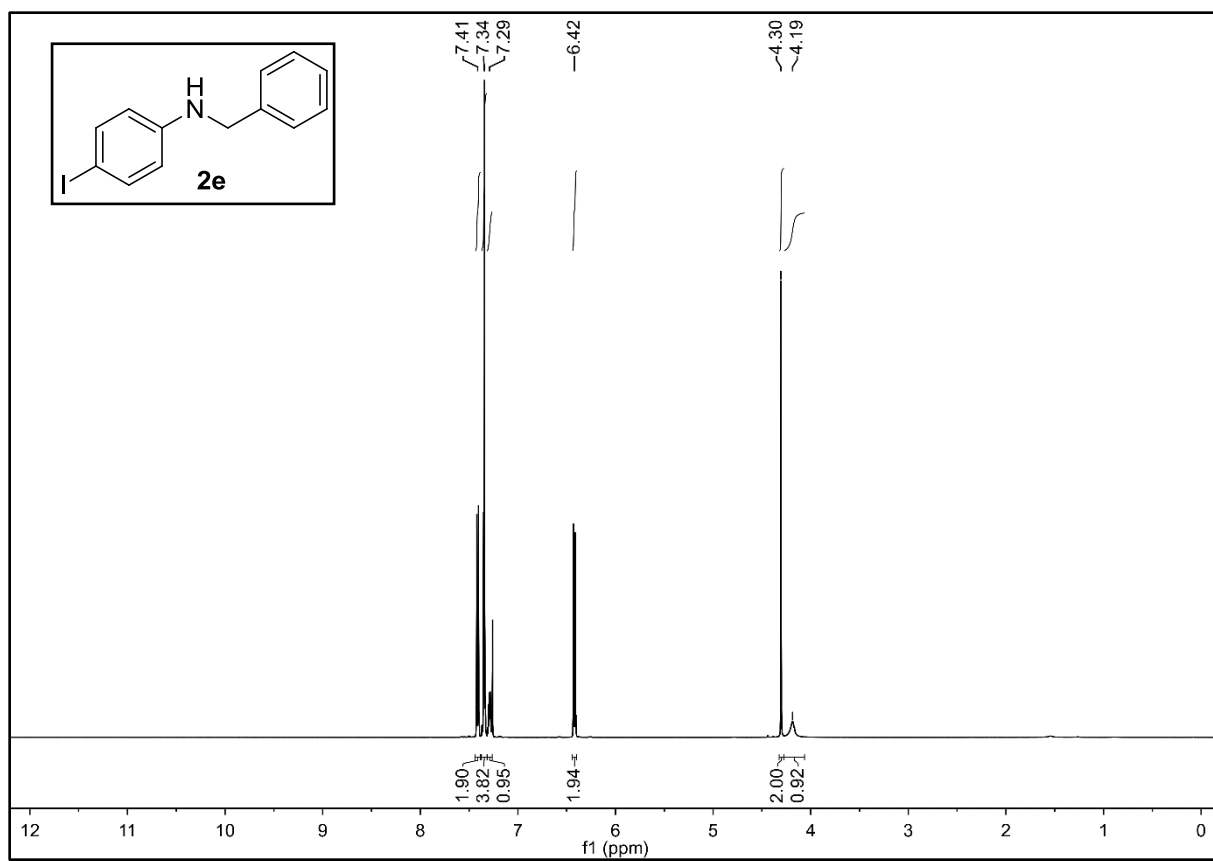
4 NMR Spectra

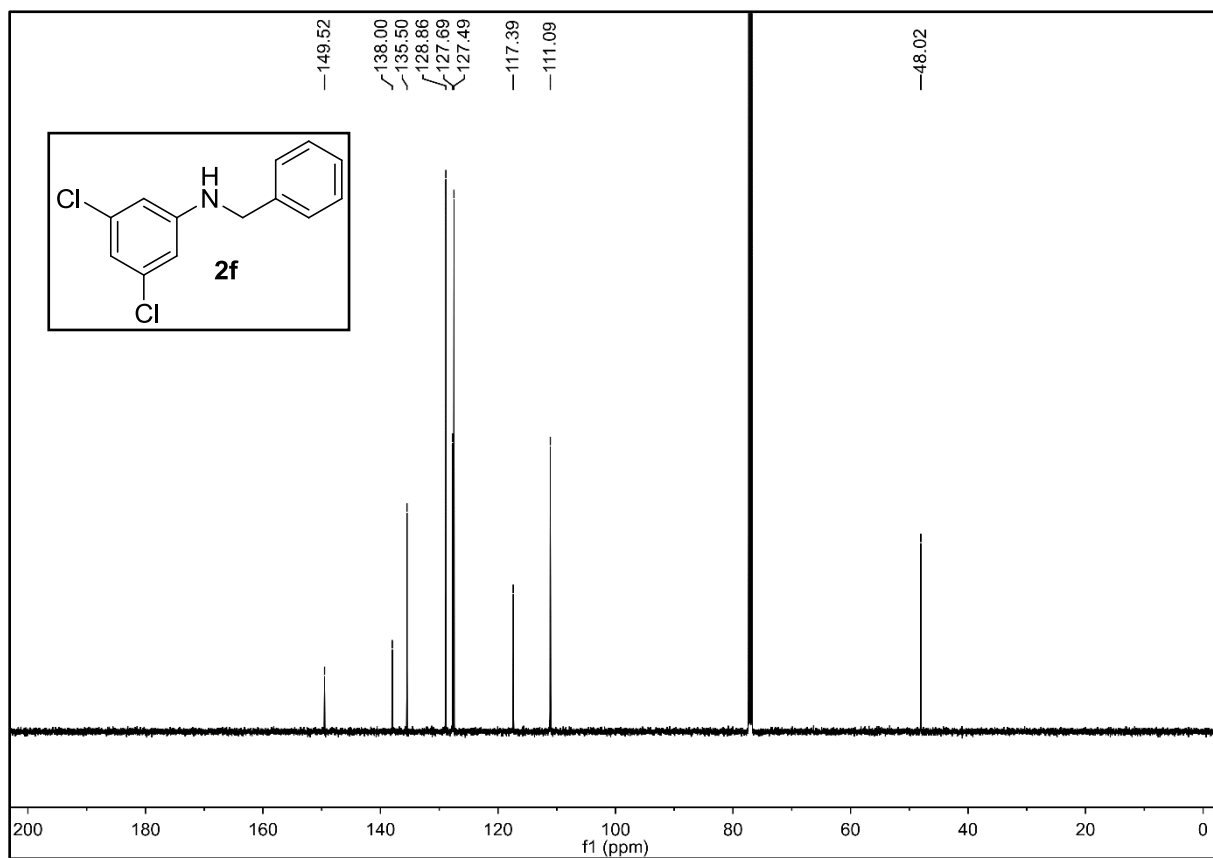
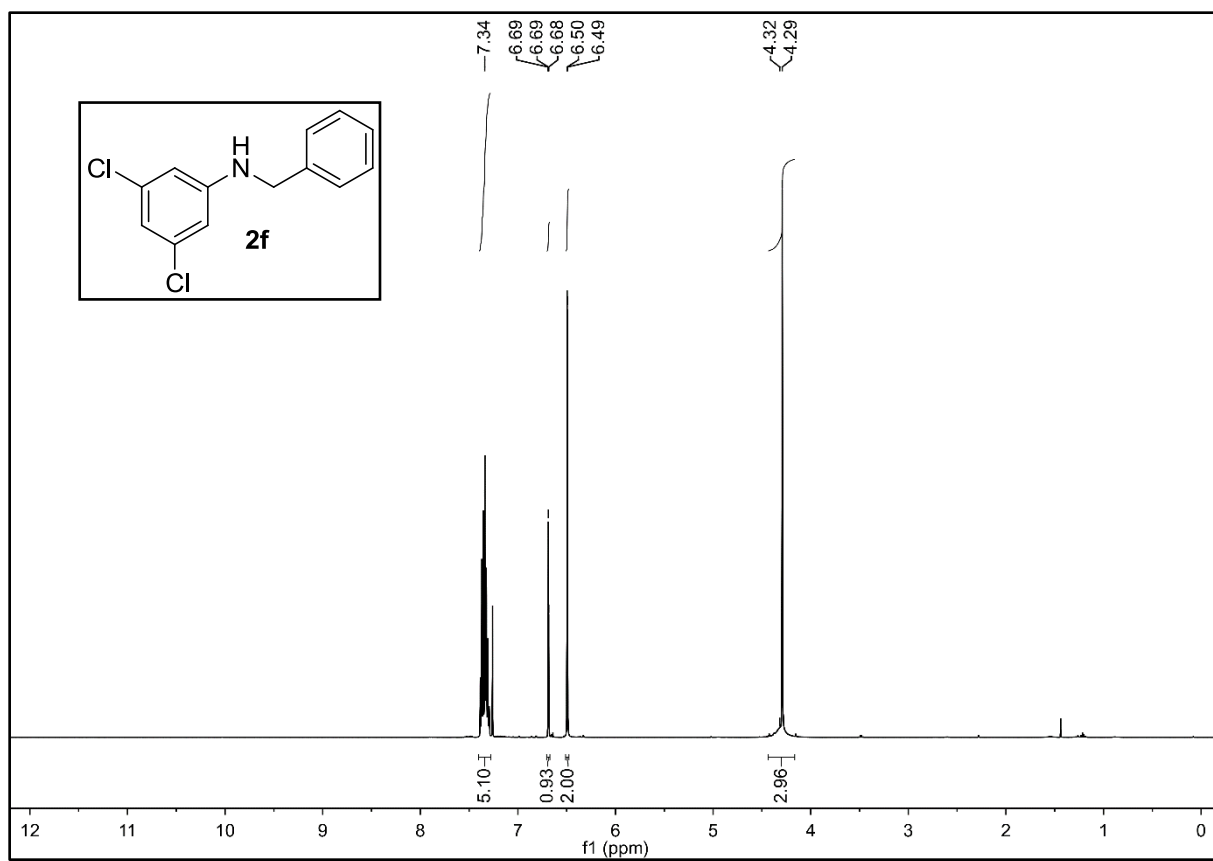


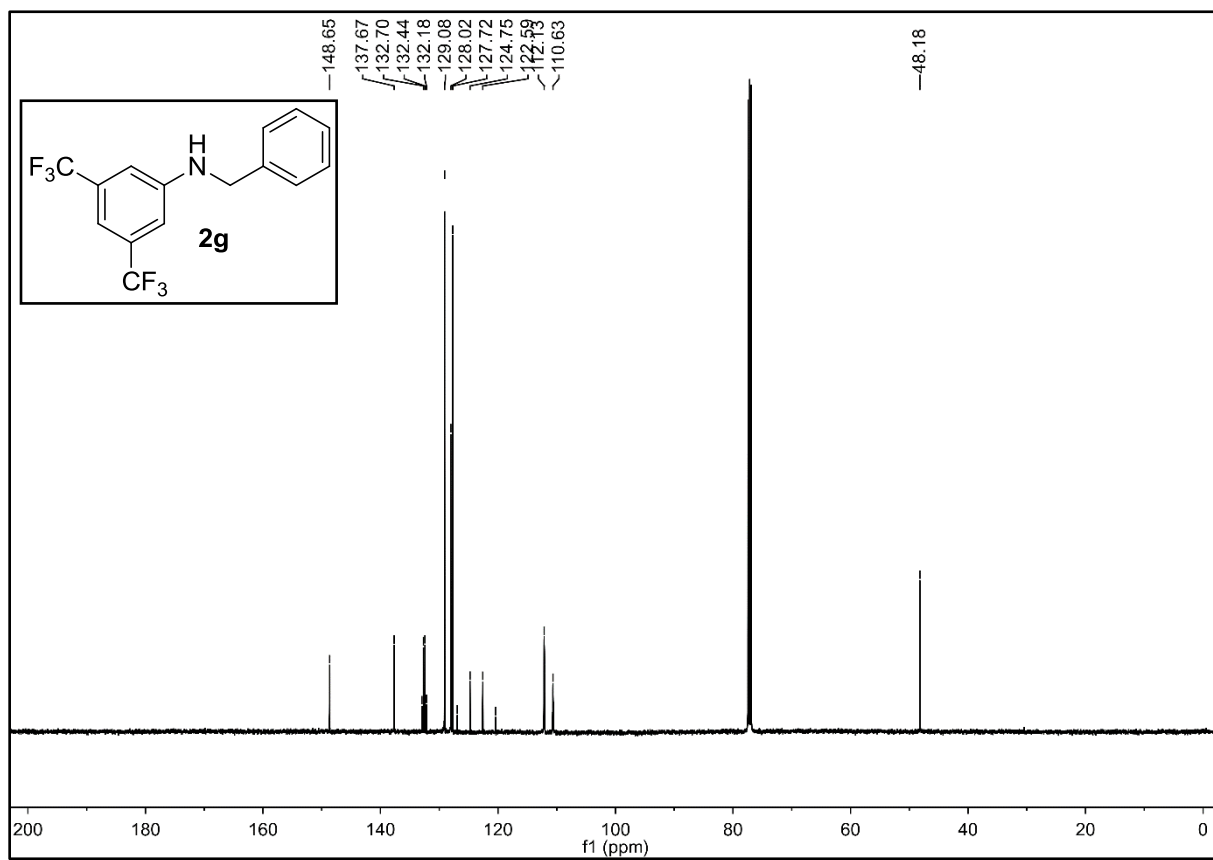
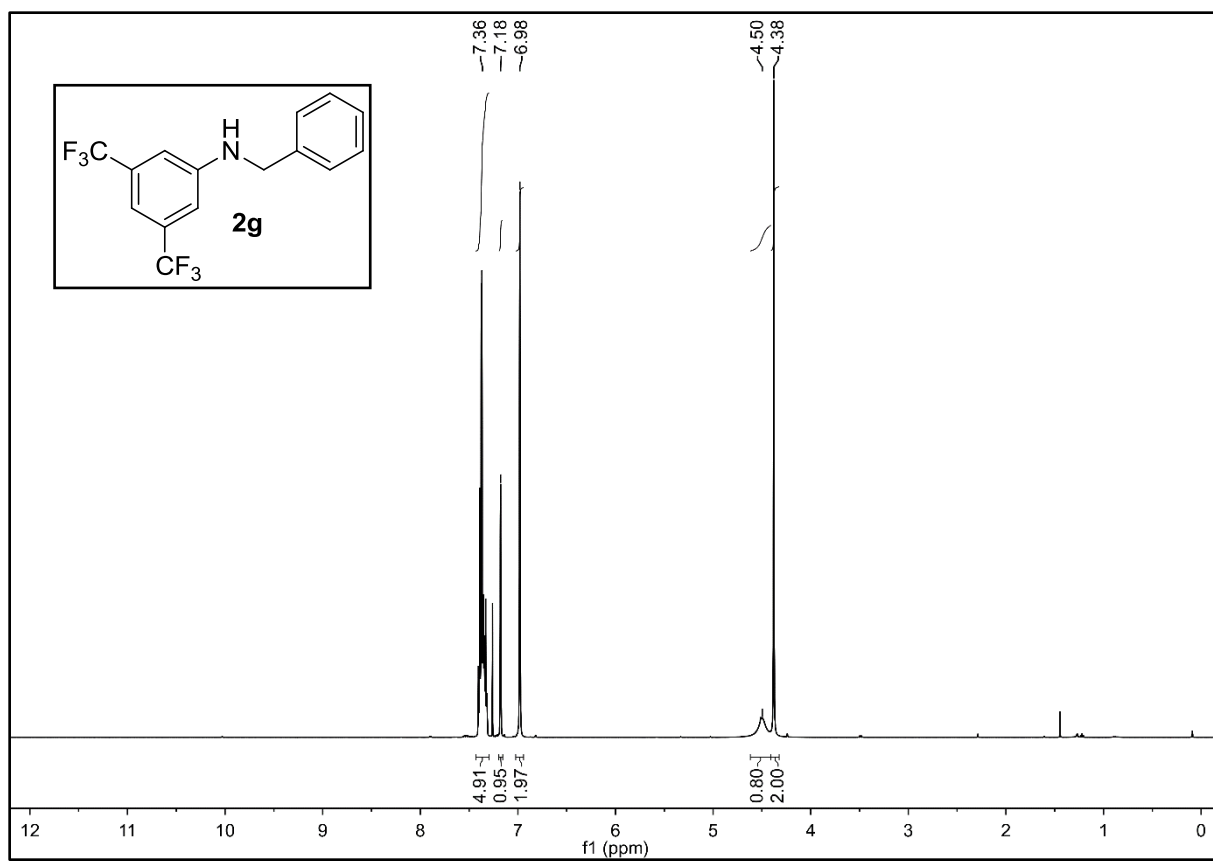


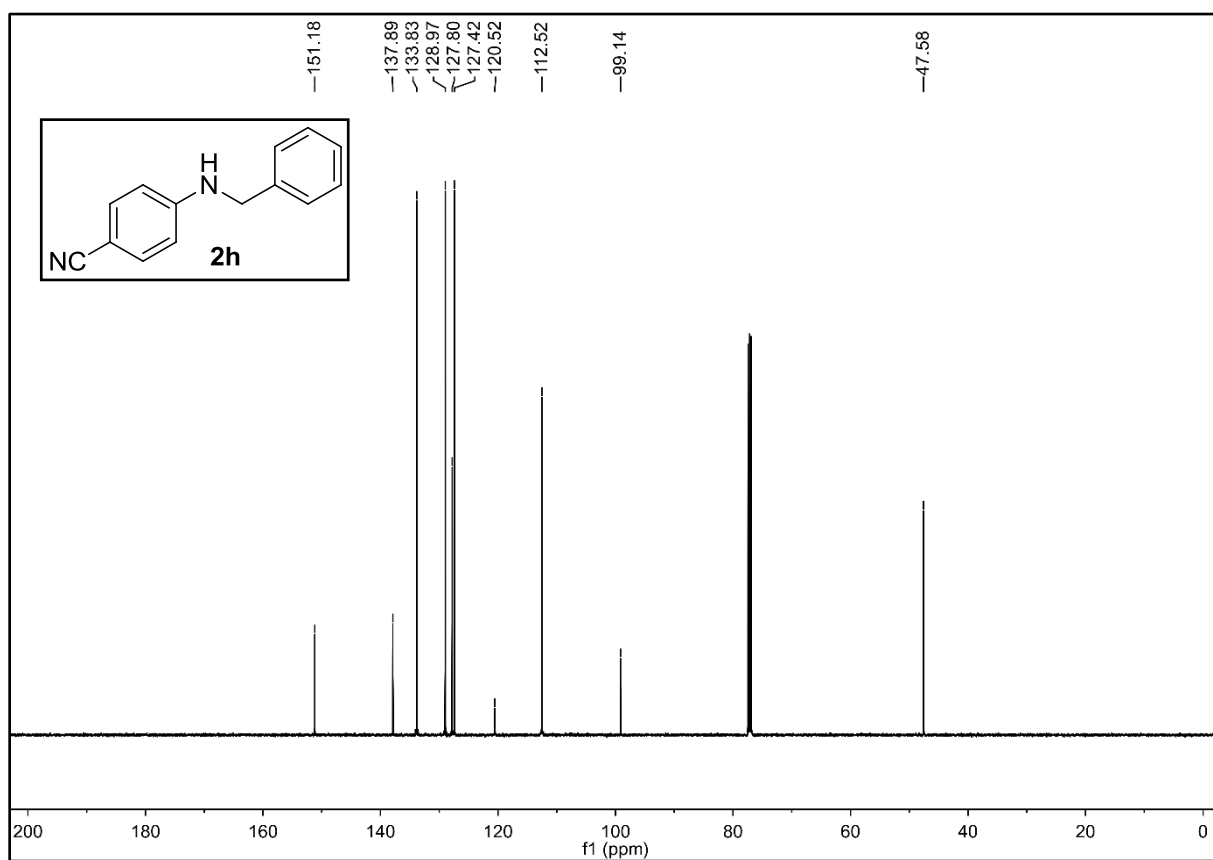
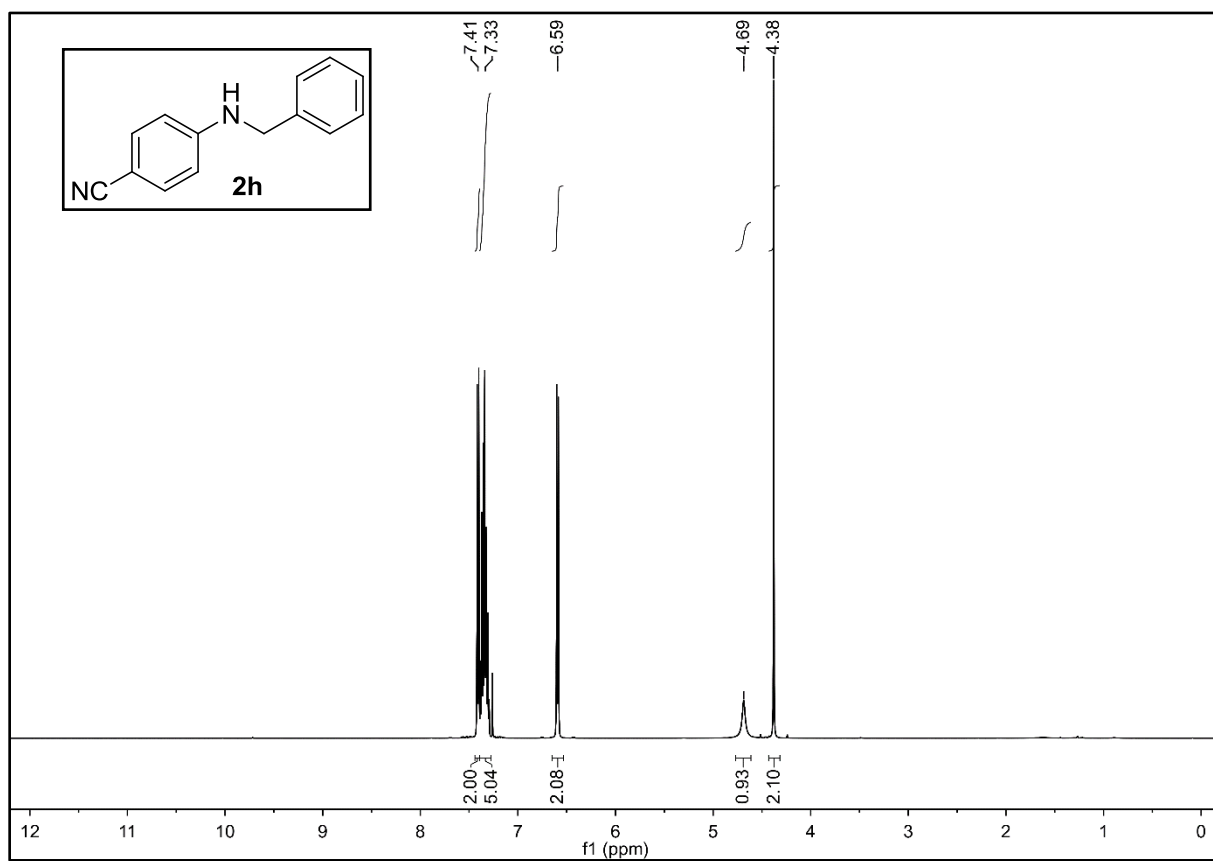


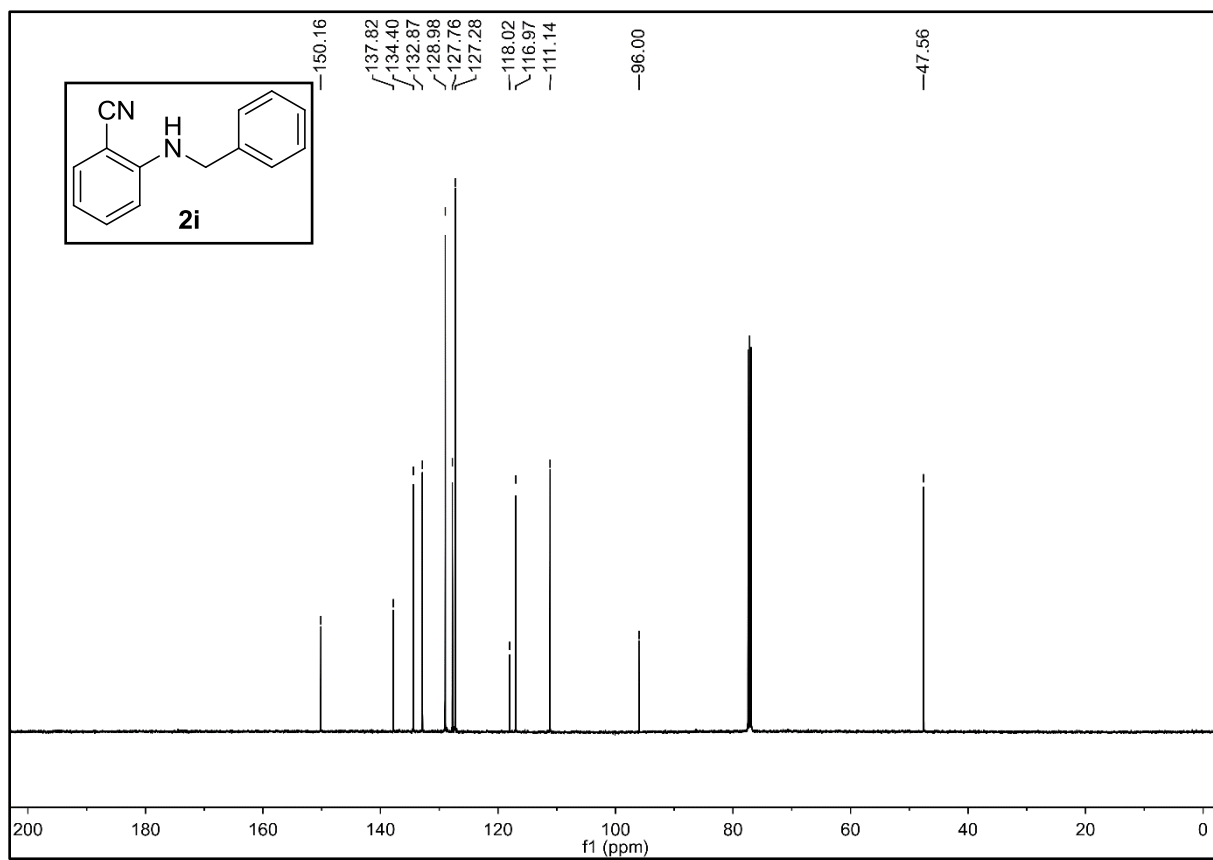
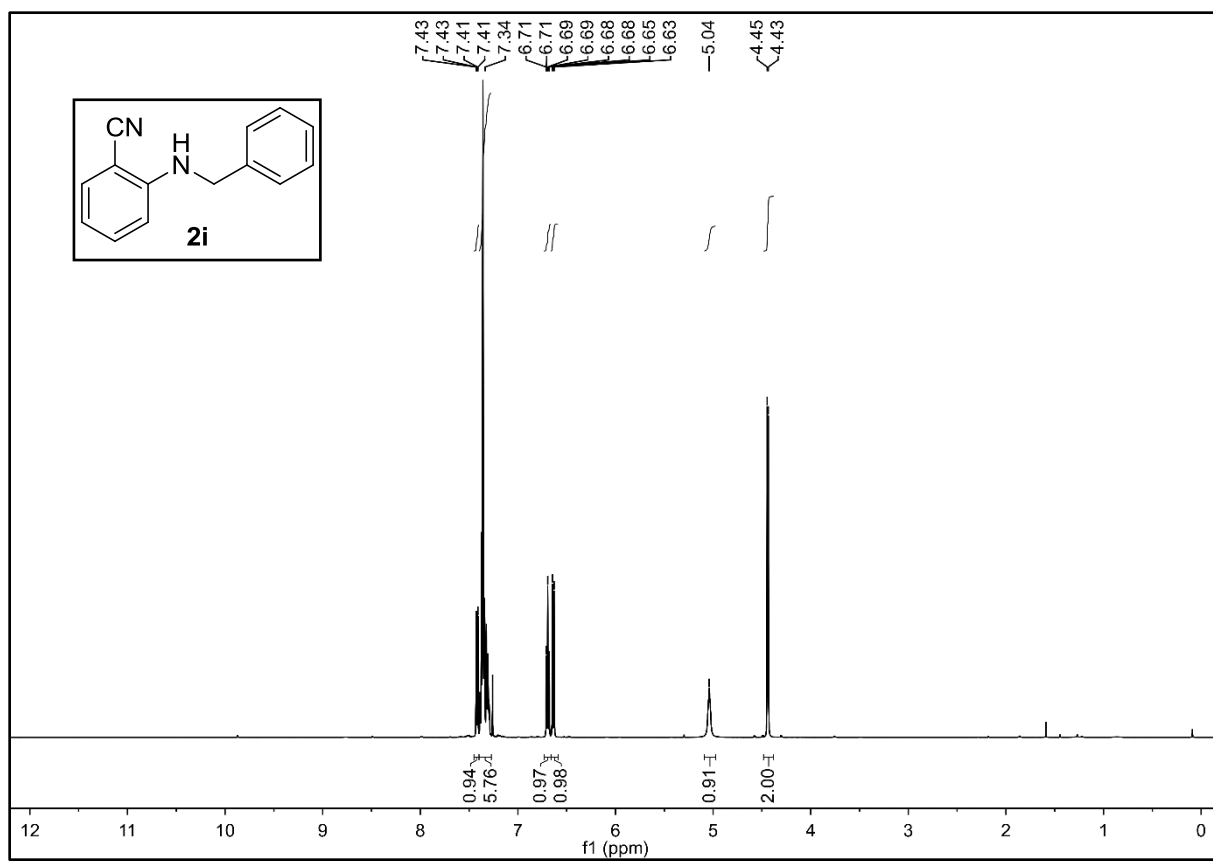


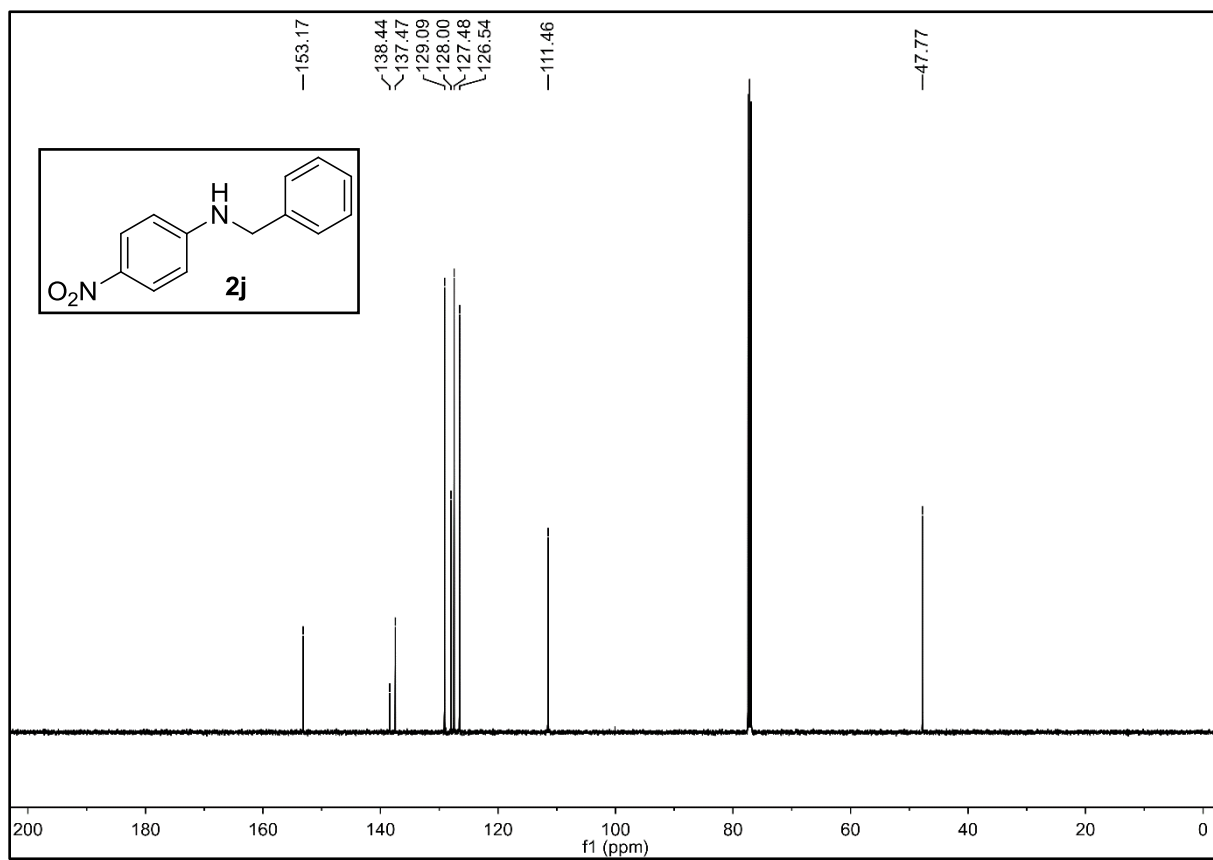
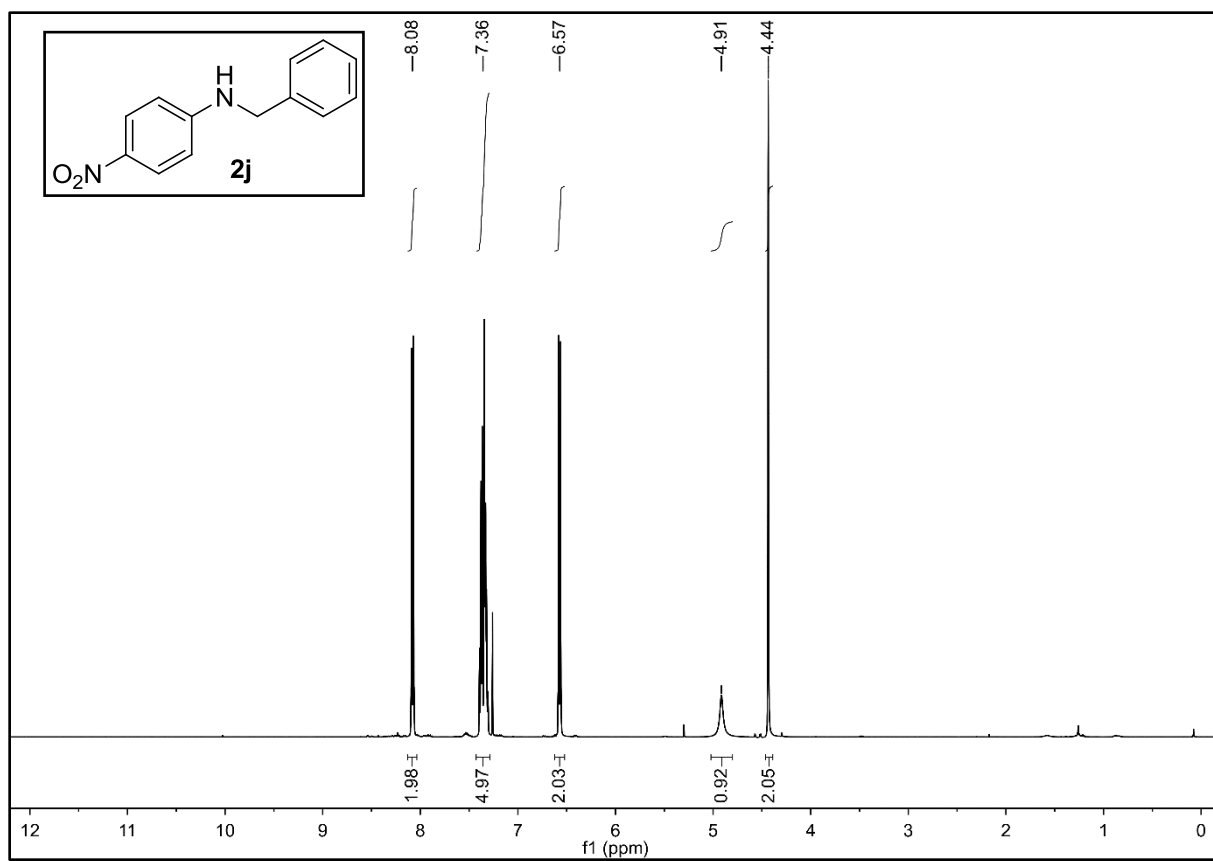


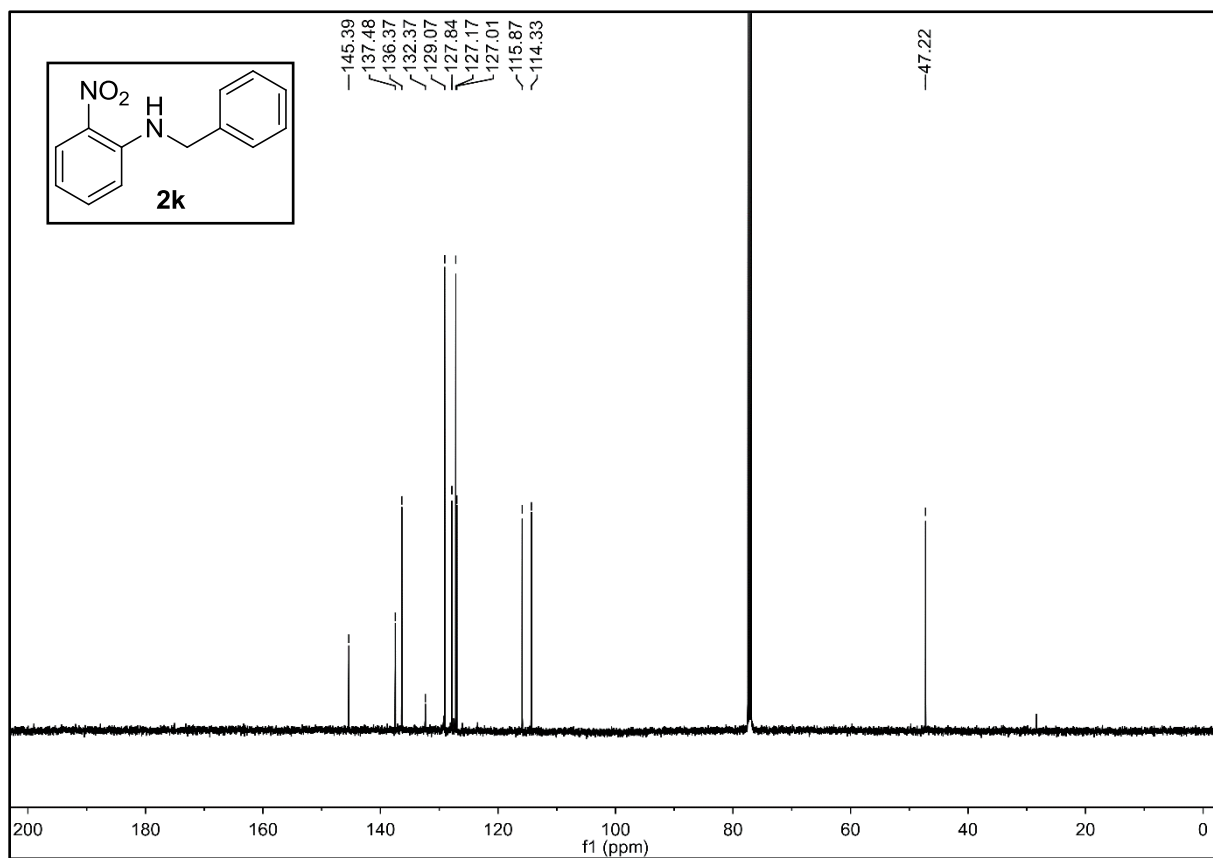
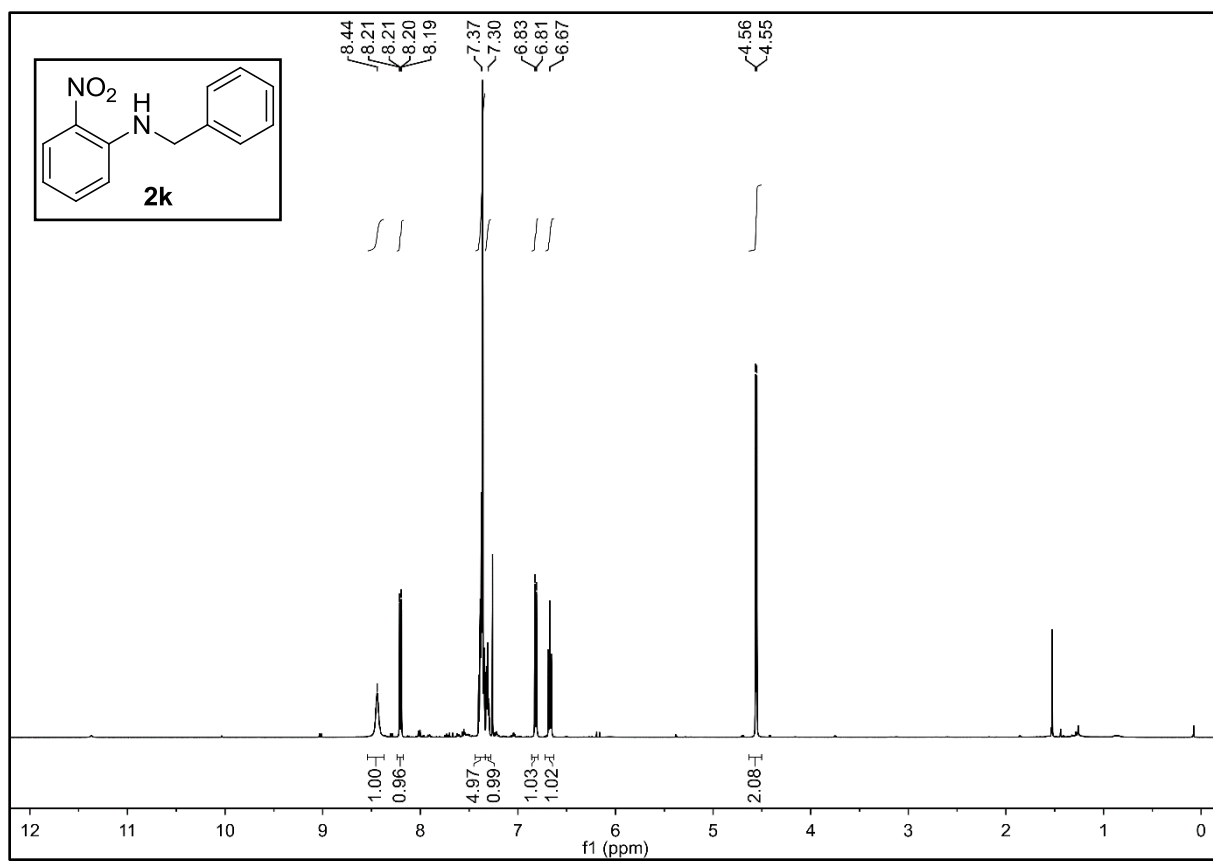


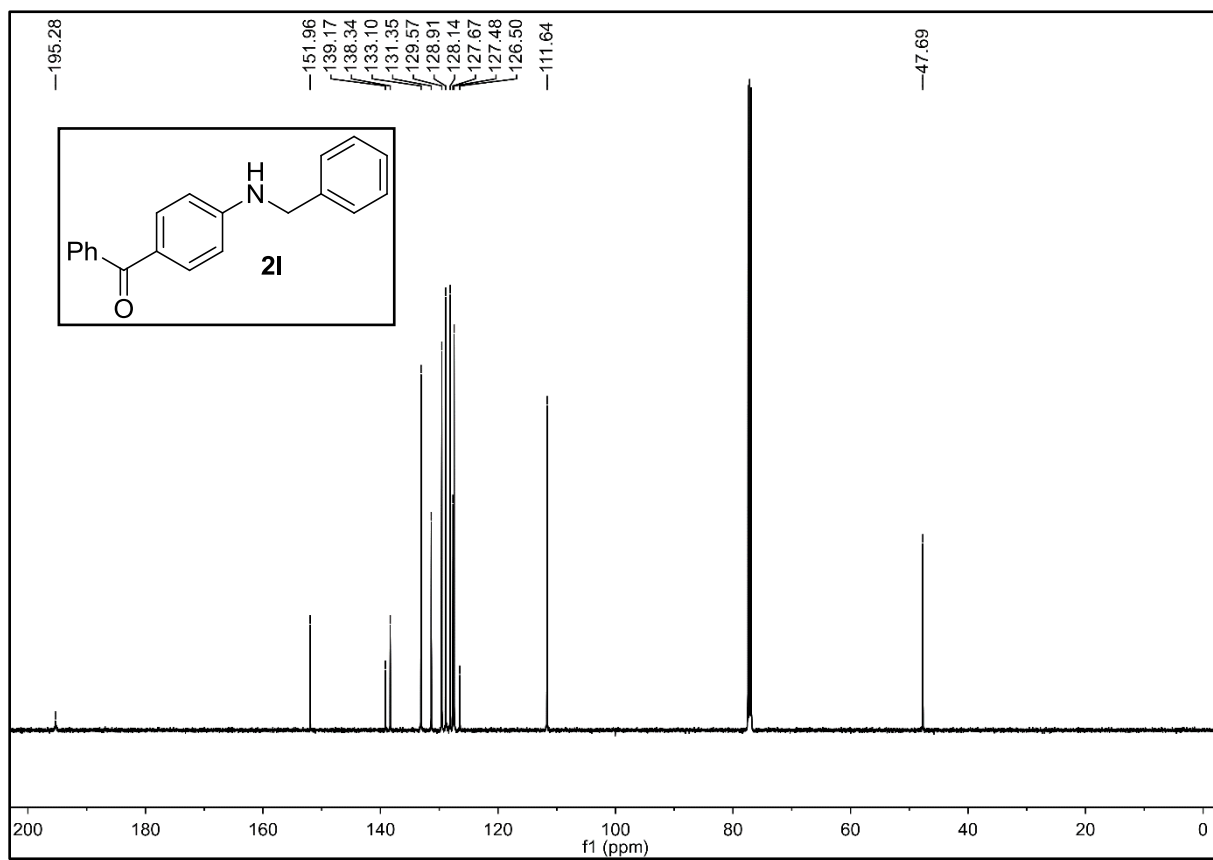
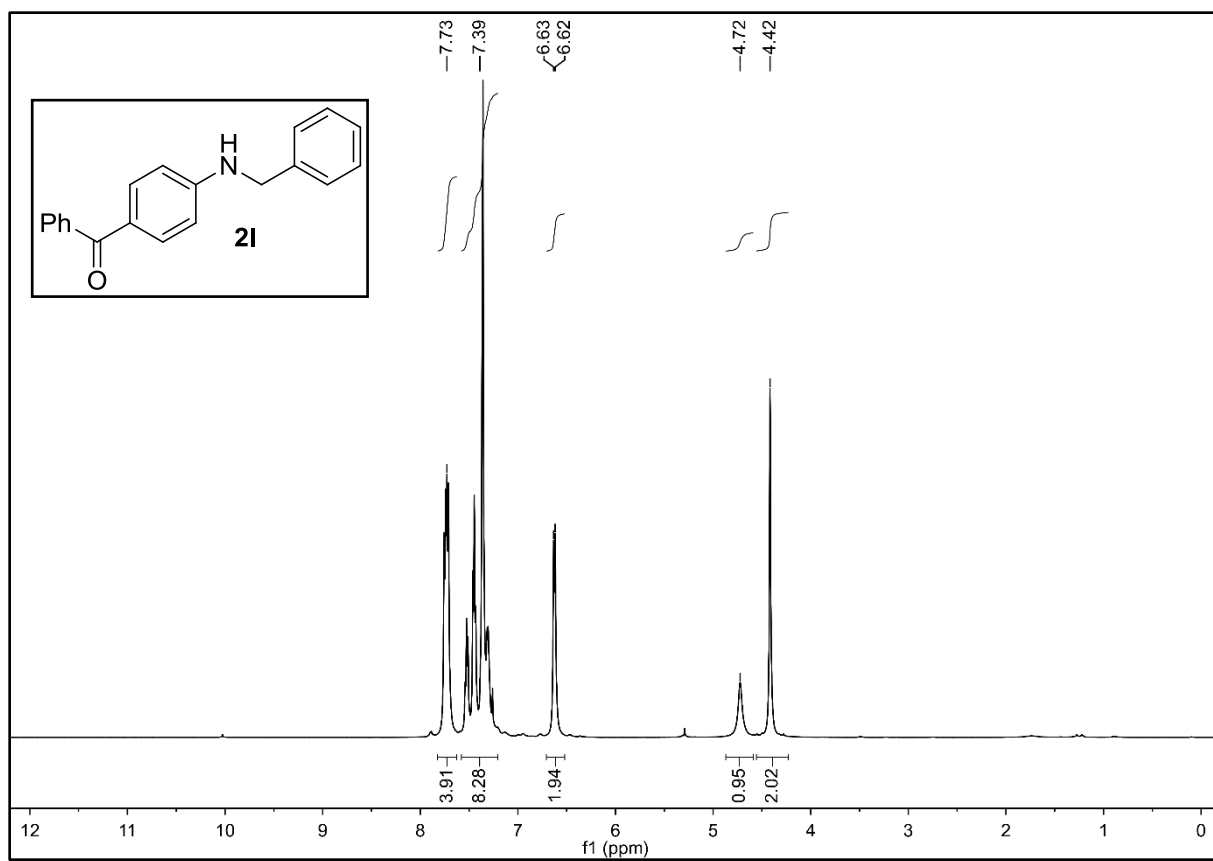


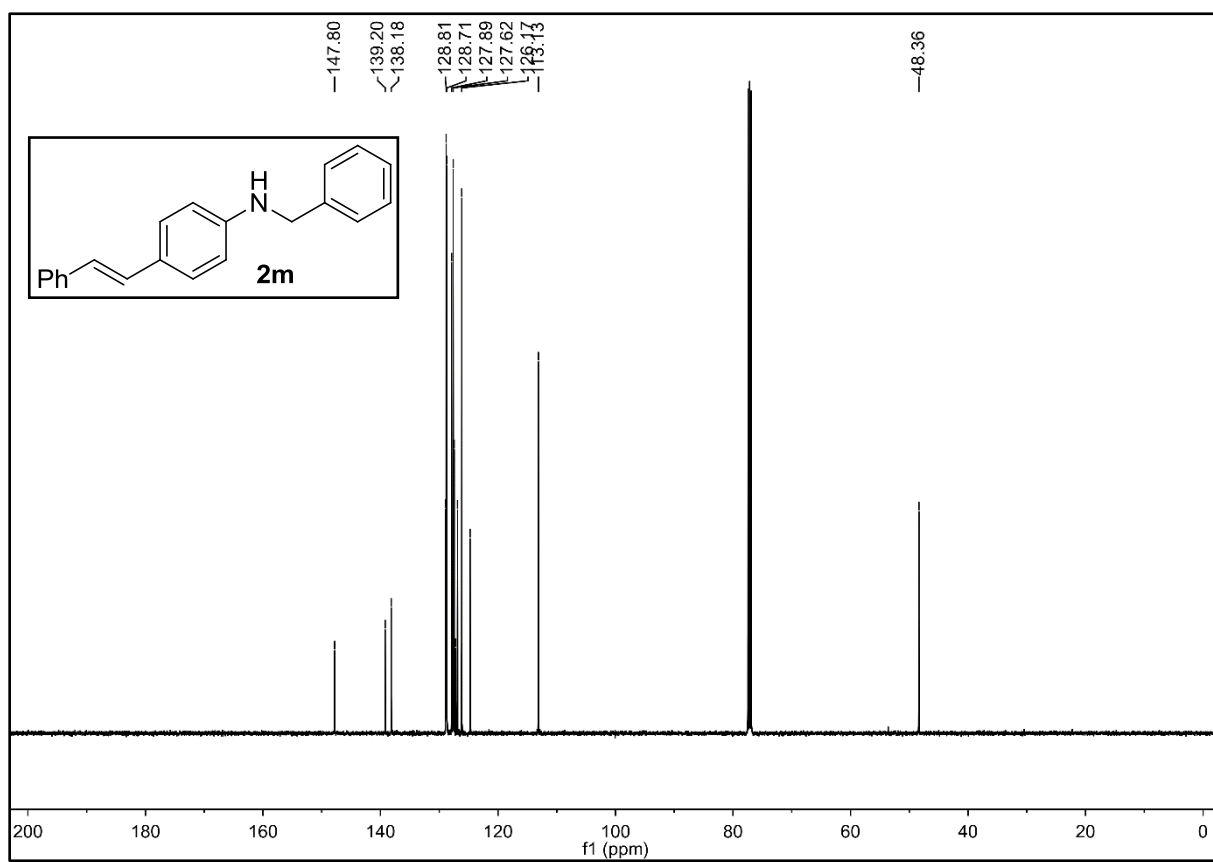
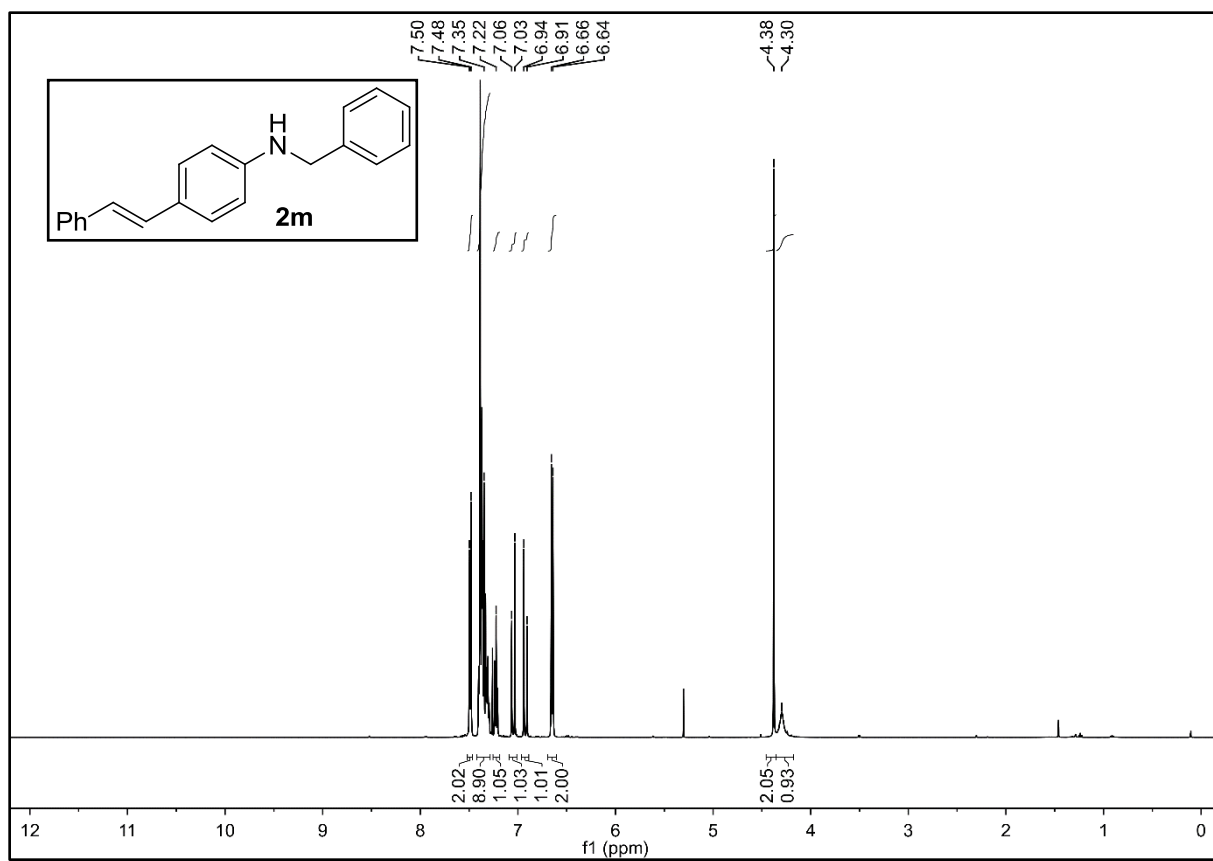


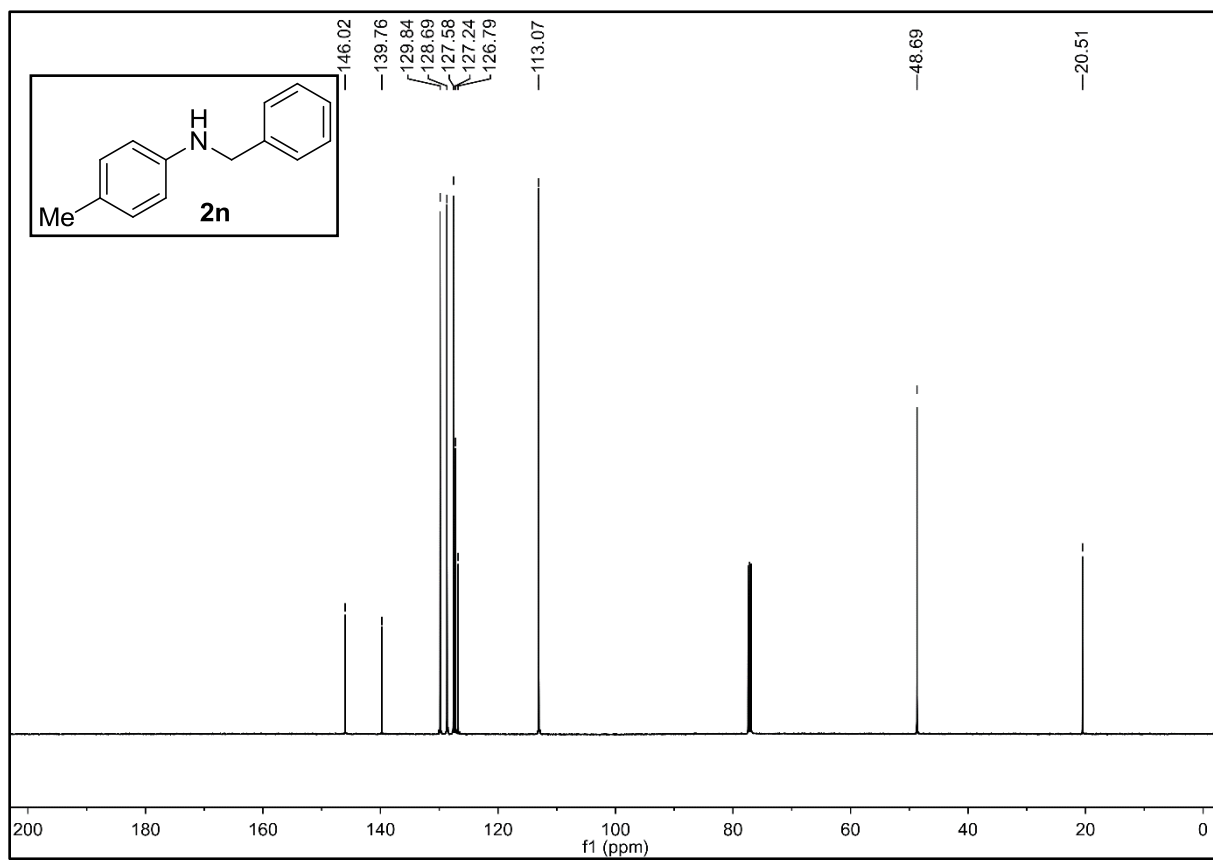
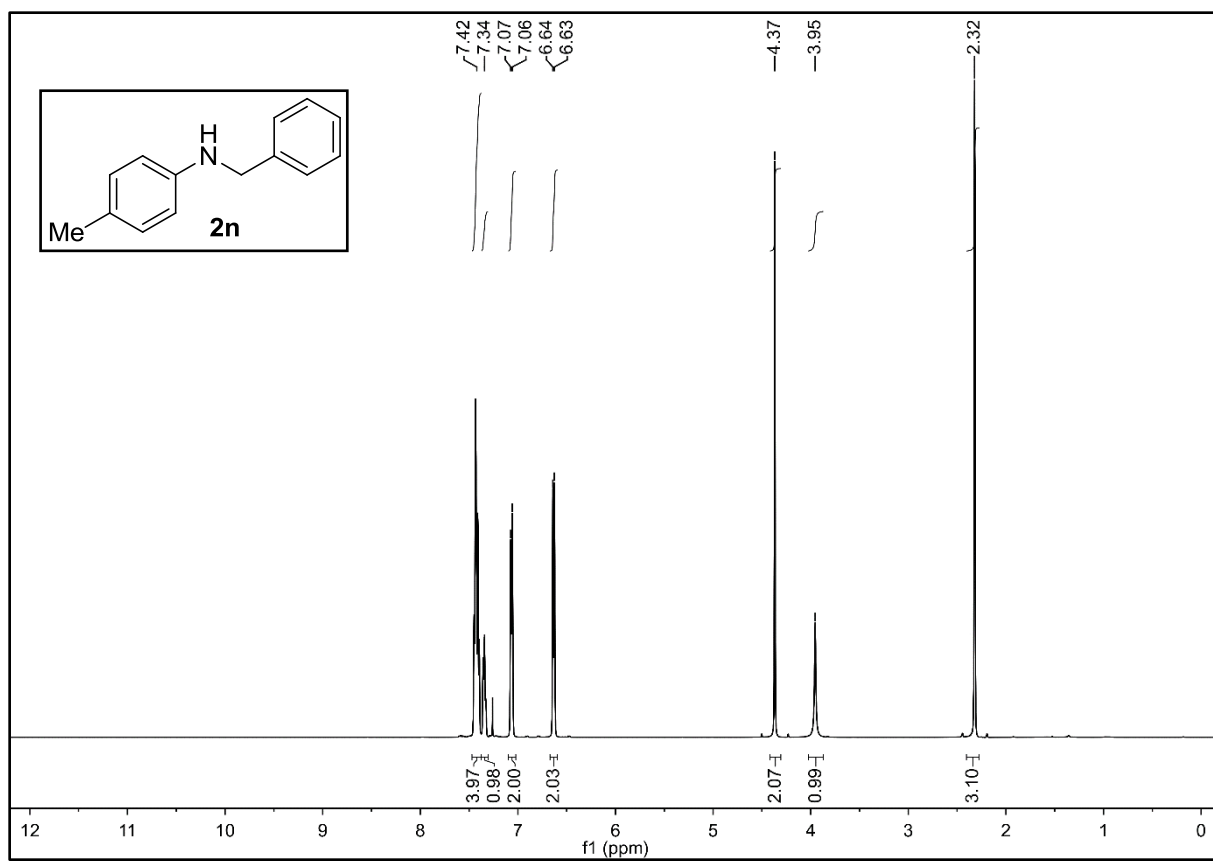


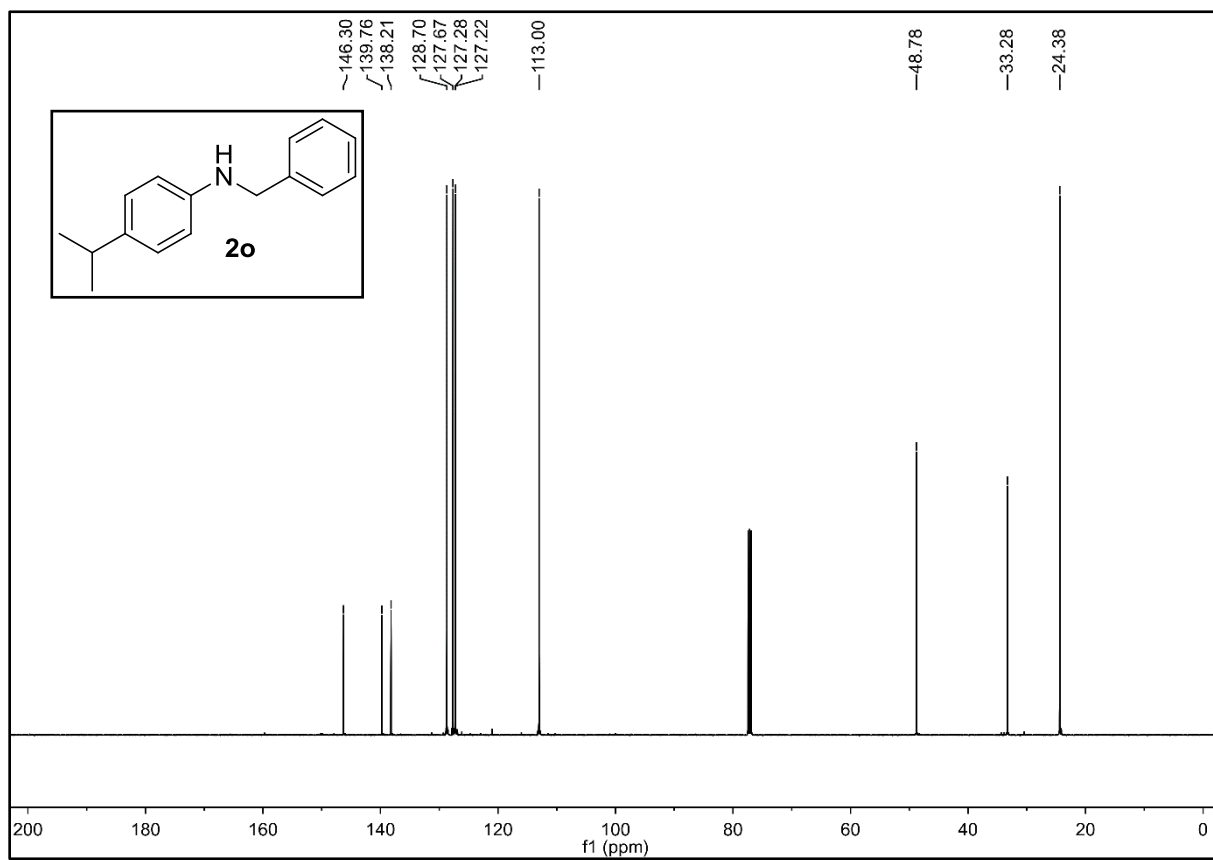
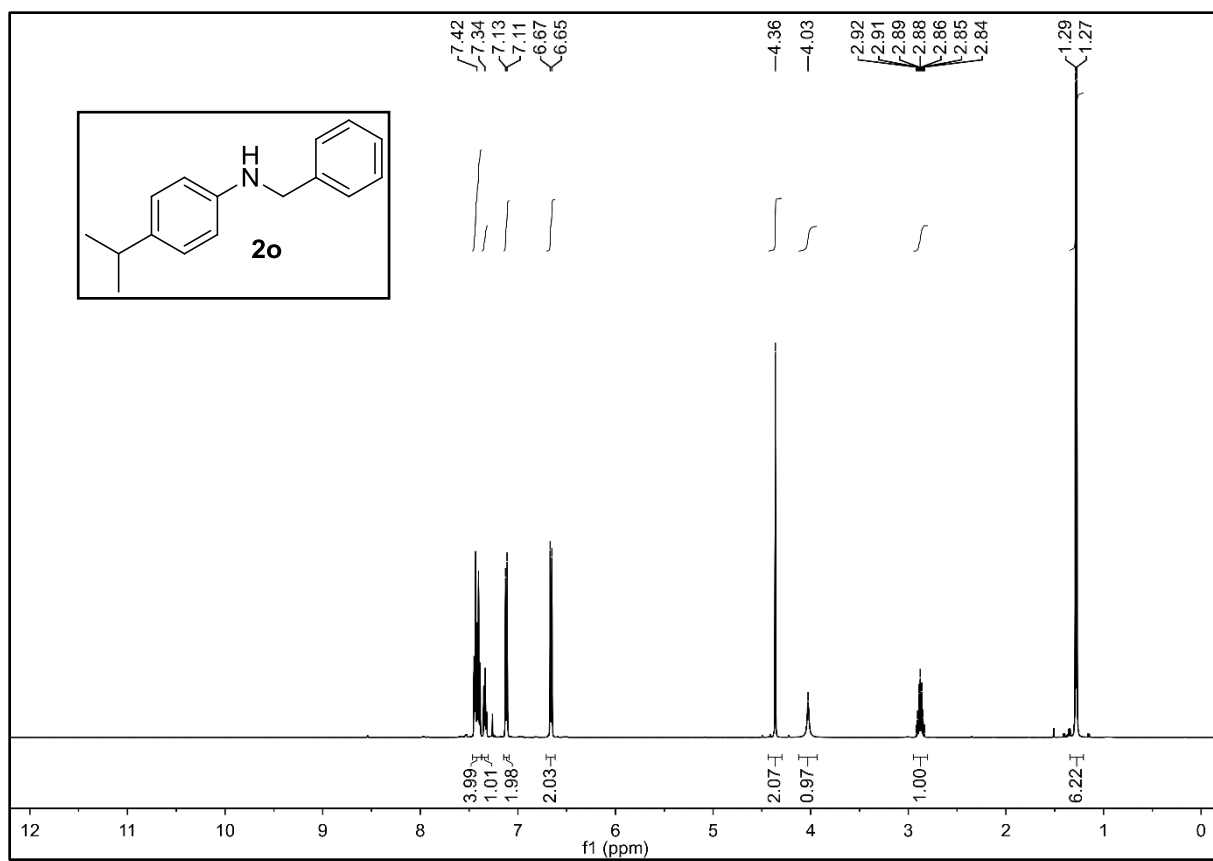


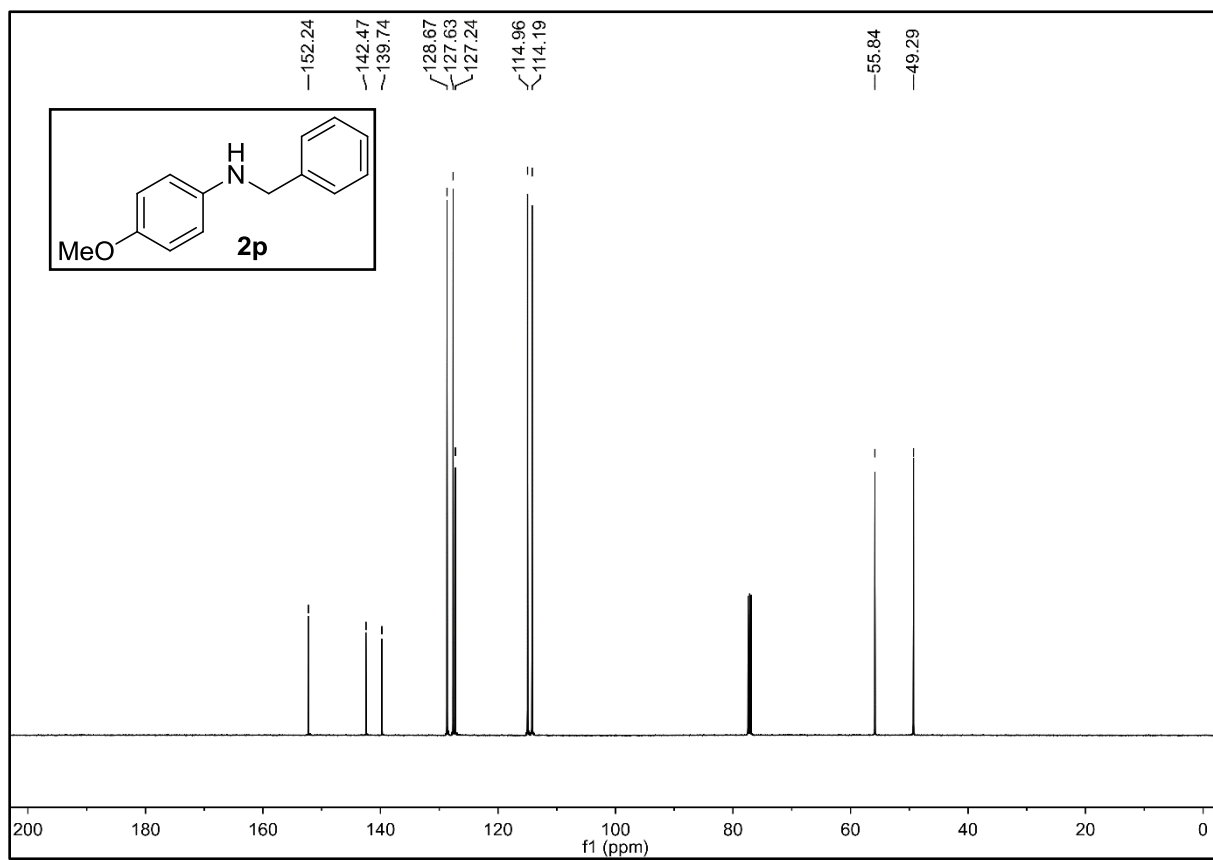
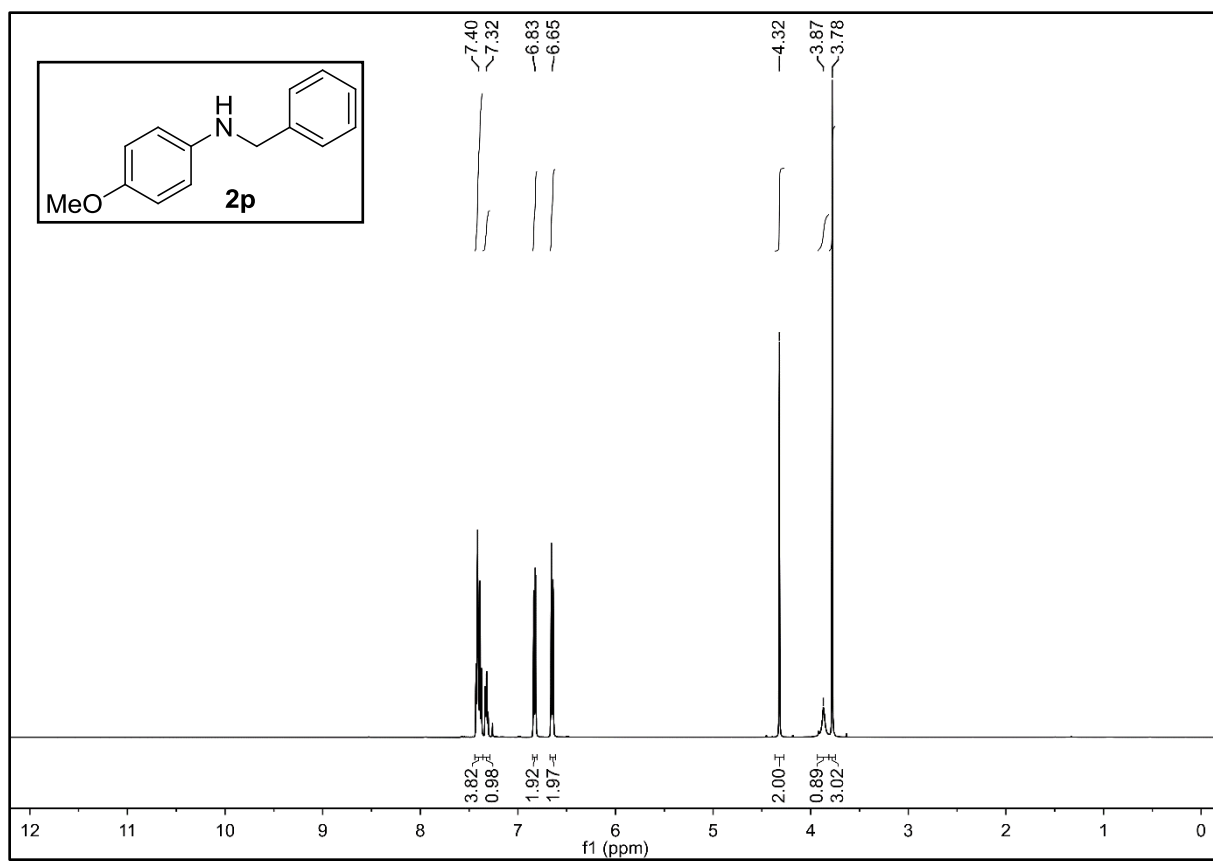


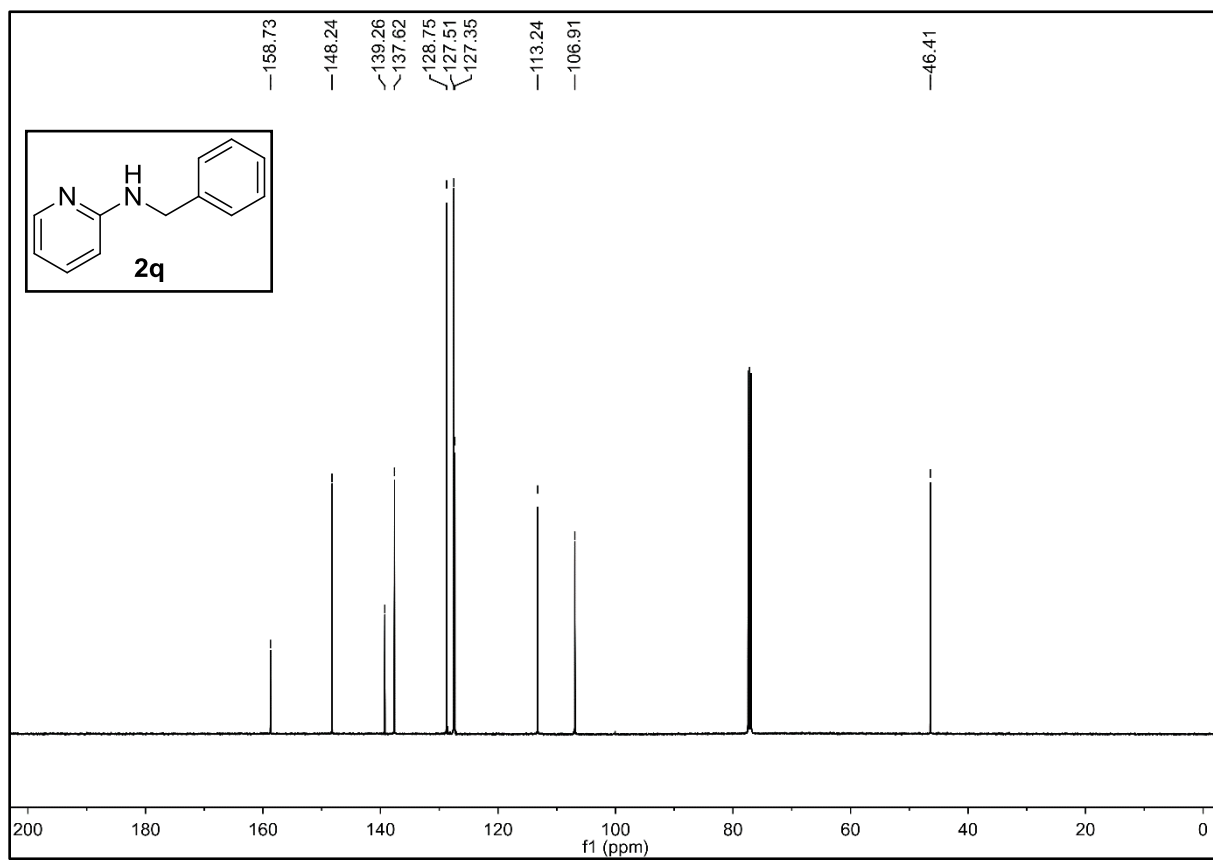
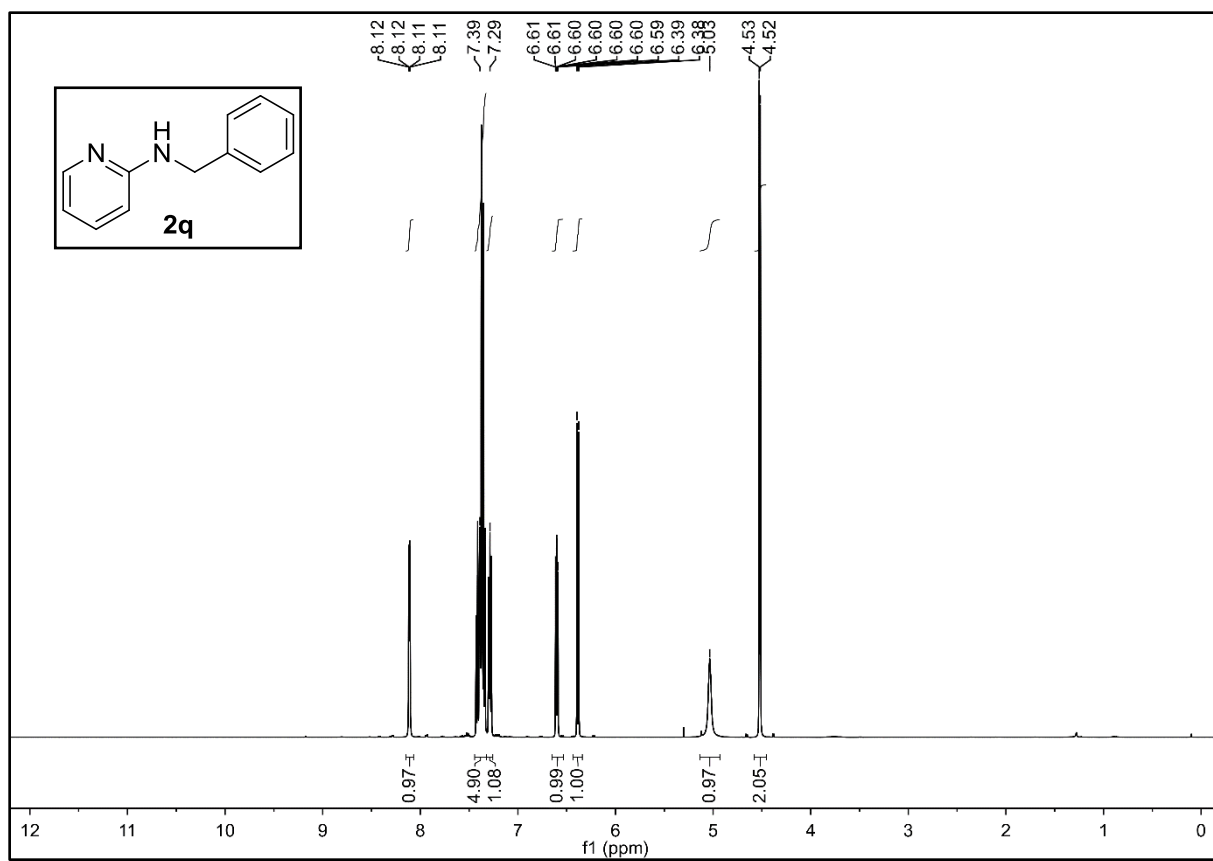


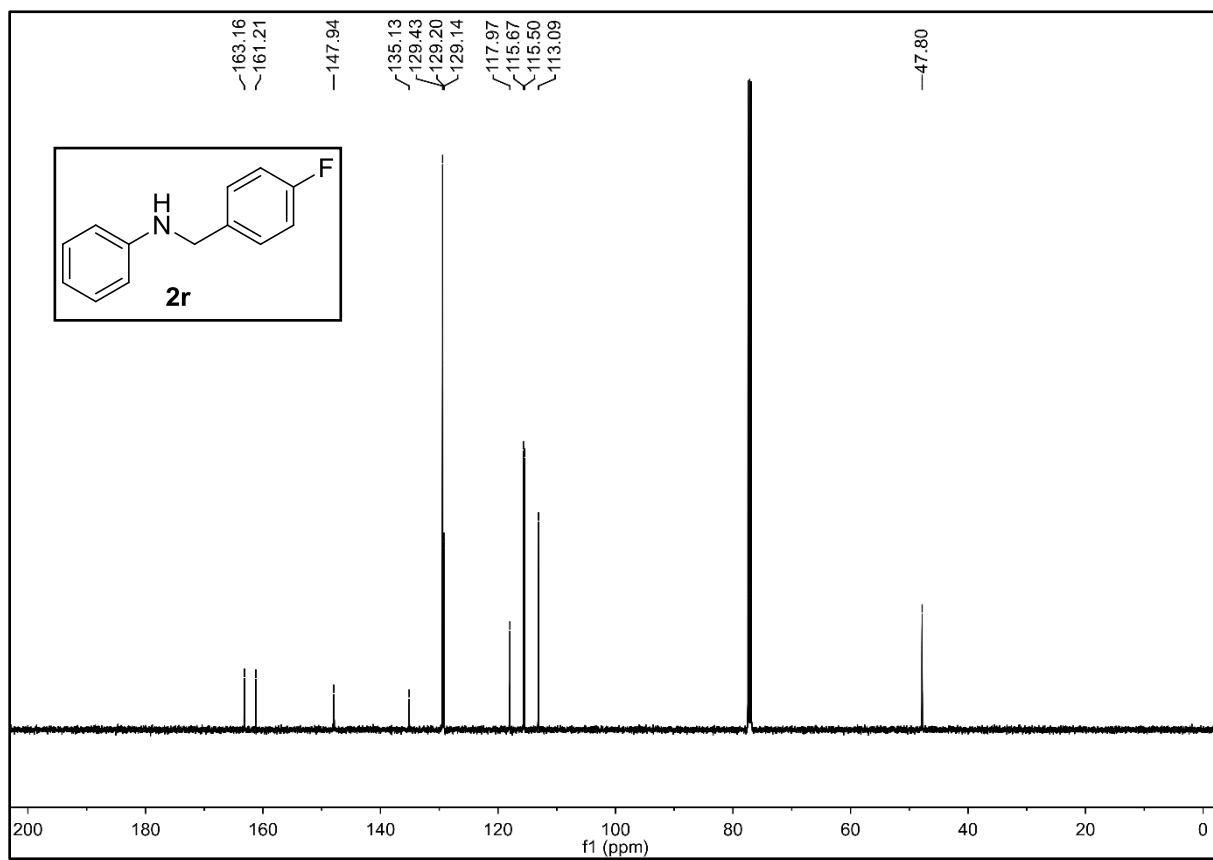
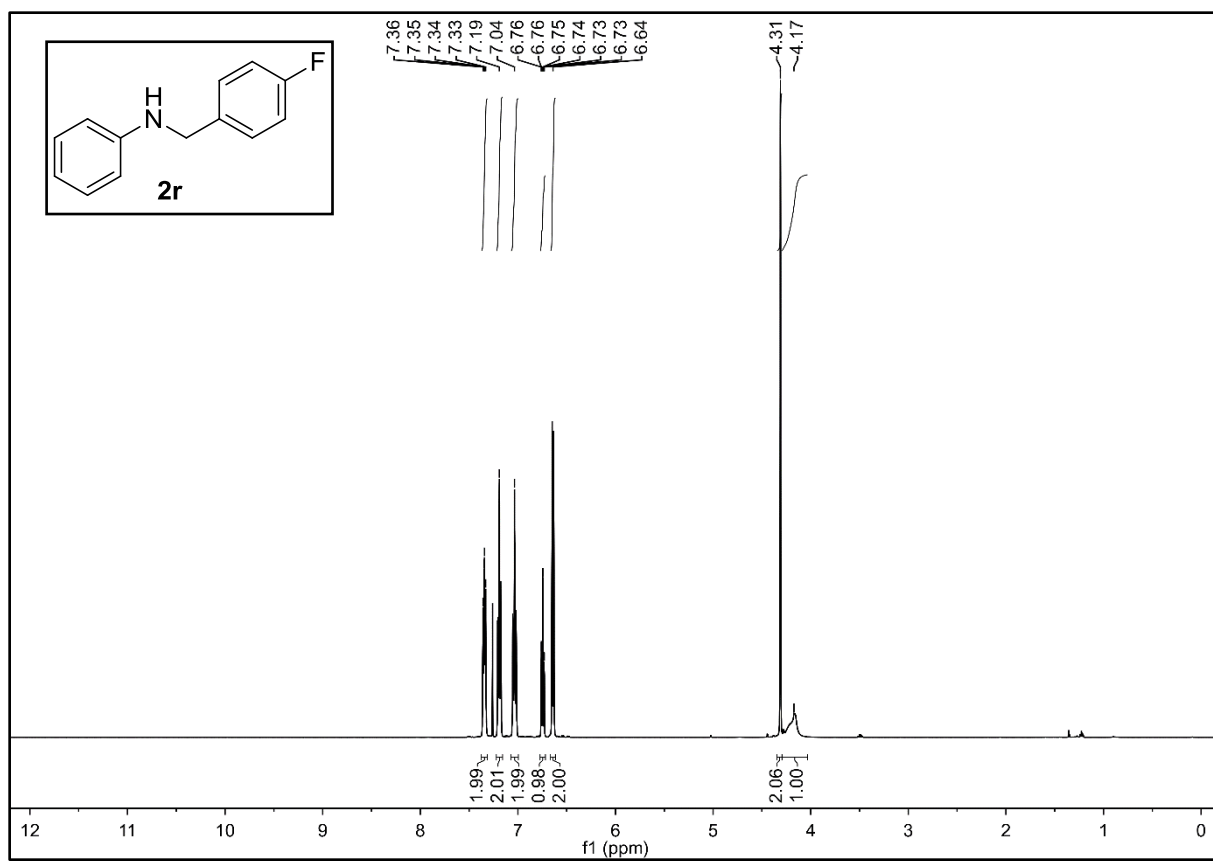


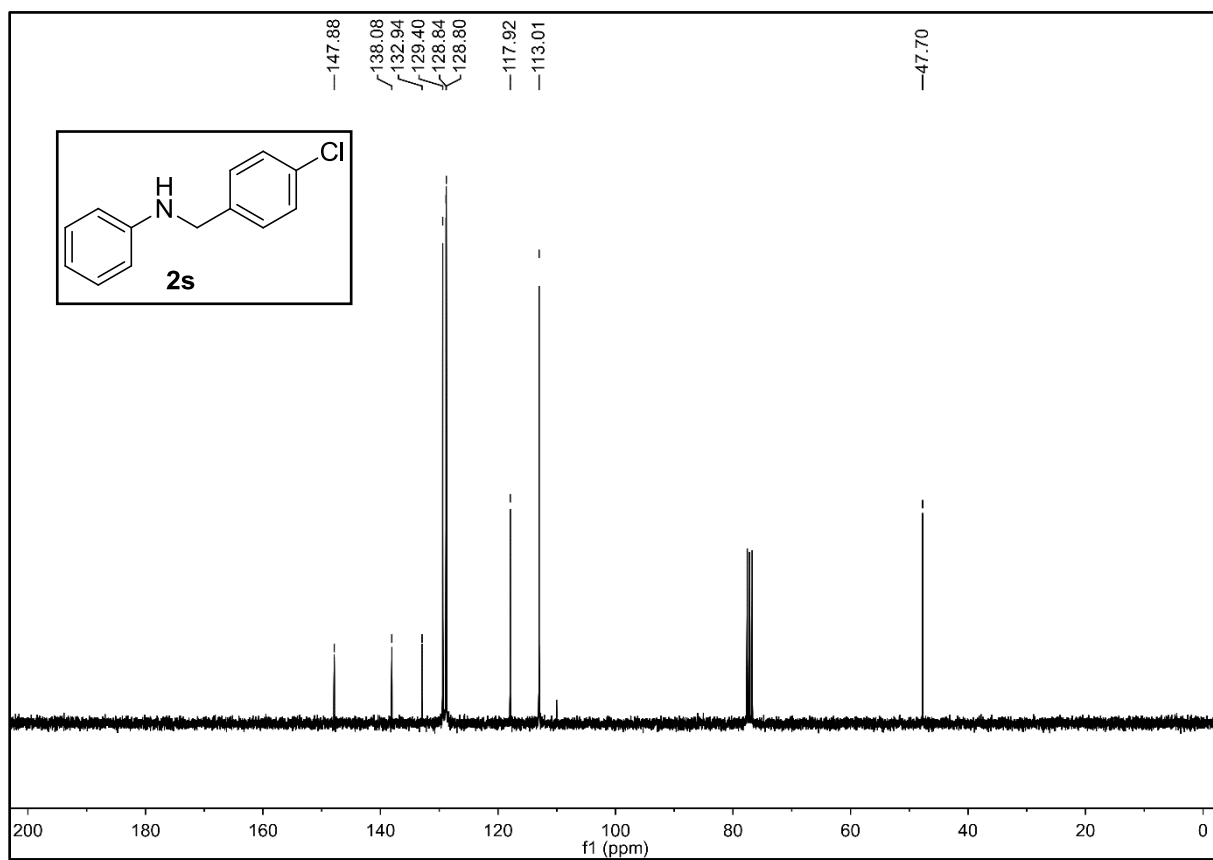
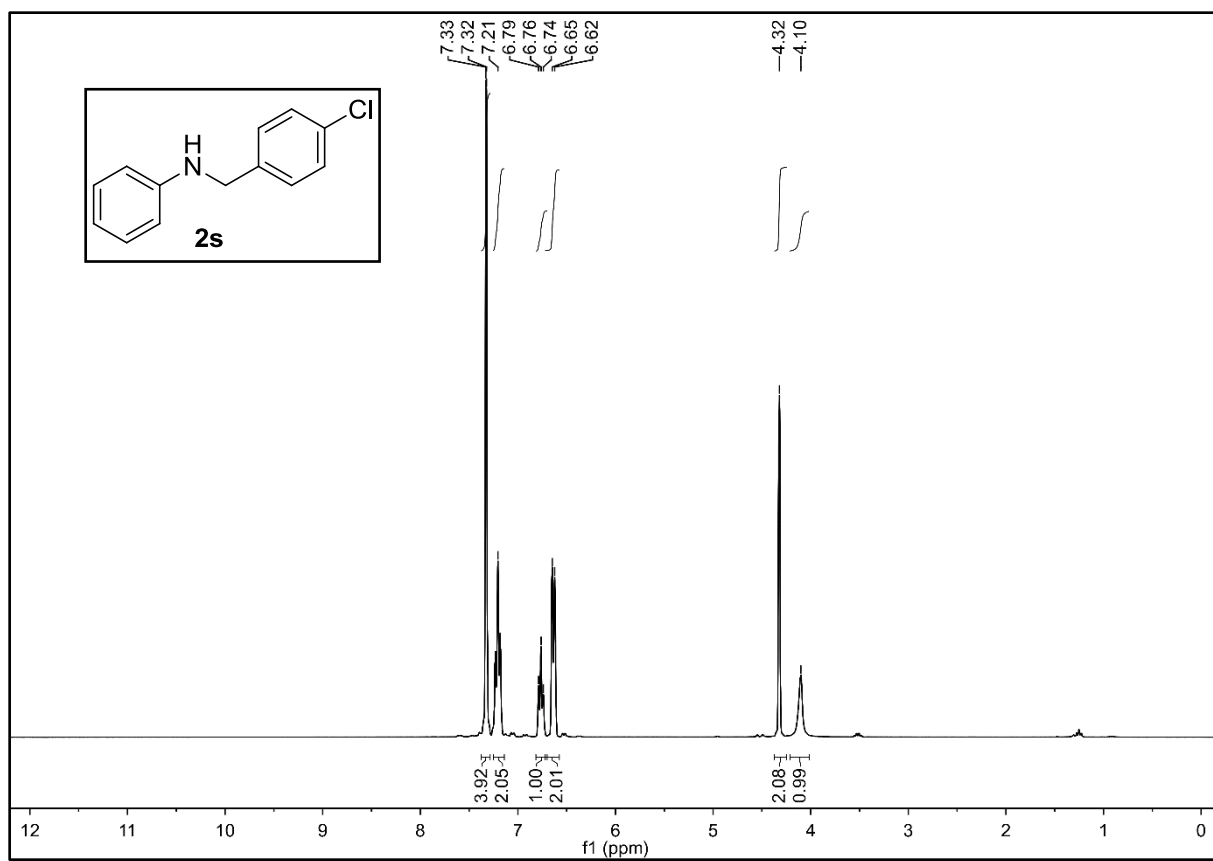


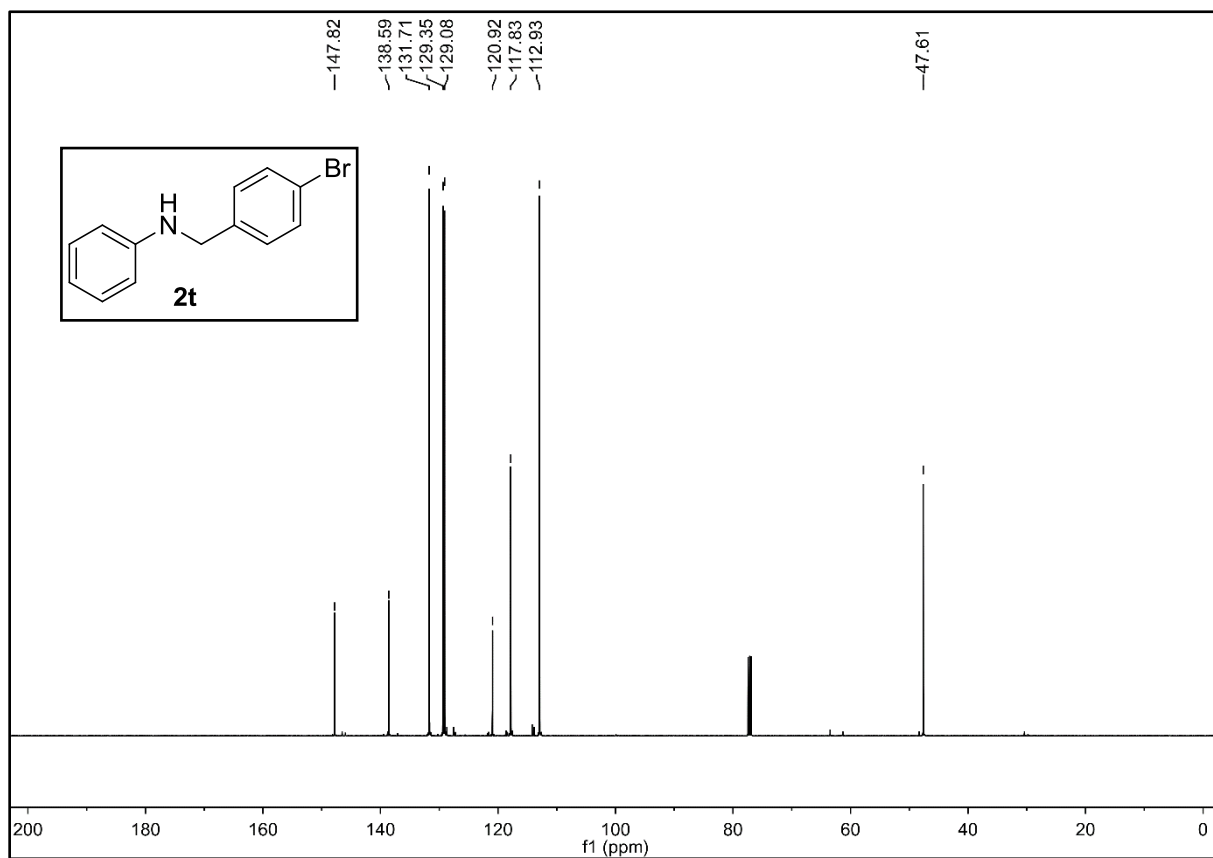
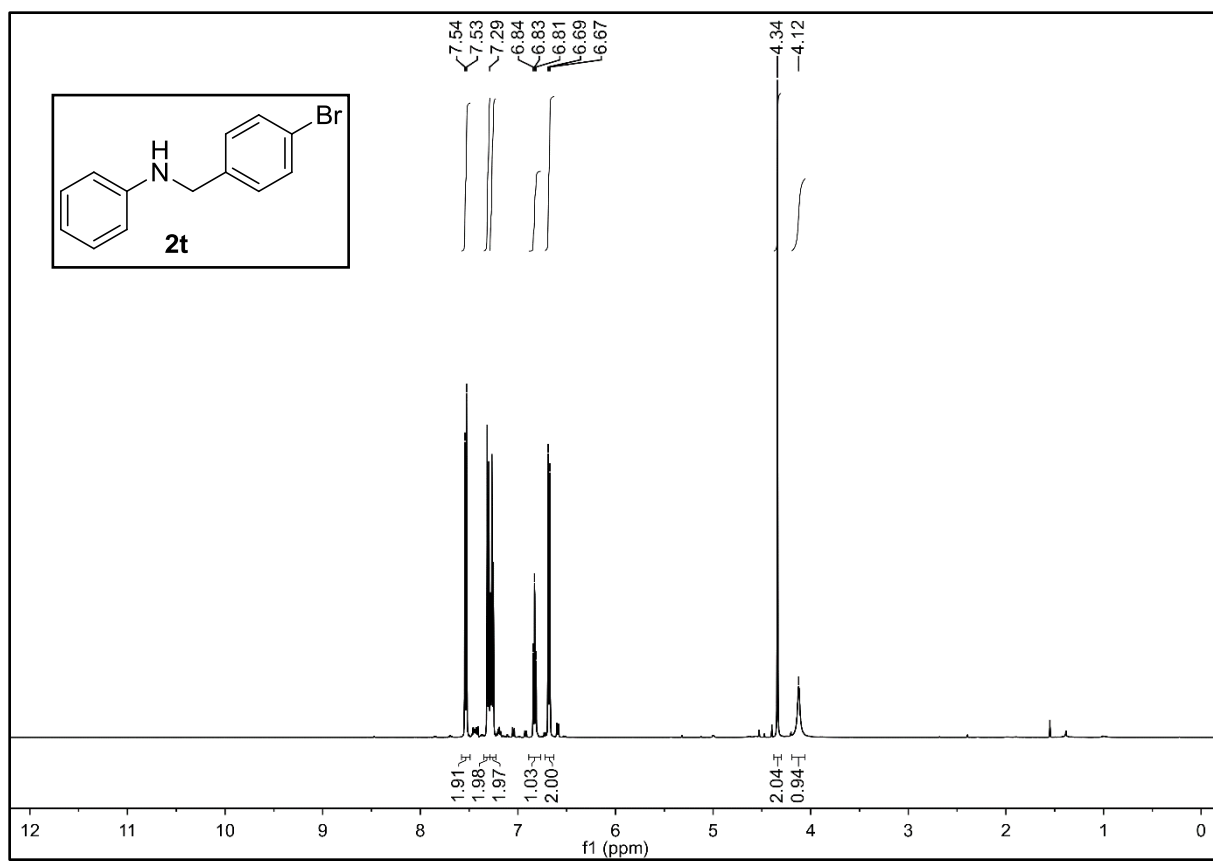


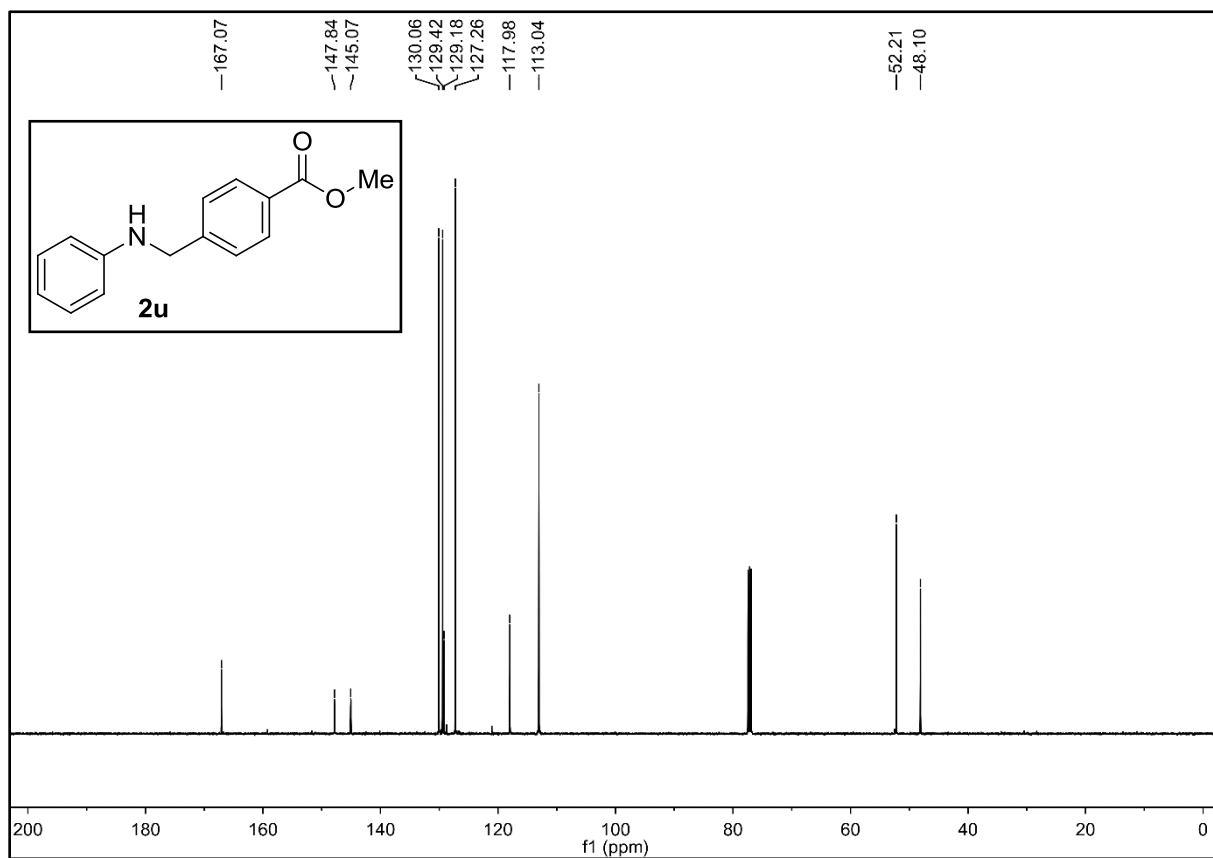
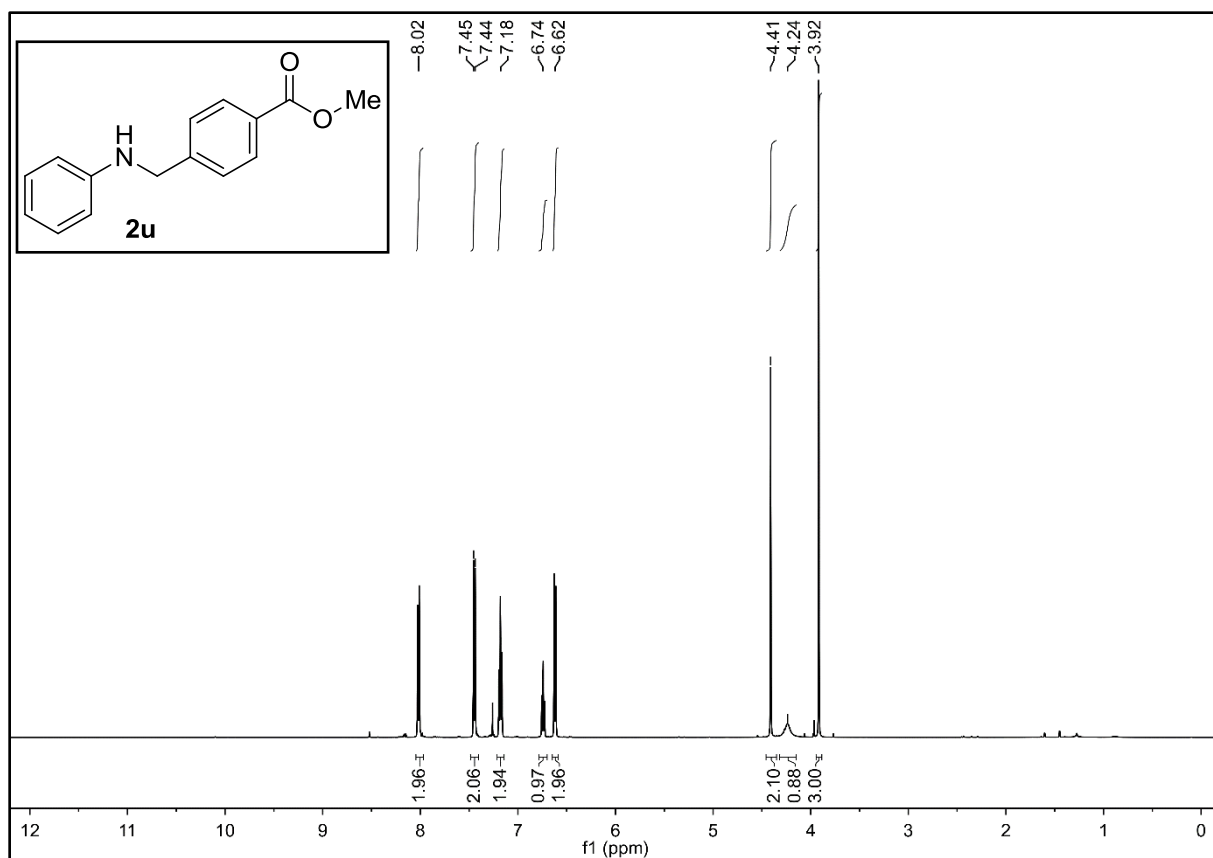


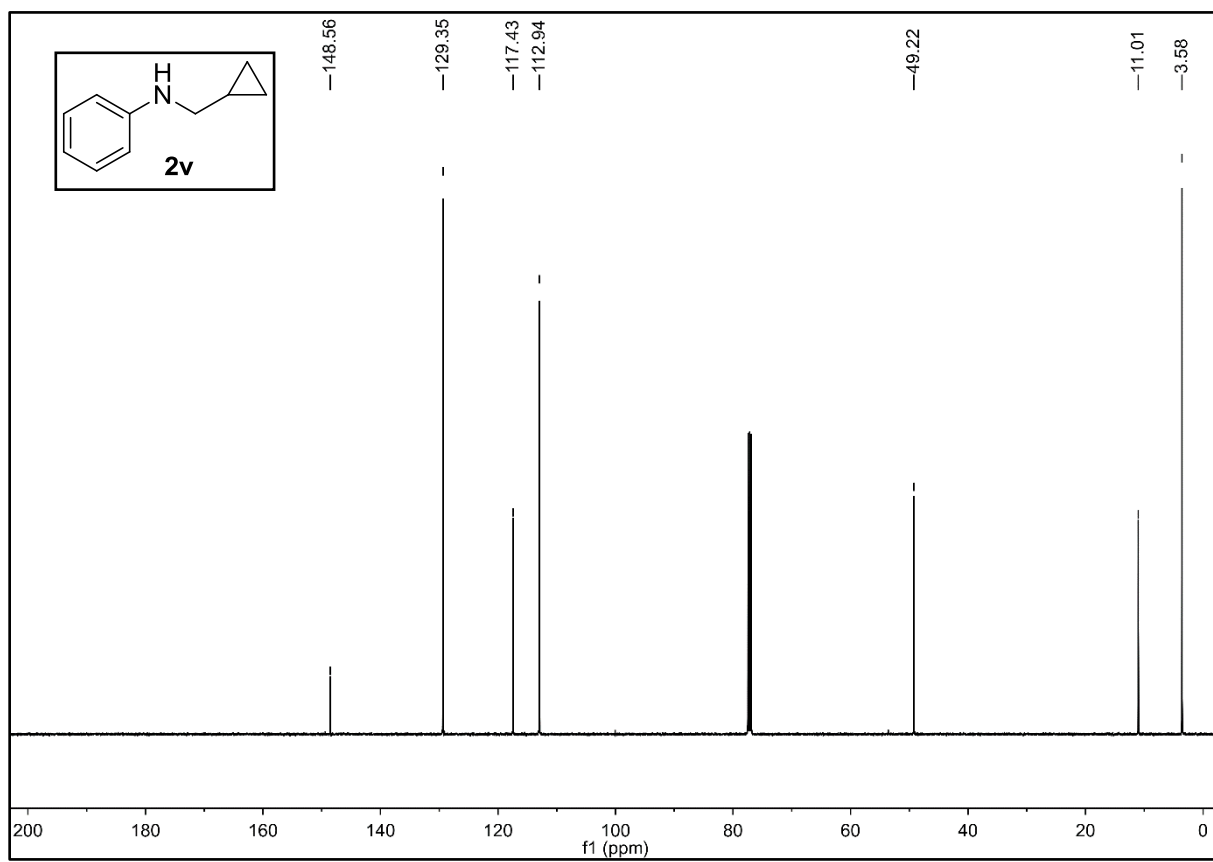
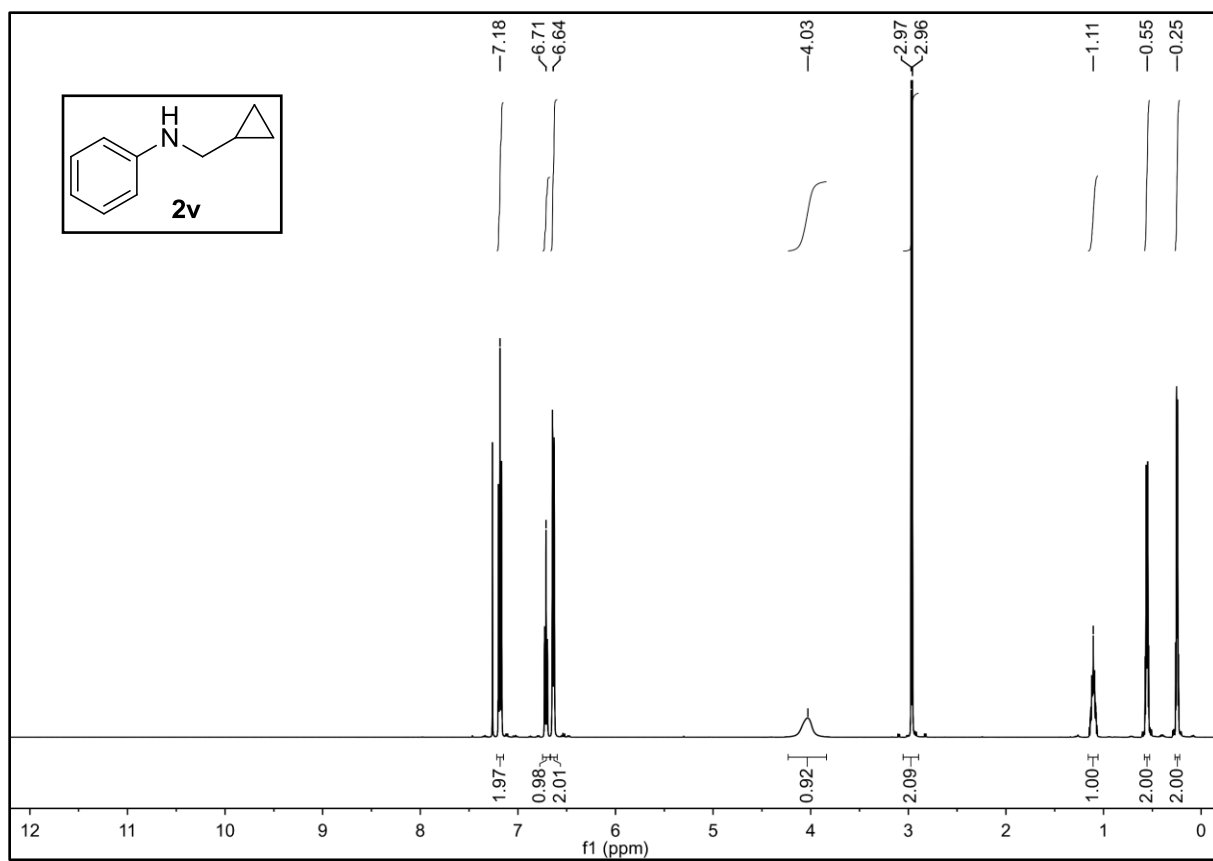


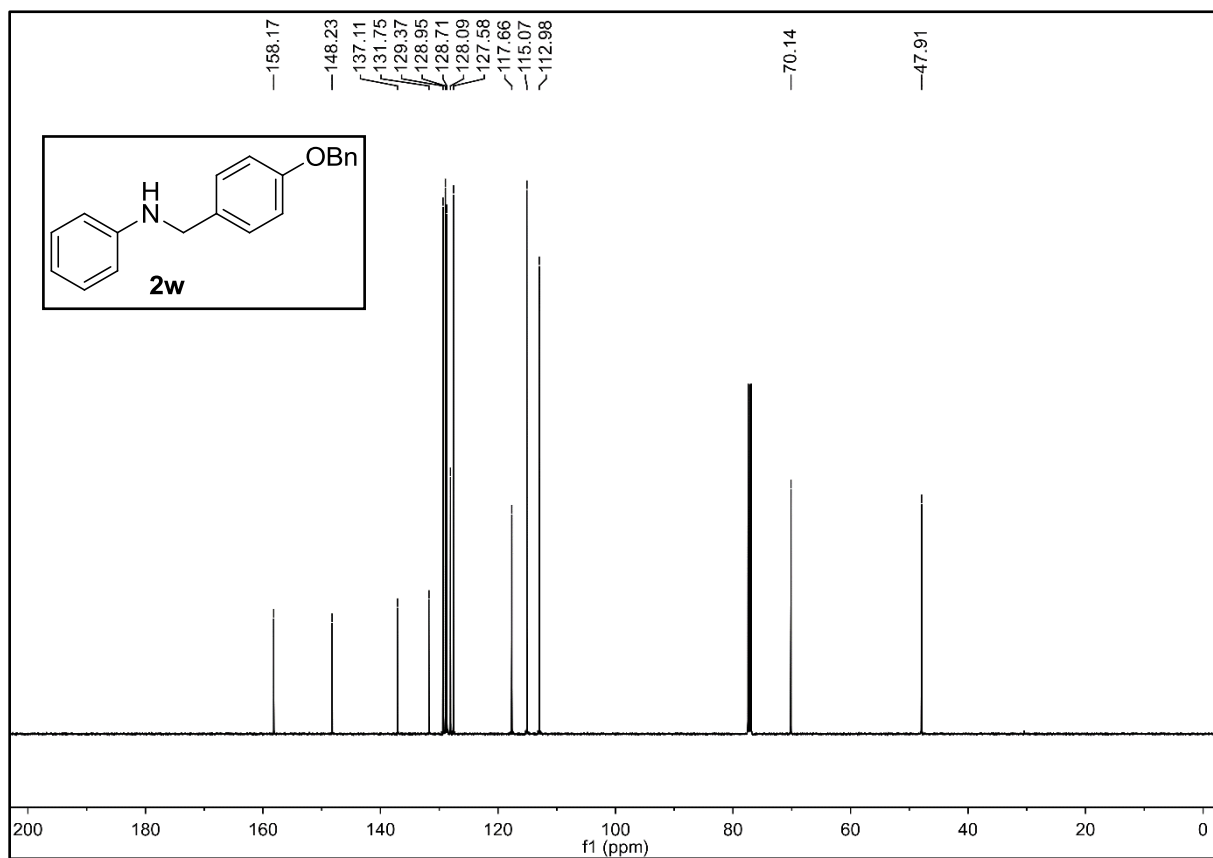
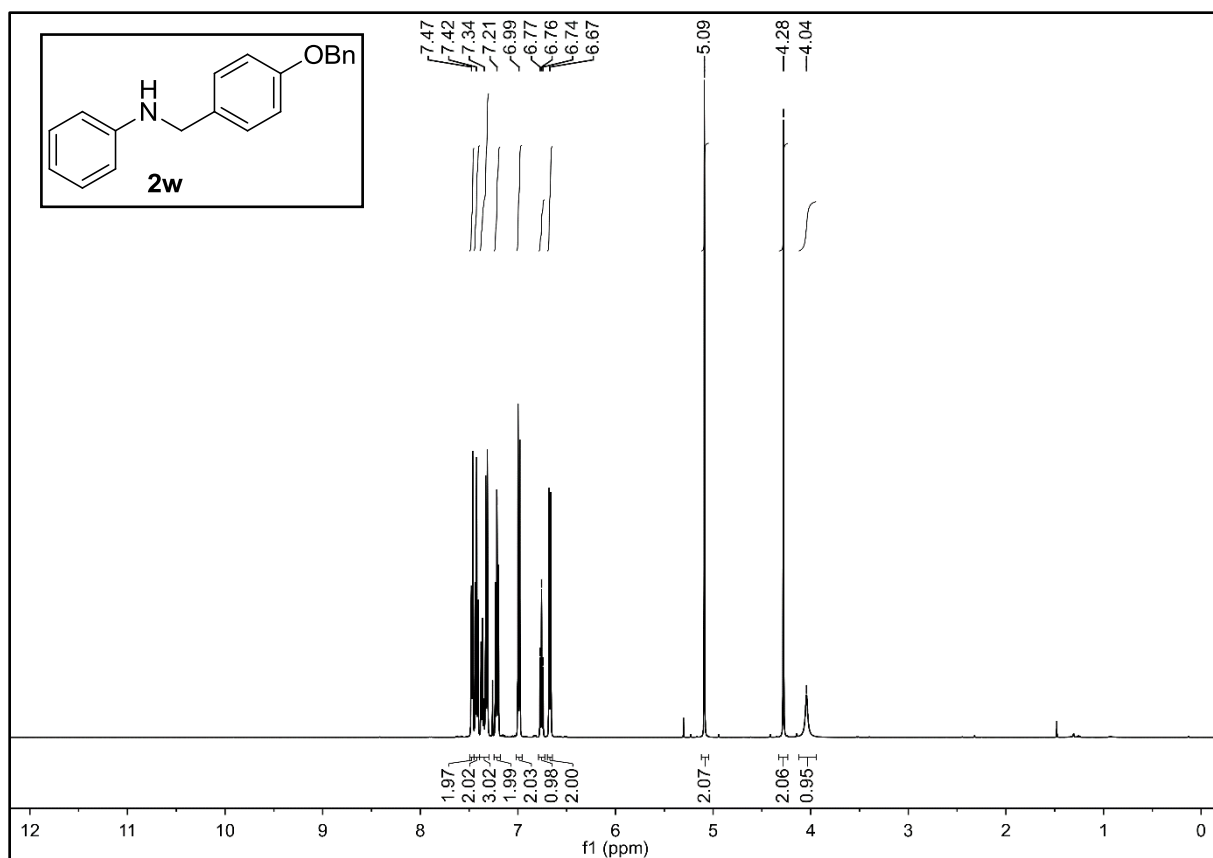


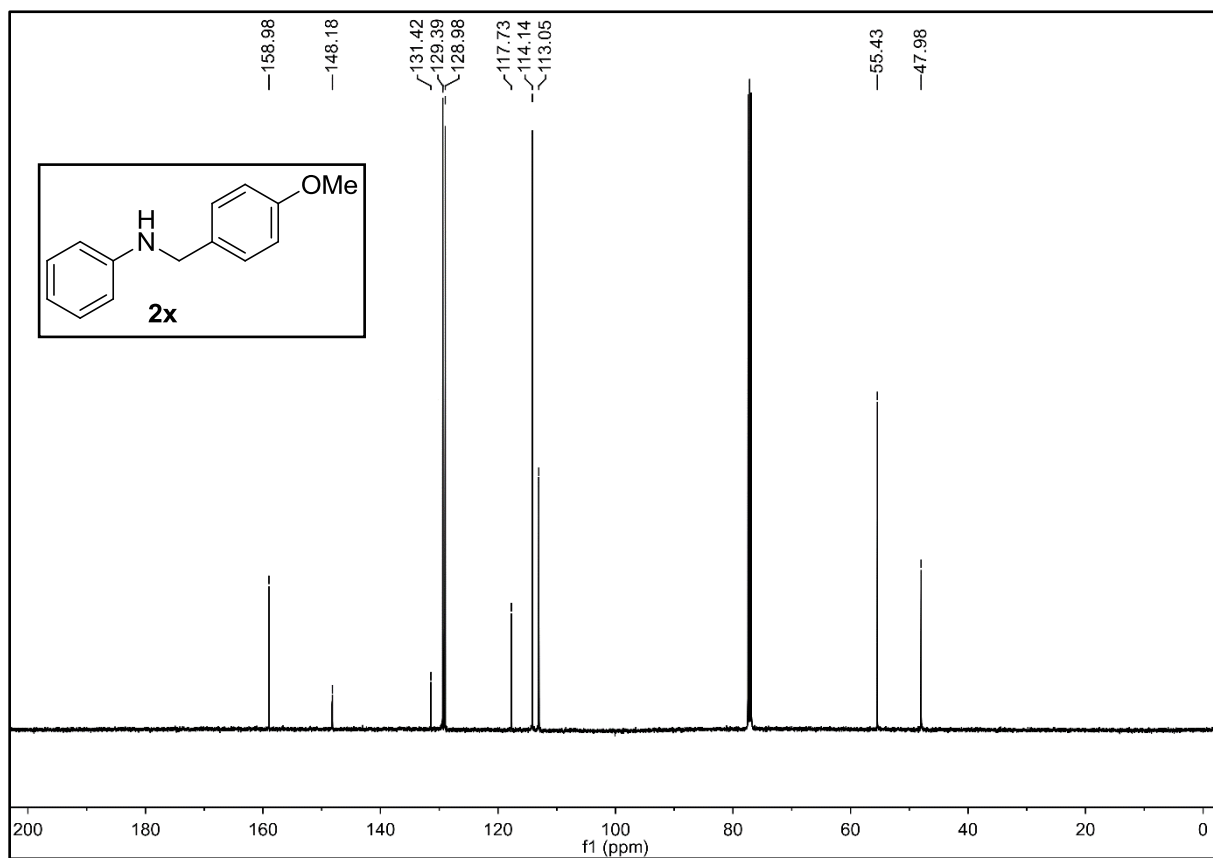
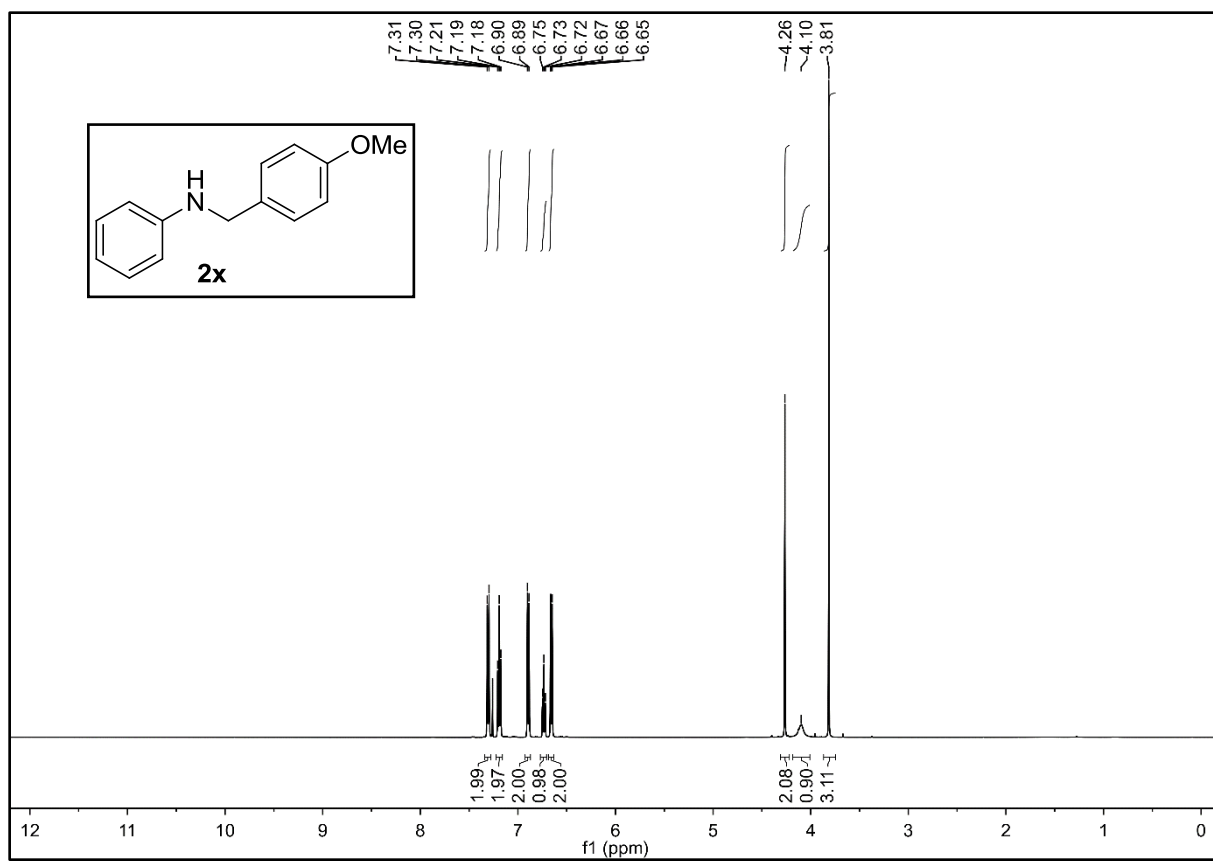


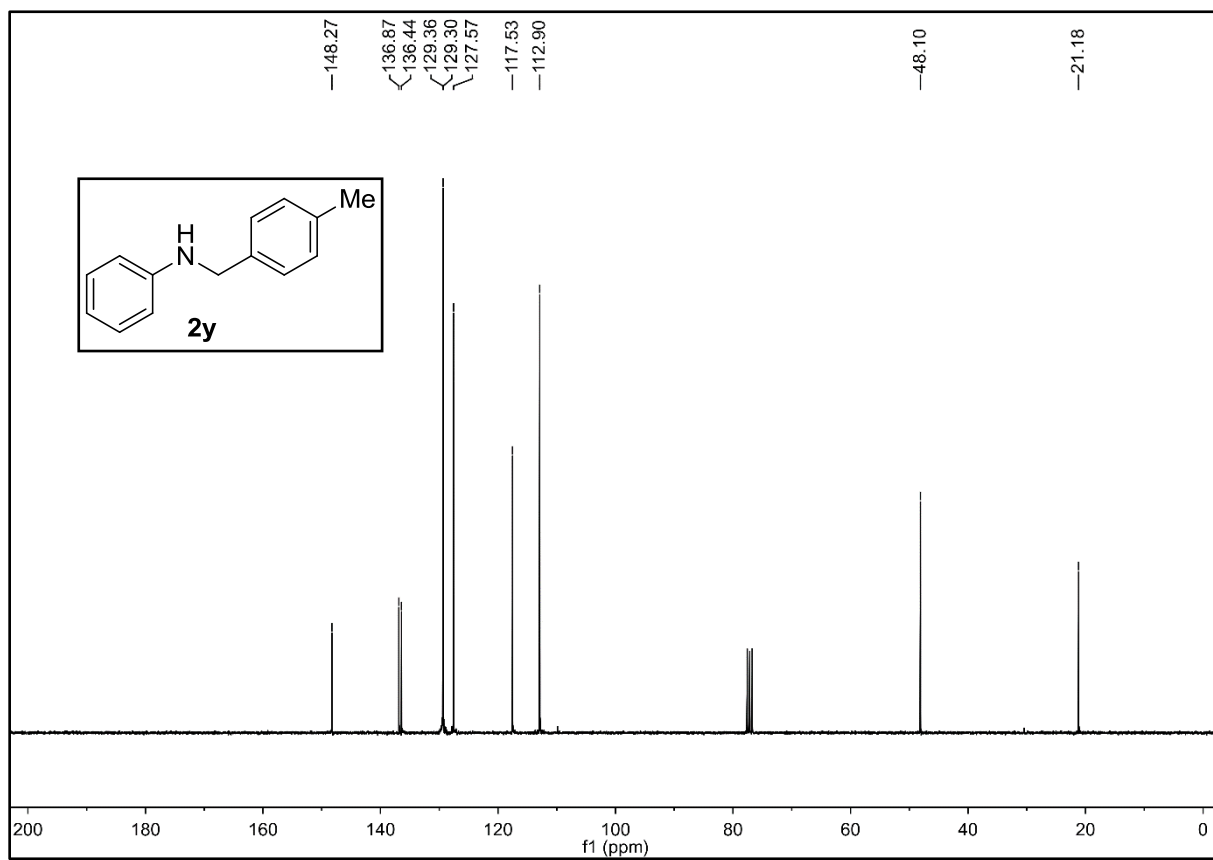
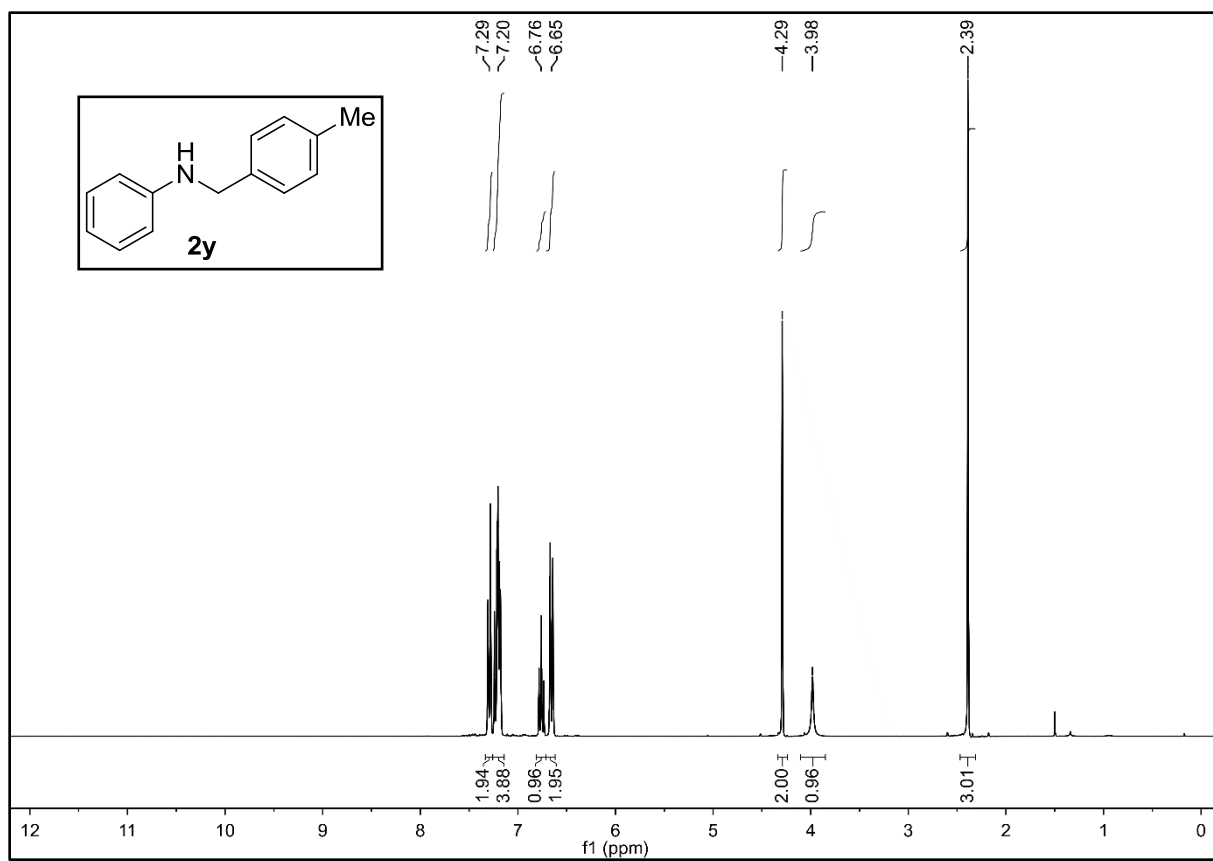


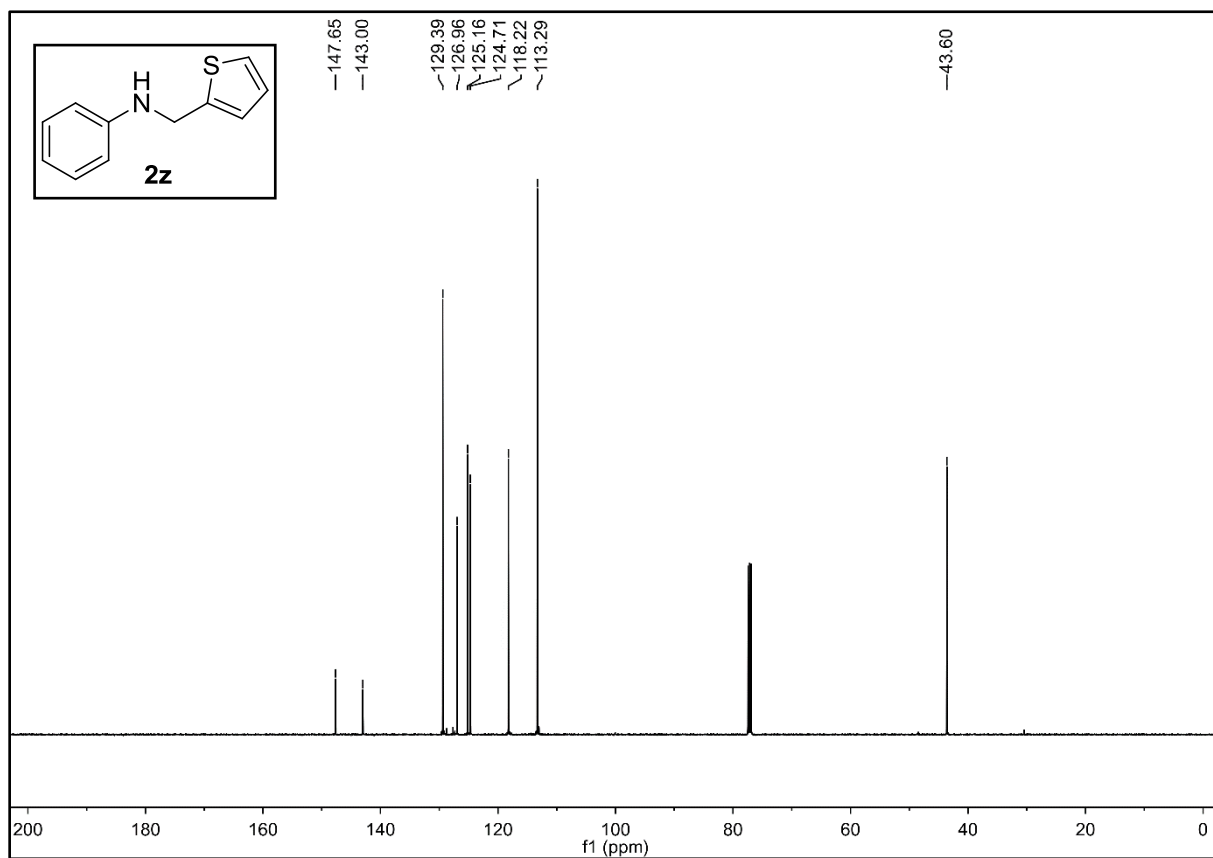
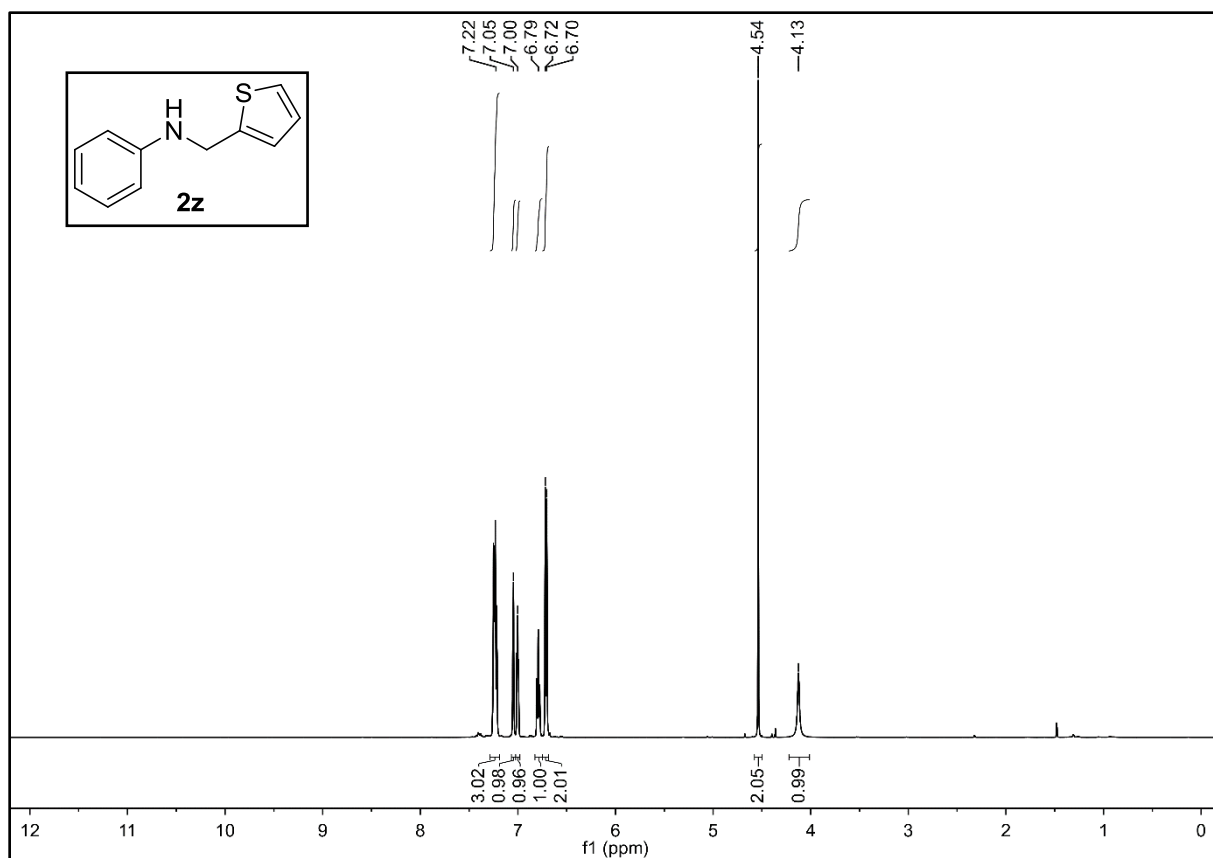


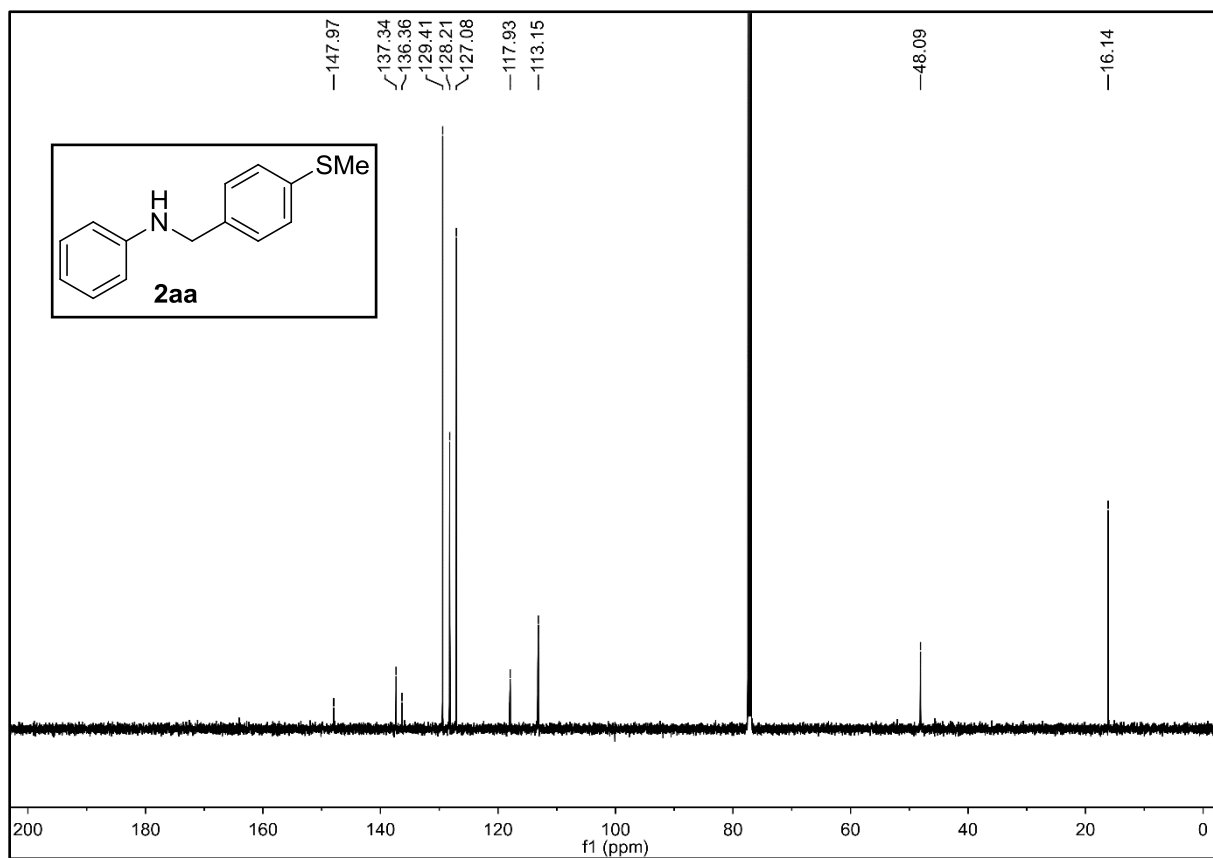
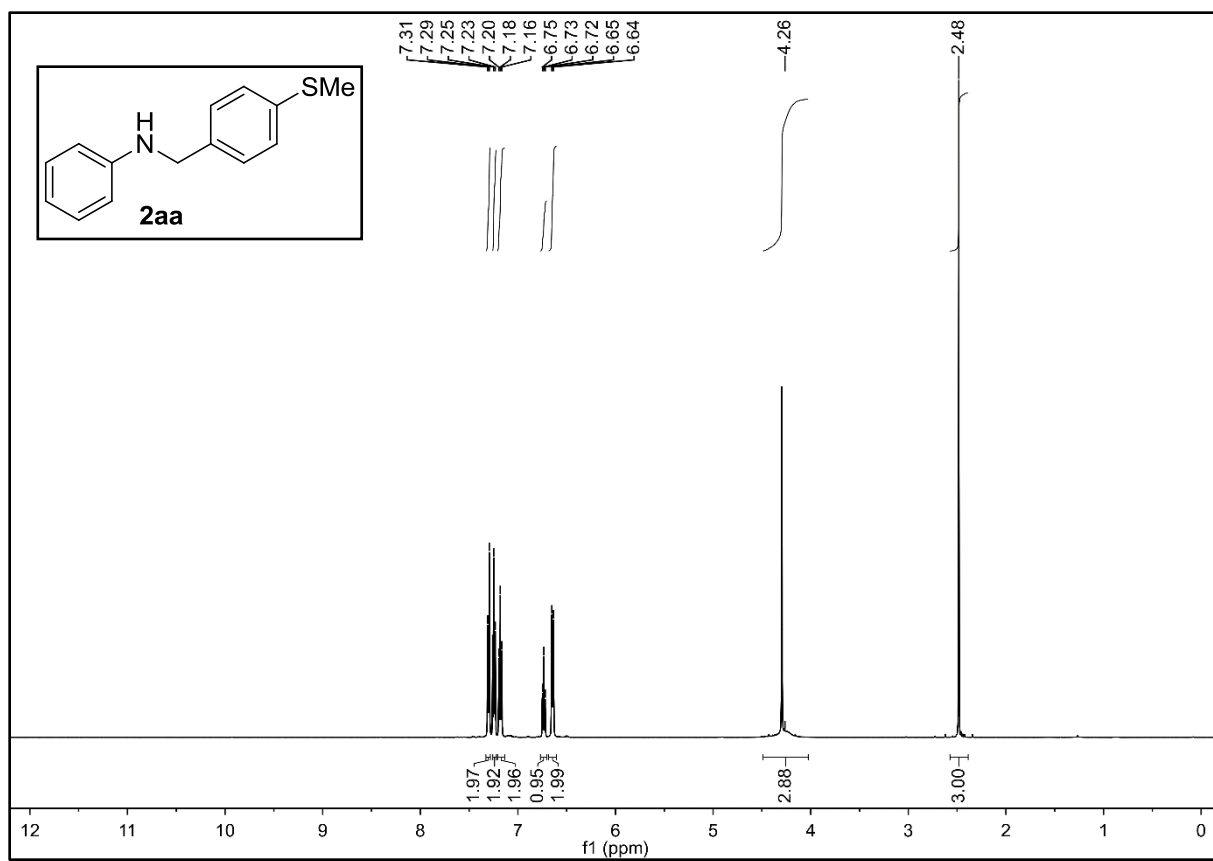


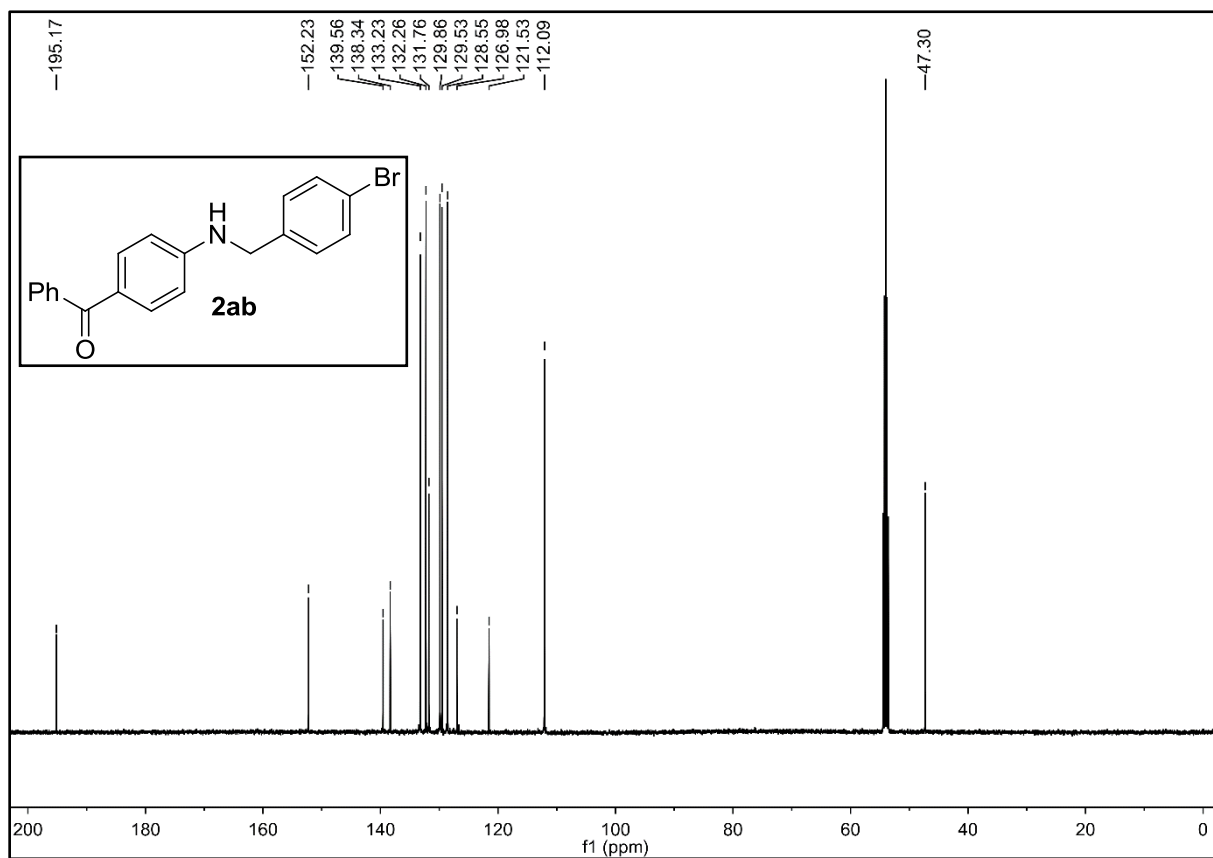
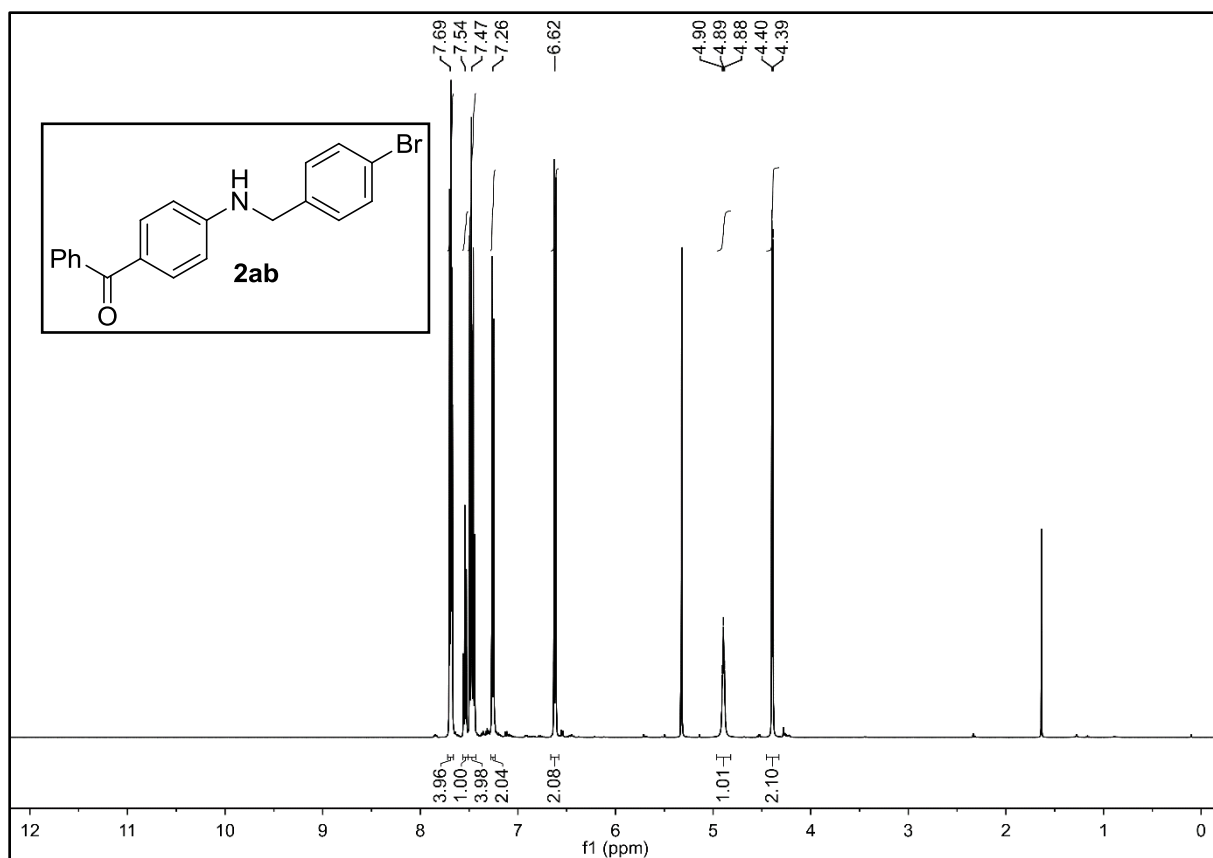


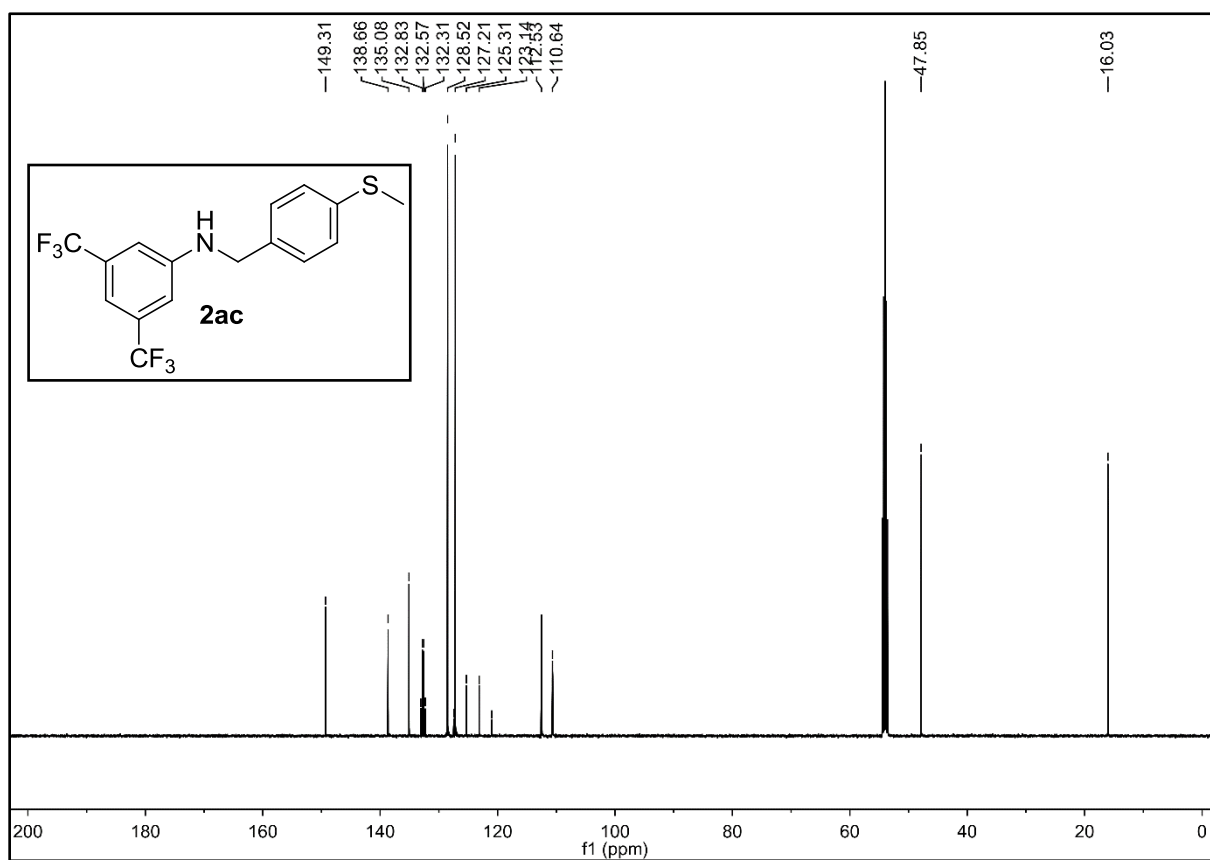
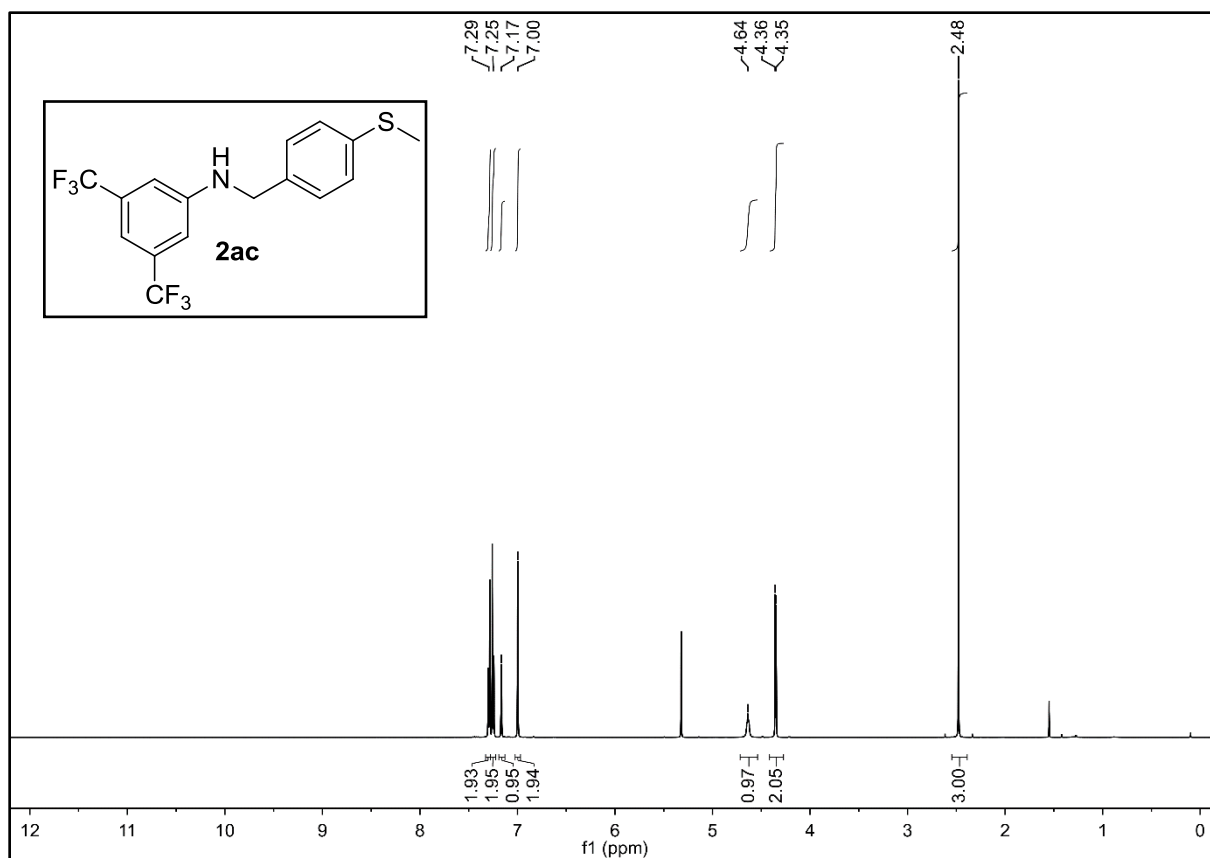


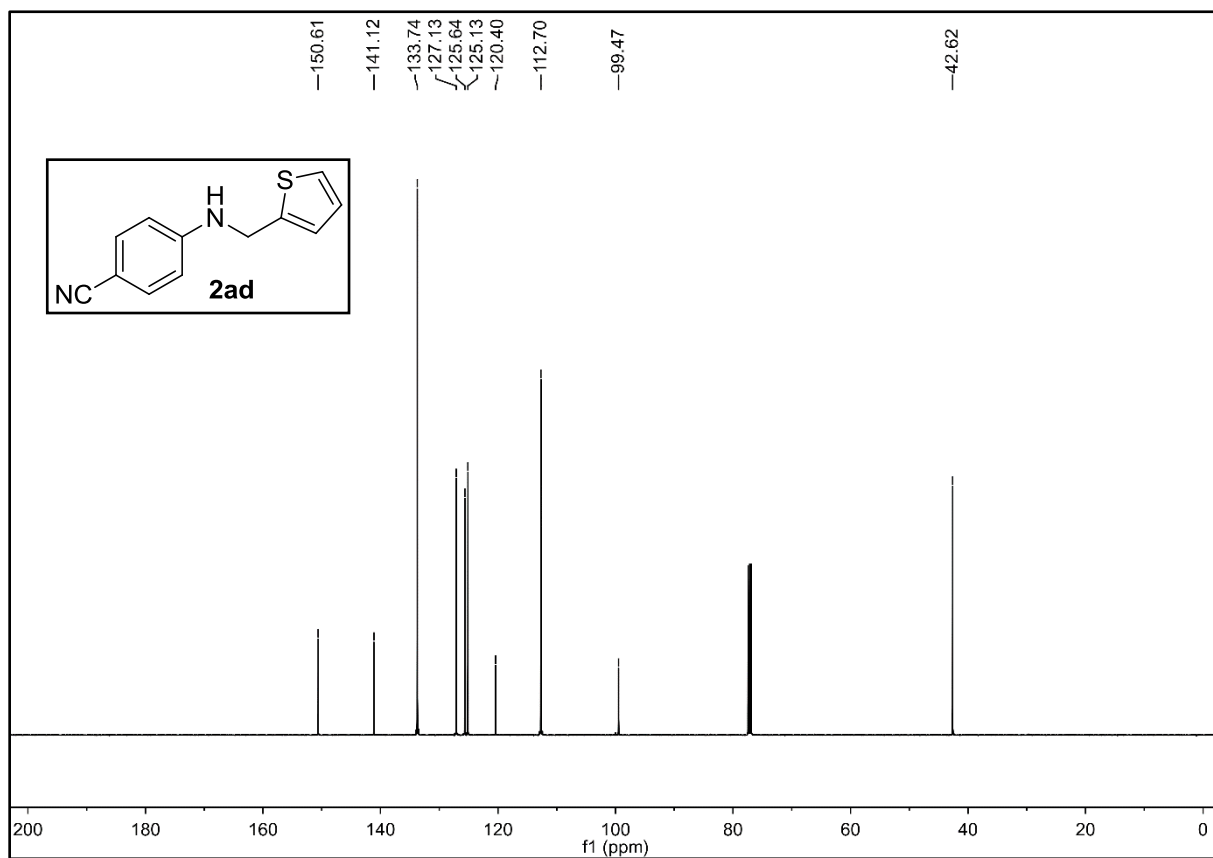
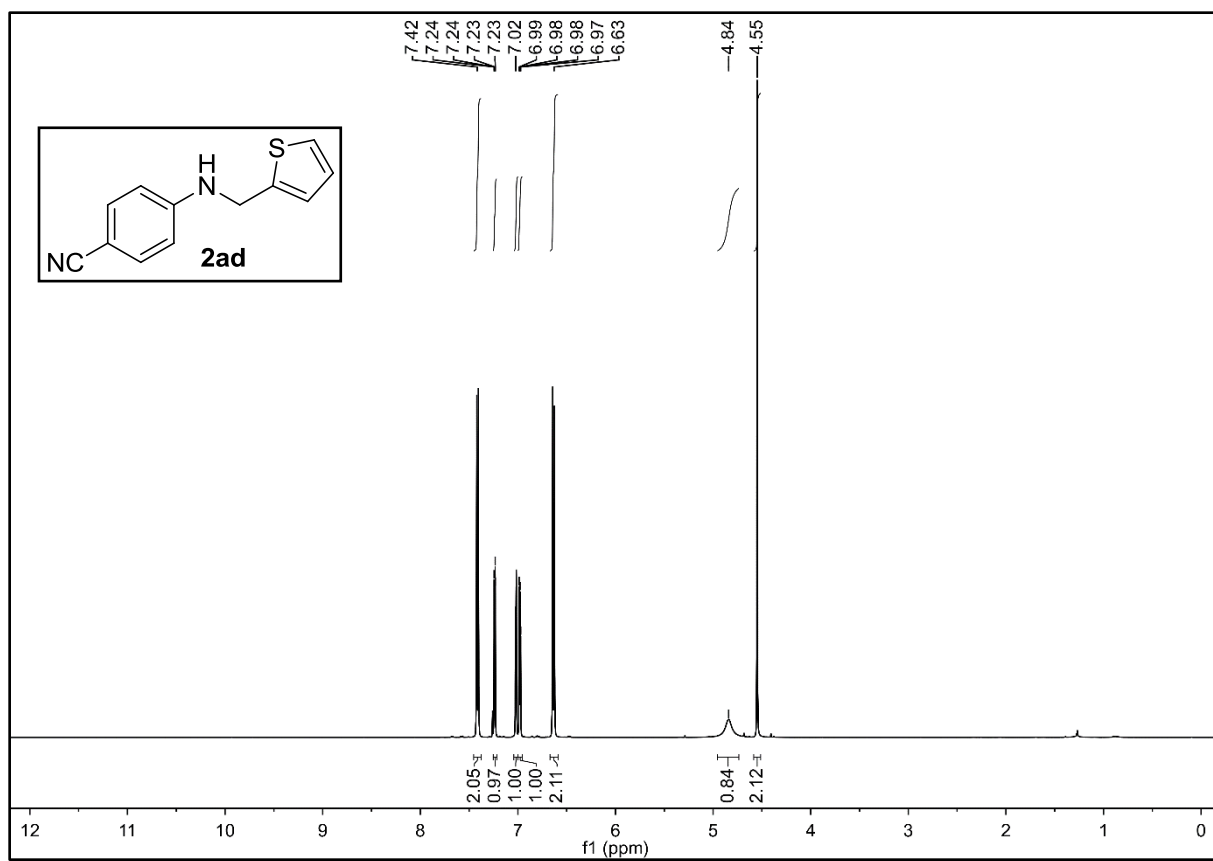


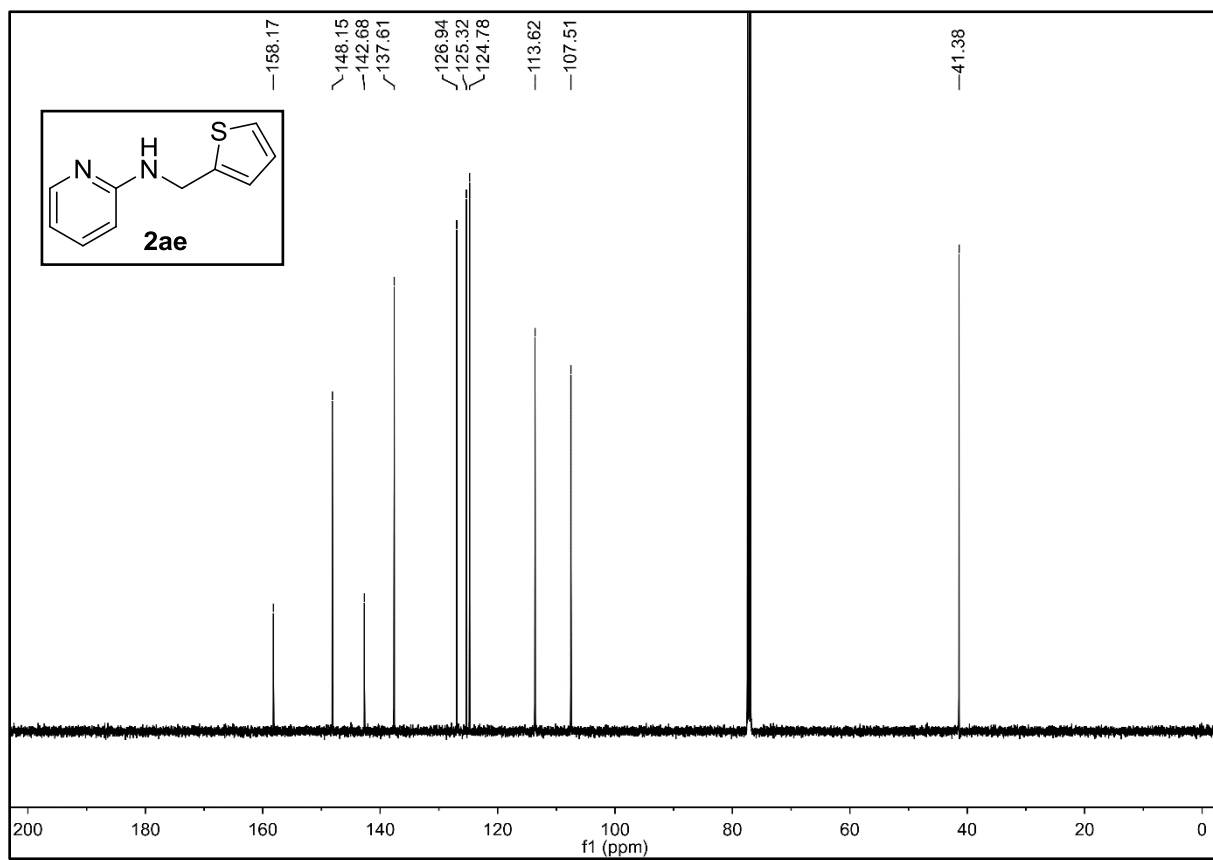
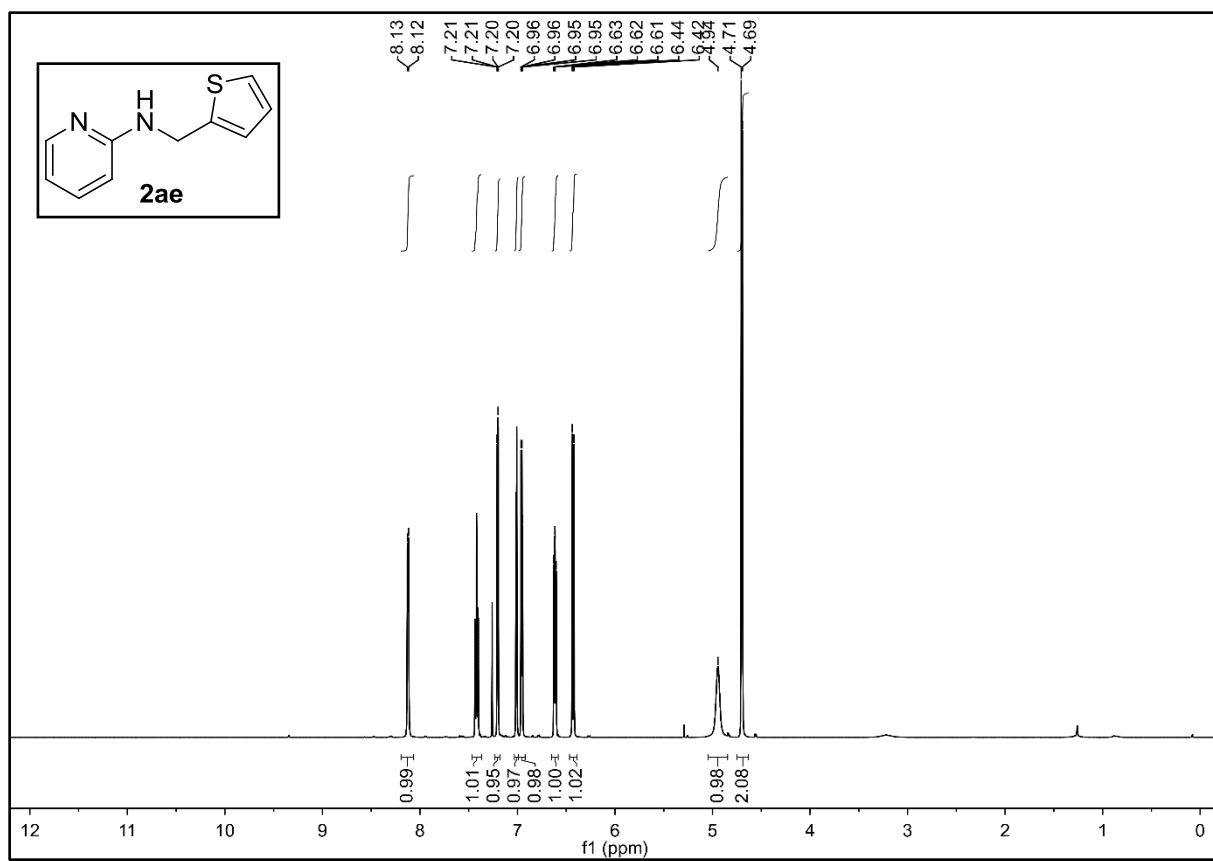


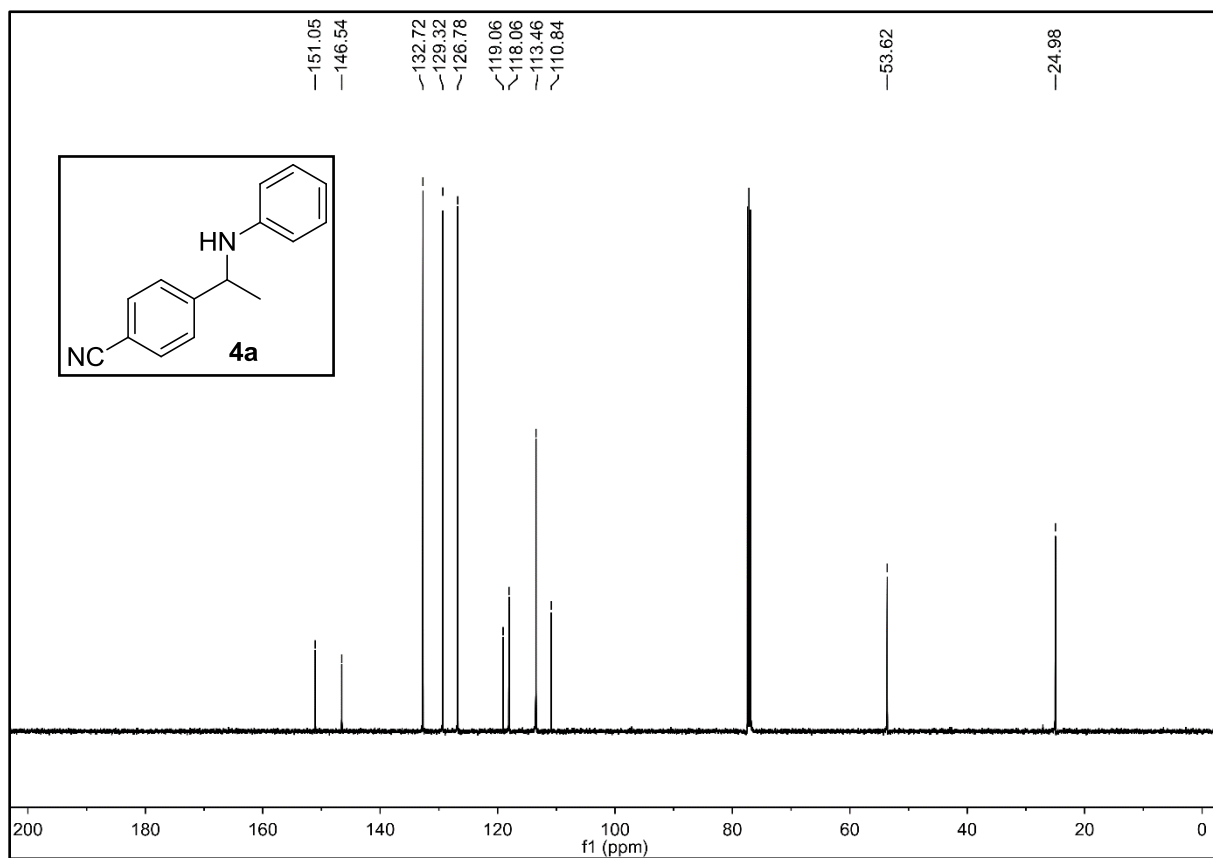
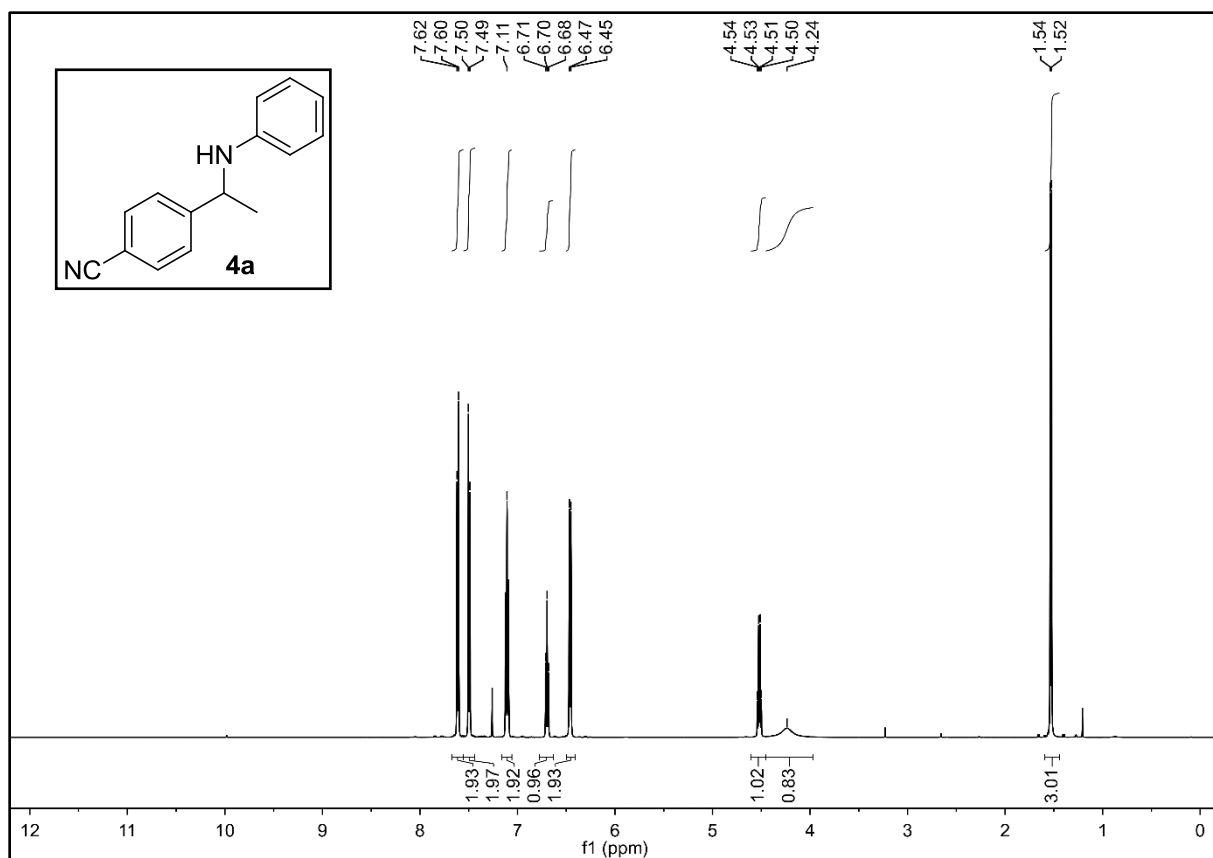


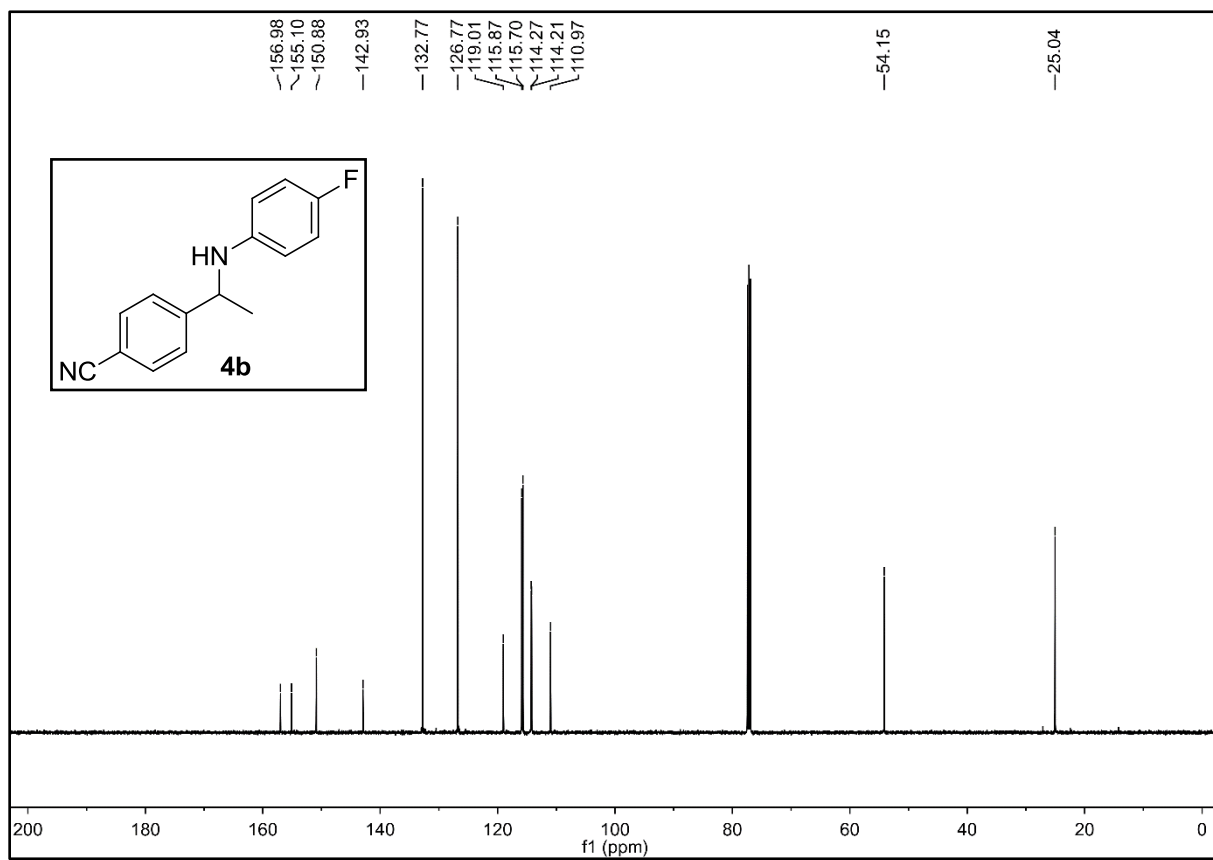
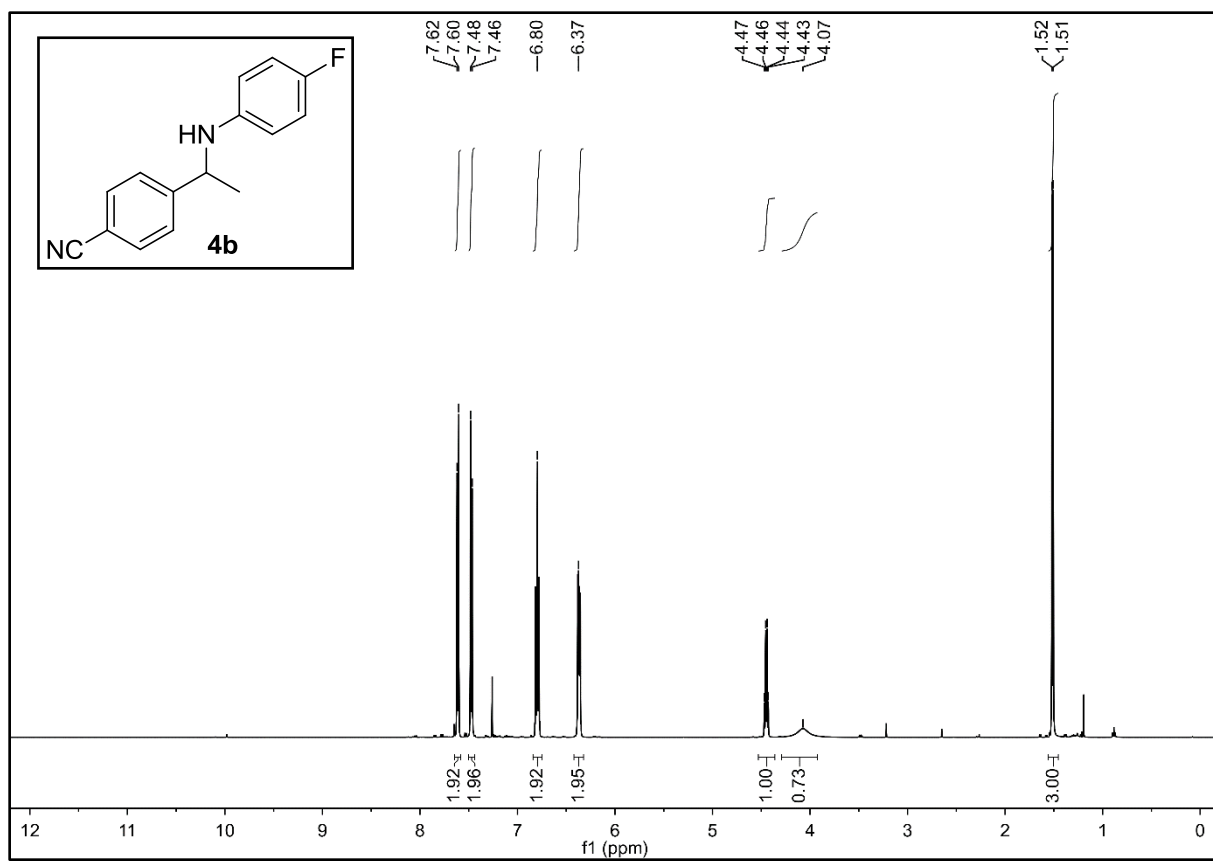


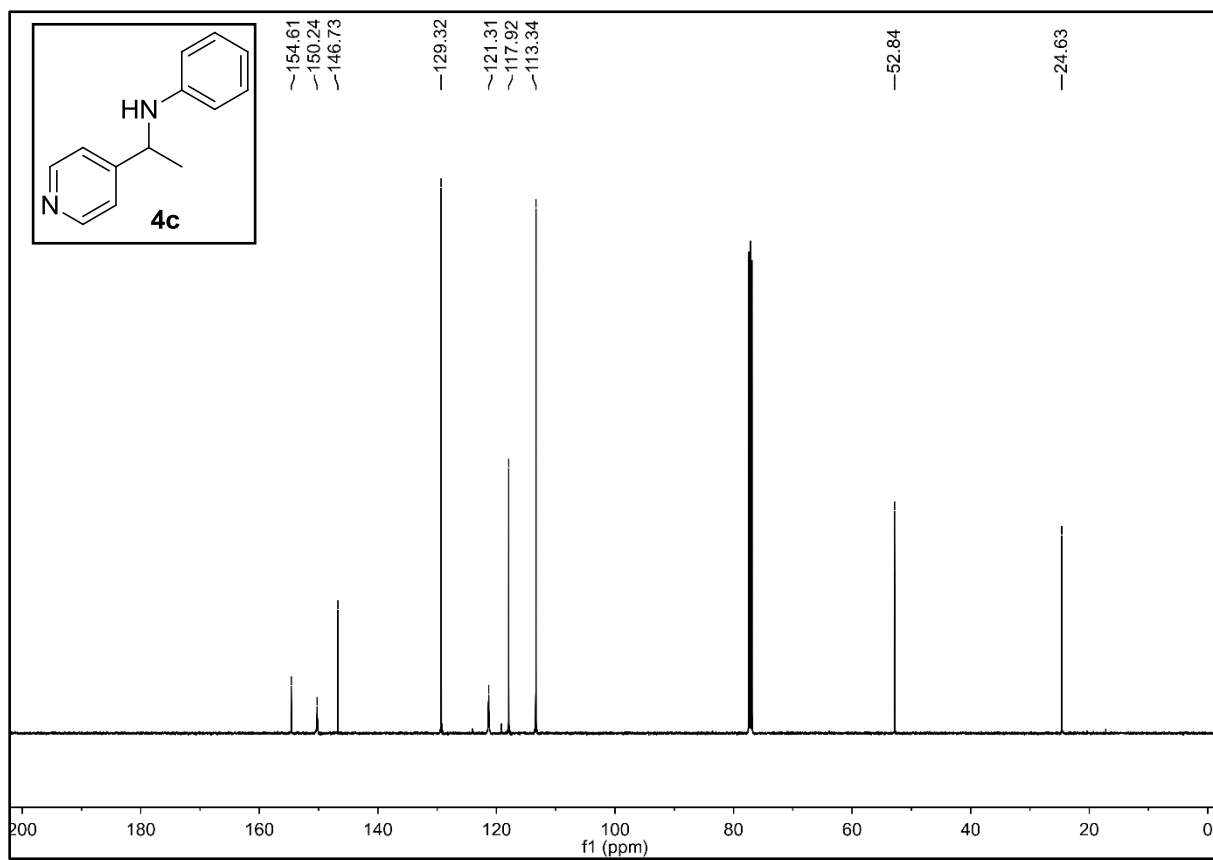
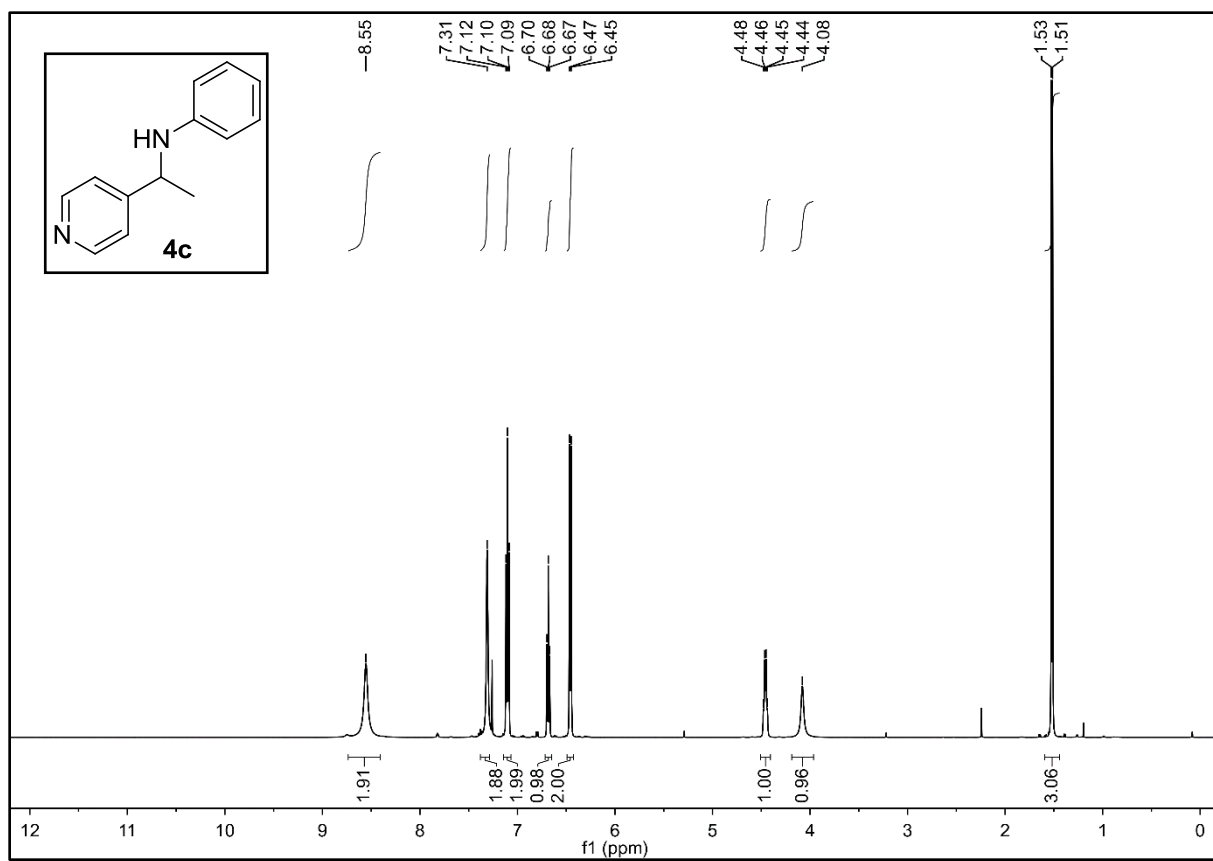


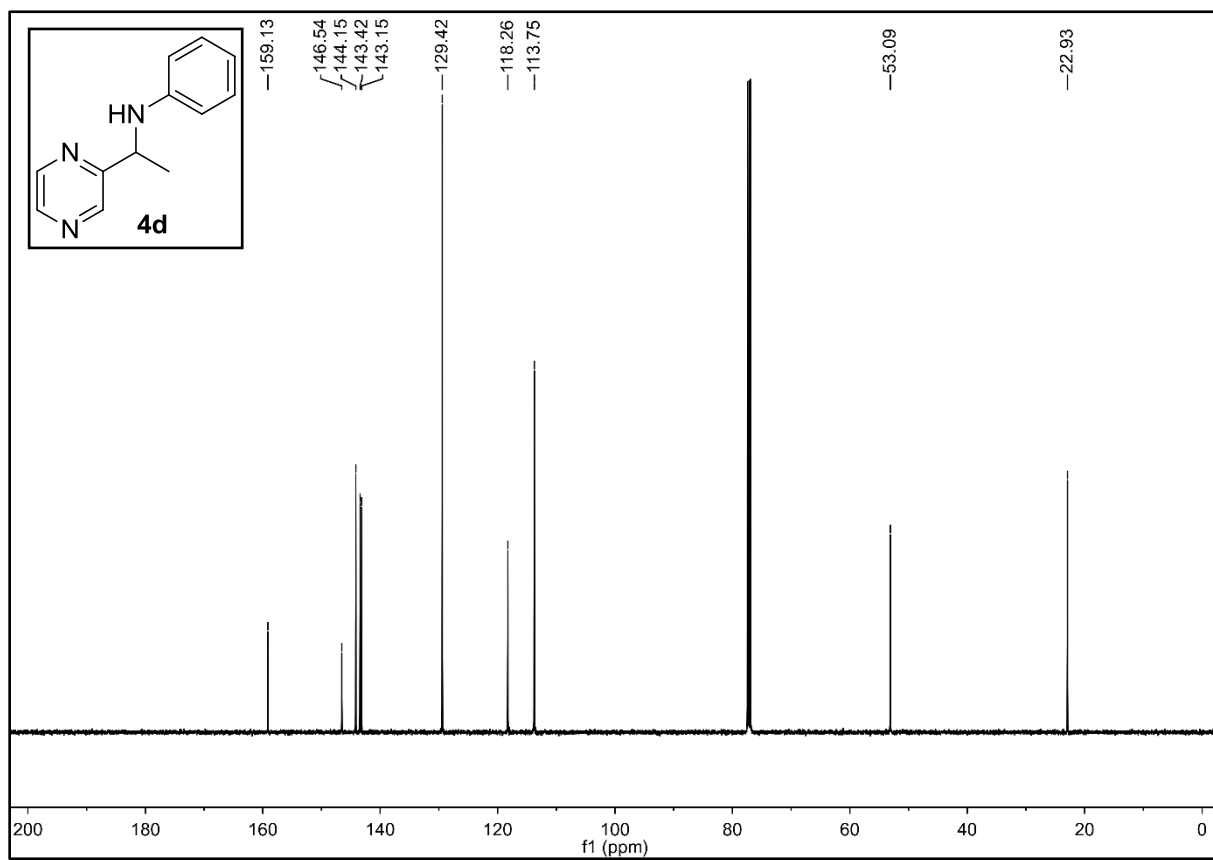
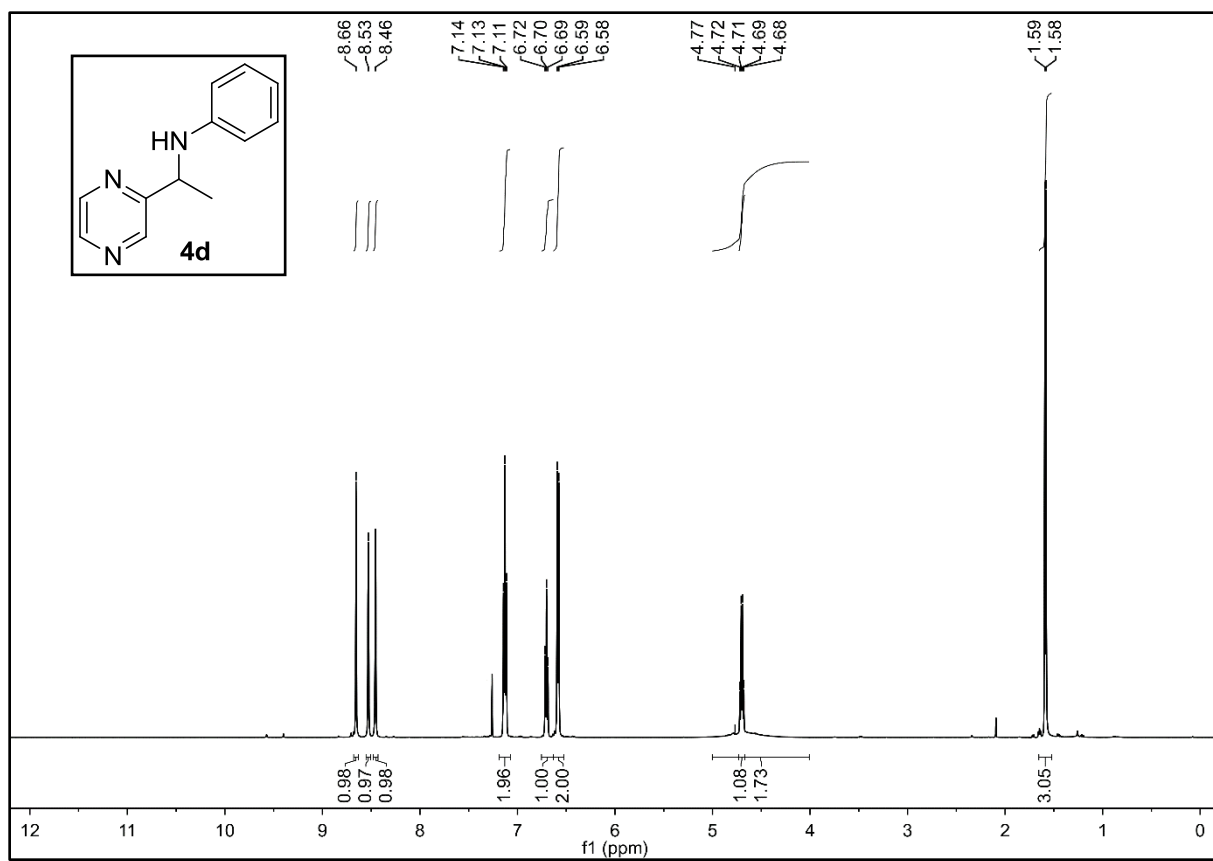


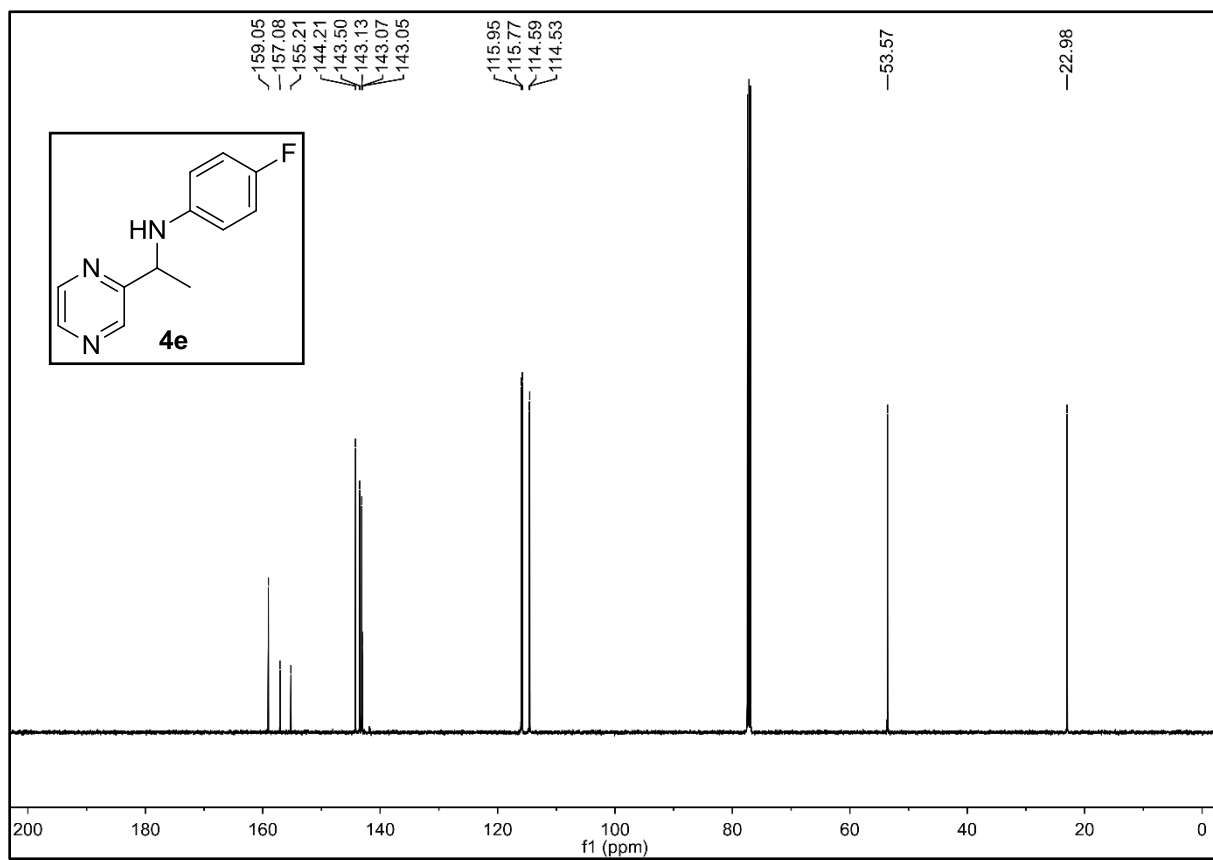
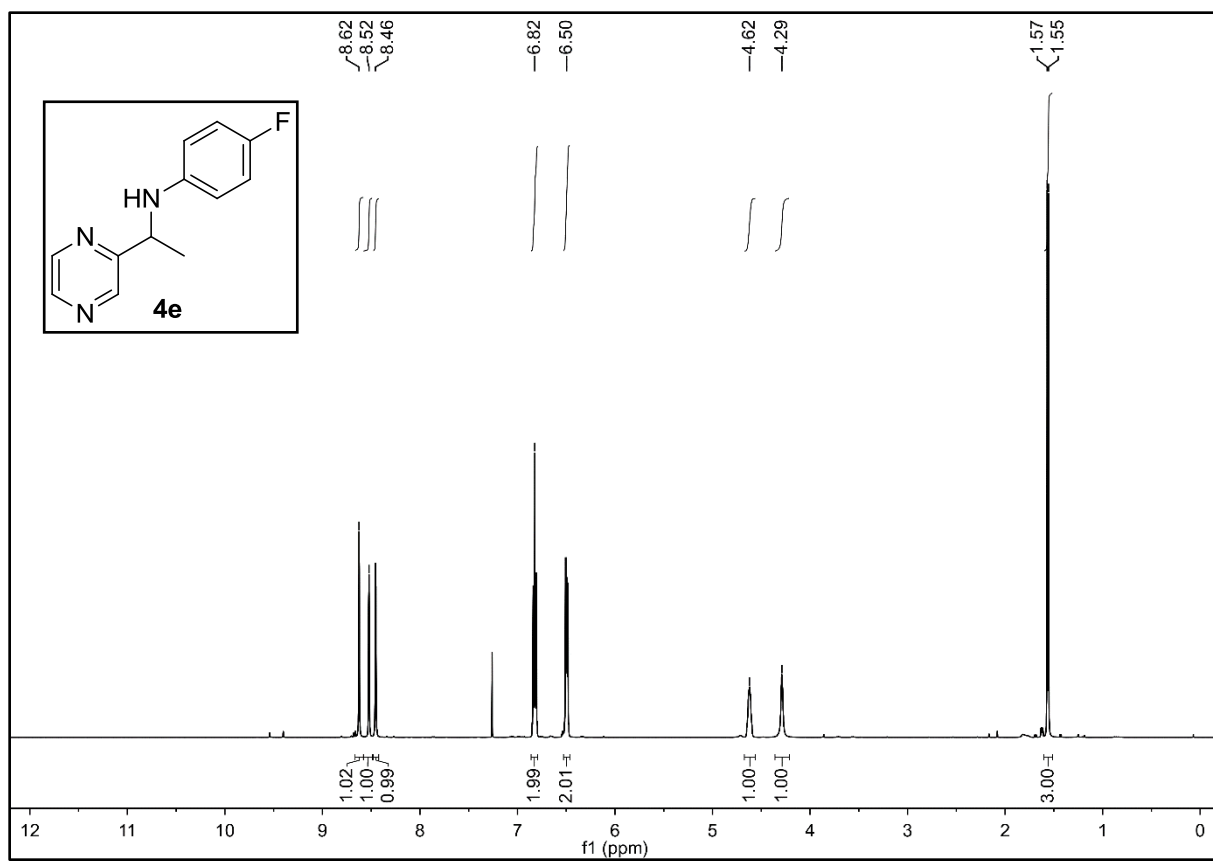












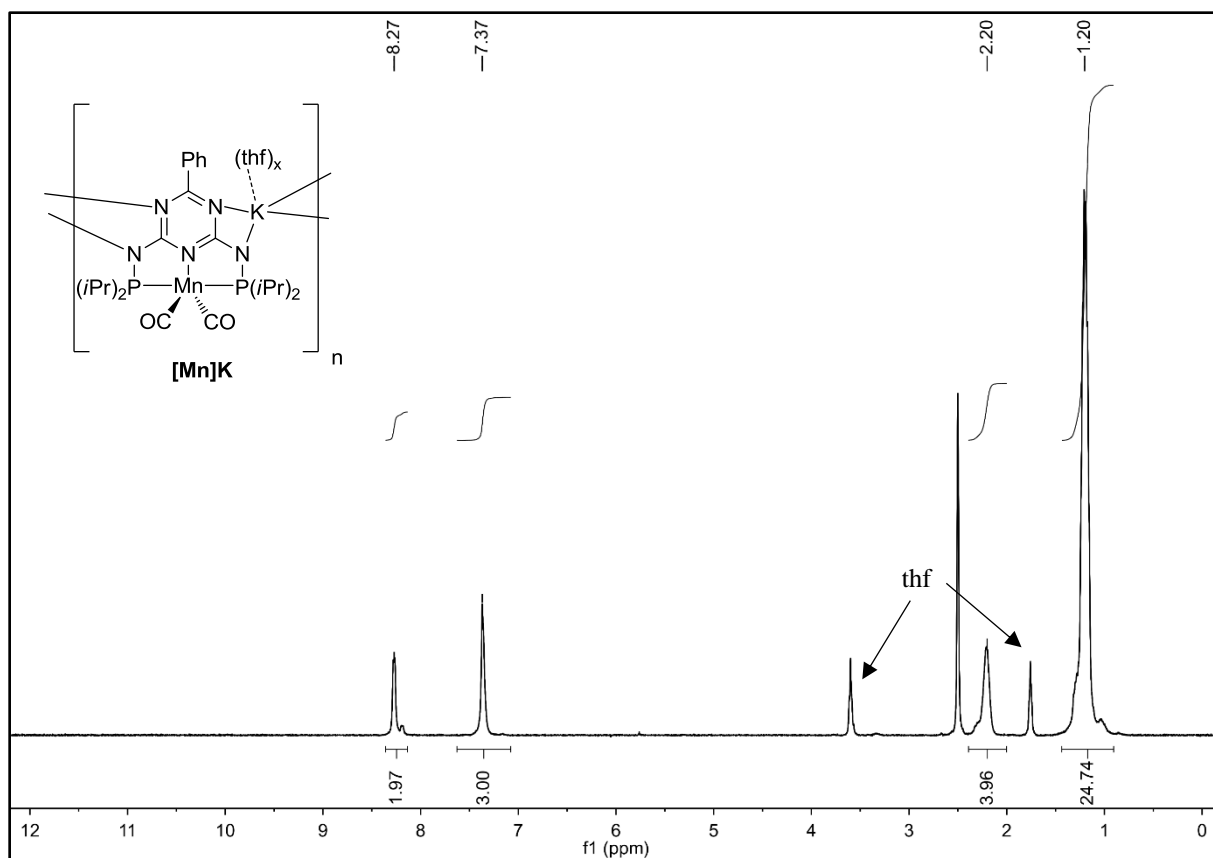


Figure S 33. 1H NMR of $[Mn]K$ in DMSO.

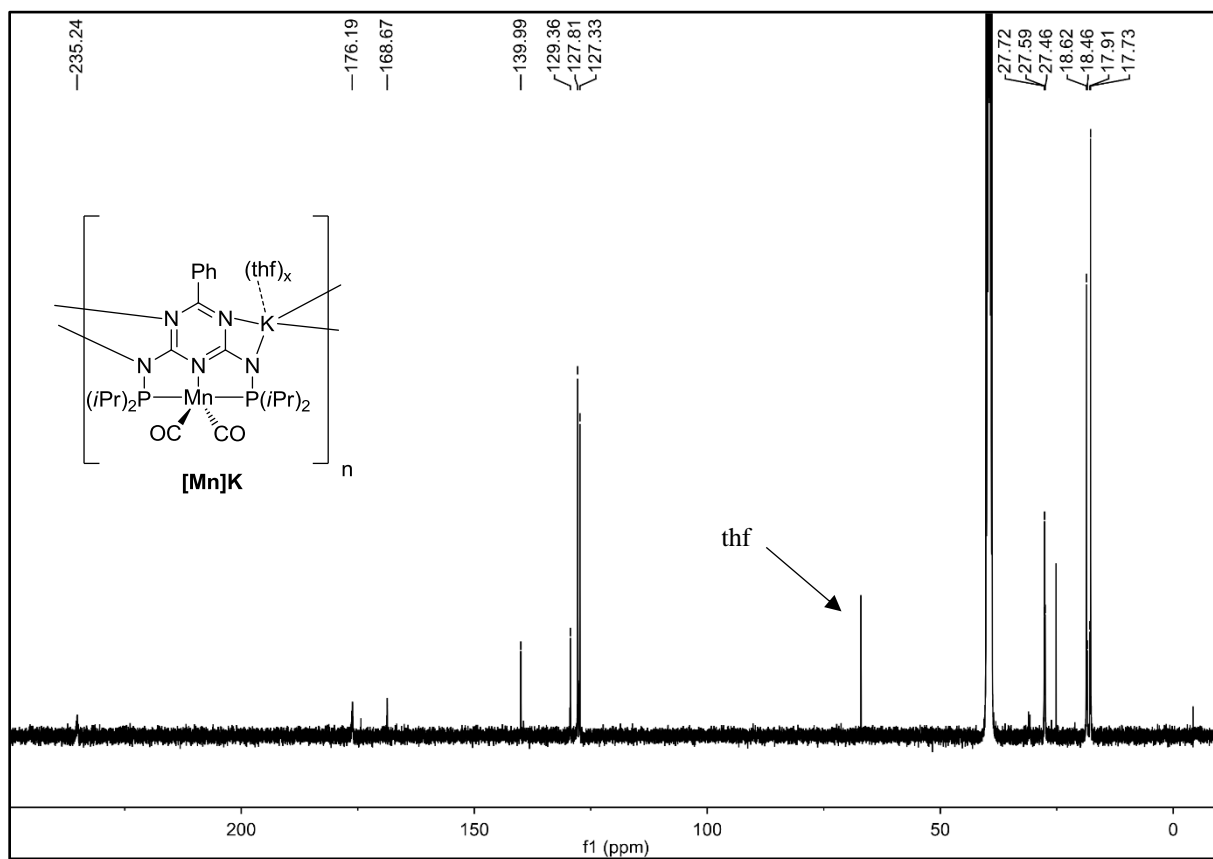


Figure S 34. ^{13}C NMR of $[Mn]K$ in DMSO.

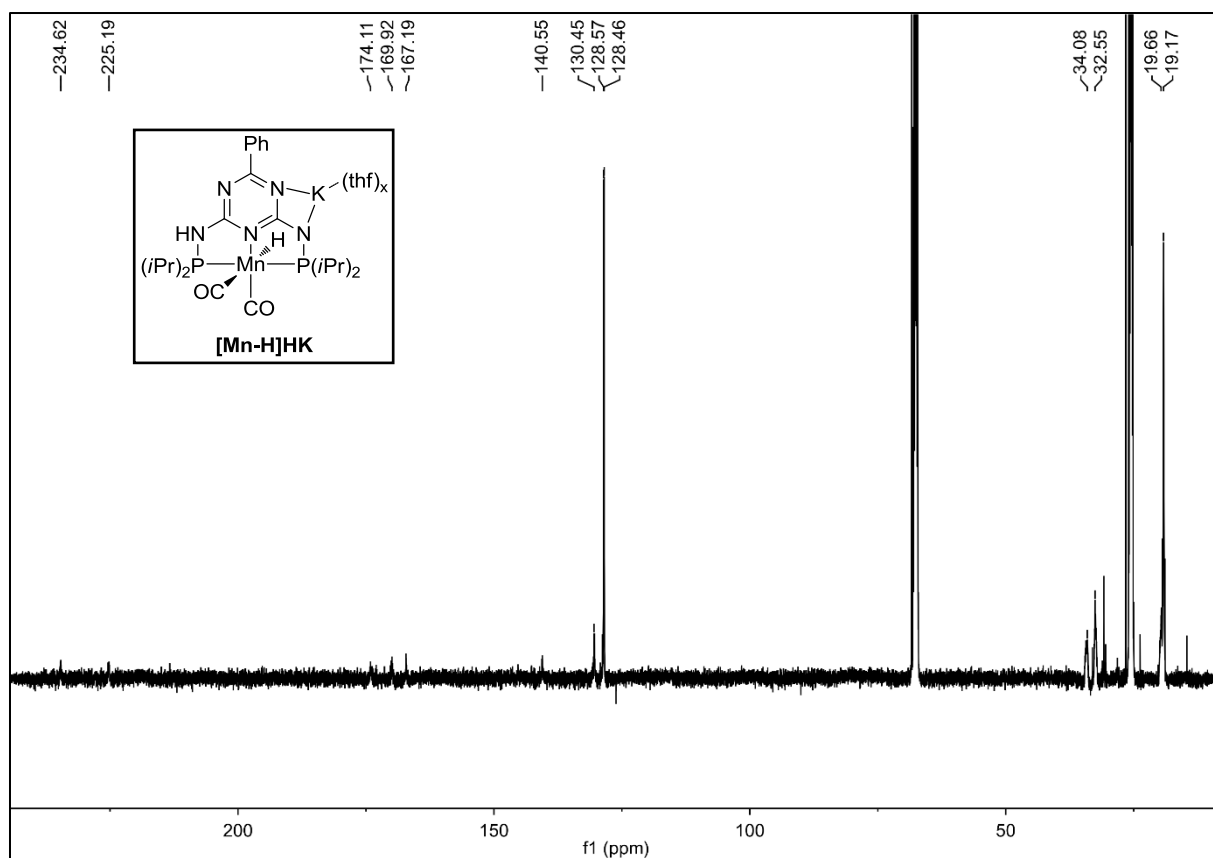


Figure S 37. ^{13}C NMR of $[\text{Mn-H}]\text{HK}$ in thf_D8 .

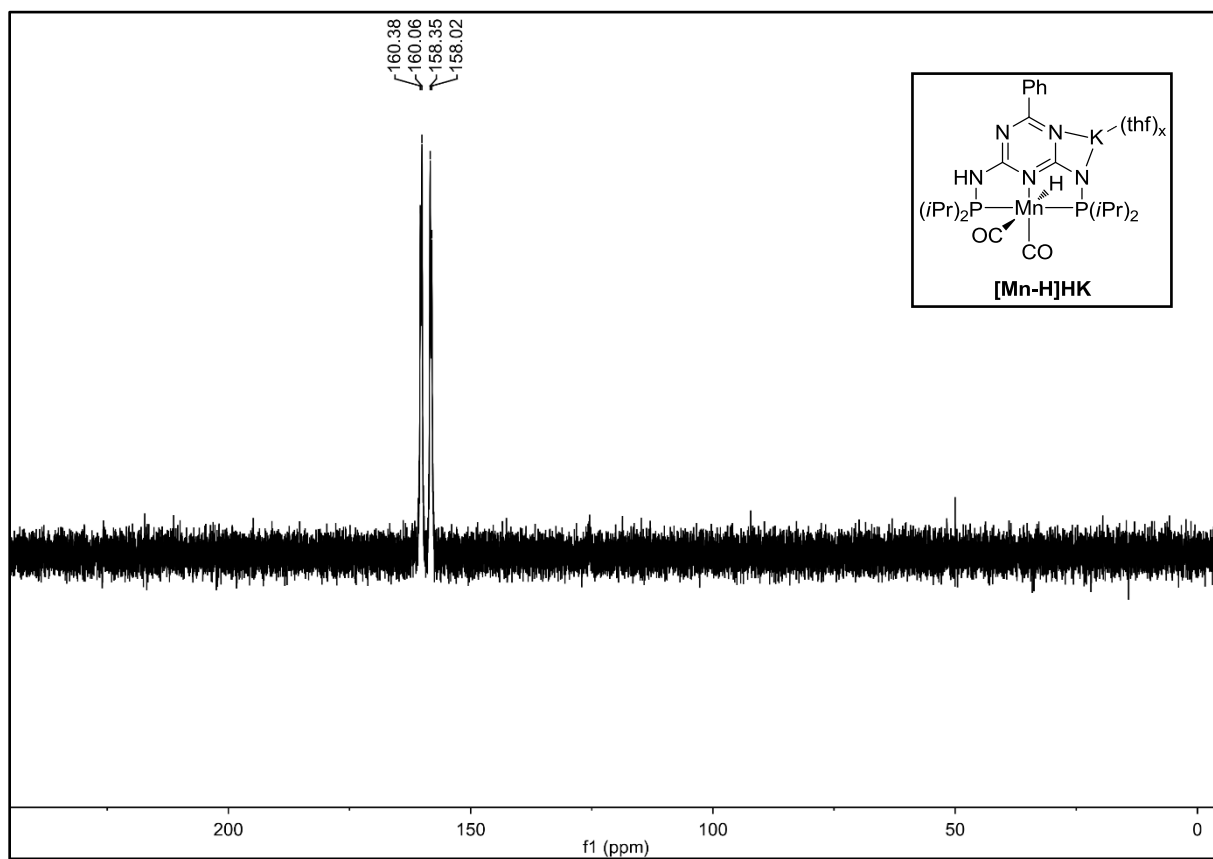


Figure S 38. ^{31}P NMR of $[\text{Mn-H}]\text{HK}$ in thf_D8 .

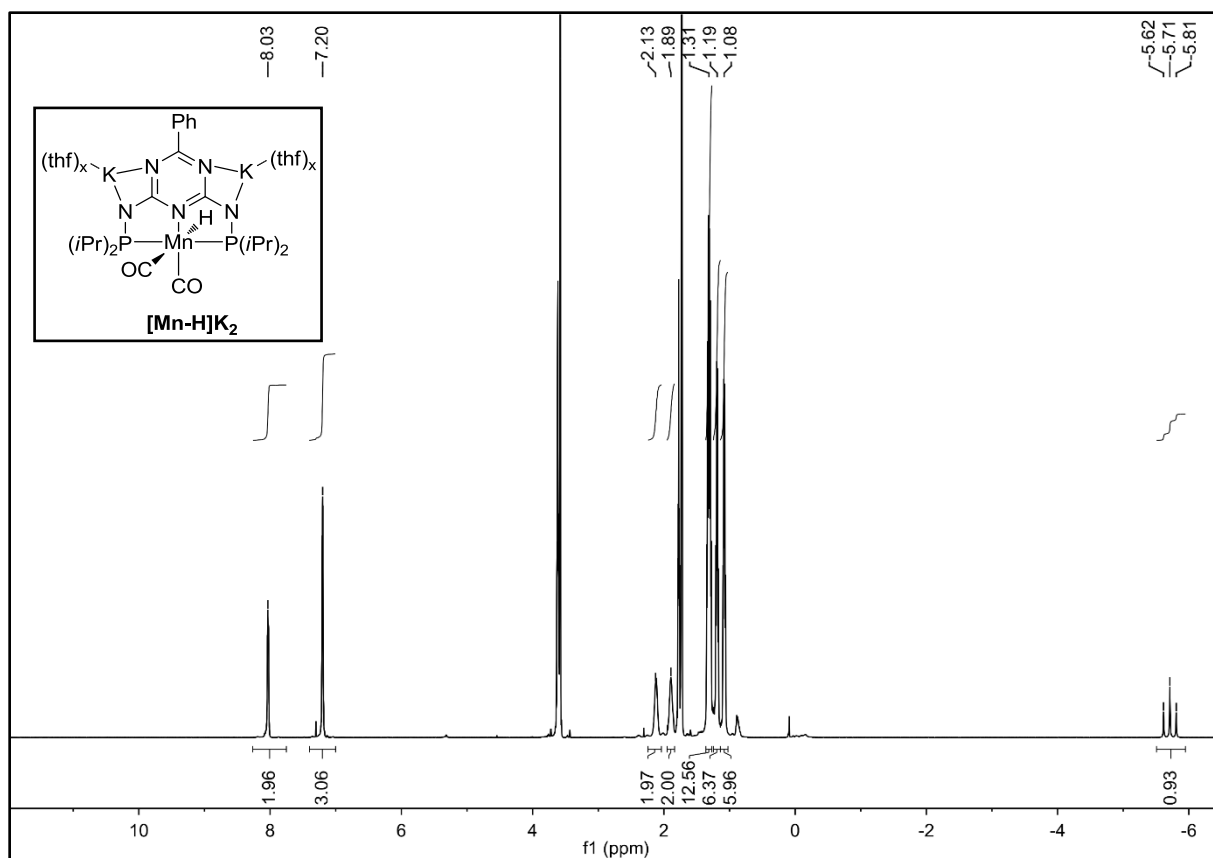


Figure S 39. ^1H NMR of $[\text{Mn-H}]\text{K}_2$ in thfD_8 .

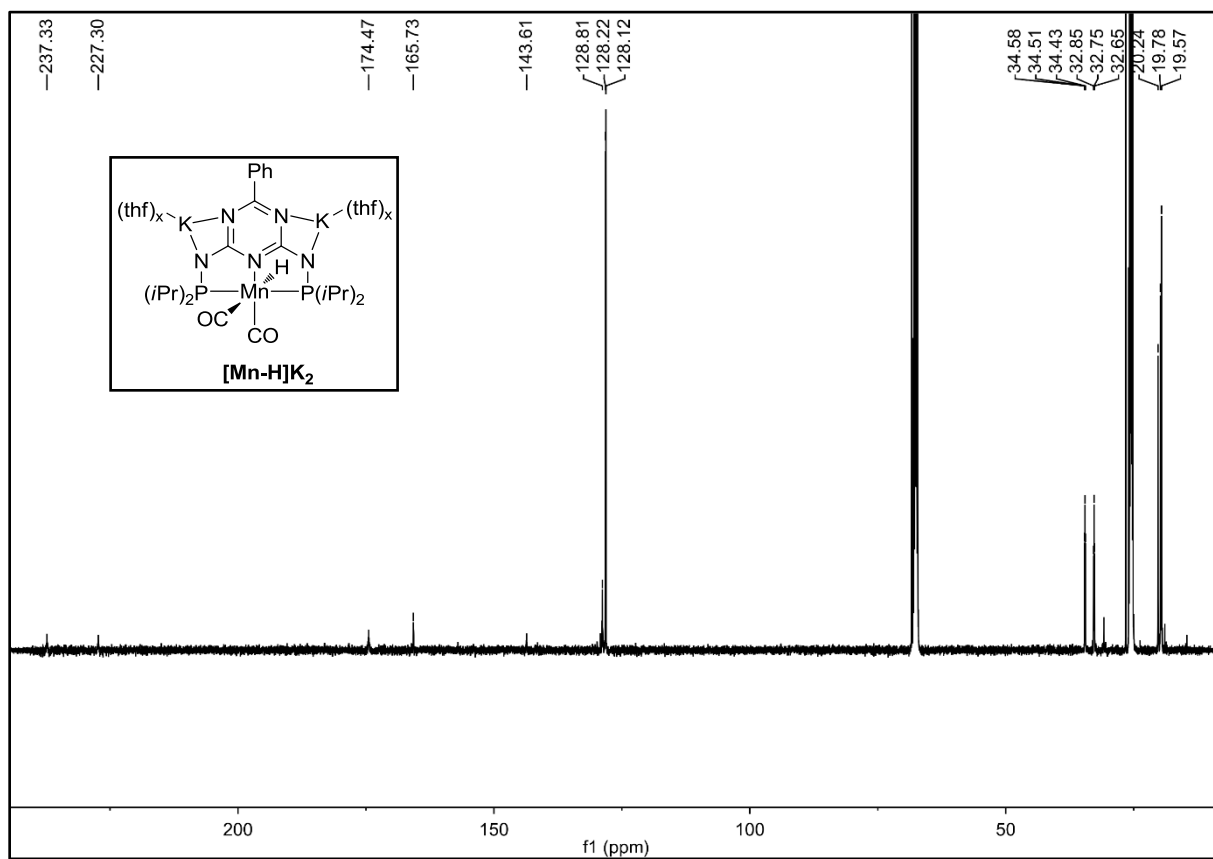


Figure S 40. ^{13}C NMR of $[\text{Mn-H}]\text{K}_2$ in thfD_8 .

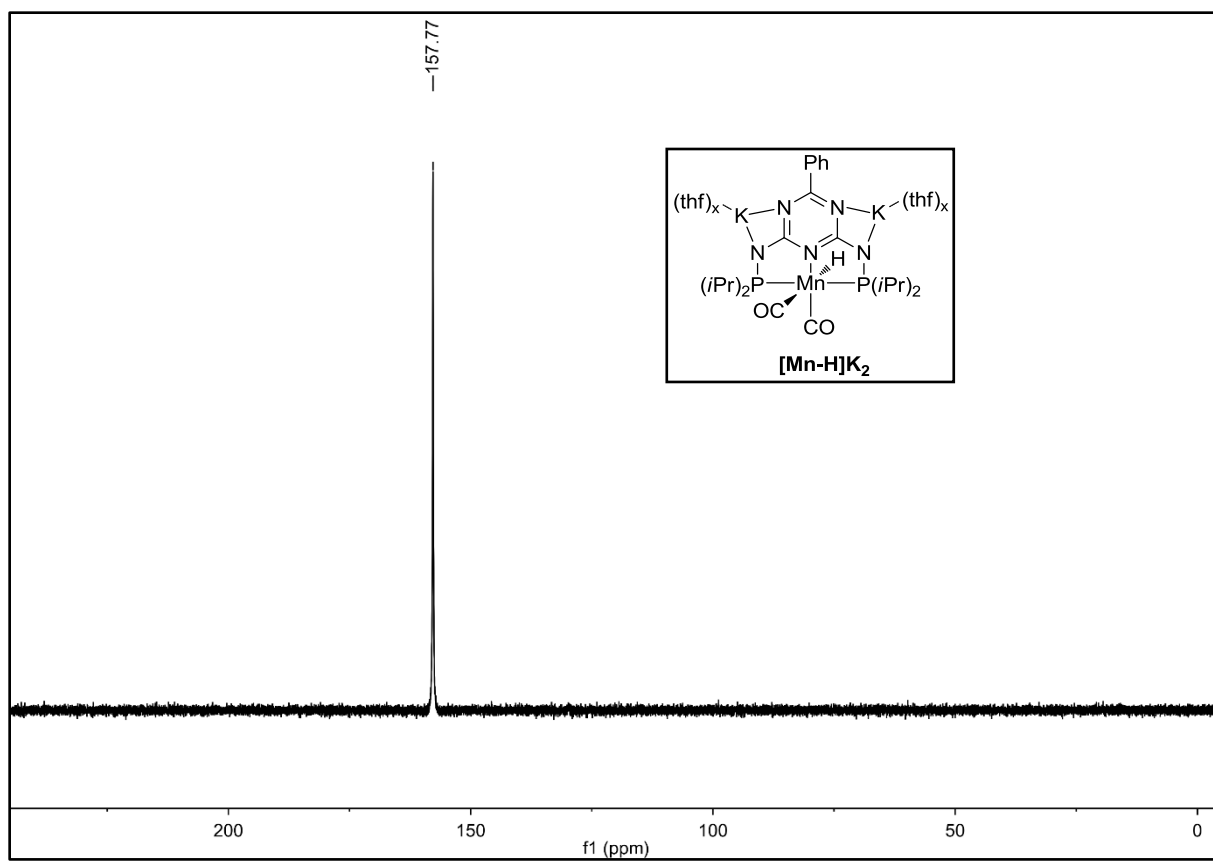


Figure S 41. ^{31}P NMR of $[\text{Mn-H}]\text{K}_2$ in thf-D_8 .

5 UV-vis Data

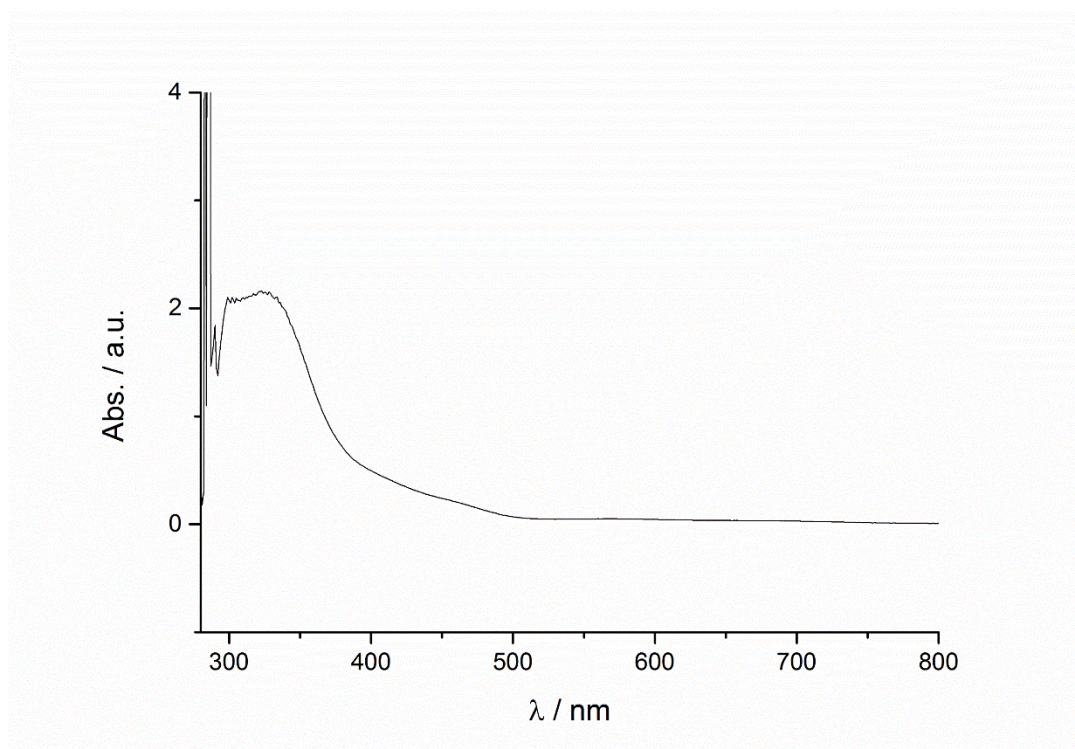


Figure S 42. UV-vis spectrum of [Mn]K.

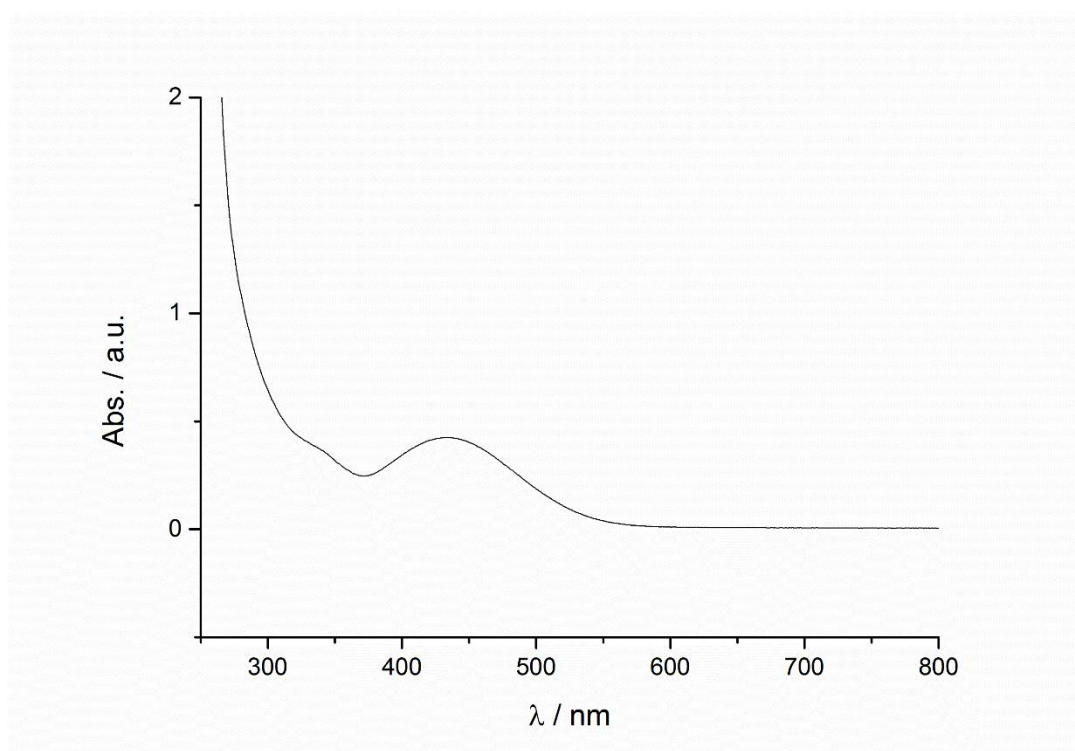


Figure S 43. UV-vis spectrum of [Mn-H]HK.

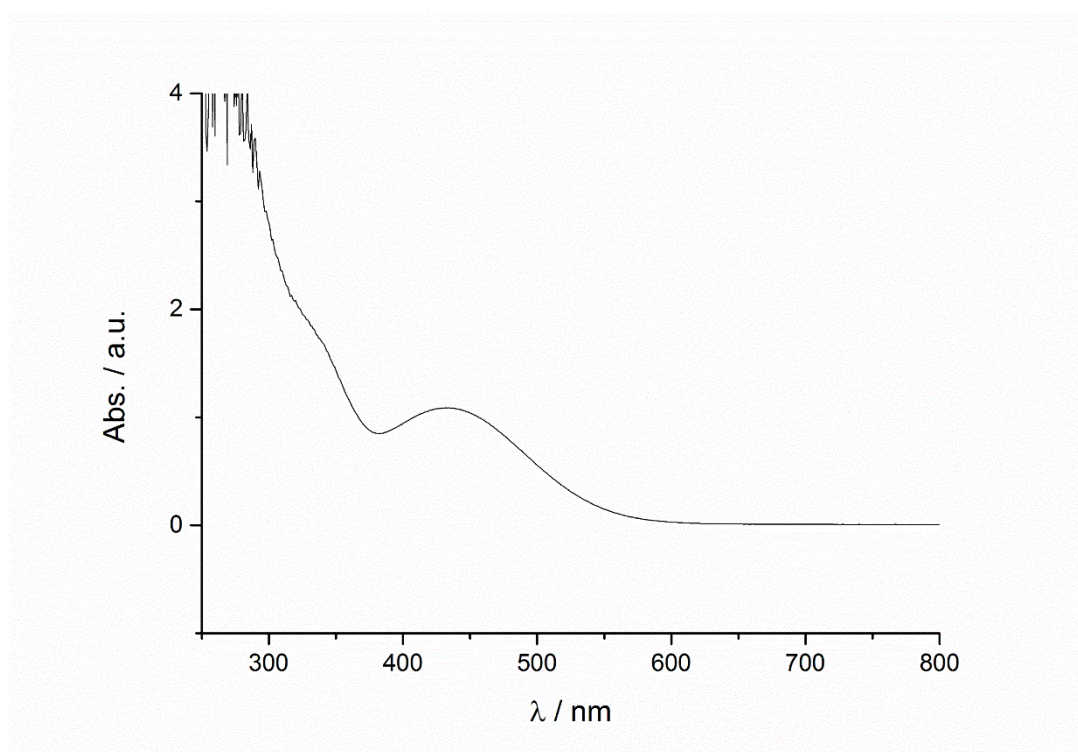


Figure S 44: UV-vis spectrum of $[\text{Mn-H}]\text{K}_2$.

6 IR Data

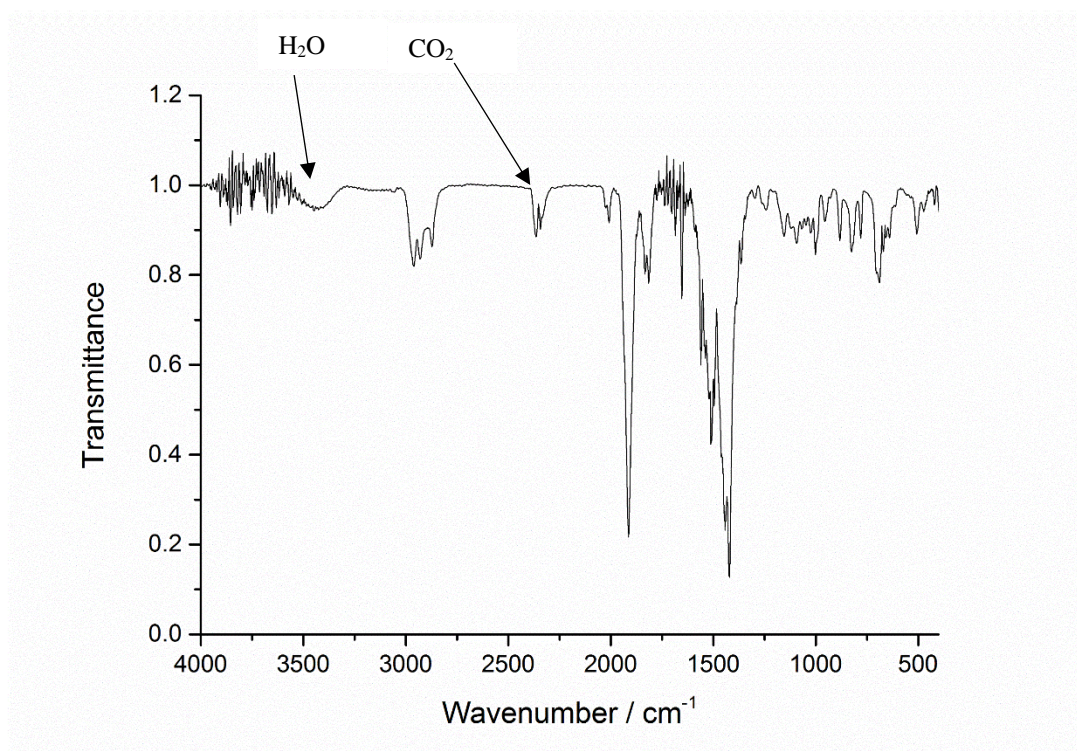


Figure S 45. IR spectrum of **[Mn]K**.

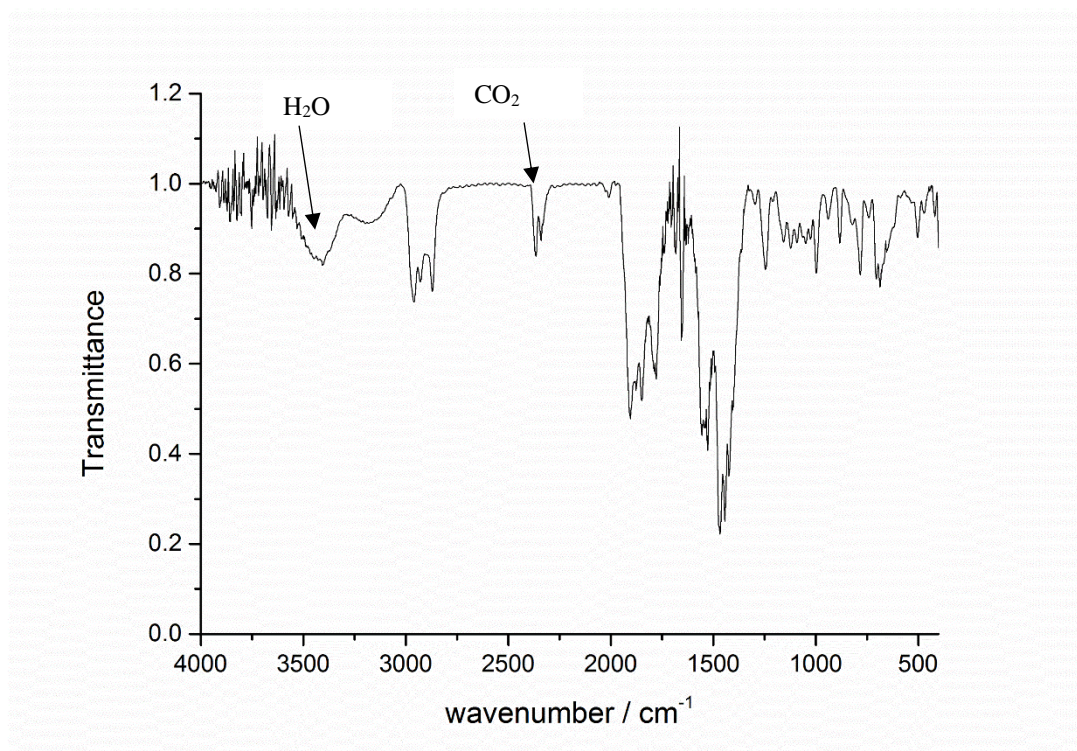


Figure S 46. IR spectrum of **[Mn-H]HK**.

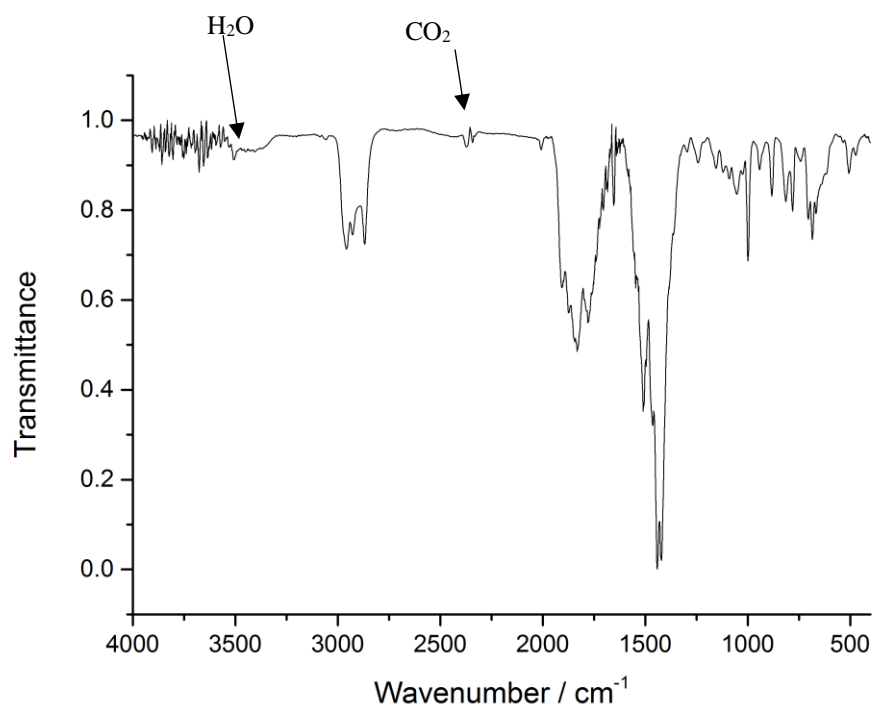
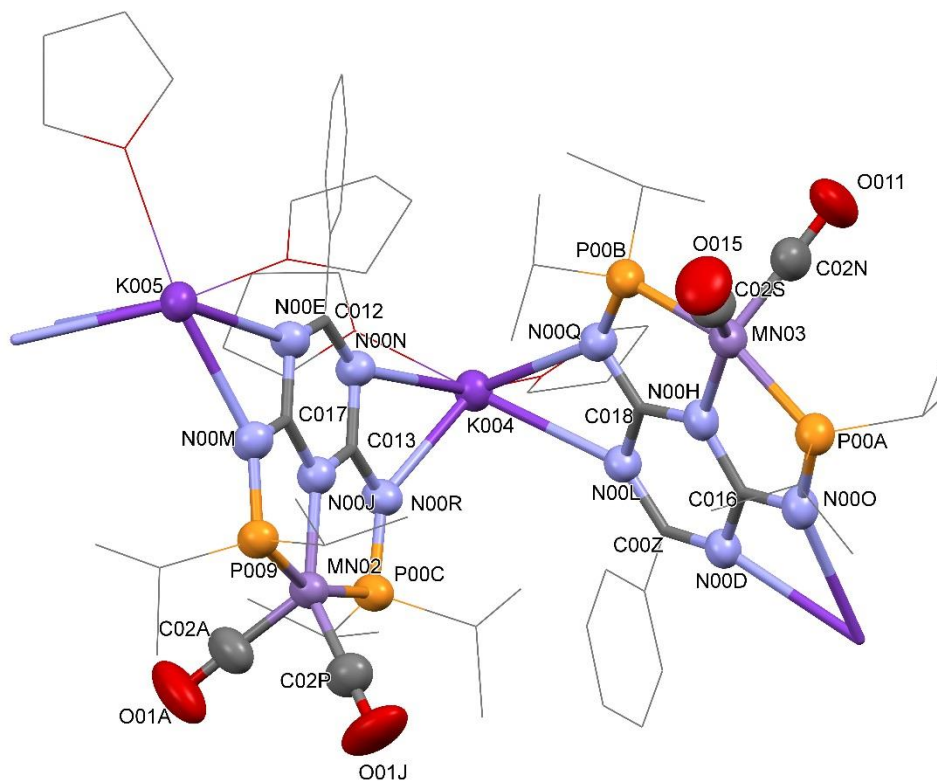


Figure S 47. IR spectrum of **[Mn-H]K₂**.

7 Crystallographic Data



checkCIF/PLATON (basic structural check) for [Mn]K

Structure factors have been supplied for datablock(s) sv493_1a1_m_p21n_sx
 THIS REPORT IS FOR GUIDANCE ONLY. IF USED AS PART OF A REVIEW PROCEDURE FOR PUBLICATION, IT SHOULD NOT REPLACE THE EXPERTISE OF AN EXPERIENCED CRYSTALLOGRAPHIC REFEREE.

No syntax errors found.
 Please wait while processing

CIF dictionary
 Interpreting this report

Structure factor report

Datablock: sv493_1a1_m_p21n_sx

Bond precision:	C-C = 0.0093 Å	Wavelength=0.71073
Cell:	a=12.840 (3) b=45.110 (9) c=20.490 (4)	
	alpha=90 beta=96.90 (3) gamma=90	
Temperature: 133 K		
	Calculated	Reported
Volume	11782 (4)	11782 (4)
Space group	P 21/n	P 21/n 1
Hall group	-P 2yn	-P 2yn
Moiety formula	C93 H147 K3 Mn3 N15 O12 P6, C4 H8 O [+ solvent]	0.25 (C93 H147 K3 Mn3 N15 O12 P6), 0.25 (C4 H8 O)
Sum formula	C97 H155 K3 Mn3 N15 O13 P6 [+ solvent]	C24.25 H38.75 K0.75 Mn0.75 N3.75 O3.25 P1.50
Mr	2207.31	551.82

Dx,g cm-3	1.244	1.244
Z	4	16
Mu (mm-1)	0.564	0.564
F000	4672.0	4672.0
F000'	4682.31	
h,k,lmax	17,60,27	17,59,27
Nref	30347	28052
Tmin,Tmax	0.972,0.990	0.983,0.994
Tmin'	0.944	

Correction method= # Reported T Limits: Tmin=0.983 Tmax=0.994 AbsCorr = NONE

Data completeness= 0.924 Theta(max)= 28.662

R(reflections)= 0.0983(15175) wR2(reflections)= 0.3280(28052)

S = 1.060 Npar= 1305

The following ALERTS were generated. Each ALERT has the format
[test-name](#) [ALERT](#) [alert-type](#) [alert-level](#).
Click on the hyperlinks for more details of the test.

Alert level B

PLAT973_ALERT_2_B Check Calcd Positive Resid. Density on	Mn01	1.74 eA-3
--	------	-----------

And 2 other PLAT973 Alerts

PLAT973_ALERT_2_B Check Calcd Positive Resid. Density on	Mn02	1.67 eA-3
PLAT973_ALERT_2_B Check Calcd Positive Resid. Density on	Mn03	1.56 eA-3

Alert level C

ABSTY03_ALERT_1_C The _exptl_absorpt_correction_type has been given as none.
However values have been given for Tmin and Tmax. Remove these if an absorption correction has not been applied.

From the CIF: _exptl_absorpt_correction_T_min 0.983
From the CIF: _exptl_absorpt_correction_T_max 0.994

PLAT084_ALERT_3_C High wR2 Value (i.e. > 0.25)	0.33	Report
PLAT094_ALERT_2_C Ratio of Maximum / Minimum Residual Density	2.01	Report
PLAT220_ALERT_2_C Non-Solvent Resd 1 C Ueq(max)/Ueq(min) Range	6.0	Ratio
PLAT222_ALERT_3_C Non-Solv. Resd 1 H Uiso(max)/Uiso(min) Range	5.1	Ratio
PLAT241_ALERT_2_C High 'MainMol' Ueq as Compared to Neighbors of	C038	Check

And 7 other PLAT241 Alerts

PLAT241_ALERT_2_C High 'MainMol' Ueq as Compared to Neighbors of	C03C	Check
PLAT241_ALERT_2_C High 'MainMol' Ueq as Compared to Neighbors of	C03F	Check
PLAT241_ALERT_2_C High 'MainMol' Ueq as Compared to Neighbors of	C03I	Check
PLAT241_ALERT_2_C High 'MainMol' Ueq as Compared to Neighbors of	C03J	Check
PLAT241_ALERT_2_C High 'MainMol' Ueq as Compared to Neighbors of	C03K	Check
PLAT241_ALERT_2_C High 'MainMol' Ueq as Compared to Neighbors of	C03O	Check
PLAT241_ALERT_2_C High 'MainMol' Ueq as Compared to Neighbors of	C03R	Check
PLAT242_ALERT_2_C Low 'MainMol' Ueq as Compared to Neighbors of	O00U	Check

And 4 other PLAT242 Alerts

PLAT242_ALERT_2_C Low 'MainMol' Ueq as Compared to Neighbors of	O00W	Check
PLAT242_ALERT_2_C Low 'MainMol' Ueq as Compared to Neighbors of	C02W	Check
PLAT242_ALERT_2_C Low 'MainMol' Ueq as Compared to Neighbors of	C032	Check
PLAT242_ALERT_2_C Low 'MainMol' Ueq as Compared to Neighbors of	C036	Check
PLAT260_ALERT_2_C Large Average Ueq of Residue Including	O02U	0.124 Check
PLAT341_ALERT_3_C Low Bond Precision on C-C Bonds	0.00929	Ang.
PLAT360_ALERT_2_C Short C(sp3)-C(sp3) Bond C03B - C03N .	1.40	Ang.

And 5 other PLAT360 Alerts

PLAT360_ALERT_2_C Short C(sp3)-C(sp3) Bond C03B - C03O .	1.43	Ang.
PLAT360_ALERT_2_C Short C(sp3)-C(sp3) Bond C03F - C03H .	1.42	Ang.
PLAT360_ALERT_2_C Short C(sp3)-C(sp3) Bond C03H - C03R .	1.42	Ang.
PLAT360_ALERT_2_C Short C(sp3)-C(sp3) Bond C03D - C03M .	1.40	Ang.
PLAT360_ALERT_2_C Short C(sp3)-C(sp3) Bond C03G - C03L .	1.43	Ang.
PLAT410_ALERT_2_C Short Intra H...H Contact H03M ..H23D .	1.93	Ang.

x,y,z = 1_555 Check

PLAT911_ALERT_3_C Missing FCF Refl Between Thmin & STh/L=	0.600	302 Report
PLAT973_ALERT_2_C Check Calcd Positive Resid. Density on	K006	1.26 eA-3
PLAT973_ALERT_2_C Check Calcd Positive Resid. Density on	K004	1.23 eA-3
PLAT977_ALERT_2_C Check Negative Difference Density on H23A		-0.31 eA-3

And 3 other PLAT977 Alerts

PLAT977_ALERT_2_C Check Negative Difference Density on Hz		-0.38 eA-3
PLAT977_ALERT_2_C Check Negative Difference Density on H7CA		-0.32 eA-3
PLAT977_ALERT_2_C Check Negative Difference Density on H1CA		-0.34 eA-3
PLAT978_ALERT_2_C Number C-C Bonds with Positive Residual Density.	0	Info

Alert level G

PLAT002_ALERT_2_G Number of Distance or Angle Restraints on AtSite	11	Note
--	----	------

PLAT003_ALERT_2_G	Number of Uiso or Uij Restrained non-H Atoms ...	18	Report
PLAT004_ALERT_5_G	Polymeric Structure Found with Maximum Dimension	1	Info
PLAT042_ALERT_1_G	Calc. and Reported MoietyFormula Strings Differ		Please Check
PLAT045_ALERT_1_G	Calculated and Reported Z Differ by a Factor ...	0.25	Check
PLAT072_ALERT_2_G	SHELXL First Parameter in WGHT Unusually Large	0.20	Report
PLAT176_ALERT_4_G	The CIF-Embedded .res File Contains SADI Records	13	Report
PLAT178_ALERT_4_G	The CIF-Embedded .res File Contains SIMU Records	4	Report
PLAT180_ALERT_4_G	Check Cell Rounding: # of Values Ending with 0 =	4	Note
PLAT301_ALERT_3_G	Main Residue Disorder(Resd 1)	4%	Note
PLAT398_ALERT_2_G	Deviating C-O-C Angle From 120 for O02U	103.9	Degree
PLAT605_ALERT_4_G	Largest Solvent Accessible VOID in the Structure	134	A**3
PLAT720_ALERT_4_G	Number of Unusual/Non-Standard Labels	288	Note
PLAT794_ALERT_5_G	Tentative Bond Valency for Mn01 (I) .	1.02	Info
And 2 other PLAT794 Alerts			
PLAT794_ALERT_5_G	Tentative Bond Valency for Mn02 (I) .	1.02	Info
PLAT794_ALERT_5_G	Tentative Bond Valency for Mn03 (I) .	1.03	Info
PLAT860_ALERT_3_G	Number of Least-Squares Restraints	109	Note
PLAT868_ALERT_4_G	ALERTS Due to the Use of _smtbx_masks Suppressed		! Info
PLAT883_ALERT_1_G	No Info/Value for _atom_sites_solution_primary .		Please Do !
PLAT910_ALERT_3_G	Missing # of FCF Reflection(s) Below Theta(Min).	1	Note
PLAT912_ALERT_4_G	Missing # of FCF Reflections Above STh/L= 0.600	1973	Note

0 **ALERT level A** = Most likely a serious problem - resolve or explain
3 **ALERT level B** = A potentially serious problem, consider carefully
35 **ALERT level C** = Check. Ensure it is not caused by an omission or oversight
21 **ALERT level G** = General information/check it is not something unexpected

4 ALERT type 1 CIF construction/syntax error, inconsistent or missing data
37 ALERT type 2 Indicator that the structure model may be wrong or deficient
7 ALERT type 3 Indicator that the structure quality may be below
7 ALERT type 4 Improvement, methodology, query or suggestion
4 ALERT type 5 Informative message, check

It is advisable to attempt to resolve as many as possible of the alerts in all categories. Often the minor alerts point to easily fixed oversights, errors and omissions in your CIF or refinement strategy, so attention to these fine details can be worthwhile. In order to resolve some of the more serious problems it may be necessary to carry out additional measurements or structure refinements. However, the purpose of your study may justify the reported deviations and the more serious of these should normally be commented upon in the discussion or experimental section of a paper or in the "special_details" fields of the CIF. checkCIF was carefully designed to identify outliers and unusual parameters, but every test has its limitations and alerts that are not important in a particular case may appear. Conversely, the absence of alerts does not guarantee there are no aspects of the results needing attention. It is up to the individual to critically assess their own results and, if necessary, seek expert advice.

Publication of your CIF in IUCr journals

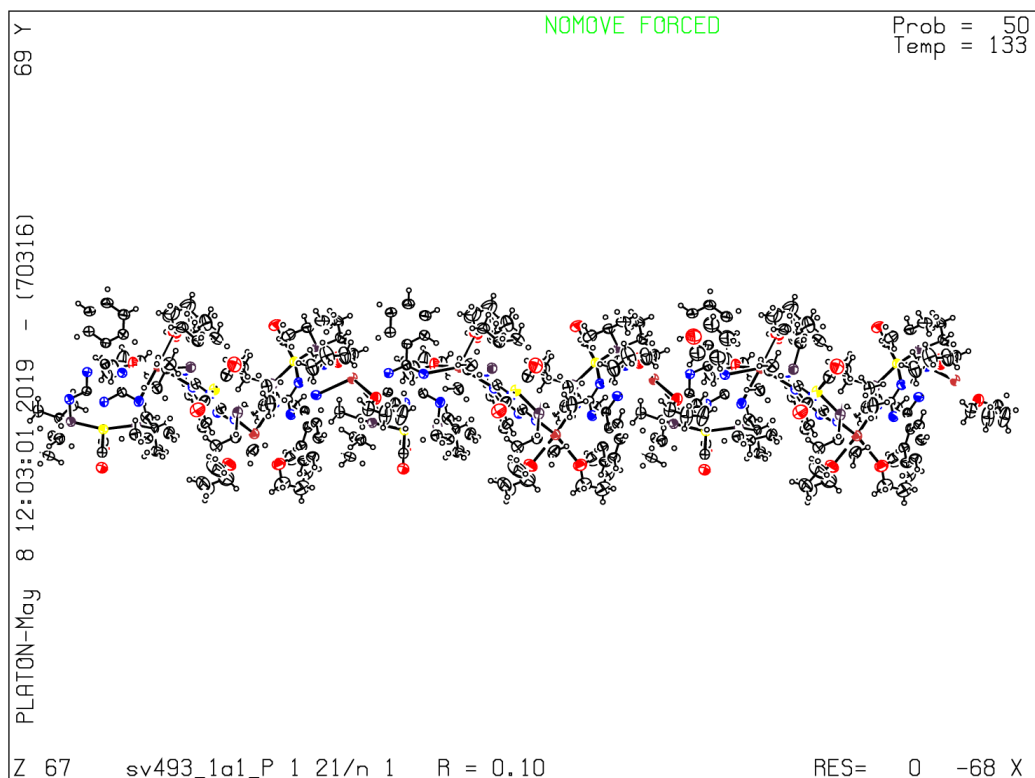
A basic structural check has been run on your CIF. These basic checks will be run on all CIFs submitted for publication in IUCr journals (*Acta Crystallographica*, *Journal of Applied Crystallography*, *Journal of Synchrotron Radiation*); however, if you intend to submit to *Acta Crystallographica Section C* or *E* or *IUCrData*, you should make sure that full publication checks are run on the final version of your CIF prior to submission.

Publication of your CIF in other journals

Please refer to the *Notes for Authors* of the relevant journal for any special instructions relating to CIF submission.

PLATON version of 03/05/2019; check.def file version of 29/04/2019

Datablock sv493_1a1_m_p21n_sx - ellipsoid plot



8 References

- ¹ Lai, P. S.; Dubland, J. A.; Sarwar, M. G.; Chudzinski, M. G.; Taylor, M. S. *Tetrahedron* **2011**, 67, 7586-7592.
- ² Perrone, S.; Salomone, A.; Caroli, A.; Falcicchio, A.; Citti, C.; Cannazza, G.; Troisi, L. *Eur. J. Org. Chem.* **2014**, 5932-5938.
- ³ Freitag, F.; Irrgang, T.; Kempe, R. *Chem. Eur. J.* **2017**, 23, 12110-12113.
- ⁴ Kallmeier, F.; Irrgang, T.; Dietel, T.; Kempe, R. *Angew. Chem. Int. Ed.* **2016**, 55, 11806-11809.
- ⁵ Dolomanov, O. V.; Bourhis, L. J.; Gildea, R. J.; Howard, J. A. K.; Puschmann, J. *Appl. Cryst.* **2009**, 42, 339-341.
- ⁶ Sheldrick, G. M. *Acta Cryst.* **2015**, C71, 3-8.
- ⁷ Farrugia, L. J. *J. Appl. Cryst.* **2012**, 45, 849-854.
- ⁸ Macrae, C. F.; Bruno, I. J.; Chisholm, J. A.; Edgington, P. R.; McCabe, P.; Pidcock, E.; Rodriguez-Monge, L.; Taylor, R.; van de Streek, J.; Wood, P. A. *J. Appl. Cryst.* **2008**, 41, 466-470.
- ⁹ Yamane, Y.; Liu, X.; Hamasaki, A.; Ishida, T.; Haruta, M.; Yokoyama, T.; Tokunaga, M. *Org. Lett.* **2009**, 11, 5162-5165.

-
- ¹⁰ Elangovan, S.; Neumann, J.; Sortais, J.; Junge, K.; Darcel, C.; Beller, M. *Nat. Commun.* **2016**, *7*, 12641.
- ¹¹ Thakur, M. S.; Nayal, O. S.; Sharma, A.; Rana, R.; Kumar, N.; Maurya, S. K. *Eur. J. Org. Chem.* **2018**, 6729–6732.
- ¹² Abdukader, A.; Jin, H.; Cheng, Y.; Zhu, C. *Tetrahedron Lett.* **2014**, *55*, 4172–4174.
- ¹³ Landge, V. G.; Mondal, A.; Kumar, V.; Nandakumar, A.; Balaraman, E. *Org. Biomol. Chem.* **2018**, *16*, 8175–8180.
- ¹⁴ Kawahara, R.; Fujita, K.; Yamaguchi, R. *Adv. Synth. Catal.* **2011**, *353*, 1161 – 1168.
- ¹⁵ Zhou, Y.; Zhou, H.; Liu, S.; Pi, D.; Shen, G. *Tetrahedron* **2017**, *73*, 3898–3904.
- ¹⁶ Fernandes, A.; Royo, B. *ChemCatChem* **2017**, *9*, 3912 –3917.
- ¹⁷ Likhar, P.; Arundhathi, R.; Kantam, M.; Prathima, P. *Eur. J. Org. Chem.* **2009**, 5383–5389.
- ¹⁸ Yang, C.; Fu, Y.; Huang, Y.; Yi, J.; Guo, Q; Liu, L. *Angew. Chem. Int. Ed.* **2009**, *48*, 7398 –7401.
- ¹⁹ Fertig, R.; Irrgang, T.; Freitag, F.; Zander, J.; Kempe, R. *ACS Catal.* **2018**, *8*, 8525–8530.
- ²⁰ Rösler, S.; Ertl, M.; Irrgang, T.; Kempe, R. *Angew. Chem. Int. Ed.* **2015**, *54*, 15046–15050.
- ²¹ Wong, C.; McBurney, R.; Binding, S.; Peterson, M.; Gonçalves, V.; Gooding, J.; Messerle, B. *Green Chem.* **2017**, *19*, 3142–3151.
- ²² Woo, L.; Wood, P.; Bubert, C.; Thomas, M.; Purohit, A.; Potter, B. *ChemMedChem* **2013**, *8*, 779 – 799.
- ²³ MacQueen, P.; Stradiotto, M. *Synlett* **2017**, *28*, 1652–1656.
- ²⁴ Villa-Marcos, B.; Tang, W.; Wu, X.; Xiao, J. *Org. Biomol. Chem.* **2013**, *11*, 6934–6939.
- ²⁵ Aziz, J.; Brion, J.; Hamze, A.; Alami, M. *Adv. Synth. Catal.* **2013**, *355*, 2417 – 2429.
- ²⁶ Hansch, C.; Leo, A.; Taft, R. *Chem. Rev.* **1991**, *91*, 165–195.
- ²⁷ Keinicke, L.; Fristrup, P.; Norrby, P.-O.; Madsen, R. *J. Am. Chem. Soc.* **2005**, *127*, 15756–15761.
- ²⁸ Creary, X.; Mehrsheikh-Mohammadi, M.; McDonald, S. *J. Org. Chem.* **1987**, *52*, 3254–3263.